NATIONAL AERONAUTICS AND SPACE ADMINISTRATION

Technical Report 32-1292

The Surveyor III and Surveyor IV Flight Paths and Their Determination From Tracking Data

W.J. O'Neil
R.G. Labrum
S.K. Wong
G. W. Reynolds

JET PROPULSION LABORATORY
CALIFORNIA INSTITUTE OF TECHNOLOGY
PASADENA, CALIFORNIA
August 15, 1968

TECHNICAL REPORT 32-1292

Prepared Under Contract No. NAS 7-100
National Aeronautics and Space Administration

Preface

The work described in this report was performed by the Systems Division of the Jet Propulsion Laboratory. Mr. W. J. O'Neil, who served as the Systems Analysis Project Engineer and a mission advisor, wrote the Introduction and integrated the sections of the report. Those sections were jointly prepared by Mr. S. K. Wong and Mr. R. G. Labrum with the following exceptions. Analysis of the AFETR tracking data for *Surveyor III* was provided by Mr. Labrum; and the corresponding analysis for *Surveyor IV* was provided by Mr. G. W. Reynolds, who also assisted with Section IX.

Foreword

This is the second in a series of three reports concerning the determination of the flight paths of the seven *Surveyor* spacecraft. The *Surveyor I* and *Surveyor II* flight path determinations are described in Technical Report 32-1285. The flight path determinations for *Surveyors V*, *VI* and *VII* are described in Technical Report 32-1302. This report describes the current best estimate of the *Surveyor III* and *Surveyor IV* flight paths and the way in which they were determined. Postflight analysis of the tracking data has verified the adequacy of the inflight orbit determinations and provided valuable information regarding tracking station locations and physical constants.

Surveyor III and *Surveyor IV* were launched from Cape Kennedy on April 17 and July 14, 1967, respectively. *Surveyor III* successfully soft-landed on the moon at its prime target located at approximately 3°S lat and 23°W lon. It was the first *Surveyor* to carry the soil mechanics/surface sampler (SMSS) experiment. Extensive data were obtained with both the SMSS and the television experiment. Communications with *Surveyor IV* were permanently lost during its terminal descent phase approximately 2 min 31 s before the predicted touchdown time. The cause of this failure could not be determined.

This report is divided into three major parts. The first part, which consists of Sections I through IV, applies to both *Surveyors III* and *IV*. It summarizes the key flight path events and describes the basic orbit determination process, the tracking stations, and the inflight computational sequence. Parts two and three pertain to *Surveyor III* and *Surveyor IV*, respectively. Each of these parts discusses the inflight orbit solutions, the postflight analysis, the comparison of the inflight and postflight results, and the analysis of the Air Force Eastern Test Range (AFETR) tracking data for the respective *Surveyor* flight.

Contents

I. Introduction 1

A. *Surveyor III* Flight Path Events 2

B. *Surveyor IV* Flight Path Events 3

II. Computational Philosophy 3

A. Orbit Determination Program 3

B. Data Weighting and Error Sources 5

C. Data Sample Rate 10

D. Data Editing 10

III. Description of DSIF Tracking Stations 10

IV. Inflight Sequence and Types of Solutions 14

V. *Surveyor III* Inflight Orbit Determination Analysis 16

A. View Periods and Tracking Patterns 16

B. Premaneuver Orbit Estimates 16

C. Postmaneuver Orbit Estimates 29

D. AMR Backup Computations 31

VI. *Surveyor III* Postflight Orbit Determination Analysis 35

A. Introduction 35

B. Premaneuver Orbit Estimates 36

C. Postmaneuver Orbit Estimates 37

D. Evaluation of Midcourse Maneuver From DSIF Tracking Data 38

E. Estimated Tracking Station Locations and Physical Constants 39

VII. Observations and Conclusions From *Surveyor III* Mission 47

A. Tracking Data Evaluation 47

B. Comparison of Inflight and Postflight Results 47

VIII. Analysis of Air Force Eastern Test Range Tracking Data—*Surveyor III* 51

A. Introduction 51

B. Analysis of the Parking Orbit Data 52

C. Analysis of the Transfer Orbit Data 52

Contents (contd)

D. Analysis of the Postretro Orbit Data 56

E. Conclusions 56

IX. *Surveyor IV* Inflight Orbit Determination Analysis 57

A. View Periods and Tracking Patterns 57

B. Premaneuver Orbit Estimates 57

C. Postmaneuver Orbit Estimates 64

D. AMR Backup Computations 64

X. *Surveyor IV* Postflight Orbit Determination Analysis 78

A. Introduction 78

B. Premaneuver Orbit Estimates 78

C. Postmaneuver Orbit Estimates 81

D. Evaluation of Midcourse Maneuver From DSIF Tracking Data 84

E. Estimated Tracking Station Locations and Physical Constants 87

XI. Observations and Conclusions From *Surveyor IV* 89

A. Tracking Data Evaluation 89

B. Comparison of Inflight and Postflight Results 89

XII. Analysis of Air Force Eastern Test Range Tracking Data—*Surveyor IV* 92

A. Introduction 92

B. Analysis of the Transfer Orbit Data 92

C. Analysis of the Postretro Orbit Data 98

D. Conclusions 99

Appendix A. Definition of Doppler Data Types 100

Appendix B. Definition of the Miss Parameter **B** 101

Glossary 102

References 103

Tables

1. DSS locations, *Surveyor III* 13

2. DSS locations, *Surveyor IV* 13

Contents (contd)

Tables (contd)

3. DSS general tracking capabilities 13

4. Nominal schedule for orbit computations 14

5. Physical constants used for *Surveyors III* and *IV* 15

6. Summary of premaneuver and postmaneuver data used in orbit determination for *Surveyor III* 21

7. Premaneuver computations for *Surveyor III* 24

8. Premaneuver position and velocity at injection epoch for *Surveyor III* 25

9. Summary of premaneuver DSS tracking data used in orbit computations for *Surveyor III* 26

10. Postmaneuver computations for *Surveyor III* 30

11. Postmaneuver position and velocity for *Surveyor III* at injection epoch . . . 31

12. Summary of postmaneuver DSS tracking data used in orbit computations for *Surveyor III* 33

13. Inflight results of orbit determination AMR backup computations, *Surveyor III* 35

14. Comparisons of inflight and postflight AMR backup computations, *Surveyor III* 35

15. Summary of postflight orbit parameters, *Surveyor III* 36

16. Summary of data used in postflight orbit solutions, *Surveyor III* 37

17. Midcourse maneuver evaluated at midcourse epoch, *Surveyor III* 39

18. Lunar unbraked impact points, *Surveyor III* 39

19. Station locations and statistics, *Surveyor III* (referenced to 1903.0 pole) . . . 44

20. Physical constants and statistics, *Surveyor III* 45

21. Correlation matrix of estimated parameters, *Surveyor III* (solution on postmaneuver data with premaneuver data as *a priori* at maneuver epoch) 46

22. Summary of target impact parameters, *Surveyor III* 51

23. Parking orbit injection conditions, *Surveyor III* 52

24. Summary of AFETR tracking data used in orbit computations for *Surveyor III/Centaur* 55

25. Converged conditions at injection epoch in space-fixed cartesian coordinates, *Surveyor III* 55

26. Transfer orbit parameter solutions, *Surveyor III* 56

27. Postretro parameter solutions, *Surveyor III* 57

Contents (contd)

Tables (contd)

28. Summary of premaneuver and postmaneuver data used in orbit determination for *Surveyor IV* 63

29. Premaneuver computations for *Surveyor IV* 65

30. Premaneuver position and velocity at injection epoch, *Surveyor IV* 66

31. Summary of premaneuver DSS tracking data used in orbit computations for *Surveyor IV* 67

32. Postmaneuver computations for *Surveyor IV* 72

33. Postmaneuver position and velocity for *Surveyor IV* at injection epoch . . . 73

34. Summary of postmaneuver DSS tracking data used in orbit computations for *Surveyor IV* 76

35. Inflight results of orbit determination AMR backup computations for *Surveyor IV* 77

36. Summary of postflight orbit parameters, *Surveyor IV* 79

37. Summary of data used in postflight orbit solutions, *Surveyor IV* 79

38. Comparisons of inflight and postflight AMR backup computations for *Surveyor IV* 84

39. Midcourse maneuver evaluated at midcourse epoch, *Surveyor IV* 85

40. Lunar unbraked impact points, *Surveyor IV* 85

41. Station locations and statistics, *Surveyor IV* (referenced to 1903.0 pole) . . . 86

42. Physical constants and statistics, *Surveyor IV* 87

43. Correlation matrix of estimated parameters, *Surveyor IV* (solution on postmaneuver data with premaneuver data as *a priori* at maneuver epoch) 88

44. Summary of target impact parameters, *Surveyor IV* 90

45. AFETR station locations used for *Surveyor IV* 92

46. Transfer orbit solutions, *Surveyor IV* 94

47. Statistics of real-time transfer orbit tracking data residuals, *Surveyor IV* 94

48. Postflight transfer orbit solutions, *Surveyor IV* 97

49. Statistics of postflight transfer orbit tracking data residuals, *Surveyor IV* 97

50. Summary of *Centaur* postretro orbit injection conditions, *Surveyor IV* 98

51. Statistics of JPL postflight *Centaur* postretro orbit tracking data residuals, *Surveyor IV* 98

Contents (contd)

Figures

1. DSS 42 uncorrected premaneuver angular residuals for *Surveyor III* 6
2. DSS 42 corrected premaneuver angular residuals for *Surveyor III* 7
3. DSS 51 uncorrected premaneuver angular residuals for *Surveyor III* 8
4. DSS 51 corrected premaneuver angular residuals for *Surveyor III* 9
5. S-band functional diagram 11
6. Tracking station view periods and doppler data coverage for *Surveyor III* 16
7. DSS 42 stereographic projection for *Surveyor III* 17
8. DSS 51 stereographic projection for *Surveyor III* 18
9. DSS 61 stereographic projection for *Surveyor III* 19
10. DSS 11 stereographic projection for *Surveyor III* 20
11. Estimated premidcourse unbraked impact point for *Surveyor III* 22
12. Premaneuver two-way doppler residuals for *Surveyor III* 23
13. Estimated postmidcourse unbraked impact point for *Surveyor III* 32
14. *Surveyor III* postmaneuver two-way doppler residuals, trajectory not corrected for perturbations 40
15. *Surveyor III* postmaneuver two-way doppler residuals, trajectory corrected for perturbations 42
16. Station coordinate system 45
17. DSS 11 midcourse maneuver doppler data for *Surveyor III* 48
18. DSS 11 main retromotor burn phase doppler for *Surveyor III* 49
19. *Surveyor III* estimated landed location on lunar surface 50
20. AFETR tracking coverage for *Surveyor III* 52
21. AFETR tracking data residuals for *Surveyor III* 53
22. Tracking station view periods and doppler coverage for *Surveyor IV* 57
23. DSS 72 stereographic projection for *Surveyor IV* 58
24. DSS 51 stereographic projection for *Surveyor IV* 59
25. DSS 61 stereographic projection for *Surveyor IV* 60
26. DSS 11 stereographic projection for *Surveyor IV* 61
27. DSS 42 stereographic projection for *Surveyor IV* 62
28. Premaneuver two-way doppler residuals for *Surveyor IV*, trajectory not corrected for perturbations 69
29. Estimated premidcourse unbraked impact point for *Surveyor IV* 71

Contents (contd)

Figures (contd)

30. Estimated postmidcourse unbraked impact point for *Surveyor IV* 74

31. Postmaneuver two-way doppler residuals for *Surveyor IV*, trajectory not corrected for perturbations 75

32. Premaneuver two-way doppler residuals for *Surveyor IV*, trajectory corrected for perturbations 80

33. Postmaneuver two-way doppler residuals for *Surveyor IV*, trajectory corrected for perturbations 82

34. Midcourse maneuver doppler for *Surveyor IV* 90

35. Main retromotor burn phase doppler for *Surveyor IV* 91

36. AFETR tracking coverage for *Surveyor IV* 93

37. AFETR station elevation angles for *Surveyor IV* 93

38. AFETR tracking data residuals for *Surveyor IV* 95

B-1. Definition of **B** • **T**, **B** • **R** system 101

Abstract

This report describes the current best estimate of the *Surveyor III* and the *Surveyor IV* spacecraft flight paths and the way in which they were determined. The inflight orbit determination analysis is presented. The results of inflight and postflight analyses on the tracking data are presented along with the determination of certain physical constants and station locations.

The *Surveyor III* and *Surveyor IV* Flight Paths and Their Determination From Tracking Data

I. Introduction

This report describes the current best estimates of the *Surveyor III* and *Surveyor IV* flight paths and the way in which they were determined. Postflight analysis of the Deep Space Instrumentation Facility (DSIF) tracking data has verified the adequacy of the inflight orbit determinations. For example, the current best estimates of the premidcourse maneuver unbraked lunar impact points differ from those obtained during the flight by only 0.95 km for *Surveyor III* and 4.43 km for *Surveyor IV*.

The overall objectives of the *Surveyor* Project are

(1) To accomplish successful soft landings on the moon as demonstrated by operations of the spacecraft subsequent to landing.

(2) To provide basic data in support of *Apollo*.

(3) To perform operations on the lunar surface which will contribute new scientific knowledge about the moon and provide further information in support of *Apollo*.

Surveyor III, which was launched from Cape Kennedy on April 17, 1967 and which successfully landed on the moon on April 20, 1967, more than fulfilled its objectives. *Surveyor IV* was launched from Cape Kennedy on July 14, 1967, but its signal was permanently lost during the terminal descent phase approximately 2 min 31 s before the predicted touchdown time. Although the *Surveyor IV* mission ended prematurely, all flight path functions had already been completed. Therefore, the scope of the inflight and postflight flight path analyses is essentially the same for both *Surveyor III* and *Surveyor IV*.

The inflight *Surveyor* flight path analysis is the responsibility of the *Surveyor* Flight Path Analysis and Command (FPAC) team, which is staffed jointly by Hughes and the Jet Propulsion Laboratory (JPL). The FPAC team comprises the following functional groups: tracking data analysis (TDA), orbit determination (OD), maneuver analysis (MA), trajectory (TRAJ), and computer support (CS).

In order to provide perspective into the overall flight path activities, the key flight path events of *Surveyor III* and *Surveyor IV*, which are reported in greater detail in Refs. 1 and 2, are briefly summarized in this introduction. The main purpose of this report is to give additional insight into the overall performance of the orbit determination function specifically.

Only data taken during free flight are used for orbit solutions. This results in a discontinuity at the midcourse maneuver epoch that logically divides the tracking data into two blocks: (1) data taken before midcourse maneuver execution, and (2) data taken after midcourse maneuver execution. Results of the inflight orbit solutions arrived at from these two blocks of data, are used primarily by the maneuver analysis group to compute the midcourse and terminal maneuvers, and to provide the best estimate of the time at which a ground command should be sent to initiate the terminal retroignition sequence in the event that the onboard altitude marking radar (AMR) does not function. The solutions are also used by the trajectory group to obtain spacecraft trajectory information and view-period summaries, and by the tracking data analysis group to generate predictions of the observables for the Deep Space Stations.

A. *Surveyor III* Flight Path Events

The *Surveyor III* spacecraft was launched from the AFETR launch site 36B at Cape Kennedy, Florida, at 07:05:01.59 GMT on April 17, 1967. A 9.83-min *Atlas/Centaur* first burn injected the vehicle into a parking orbit having an altitude of approximately 90 nmi. After a coast of 22.1 min., a 1.86-min. *Centaur* second burn accurately injected the spacecraft into the desired lunar transfer trajectory. All event times for the launch phase were close to nominal except for the duration of the *Centaur* burns, which were longer than expected because of the 2% to 3% low main-engine thrust. This launch marked the first operational use of the *Centaur* in the parking orbit ascent mode.

Initial DSIF acquisition by the Tidbinbilla station (DSS 42) was close to optimum. Station 42 reported good one-way data at 07:55:42 GMT, only seconds after the predicted rise over the horizon mask of the station. Good two-way data were reported at 08:01:50. After DSS 42 acquisition, the DSIF stations continued to provide good two-way doppler data for the remainder of the flight with few exceptions.

The landing site, which was used in targeting the ascent trajectory was in an area of lunar maria of interest to the *Apollo* program, located at 3.33° S lat and 23.17° W lon. The *Centaur* injection was so accurate that the uncorrected, unbraked impact point was only about 466 km southwest of this site. The preflight site selection assumed the 99% landing site dispersions to be a 30-km radius circle on the lunar surface. However, primarily because of the small midcourse correction required and the high quality of the tracking data, the 99% dispersion that was computed during the flight from the predicted midcourse execution errors and orbit determination errors was a 10.6-km × 15.1-km ellipse. Because of this smaller dispersion, and the hazardous features of the lunar terrain that were observed in the high-resolution *Lunar Orbiter III* photographs, the midcourse aim point was biased 0.42 deg approximately north of the site selected preflight in order to enhance the probability of soft landing.

A midcourse correction of 4.19 m/s was successfully executed during the first Goldstone view period at approximately 05:00 GMT on April 18, 1967. This velocity increment was required in the critical plane to correct for "miss only." The velocity component normal to the critical plane is referred to as the *noncritical component* since it does not affect the miss to first order. The noncritical component principally influences the flight time, main retro burnout velocity, vernier propellant margin, and landing site dispersions. A noncritical component of zero was selected to minimize landing site dispersions since there were ample margins in all of the above parameters. Execution of the midcourse correction during the second Goldstone view period (approximately 46 h after injection) would have doubled the required velocity correction while reducing the expected landing site dispersions by one-fourth because of the reduction in orbit determination errors with the additional tracking data. However, the very small net gain in soft landing probability did not warrant the 24-h reduction in the time available after midcourse to diagnose and correct failures which might have occurred as a result of the midcourse execution.

A terminal attitude maneuver, consisting of −157.90 deg yaw, −76.78 deg pitch, and −63.92 deg roll, was initiated 38 min before retroignition to properly orient the spacecraft for the powered descent. The terminal roll attitude of the spacecraft was constrained by a problem with sidelobe crosscoupling of the radar altimeter and doppler velocity sensor (RADVS). The terminal descent was near nominal with the exception that the vernier engines were not automatically shut off at the 14-ft altitude mark. Consequently, the spacecraft bounced off the surface twice before the engines were shut off by ground command. Initial touchdown occurred at 00:04:17 GMT on April 20, 1967, at a mission time of $L + 64$ h 09 min.

Early television pictures from *Surveyor III* indicated that the spacecraft had landed within a crater having a diameter of about 200 m. The *Lunar Orbiter III* high-resolution photographs of the general landing area were scanned, and a crater was discovered in surroundings which resembled those appearing in the *Surveyor* pictures.

Closer examination of the photographs revealed sufficient landmarks recognizable in both the *Surveyor* and *Lunar Orbiter* pictures to conclude with high confidence that *Surveyor* was, indeed, in this particular crater. With the use of simple triangulation methods, the *Surveyor III* spacecraft was found to be at 2.94° S lat and 23.34° W lon, a mere 2.8 km from the final aim point.

B. *Surveyor IV* Flight Path Events

The *Surveyor IV* spacecraft was launched from the AFETR launch site 36A at Cape Kennedy, at 11:53:29.215 GMT on July 14, 1967. Since this was a direct ascent flight, a single *Atlas/Centaur* burn of 11.46-min injected the spacecraft into the desired lunar transfer trajectory. All event times were well within the 3-σ tolerances.

The tracking by the DSIF stations provided virtually continuous, high-quality, two-way doppler data with few exceptions throughout the mission. Initial DSIF acquisition was smoothly accomplished by DSS 72 at Ascension Island. Station 72 reported good one-way doppler data at 12:10:03 GMT only seconds after the predicted spacecraft rise at the station. Good two-way data was reported at 12:16:23 GMT.

The landing site initially selected for *Surveyor IV*, which was used in targeting the launch vehicle ascent trajectory, was in Sinus Medii at 0.58°N lat and 0.83°W lon. This site was selected because of its prime interest to the *Apollo* program. Subsequently, NASA Headquarters directed a refinement of the aim point to 0.417°N lat and 1.333°W lon at the request of the *Apollo* program office. The precision of the *Centaur* injection achieved an uncorrected, unbraked impact point that was only about 176 km southwest of the initial target point. Primarily because of the small midcourse correction required, and the high quality of the tracking data, the 99% landing site dispersion that was computed from the predicted midcourse execution errors and the orbit determination errors for a correction during the second Goldstone view period (about $L + 38$ h) was a 7.2 km × 10.8 km ellipse. The midcourse correction was delayed until the second Goldstone view period because the predicted landing site dispersions were substantially less than those predicted for a midcourse correction during the first Goldstone view period. Landing accuracy was particularly critical on this mission because of the hazardous surface features seen near the desired landing site in the high resolution *Lunar Orbiter* photographs. This was the only *Surveyor* mission in which midcourse correction was delayed until the second Goldstone view period.

A midcourse correction of 10.27 m/s was commanded and successfully executed at about 02:30 GMT on July 16, 1967. The velocity component in the critical plane to correct "miss only" was 2.47 m/s. The noncritical component of −10.0 m/s (negative sign indicates reduction in flight time) was selected because (1) predicted landing site dispersions were fairly constant out to this value, (2) the main retro burnout velocity would be reduced to a more comfortable level of about 500 ft/s, and (3) the Goldstone post-arrival visibility time would be increased.

A terminal attitude maneuver, consisting of +80.85 deg roll, +92.68 deg yaw, and −25.24 deg roll, was initiated approximately 38 min before retroignition in order to properly orient the spacecraft for the powered descent. The final roll maneuver was performed to achieve a spacecraft roll attitude that would satisfy the constraints of the radar altimeter and doppler velocity sensor and of the post-landing operations. Sudden loss of the spacecraft signal occurred about 41 s after main retroignition at 02:02:40 GMT on July 17, 1967 at a mission time of $L + 62{:}09{:}10$. This was about 2.5 min before the predicted touchdown time. Since all control of the powered descent is performed automatically onboard the spacecraft, it is possible that the *Surveyor IV* spacecraft soft-landed even though all communication was lost. The best estimate of the landing site, assuming soft landing occurred, is 0.37°N lat and 1.55°W lon. This point is 6.6 km approximately due west of the final aim point.

II. Computational Philosophy

A. Orbit Determination Program

The Single Precision Orbit Determination Program (SPODP) of the Jet Propulsion Laboratory (Ref. 3) is the principal analysis tool used for *Surveyor* orbit determination. This program uses an iterative, modified-least-squares technique to find that set of initial conditions at a given epoch which causes the weighted sum of squares of the tracking data residuals (defined as observed values minus computed values [O − C]) to be minimized. Here the term *modified* is used to indicate that the weighting of individual data types is accomplished in a different manner than in the usual least-squares method. The Single Precision Cowell Trajectory Program, SPACE (Ref. 4), and the double precision JPL Development Ephemeris No. 19, DE-19, are used in conjunction with the SPODP.[1]

[1]Before the *Surveyor IV* mission, the JPL Ephemeris EPHEM-1 was used.

The weighted-least-squares technique used for the parameter estimates has the refinement that *a priori* information on the parameters together with their statistics influence the estimate. The basic equations are

$$\Delta \mathbf{q}_i = [\mathbf{A}^T\mathbf{W}\mathbf{A} + \tilde{\mathbf{\Gamma}}^{-1}]^{-1} [\mathbf{A}^T\mathbf{W}(\mathbf{O} - \mathbf{C}) + \tilde{\mathbf{\Gamma}}^{-1} \Delta \mathbf{q}_i]$$

and

$$\mathbf{q}_{i+1} = \mathbf{q}_i + \Delta \mathbf{q}_i$$

where

$\mathbf{q}_i$ = the estimate of the solution parameter vector $(m \times 1)$ on the ith iteration.

$\mathbf{A}$ = the matrix of first-order partial derivatives on each observable with respect to each solution parameter $(n \times m)$.

$\mathbf{W}$ = the diagonal weighting matrix formed by taking the reciprocal of the *a priori* estimated effective variance on each observable $(n \times n)$.

$\tilde{\mathbf{\Gamma}}$ = the *a priori* covariance matrix on the solution parameters $(m \times m)$.

$\mathbf{O} - \mathbf{C}$ = the vector of differences between the observed data and the calculated data $(n \times 1)$.

$\Delta \mathbf{q}_i$ = the difference between the *a priori* solution estimate and the ith iteration estimate $(m \times 1)$.

The statistics associated with the parameter estimates are given in the covariance matrix $[\mathbf{A}^T\mathbf{W}\mathbf{A} + \tilde{\mathbf{\Gamma}}^{-1}]^{-1}$, from which it can be seen that the statistics are a direct reflection of the data weights.

Trajectory perturbations caused by gas leaks in the attitude control systems were observed during the *Mariner IV* and *Pioneer 6* missions. The postflight analysis of *Mariner IV* data by G. W. Null[2] led to an improved model for handling nongravitational, nondrag trajectory perturbations that was included in the Mod II version of the SPODP. The equations for this model are as follows:

$$\begin{aligned}\Delta \ddot{\mathbf{r}} = &\left[f_1 (1 - \alpha_1 \tau - \alpha_2 \tau^2) + \frac{A_p}{m_p} \frac{SC}{r_{sp}^2} (1 + G_R + \Delta G_R) \right] \mathbf{U} \\ &+ \left[f_2 (1 - \alpha_1 \tau - \alpha_2 \tau^2) + \frac{A_p}{m_p} \frac{SC}{r_{sp}^2} (G_T + \Delta G_T) \right] \mathbf{T} \\ &+ \left[f_3 (1 - \alpha_1 \tau - \alpha_2 \tau^2) + \frac{A_p}{m_p} \frac{SC}{r_{sp}^2} (G_N + \Delta G_N) \right] \mathbf{N}\end{aligned} \qquad (1)$$

[2]From Jet Propulsion Laboratory.

$[\Delta \ddot{\mathbf{r}}]$ = change of acceleration of probe caused by solar radiation pressure and small forces such as gas leaks in attitude control system, noncoupled attitude control jets, etc.

where

(1) The parameters to be solved for are

f_1, f_2, f_3 = accelerations due to gas leaks

α_1, α_2 = coefficients of polynomial in τ

G_R, G_T, G_N = solar radiation coefficients in the radial, tangential and normal directions

(2) The constants, or parameters not to be solved for, are

$\tau = T_c - T_0$, where T_c = current time, T_0 = initial epoch

A_p = nominal area of spacecraft projected onto plane normal to sun–probe line, m^2

m_p = instantaneous mass of probe, kg

r_{sp} = distance from sun to probe, km

SC = spacecraft solar radiation constant

$$= \frac{J\,(AU)^2}{c} \times \frac{1\,\text{km}^2}{10^6\,\text{m}^2}$$

$$= 1.031 \times 10^8 \frac{\text{km}^3\,\text{kg}}{\text{s}^2\,\text{m}^2}$$

where

J = solar radiation constant

$= 1.383 \times 10^3$ W/m^2

$= 1.383 \times 10^3$ kg/s^2

AU = astronomical unit

$= 1.496 \times 10^8$ km

c = speed of light

$= 2.997925 \times 10^5$ km/s

$\mathbf{U}$ = a unit vector directed out from the sun as in the case of a radiation pressure force. For *Surveyor* this corresponds to the spacecraft +Z direction (roll axis)

$\mathbf{T}$ = a unit vector in the direction of the projection of the spacecraft–Canopus vector in the plane normal to $\mathbf{U}$. For *Surveyor* this corresponds to the spacecraft $+X$ direction (pitch axis)

$\mathbf{N}$ = a unit vector in the direction required to make $\mathbf{T}$, $\mathbf{N}$, and $\mathbf{U}$ a right-hand orthogonal system. For *Surveyor* this corresponds to the spacecraft $+Y$ direction (yaw axis)

$\Delta G_R, \Delta G_T, \Delta G_N$ = input values specified at up to 100 time-points with linear interpolation between points

The portion of the trajectory during which these accelerations are estimated is under option control. That is, during a given orbit computation the acceleration can be estimated either for specific parts of the trajectory or for the entire trajectory.

B. Data Weighting and Error Sources

The philosophy used for weighting data in the SPODP is to base the calculation of a weight value on the effective (or expected) variance of a given data type. The effective variance for a given data type is determined by summing up the variances caused by all known error sources. For two-way doppler data,[3] the error sources were divided into two general classes: (1) hardware, or station equipment errors; and (2) software, i.e., computing and model errors. For the first class of errors, such items as transmitter reference oscillator stability, doppler counter roundoff error or quantization, and doppler counter error due to dropped or added cycles in the presence of a low signal-to-noise ratio were considered. Of these, the major contributor is counter quantization error which is estimated to be 0.017 Hz (equivalent to a velocity error of 0.0011 m/s) for a data sample rate of 60 s. For the second class of errors it is known that certain model errors exist which are not adequately accounted for in the SPODP and are not sufficiently known so that they may be reflected in the effective variance. Among these are planetary and earth–moon ephemerides errors. The planetary ephemerides errors are negligible for a lunar trajectory, but earth–moon ephemerides errors will affect such quantities as predicted unbraked impact time, i.e., unbraked time of arrival. This is evidenced by the fact that the predicted time tends to vary as more near-moon tracking data is included in the orbit solution. The error in the refraction correction model used to correct low elevation data contributes a maximum of 1.07×10^{-4} m/s for a 60-s sample rate. In the ODP, statistics are based upon 1-σ data weights modified by an empirical refraction formula to account for varying elevation angles. Computing errors incurred within the program are the major contributors to the two-way doppler data weight. These errors (approximately 0.012 m/s for a 60-s sample rate) are due to the fact that most of the computations are done in single precision and result in interpolation errors and the build-up of roundoff errors. Based on the above error sources, the effective two-way doppler data weight is 0.013 m/s which corresponds to 0.2 Hz for S-band stations.

[3]See Appendix A for a definition of tracking data types.

The error sources associated with angle data (hour angle–HA, and declination angle–dec; or azimuth angle–az, and elevation angle–el) are

(1) Angle jitter or variation about the aiming point caused by antenna drive servomechanisms.

(2) Angle correction errors caused by differences between the empirical correction model which is based on the antenna optical axis, and the RF pointing axis.

(3) Angle encoder readout errors caused by inaccuracies in the compensation cams. Resolution of the encoder is plus or minus one count which corresponds to 0.002 deg.

(4) Refraction correction errors due to the difference between the atmospheric model used in the SPODP and the actual atmosphere at a given time.

Of these, the dominant error sources are angle correction errors which contribute an estimated variance of 0.033 deg^2 for a sample rate of 60 s. Thus, an effective data weight of 0.18 deg was used for HA–dec and az–el data. In past missions it was observed that a bias remained after the corrections were applied to the angle data. Therefore, these data are usually omitted from the orbit solution as soon as enough two-way doppler data are available to obtain a good solution. An idea of the biases for both uncorrected and corrected angle data can be obtained by examining the residual plots for DSS 42 and 51 premaneuver angle data in Figs. 1 through 4. These residuals were obtained by passing a converged set of initial conditions through the angle data. This set of initial conditions was obtained from an orbit solution which used all premaneuver two-way doppler data in the fit; i.e., no angle data were used to obtain the conditions. The residuals are plotted vs hour angle rather than time. Thus,

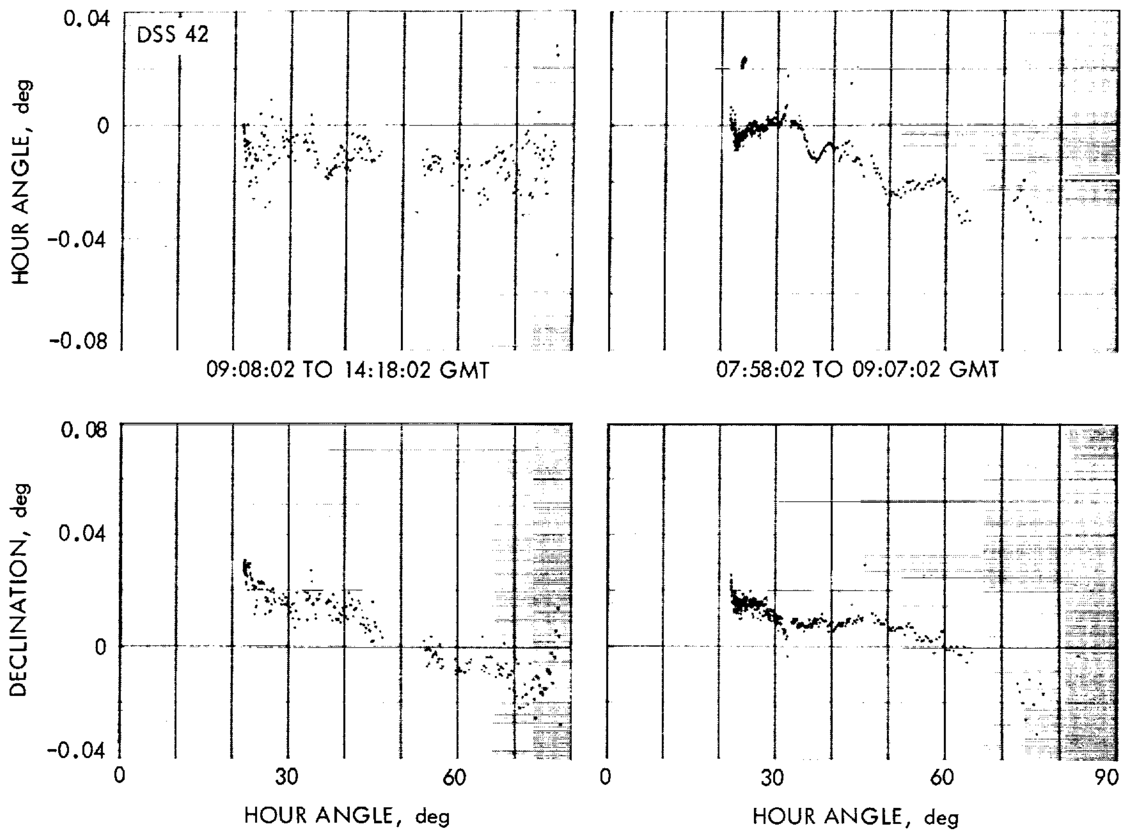

Fig. 1. DSS 42 uncorrected premaneuver angular residuals for *Surveyor III*

the shape of the uncorrected residual plots (Figs. 1 and 3) will show the total deflection or pointing error (main antenna structure deflection plus quadripod deflection) as the antenna moves from one horizon to the other. Figures 2 and 4 show the residuals of the same angle data after corrections, intended to remove the systematic pointing errors, were applied. These corrections are given in the form of polynomial coefficients based on optical horizon-to-horizon star tracks. That is, a polynomial curve fit is made to the optical pointing errors[4] resulting from a given horizon-to-horizon star track. The results of a number of such star tracks, using different stars, are combined to obtain the actual polynomial coefficients used in the orbit data generator program (ODG) to correct the angle data before it is used in the ODP. Star tracks, of stars which were not used in the polynomial curve fits, are periodically conducted to validate the coefficients. A comparison between the corrected residuals (Figs. 2 and 4) and the uncorrected residuals (Figs. 1 and 3) shows that a large percentage of the skew and curvature has been removed by the angle corrections, but some bias still exists. Similar biases have been observed in all previous lunar and planetary missions. These biases are most likely due to a difference between the antenna optical axis and the antenna RF axis. An optical ray path is directed from the source to a small telescope mounted near the bottom of the main paraboloidal reflector. On the other hand, the RF signal path is more complex. In general terms, an RF signal arriving at the main dish is reflected to a hyperboloidal reflector (part of the Cassegrain feed system) located essentially at the apex (focal point of the paraboloid) of a quadripod structure approximately 36 ft above the bottom of the paraboloidal reflector. From the hyperboloid, the signal is reflected back to the Cassegrain cone which supports the Cassegrain tracking feed. The net result is that another deflection has been introduced: that of the quadripod structure. Efforts are now under way to use RF sources such as post landing *Surveyor* tracking to generate more accurate correction coefficients. Even though the present corrections do not completely remove the systematic pointing errors, the corrected angle data are extremely valuable in converging to an orbit solution during the early part of a mission.

[4]The optical pointing error is defined as the difference between the known star position (in terms of topocentric hour angle and declination) at a given time and the corresponding antenna position at the same time.

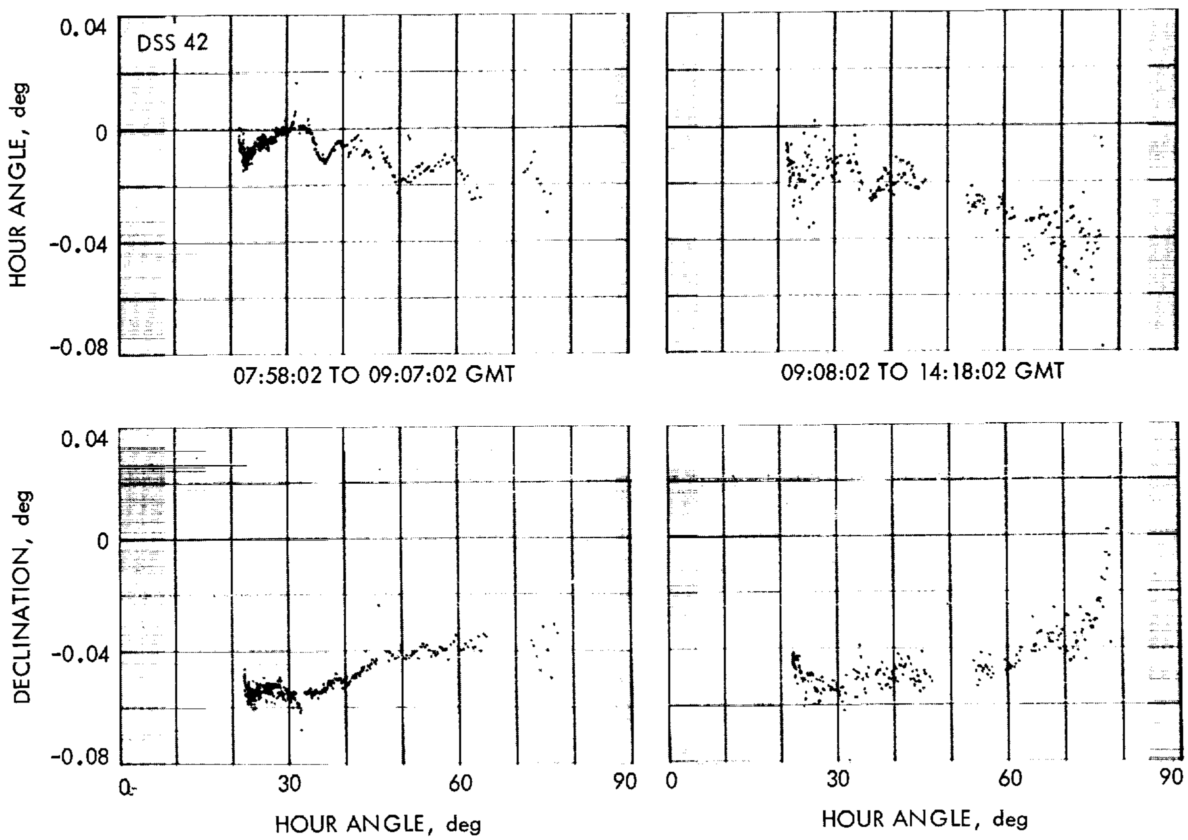

Fig. 2. DSS 42 corrected premaneuver angular residuals for *Surveyor III*

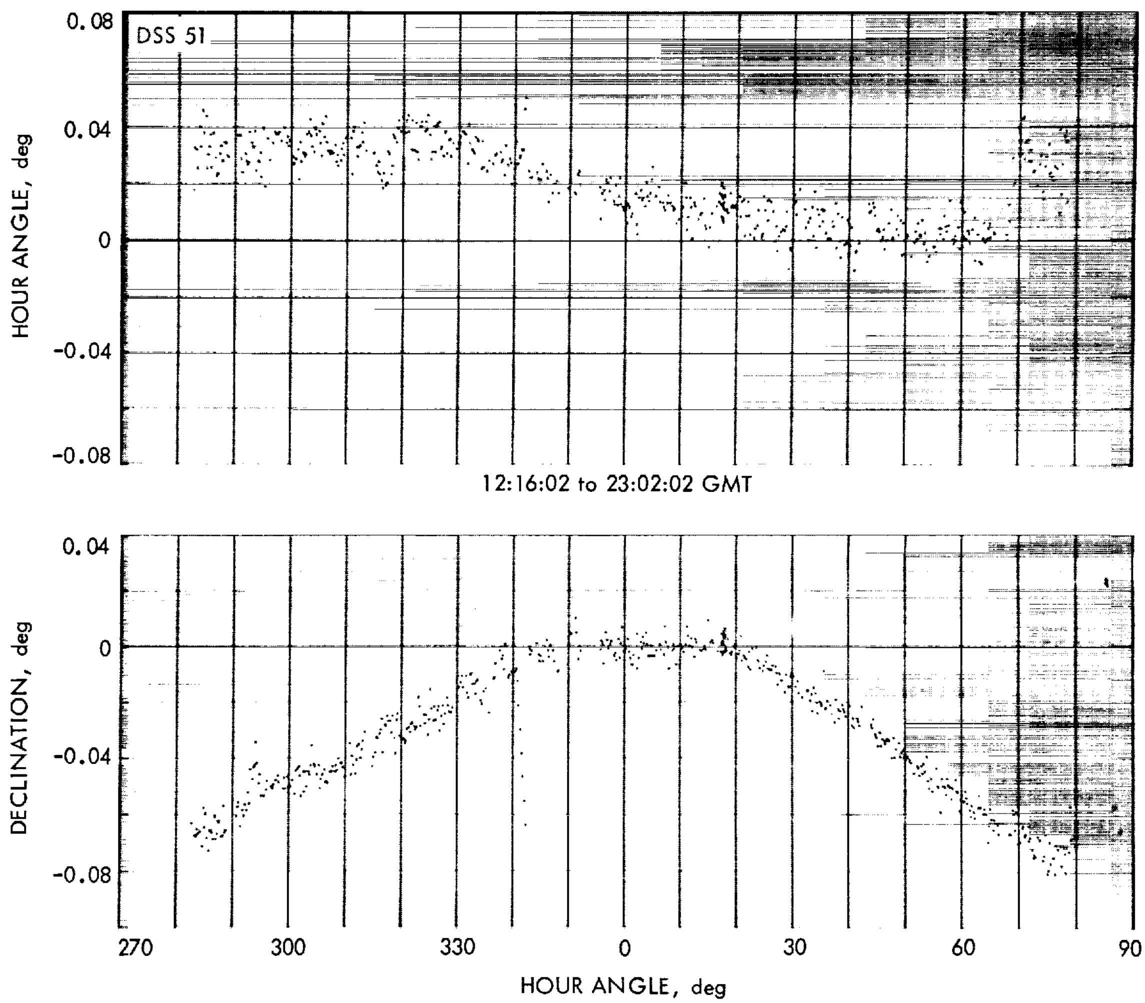

Fig. 3. DSS 51 uncorrected premaneuver angular residuals for *Surveyor III*

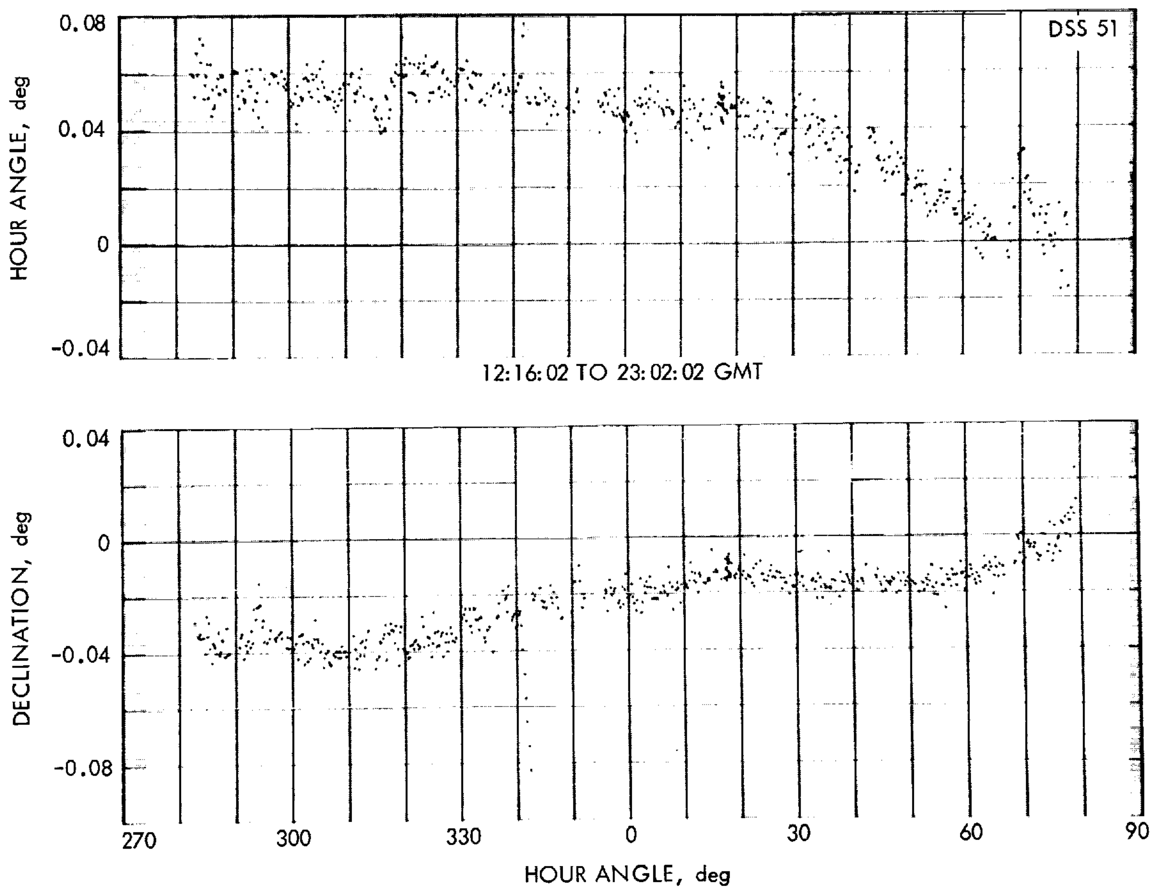

Fig. 4. DSS 51 corrected premaneuver angular residuals for Surveyor III

C. Data Sample Rate

The sample spacing to be used at the tracking station is determined by the tradeoff between doppler counter roundoff errors and truncation errors occurring in the doppler frequency computations. The expression used in the SPODP for the computations is

$$f(t_{ob}) = \int_{T-1/2\tau}^{T+1/2\tau} \ddot{F}(t)\,dt$$

where

$f(t_{ob})$ = integrated doppler frequency which should be observed by a station at time t_{ob}

$T = t_{ob} - \frac{1}{2}\tau$

τ = sample spacing

$F(t)$ = instantaneous frequency of the doppler shift which should have been observed at time t

This integral is evaluated by expanding a Taylor series about T and integrating term by term leading to

$$f(t_{ob}) = \tau F(t) + \frac{\tau^3}{24}\ddot{F}(t) + 0(F^{IV})$$

Thus, the truncation error is a function of τ and the fourth derivative of the frequency (which is dependent on the fifth derivative of range). Sample spacing has to be reduced during two phases of flight: (1) near earth, and (2) during midcourse maneuver. For these phases a sample spacing of 10 s was used. At all other times a sample spacing of 60 s was used.

D. Data Editing

The JPL tracking data processor (TDP) and orbit data generator (ODG) programs (Ref. 5) are used to edit all incoming tracking data and to prepare a data file for input to the SPODP. Data points are first read into the TDP which checks each data sample for acceptable format; i.e., it checks to determine if it is one of 30 acceptable message formats, if each item in the sample is the proper field, and if any item contains a missing or illegal character. During flight operations, time does not permit reconstruction of data points which were rejected for bad format. The next item the TDP checks is the data condition code. A data point is given a bad data condition code when automatic detectors, at the station, sense that the data would be unusable. These detectors have manual overrides which are used whenever an equipment malfunction is suspected, and during periods when the transmitter is being retuned before the transmitting assignment is transferred to another station. A coarse, in-range value check is made by the TDP to determine if each data type is within an acceptable limit; i.e., 360° for angles and 10^4 cycles for doppler. All data which have passed these checks or are not rejected by a user option are time-sorted and written on disk and magnetic tape for access by the ODG. If the ODG, upon reading the data file, finds angle data from DSS 42 or DSS 51, the values are corrected to remove systematic antenna pointing errors. Next, the doppler data is checked for monotonicity, valid tracking mode, and valid sample rate, and is converted from cycles to cycles per second by differencing adjacent samples and dividing by the sample time. Pertinent transmitter and receiver frequencies are entered on the file with each doppler sample (these frequencies are read in by the user; or, in some formats may be included with the data sample). The data are then written on disk and magnetic tape for access by the SPODP.

Blunder points are the data points rejected by the TDP and ODG during validity checks, or by application of user rejection limits during the orbit computation. These limits are based on experience gained in previous missions, and on the philosophy that it is better to immediately reject questionable points, which could create difficulties in converging to an orbit, than to attempt to salvage every point. This is particularly true when very few data are available during the early phase of the mission.

III. Description of DSIF Tracking Stations

The following Deep Space Stations provided tracking data for both *Surveyors III* and *IV*: DSS 11 (Pioneer: Goldstone, California), DSS 42 (Tidbinbilla, Australia), DSS 51 (Johannesburg, South Africa) and DSS 61 (Madrid, Spain). DSS 72 (Ascension Island) also participated as a backup station but provided two-way tracking only for *Surveyor IV*. The locations of these stations for *Surveyors III* and *IV* are given in Tables 1 and 2, respectively. The locations are mission-dependent because of the correction for polar motion, which is time-dependent. Figure 5 is a simplified functional diagram of the prime tracking stations. Table 3 summarizes the tracking capability of these stations.

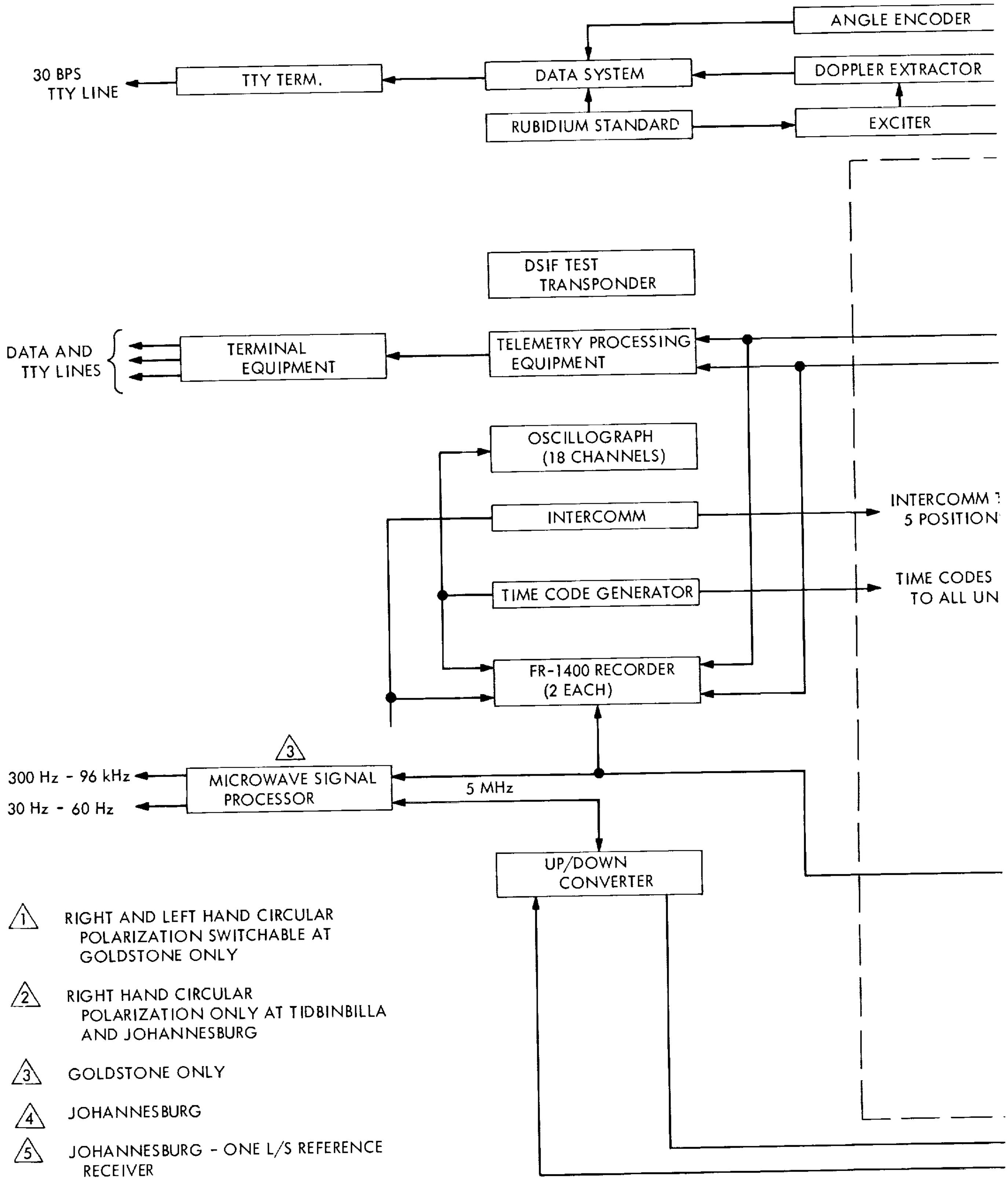
ANGLE ENCODER
30 BPS
TTY LINE
TTY TERM.
DATA SYSTEM
DOPPLER EXTRACTOR
RUBIDIUM STANDARD
EXCITER
DSIF TEST
TRANSPONDER
DATA AND
TTY LINES
TERMINAL
EQUIPMENT
TELEMETRY PROCESSING
EQUIPMENT
OSCILLOGRAPH
(18 CHANNELS)
INTERCOMM
INTERCOMM
5 POSITION
TIME CODE GENERATOR
TIME CODES
TO ALL UN
FR-1400 RECORDER
(2 EACH)
3
300 Hz - 96 kHz
30 Hz - 60 Hz
MICROWAVE SIGNAL
PROCESSOR
5 MHz
UP/DOWN
CONVERTER
1 RIGHT AND LEFT HAND CIRCULAR POLARIZATION SWITCHABLE AT GOLDSTONE ONLY
2 RIGHT HAND CIRCULAR POLARIZATION ONLY AT TIDBINBILLA AND JOHANNESBURG
3 GOLDSTONE ONLY
4 JOHANNESBURG
5 JOHANNESBURG - ONE L/S REFERENCE RECEIVER

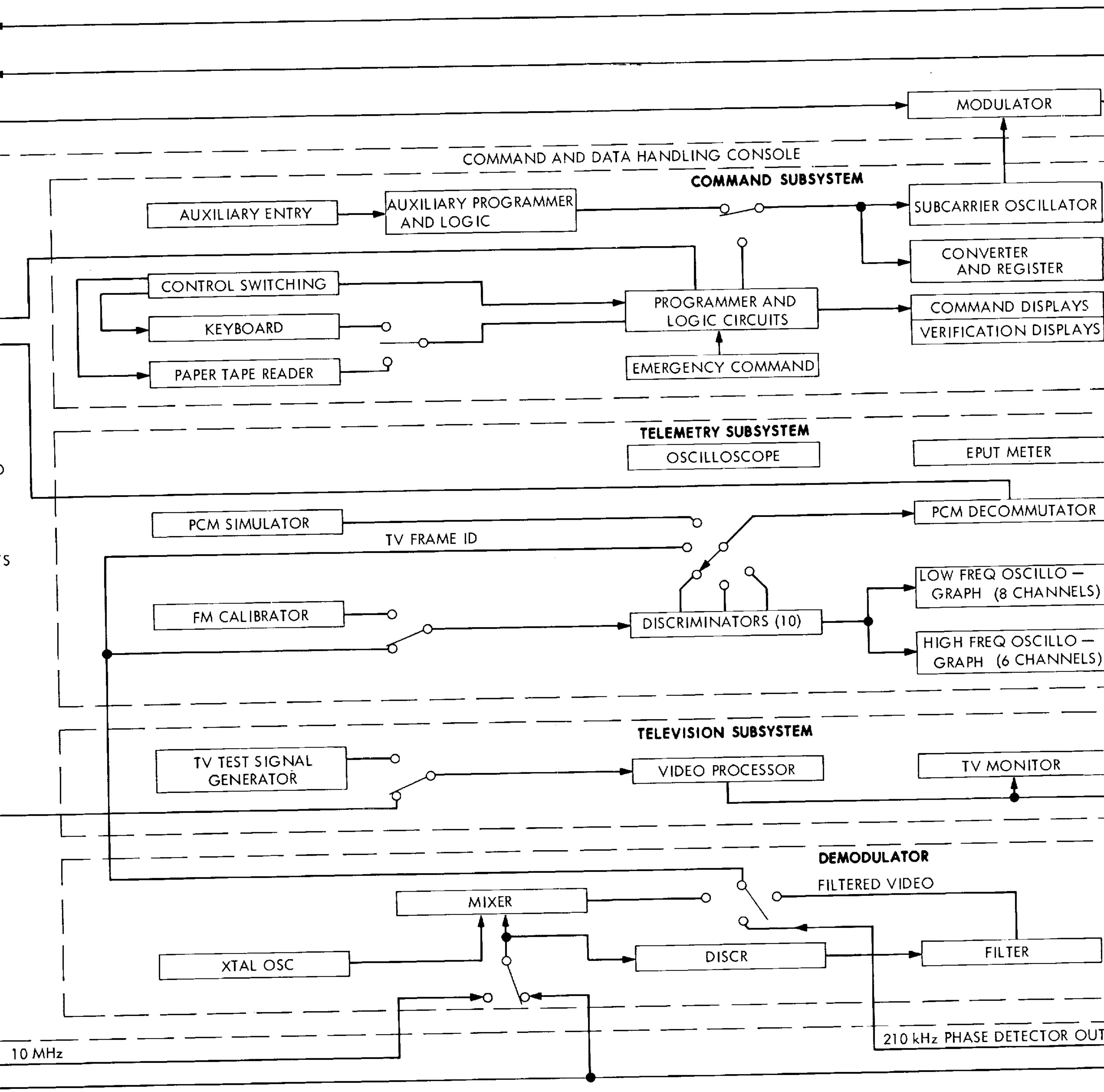

DEEP SPACE INSTRUMENTATION FACILITY, SURVEYOR CONFIGURATION

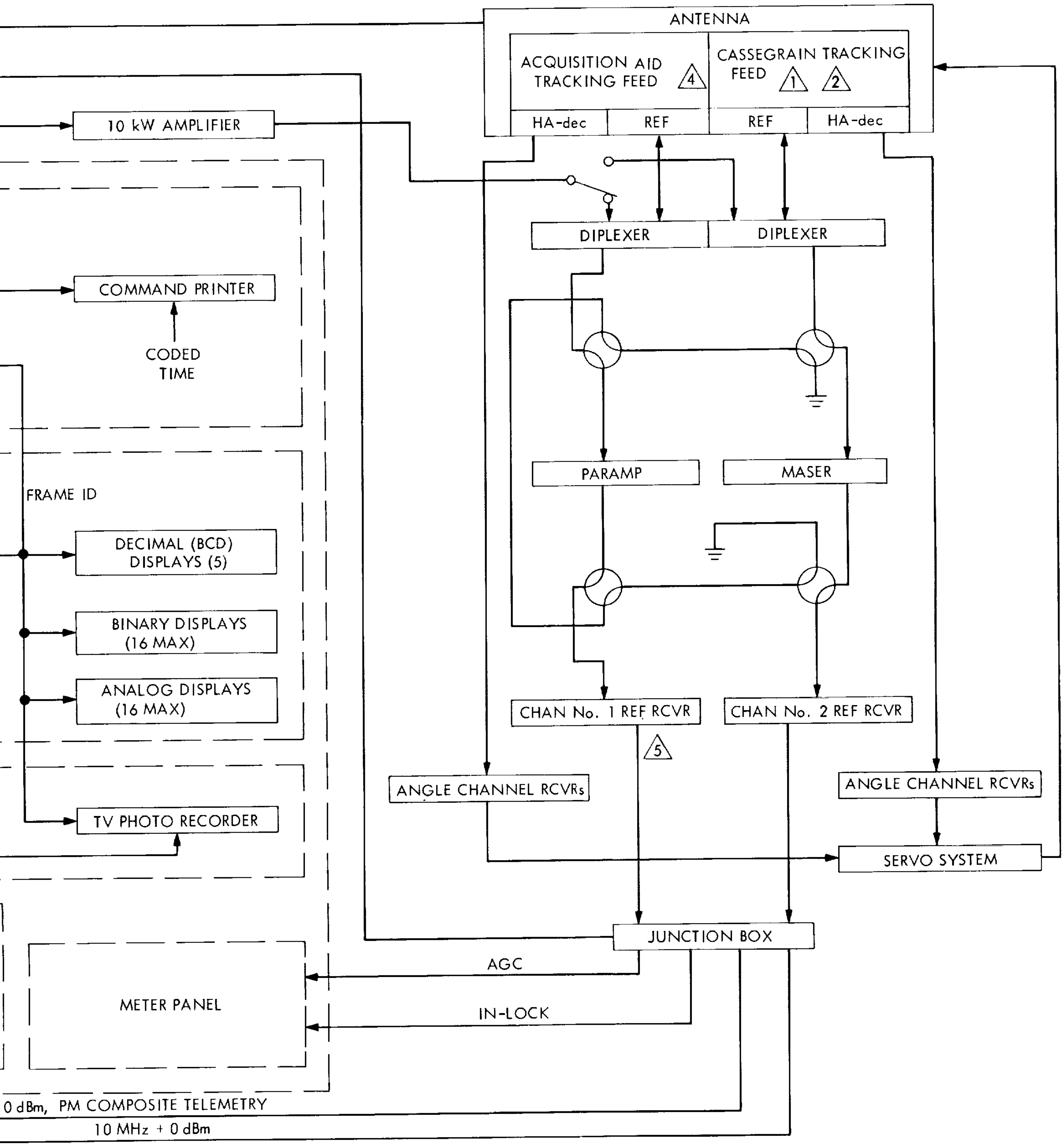

Fig. 5. S-band functional diagram

Table 1. DSS locations, *Surveyor III*

DSS	Geocentric radius, km	Geocentric latitude, deg (minus, south)	Geocentric longitude, deg
11	6372.020	35.20822	243.15070
42	6371.691	−35.21942	148.98140
51	6375.506	−25.73926	27.68568
61	6370.012	40.23882	355.75110
72	6378.239	−7.8999	345.6736

Table 2. DSS locations, *Surveyor IV*

DSS	Geocentric radius, km	Geocentric latitude, deg (minus, south)	Geocentric longitude, deg
11	6372.0107	35.208360	243.150980
42	6371.6771	−35.219193	148.981630
51	6375.5063	−25.739289	27.685671
61	6369.9955	40.238785	355.751300
72	6378.239	−7.89993	345.67362

Table 3. DSS general tracking capabilities

Deep Space Stations 11, 42, 51, 61	
Configuration	**GSDS S-band**
Antenna	
Tracking	85-ft parabolic
Mount	Polar (HA-dec)
Beamwidth ±3 dB	~0.4 deg
Gain, receiving	53.0 dB, +1.0, −0.5
Gain, transmitting	51.0 dB, +1.0, −0.5
Feed	Cassegrain
Polarization	LH or RH circular
Maximum angular tracking rate[a]	51 deg/min = 0.85 deg/s
Maximum angular acceleration	5.0 deg/s/s
Tracking accuracy (1 σ)	0.14 deg
Receiver	S-band
Typical system temperature	
with paramp	270°K ±50°K
with maser	55°K ±10°K
Loop noise bandwidth	
Threshold ($2B_{LO}$)	12, 48, or 152 Hz +0, −10%
Strong signal ($2B_{LO}$)	120, 255, or 550 Hz +0, −10%
Frequency (nominal)	2295 Mc
Frequency channel	14a

Deep Space Stations 11, 42, 51, 61	
Configuration	**GSDS S-band**
Transmitter characteristics	
Frequency (nominal)	2113 Mc
Frequency channel	14b
Power, maximum	10 kW
Tuning range	±100 kc
Modulator, phase	
Input impedance	≧1 kΩ
Input voltage	≦2.5 V peak
Frequency response (3 dB)	1 to 100 kHz
Sensitivity at carrier output frequency	1.0 rad peak per V peak
Peak deviation	2.5 rad peak
Modulation deviation stability	±5%
Rubidium standard	Yes
Stability, short term (1σ)	1×10^{-11}
Stability, long term (1σ)	5×10^{-11}
Doppler accuracy at F_{rc} (1σ)	0.2 Hz = 0.03 m/s
Data transmission, teletype	
Angle	Near-real-time
Doppler	Near-real-time
Telemetry	Near-real-time
Command and data handling console	Yes
Command capability	Yes

[a]Both axes.

IV. Inflight Sequence and Types of Solutions

During the flight the orbit solution is periodically updated as new tracking data becomes available. The nominal schedule on which these computations are made and the purpose of each computation is given in Table 4. Because a late (during DSS 11 [Goldstone] second pass) midcourse maneuver was decided upon and executed for *Surveyor IV*, the nominal schedule was modified after the normal LAPM orbit time. Since the computers are heavily loaded (i.e., a number of different engineering programs must be run at various intervals) throughout most of the mission, the type of orbit solution must be held to a minimum. That is, the number of parameters estimated in a solution must be restricted to the minimum set which will still allow the orbit determination accuracy goals to be met.[5] Experience gained from analyzing the data on *Surveyors I* and *II* and *Ranger* Block III preflight, inflight, and postflight analysis led to the determination that, in general, estimating only the position and velocity of the spacecraft at a given epoch is the best compromise between accuracy and computer time for inflight *Surveyor* orbit determination, assuming that the improved physical constants and station location parameter solutions obtained from the *Ranger* Block III and *Mariners II* and *IV* tracking data be used. Numerical values of these and other critical constants are given in Tables 1, 2, and 5.

In the premidcourse maneuver phase, all orbit solutions are obtained by estimating only the standard 6 parameters. After midcourse maneuver execution, all premidcourse tracking data from initial DSS acquisition until start of maneuver roll turn are used to obtain a best estimate premidcourse 6 × 6 orbit solution. The state vector (probe position and velocity) at injection epoch is integrated forward to the end of midcourse motor burn and incremented by the commanded midcourse velocity change. The resulting vector is then used as the initial estimate of the spacecraft postmidcourse orbit.

During the postmidcourse maneuver phase from end of midcourse motor burn until lunar encounter minus 5 h 40 min ($E - 5$ h 40 min), the orbit solutions are based

[5]The *Surveyor* guaranteed orbit determination accuracy capabilities are given in Refs. 6 and 7.

[6]This type of orbit solution is commonly referred to as a "6 × 6" or "standard 6."

Table 4. Nominal schedule for orbit computations

Orbit identification	Time of computation		Type of solution	Purpose of computation
	Beginning	Ending		
AFETR	L + 45 min	L + 1 h 10 min	6 × 6	Backup to AFETR orbit computation using AFETR C-band *Centaur* tracking data.
PROR	L + 1 h 15 min	L + 1 h 45 min	6 × 6	Estimate initial spacecraft orbit, based on DSS data; orbital elements, to generate acquisition predictions for Deep Space Stations.
ICEV	L + 2 h 20 min	L + 2 h 50 min	6 × 6	Evaluate initial injection conditions.
PREL	L + 3 h 30 min	L + 4 h 30 min	6 × 6	Provide orbital and target information for preliminary midcourse study, and elements for updating acquisition predictions.
DACO	MC − 11 h 45 min	MC − 8 h 45 min	6 × 6	Check data consistency computations; i.e., validate consistency of all available data.
LAPM	MC − 4 h 30 min	MC − 3 h	6 × 6	Final premidcourse orbit for determining midcourse maneuver corrections.
PRCL	MC + 2 h	MC + 4 h	6 × 6	Clean up orbit for generating *a priori* covariance matrix for postmidcourse orbit computations.
1 POM	MC + 7 h	MC + 9 h 40 min	6 × 6	Make preliminary evaluation of midcourse maneuver execution; provide orbital elements to generate acquisition predictions for Deep Space Stations.
2 POM	MC + 12 h 50 min	MC + 14 h 30 min	6 × 6	Update postmidcourse orbit solution based on postmidcourse data only.
3 POM	R − 24 h	R − 21 h 30 min	6 × 6	Update postmidcourse orbit solution.
4 POM	R − 14 h 5 min	R − 11 h 5 min	6 × 6	Update postmidcourse orbit solution.
5 POM	R − 5 h 40 min	R − 2 h 45 min	6 × 6	Solve final postmidcourse orbit for determining terminal spacecraft attitude maneuvers.
FINAL	R − 2 h	R − 40 min	10 × 10	Obtain best estimate of unbraked impact time for AMR backup.

Abbreviations: L = launch; MC = midcourse; R = retrofire.

Table 5. Physical constants used for *Surveyors III* and *IV*

Constant	Value		SPODP symbolic designation	SPACE symbolic designation	Basic source
	Surveyor III	*Surveyor IV*			
Earth gravitational coefficient, km^3/s^2	398601.27	398601.27	KE	GME	*Ranger* Block III (Ref. 6)
Moon gravitational coefficient, km^3/s^2	4902.6309	4902.6309	KM	GMM	Ref. 6
Earth radius to convert lunar ephemeris to km, km	6378.3106[a]	6378.1495	RE	REM	Ref. 6
Earth radius to be used in the oblate potential of earth, km	6378.1650	6378.1650		RE	Ref. 7
Ephemeris–Universal time reduction $\Delta T = ET - UT$, s	37.8	38.0	DUT	DUT	Internal publication
Earth–moon mass ratio GM_{earth}/GM_{moon}, kg-km[2]	81.304389	81.304389			*Ranger* Block III (Ref. 6)
Moments of inertia of moon for lunar oblate potential, kg-km[2]	$0.88778216 \times 10^{29}$ $0.88796612 \times 10^{29}$ $0.88833394 \times 10^{29}$	$0.88778216 \times 10^{29}$ $0.88796612 \times 10^{29}$ $0.88833394 \times 10^{29}$		A B C	Derived from *Ranger* Block III value of KM
Coefficient of second harmonic in oblateness of earth	0.00162345	0.00162345	J	J	Internal publication
Coefficient of third harmonic in oblateness of earth	−0.00000575	−0.00000575	H	H	Internal publication
Coefficient of fourth harmonic in oblateness of earth	0.000007875	0.000007875	D	D	Internal publication
Speed of light, km/s	299792.5	299792.5			Ref. 7
Lunar radius at target, km	1737.5[b]	1736.8	RSTOP		ACIC lunar charts, *Ranger*, *Surveyor*, and *Lunar Orbiter*

[a]During the AMR backup computations, this value was changed to 6378.3031 to account for estimated error of 112 m in earth–moon radial distance (as estimated by Dr. J. W. Eckert).

[b]During the postmidcourse orbit computations this value was changed to 1736.

on estimating only the standard 6 parameters. The spacecraft terminal attitude maneuvers are computed from the final 6×6 orbit solution. The rationale here is the same as that used for the premaneuver 6×6 solutions. That is, even though model errors and ephemerides errors exist, and errors that might occur because of differences between the assumed values of physical constants and station locations and the *true* values, the orbit determination accuracy goal can be achieved by estimating only the standard 6 orbital parameters.

To provide an effective backup for the *Surveyor* altitude marking radar (AMR), the type of orbit solution must be changed during the last few hours of the mission. The backup consists of transmitting a retromotor ignition sequence turn on command (from a ground station) at such a time that if a turn on pulse has not been generated by the AMR by the time the backup command reaches the spacecraft, the backup command will initiate the sequence. The transmission time is intentionally biased late, so that the AMR has ample opportunity to function, yet in time to save a significant percentage of missions in the event the AMR does not function. This requires that the SPODP be capable of predicting the unbraked impact time to within an uncertainty of approximately 0.5 s (1 σ). The uncertainty must include all error sources. Error sources, exclusive of tracking data errors, that significantly affect the predicted unbraked impact time are: (1) assumed value of lunar elevation at the impact point, (2) errors in earth-moon ephemerides, and (3) timing errors. The lunar elevation is obtained from NASA Langley Research Center and closely agrees with the elevation based on the Air Force Aeronautical Chart and Information Center (ACIC) lunar charts less 2.4 km. The 2.4 km is the amount by which elevations based on the appropriate ACIC lunar charts exceed elevations obtained from the *Rangers VI*, *VII*, and *VIII* tracking data. An *a priori* 1-σ uncertainty of ± 1 km (roughly equivalent to ± 0.4 s) is assigned to the elevation. A study using *Ranger* Block III tracking data indicated that the two remaining error sources could be adequately reduced by relying heavily on the near-moon tracking data and processing the data in the following manner:

(1) Process all available two-way doppler data from the midcourse epoch to approximately $E - 5$ h 40 min and map the resulting solution plus covariance matrix to the time of the last data point. Nothing is significant about the $E - 5$ h 40 min epoch other than its consistency with nominal sequence of events items. Degrade the diagonal elements of the mapped covariance matrix by 0.25 km^2 on position components and 1×10^{-10} km^2/s^2 on velocity components.

(2) Expand the estimate list to include geocentric radius and longitude of the two observing stations. That is, the type solution is expanded to a 10×10. *A priori* uncertainties of 12 m in spin axis distance, 40 m in station longitude, and 25 m in longitude difference between the two stations are added to the mapped covariance matrix.

(3) Reduce the effective data weight to 0.003 m/s (0.0195 Hz) to obtain realistic statistics on predicted unbraked impact time. This reduction is valid since computational errors are no longer a source of major error; i.e., the trajectory is only being integrated over a 6-h period. Also, the model errors have been taken into account by degrading the covariance matrix and by adding the station parameters to the estimate list.

V. *Surveyor III* Inflight Orbit Determination Analysis

A. View Periods and Tracking Patterns

Figure 6 summarizes the tracking station view periods and their data coverage for the period from launch to lunar touchdown. Figures 7 to 10 are stereographic projections for the prime tracking stations which show the trace of the spacecraft trajectory for the view periods of Fig. 6.

B. Premaneuver Orbit Estimates

Table 6 summarizes the tracking data used for both the inflight and postflight orbital calculations and analyses. This table provides a general picture of the performance of the data recording and handling systems.

The Air Force Eastern Test Range C-band tracking data obtained from Pretoria during the period between *Centaur* second main engine cutoff (MECO 2) and *Centaur*-spacecraft separation indicates that the Pretoria radar had problems in staying locked to the *Centaur.*

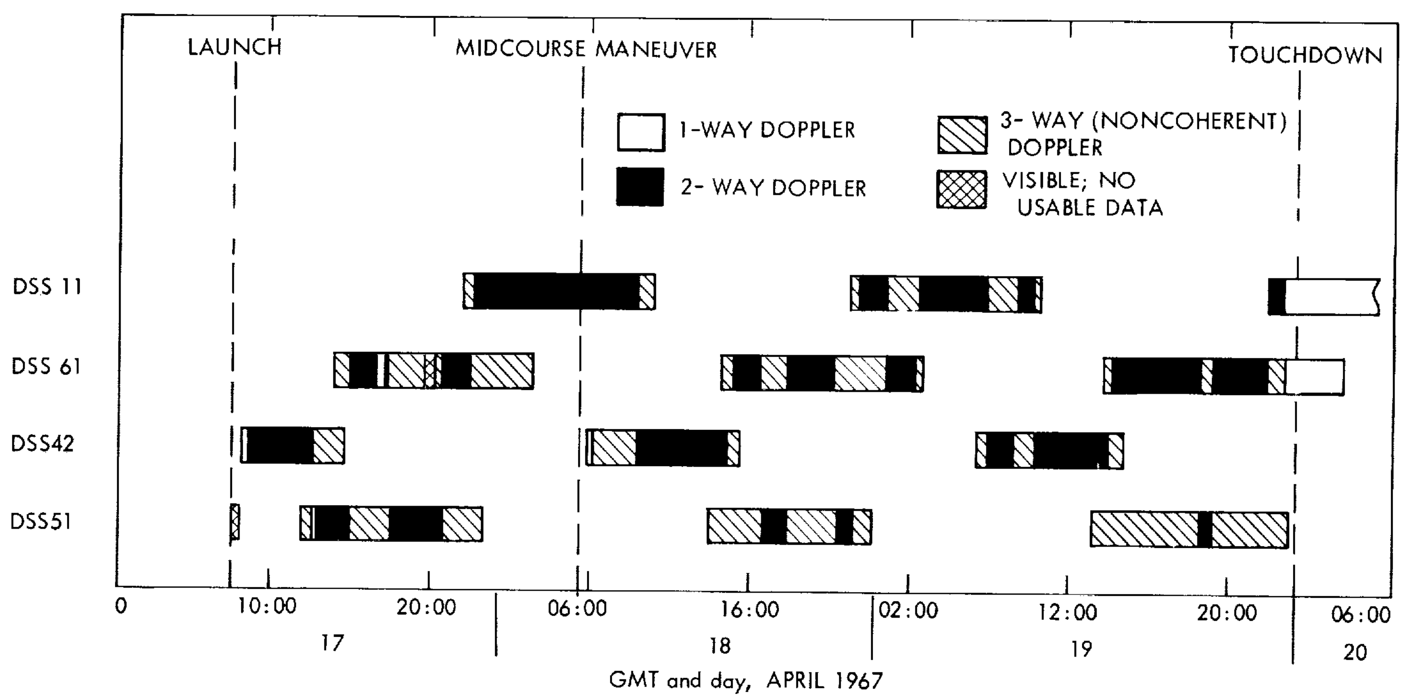

Fig. 6. Tracking station view periods and doppler data coverage for *Surveyor III*

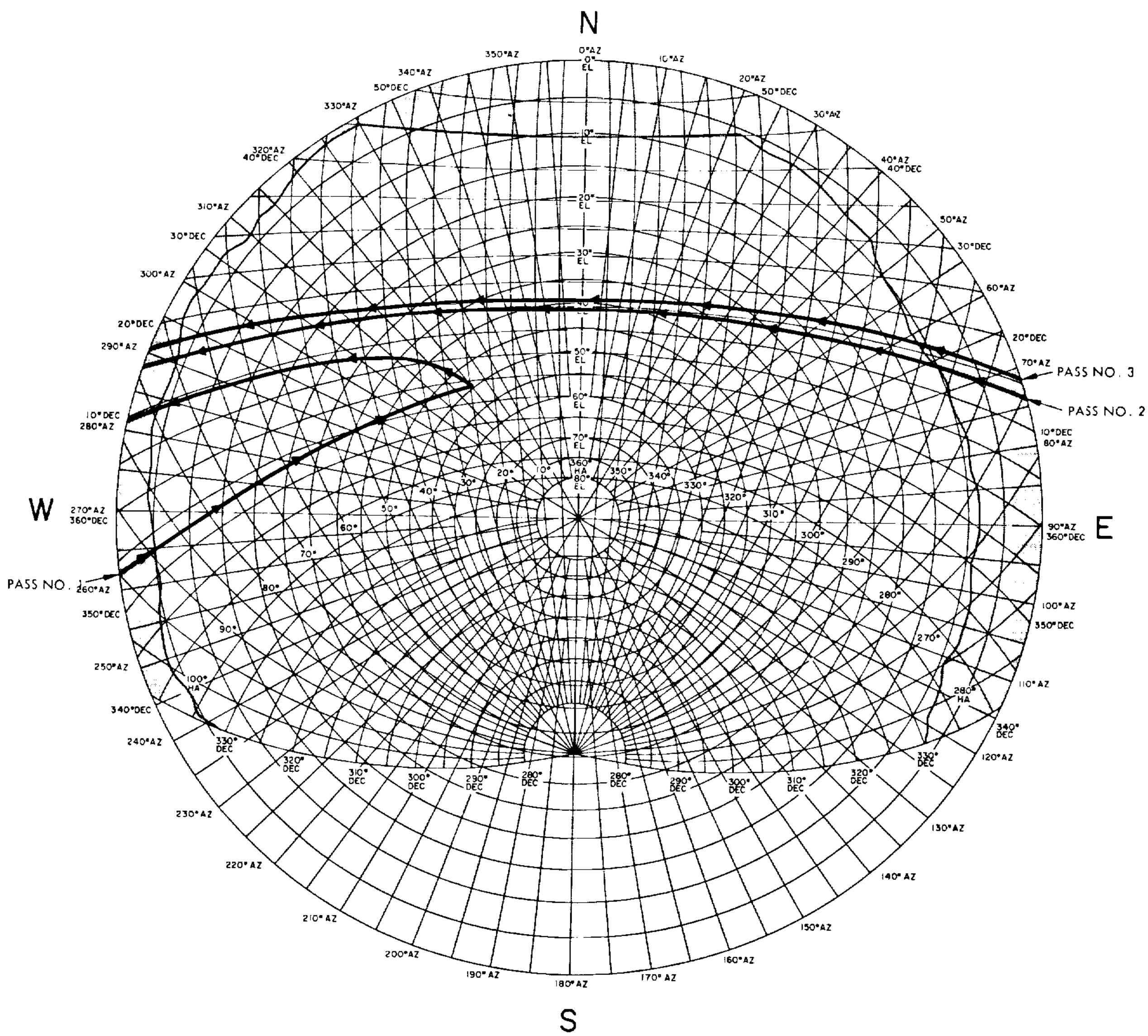

Fig. 7. DSS 42 stereographic projection for *Surveyor III*

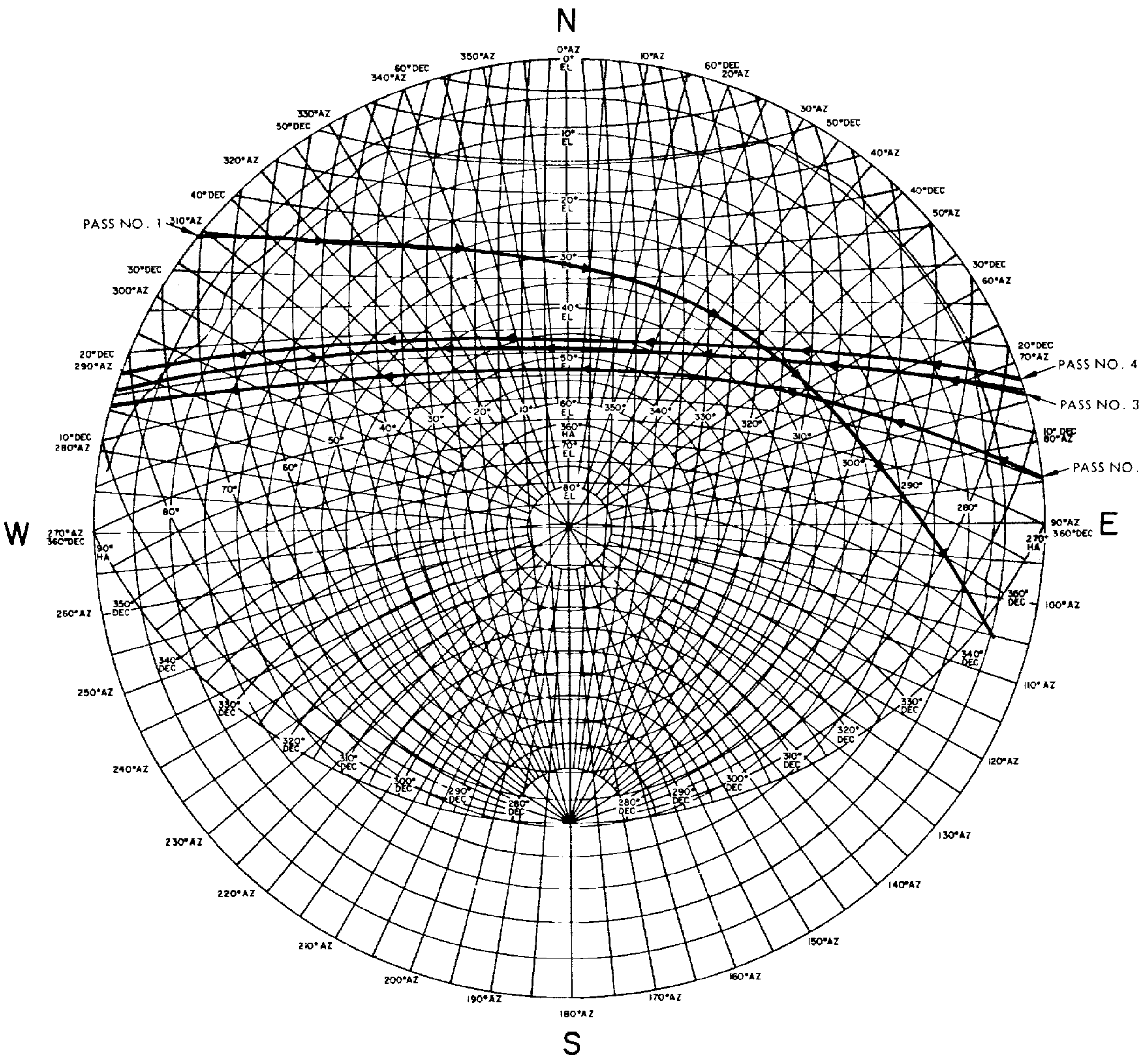

Fig. 8. DSS 51 stereographic projection for *Surveyor III*

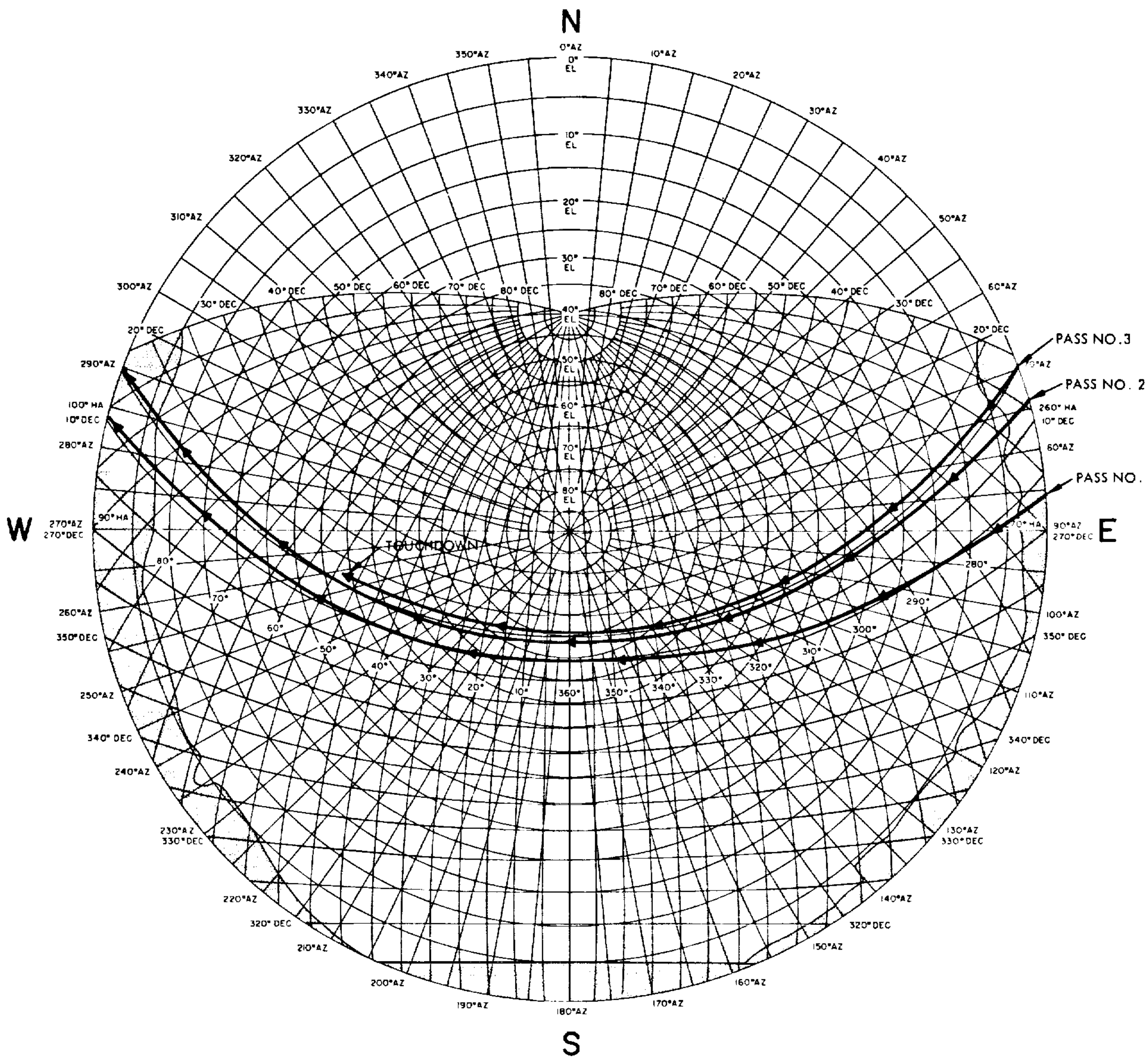

Fig. 9. DSS 61 stereographic projection for *Surveyor III*

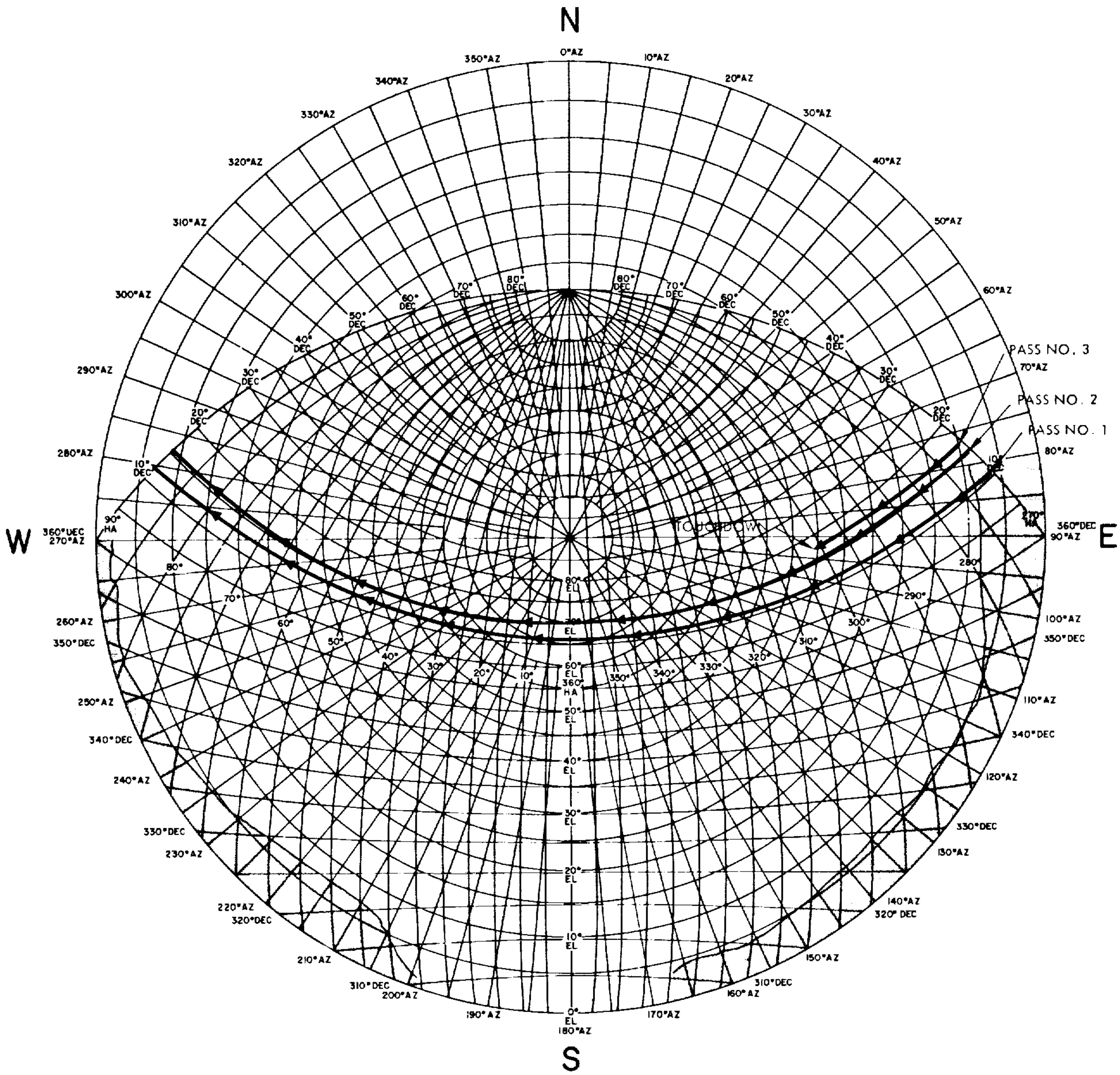

Fig. 10. DSS 11 stereographic projection for *Surveyor III*

Because of these problems, the AFETR check orbit was computed at JPL using only 5 data points of which 2 points were burn data and another 2 points were post-*Centaur*–spacecraft separation data. Only one usable data point was available between second main engine cutoff and *Centaur*–spacecraft separation. Therefore confidence in the solution was limited. Since the mark times indicated a near nominal flight, the preflight nominal injection conditions were used as starter values for the initial orbit computations.

The first estimate of the spacecraft orbit was completed at $L + 1$ h 54 min, and was based on approximately 20 min of DSS 42 angle and two-way doppler data. Mapping this solution forward to the target indicated that the correction required to achieve encounter at the prelaunch aiming point was well within the midcourse correction capability as was verified by the second (ICEV) and third (PREL) orbit computations completed at $L + 2$ h 50 min and $L + 3$ h 48 min, respectively.

During the third orbit computation period a comparison was made between solutions with and without angle (HA, dec) data. On the prime computer, the orbit computation (PREL YA) was made using DSS 42 angle and two-way doppler (CC3) data in the least-squares fit. On

Table 6. Summary of premaneuver and postmaneuver data used in orbit determination for *Surveyor III*

DSS	Data type	Points received	Number of points used in real time, % of received		Bad format, % of received		Bad data condition, % of received		Blunder points, % of received		Rejection limits on blunder points	Points used in postflight analysis
			Points	%	Points	%	Points	%	Points	%		
(A)	(B)	(C)	(D)		(E)		(F)		(G)		(H)	(I)
					Premaneuver data							
11	CC3	515	387	75.1	19	3.7	1	0.2	28	5.4	0.05 Hz	378
	HA	416	0	0	19	4.5	33	7.9	—	—	—	0
	Dec	416	0	0	19	4.5	33	7.9	—	—	—	0
42	CC3	507	429	84.6	7	1.4	3	0.6	5	1.0	0.06 Hz	418
	HA	699	383	54.8	15	2.1	66	9.4	2	0.3	0.20 deg	0
	Dec	699	383	54.8	15	2.1	66	9.4	4	0.6	0.20 deg	0
51	CC3	354	242	68.4	30	8.5	15	4.2	5	1.4	0.08 Hz	239
	HA	735	0	0	51	6.9	93	12.6	—	—	—	0
	Dec	735	0	0	51	6.9	93	12.6	—	—	—	0
61	CC3	290	140	48.3	26	9.0	48	16.5	66	22.7	0.03 Hz	69
	HA	1045	133	12.7	98	9.4	80	7.7	1	0.1	0.20 deg	0
	Dec	1045	133	12.7	98	9.4	80	7.7	1	0.1	0.20 deg	0
					Postmaneuver data							
11	CC3	792	602	76.0	6	0.8	22	2.8	18	2.3	0.08 Hz	585
42	CC3	755	593	78.5	3	0.4	17	2.3	2	0.3	0.02	590
51	CC3	204	101	49.5	6	2.9	0	0.0	1	0.5	0.10	101
61	CC3	830	581	70.0	26	3.1	48	5.8	3	0.4	0.03	551

the backup computer, the orbit computation (PREL XA) was made using only DSS 42 two-way doppler data in the fit. The comparison showed a difference in the **B**-plane target parameters of approximately 115 km in $\mathbf{B} \cdot \mathbf{T}T$ and approximately 133 km in $\mathbf{B} \cdot \mathbf{R}T$. These differences are outside the stated uncertainties, and clearly demonstrate how the orbit solution is corrupted by using the biased angle data.

During the data consistency (DACO) computation period from $MC - 11$ h 45 min to $MC - 8$ h 45 min, eight orbital solutions were obtained using various combinations of DSS 42, DSS 51, and DSS 61 data. The solutions obtained from these computations indicated that the two-way doppler data from the three Deep Space Stations were consistent. However, the DSS 61 data were excessively noisy owing to a counter problem which was corrected before the next DSS 61 rise.

At the beginning of the last premidcourse (LAPM) orbit computation time block, the following amount of two-way doppler data was available: 3 h 43 min from DSS 42, 8 h 4 min from DSS 51, 7 h 35 min from DSS 61, and 2 h 10 min from DSS 11. An orbit computation (LAPM YA) was made from these data and the solution showed that the DSS 11 data were also consistent with data from the other three Deep Space Stations. The data file was updated to include an additional 54 min of DSS 11 two-way doppler for the final premidcourse orbit computation (LAPM YC). When this solution was mapped to the moon, it indicated that the uncorrected unbraked lunar impact would occur at 10.07° S lat and 323.02° E lon, approximately 430 km west and 205 km south of the aiming point.

The numerical results of the premaneuver orbit computations are presented in Tables 7 and 8. Figure 11 is a plot showing the unbraked impact points obtained from the representative premaneuver orbit solutions. Amounts and types of tracking data used in the various orbit computations, together with the associated noise statistics, are given in Table 9. Figure 12 shows representative premidcourse residuals plots for two-way doppler data used in the orbit solutions.

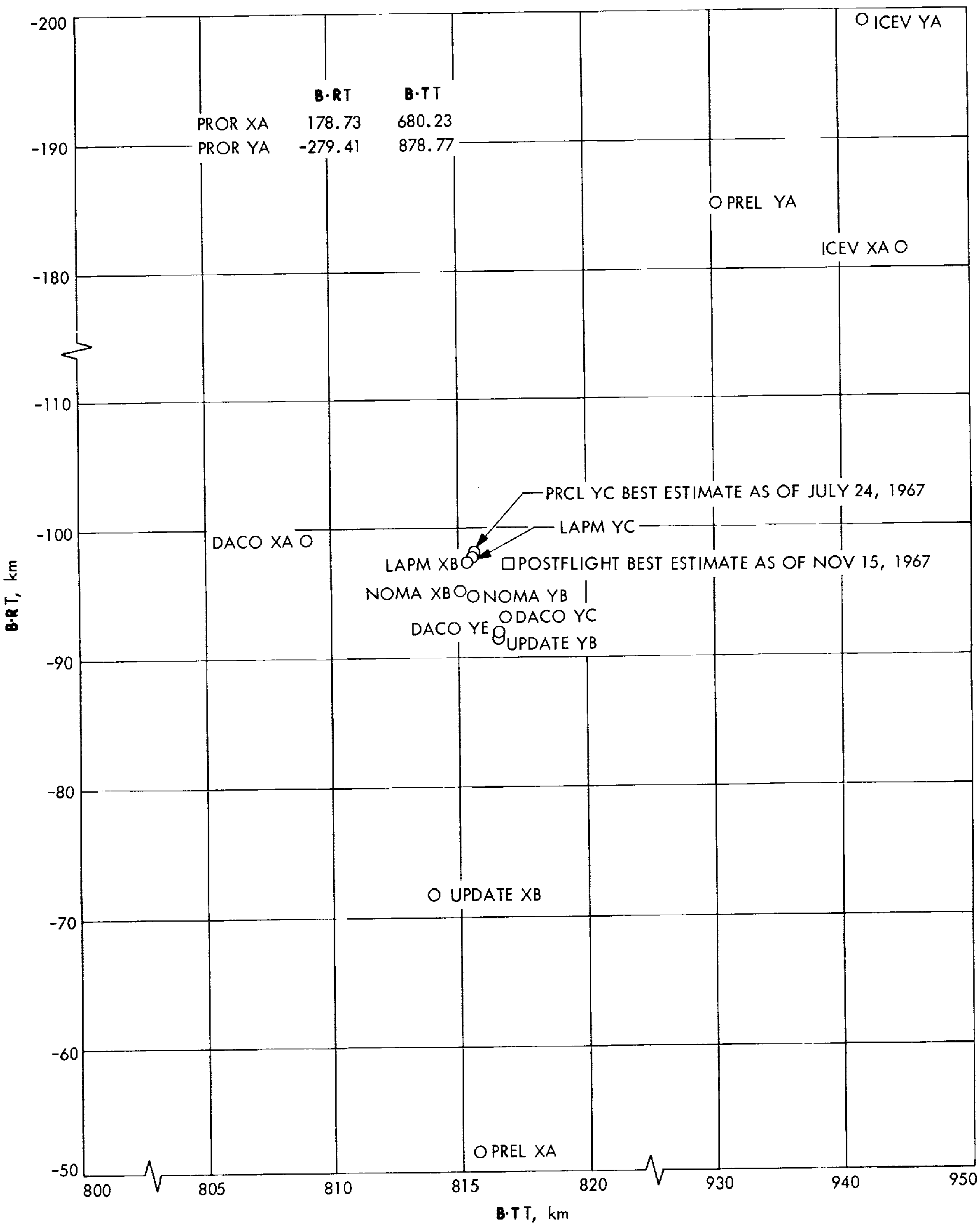

Fig. 11. Estimated premidcourse unbraked impact point for Surveyor III

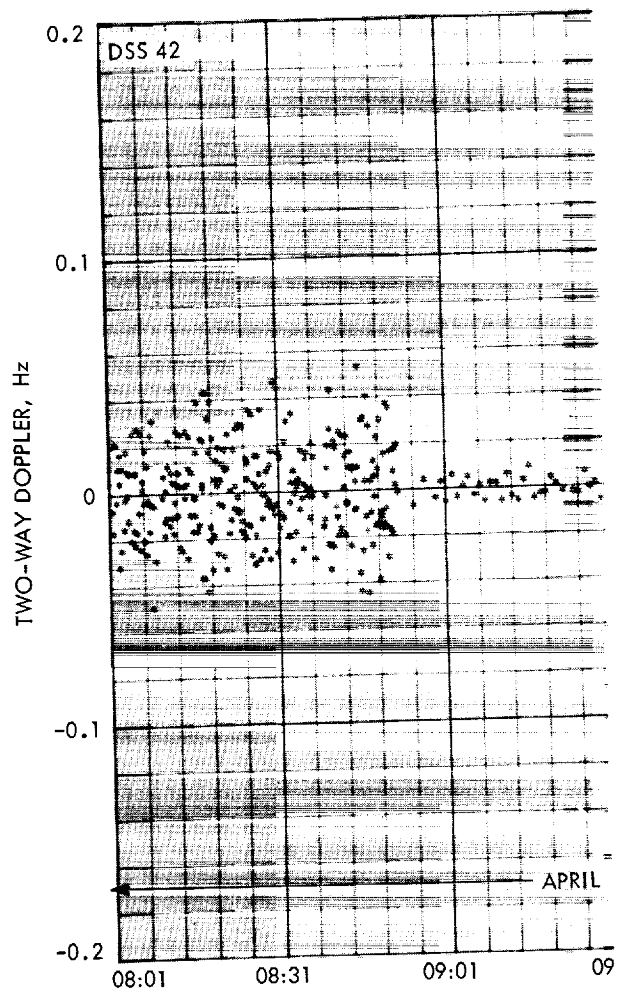

DSS 42
TWO-WAY DOPPLER, Hz
0.2
0.1
0
-0.1
-0.2
APRIL
08:01
08:31
09:01
09

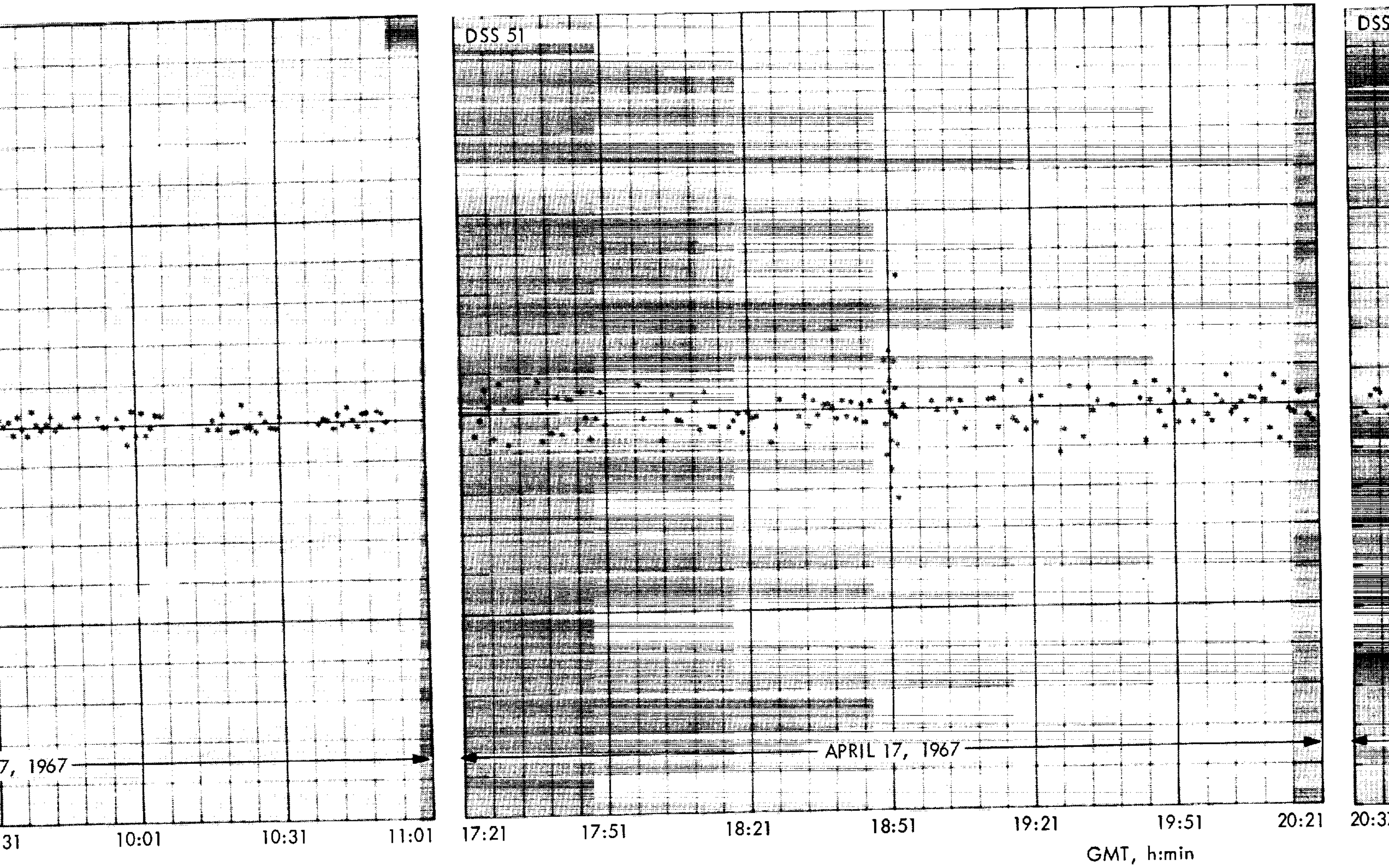
DSS 51
7, 1967
APRIL 17, 1967
31
10:01
10:31
11:01
17:21
17:51
18:21
18:51
19:21
19:51
20:21
GMT, h:min

Type solution	Data used	
	DSS	Data
6×6	42	Angles, CC3
6×6	42	Angles, CC3
6×6	42	Angles, CC3
6×6	42	Angles, CC3
6×6	42	CC3
6×6	42	Angles, CC3
6×6	42, 51	CC3
6×6	42, 51, 61	CC3
6×6	42, 51, 61	CC3
6×6	42, 61	CC3
6×6	51, 61	CC3
6×6	42, 51, 61	Angles, CC3
6×6	42, 51	Angles, CC3
	+61	Angles
6×6	42, 51	CC3
6×6	42, 51	CC3
	+51, 61	Angles
6×6	42, 51, 61	CC3
6×6	42, 51, 61	CC3
6×6	42, 51, 61	CC3
6×6	42, 51, 61	CC3
6×6	42, 51, 61, 11	CC3
6×6	42, 51, 61, 11	CC3
6×6	42, 51, 61, 11	CC3
6×6	42, 51, 61, 11	CC3
6×6	42, 51, 61, 11	CC3
6×6	42, 51, 61, 11	CC3
6×6	42, 51, 61, 11	CC3
×6	42, 51, 11	CC3

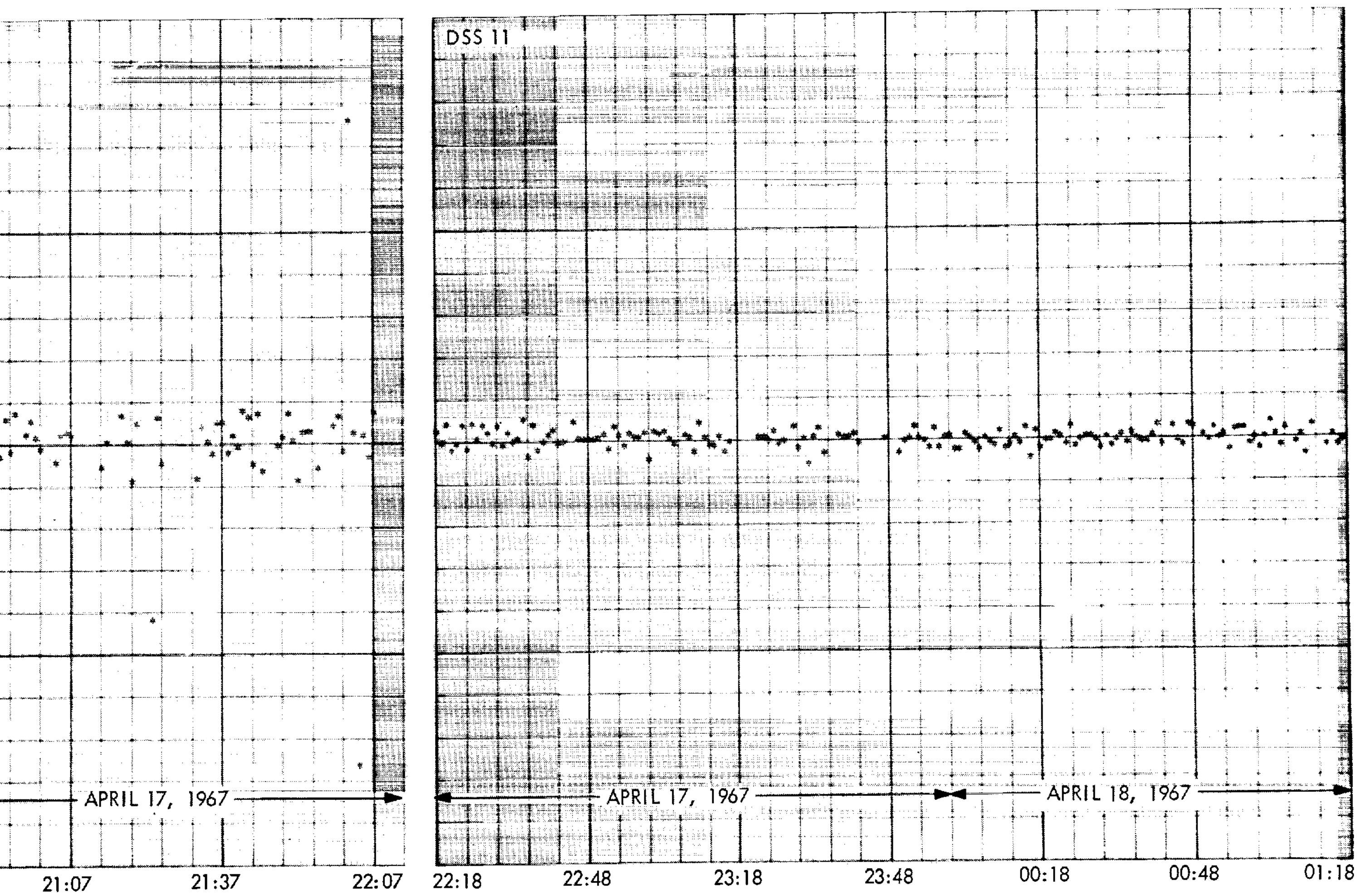

Fig. 12. Premaneuver two-way doppler residuals for *Surveyor III*

Table 7. Premaneuver computations for *Surveyor III*

Orbit identification	Time computed		Target statistics										Selenocentric conditions at unbraked impact		
	Start h:min	Stop h:min	B, km	B • TT, km	B • RT, km	T_L, h	SMAA, km (1σ)	SMIA, km (1σ)	θ_T, deg	$\sigma_{T,\,impact}$, s (1σ)	ϕ_{99}, deg	SVFIXR, km/s (1σ)	Latitude, deg (south)	Longitude, deg (east)	GMT, h:min: Apr 19 1967
PROR YA	08:28	08:59	922.123	878.773	−279.411	64.425	564.03	107.01	60.638	48.0449	7.654	0.000696	−6.277	324.184	23:57:35.
PROR XA	08:30	09:03	703.318	680.229	178.733	64.434	524.99	105.02	61.501	39.8485	7.6136	0.000656	−15.911	320.487	23:57:44.
ICEV YA	09:32	09:55	962.949	942.159	−199.016	64.424	82.216	54.19	78.017	10.2877	1.3636	0.000608	−7.832	325.613	23:57:36.
ICEV XA	09:56	10:30	962.221	944.958	−181.453	64.424	78.680	46.39	91.096	10.8191	1.2589	0.000608	−8.187	325.692	23:57:38.
PREL XA	10:33	10:53	817.395	815.762	−51.641	64.442	1668.94	98.850	90.346	252.453	24.702	0.0008834	−11.0217	323.072	23:58:23.
PREL YA	10:46	11:12	948.797	930.556	−185.153	64.425	65.835	31.176	102.07	8.23346	0.99335	0.000608	−8.1333	325.379	23:57:39.
UPDATE XB	13:56	14:18	817.107	813.935	−71.931	64.441	51.43	4.983	82.47	91.00	7.944	0.000642	−10.609	323.008	23:58:21.
UPDATE YA	15:01	15:20	821.457	816.481	−90.28	64.440	35.19	3.999	85.12	5.851	0.5387	0.000608	−10.231	323.041	23:58:17.
UPDATE YB	16:04	16:06	821.694	816.596	−91.405	64.440	24.068	3.659	87.924	3.742	0.3630	0.000608	−10.208	323.0428	23:58:17.
DACO YA	18:03	18:24	826.531	816.582	−90.046	64.44	186.6	3.752	88.73	27.68	2.790	0.0006116	−10.236	323.04	23:58:17.
DACO YB	18:31	18:49	831.165	824.561	−104.572	64.438	312.31	77.51	73.33	120.55	5.968	0.0006678	−9.928	323.199	23:58:11.
DACO XA	18:13	18:51	815.144	809.081	−99.241	64.440	14.937	3.839	86.547	2.709	0.2299	0.0006080	−10.059	322.873	23:58:17.
DACO XB	18:56	19:26	830.443	817.541	−145.818	64.437	20.794	4.604	79.271	4.367	0.3399	0.0006080	−9.095	323.003	23:58:08.
DACO YC	18:59	19:15	822.120	816.842	−93.010	64.440	23.72	4.270	81.81	4.894	0.3765	0.0006080	−10.175	323.046	23:58:17.
DACO XC	19:33	20:05	814.703	812.895	−54.260	64.442	20.88	4.571	82.32	4.554	0.3291	0.0006080	−10.972	323.007	23:58:25.
DACO XD	20:15	20:49	821.650	816.499	−91.864	64.440	14.926	3.715	89.65	2.732	0.2269	0.0006080	−10.199	323.040	23:58:17.
DACO YE	20:04	20:23	821.740	816.490	−91.863	64.440	15.696	3.335	88.959	2.865	0.2390	0.0006080	−10.199	323.042	23:58:17.
NOMA XA	22:17	22:43	820.708	815.806	−89.554	64.441	14.804	3.087	89.412	2.755	0.2250	0.0006080	−10.247	323.028	23:58:18.
NOMA YA	22:21	23:00	820.824	815.876	−89.990	64.441	15.147	2.810	89.673	2.750	0.2295	0.0006080	−10.238	323.029	23:58:18.
NOMA YB	23:19	23:24	820.976	815.527	−94.429	64.440	10.319	2.573	84.534	2.193	0.1623	0.0006079	−10.148	323.016	23:58:17.
NOMA XB	23:46	00:13	820.659	815.142	−95.003	64.440	9.080	2.598	79.792	2.161	0.1483	0.0006079	−10.137	323.008	23:58:17.5
LAPM YA	00:44	01:02	821.231	815.461	−97.171	64.440	6.763	1.779	71.860	1.8025	0.1162	0.0006079	−10.092	323.012	23:58:17.0
LAPM XA	00:35	00:42	820.711	815.050	−96.225	64.440	7.300	1.950	71.204	1.9764	0.1263	0.0006079	−10.112	323.004	23:58:17.
LAPM YB	01:10	01:26	821.351	815.527	−97.644	64.440	6.644	1.774	71.579	1.776	0.1143	0.0006079	−10.082	323.013	23:58:16.8
LAPM XB	00:48	01:25	821.097	815.303	−97.373	64.440	6.948	1.886	70.049	1.900	0.1210	0.0006079	−10.088	323.008	23:58:17.0
LAPM YC[a]	01:33	01:54	821.443	815.595	−97.845	64.440	6.633	1.771	71.395	1.767	0.1142	0.0006079	−10.078	323.014	23:58:16.8
PRCL YL[b]	08:00	08:53	821.533	815.644	−98.192	64.440	10.18	1.779	70.77	2.74	0.176	0.000607	−10.071	323.015	23:58:16.5

[a]Orbit used for midcourse computations.

[b]Current best estimate, premaneuver as of July 24, 1967.

NOTE

SMAA = Semimajor axis of dispersion ellipse.

SMIA = Semiminor axis of dispersion ellipse.

θ_T = Orientation angle of dispersion ellipse measured counterclockwise from B • TT axis.

$\sigma_{T,\,impact}$ = Uncertainty in predicted unbraked impact time.

ϕ_{99} = 99% velocity vector pointing error.

SVFIXR = Uncertainty in magnitude of velocity vector at unbraked impact.

Table 8. Premaneuver position and velocity at injection epoch for *Surveyor III*

Orbit identification	Geocentric space-fixed position, km			Geocentric space-fixed velocity, km/s			Uncertainties (1σ)					
							Position, km			Velocity, m/s		
	X	Y	Z	DX	DY	DZ	σ_X	σ_Y	σ_Z	σ_{DX}	σ_{DY}	σ_{DZ}
PROR YA	5841.6414	−1727.0861	−2420.0416	1.8261961	10.099453	−3.842853	1.6754	2.2304	9.5415	7.5074	1.6742	3.4360
PROR XA	5840.2444	−1728.6297	−2410.6895	1.8340982	10.100999	−3.8456459	1.7286	2.2802	9.6332	7.9193	1.8916	2.9030
ICEV YA	5840.5008	−1728.4595	−2419.0524	1.8285653	10.098959	−3.8453789	0.8908	1.2694	2.0897	2.9159	0.6433	1.1558
ICEV XA	5840.4074	−1728.5290	−2418.8681	1.8286530	10.098813	−3.8460368	0.9108	1.3050	2.0598	3.0468	0.6369	1.1996
PREL XA	5839.3624	−1730.8779	−2412.1385	1.8372045	10.102435	−3.8392922	19.92	30.88	50.01	78.91	15.41	11.40
PREL XA	5840.5200	−1728.4157	−2418.7000	1.8287019	10.099046	−3.8453984	0.8098	1.161	1.681	2.696	0.5278	1.060
UPDATE XB	5839.6214	−1730.4804	−2412.7323	1.8362213	10.102260	−3.8393942	5.798	9.373	16.771	25.313	5.959	6.339
UPDATE YA	5839.8268	−1730.1482	−2413.3323	1.8353244	10.102049	−3.8396109	0.4195	0.6775	1.130	1.774	0.4015	0.4744
UPDATE YB	5839.8395	−1730.1277	−2413.3690	1.8352694	10.102037	−3.8396234	0.3043	0.4920	0.7646	1.254	0.2743	0.3598
DACO YA	5839.8226	−1730.1546	−2413.3258	1.8353389	10.102051	−3.8396090	2.121	3.271	5.508	8.466	1.653	1.055
DACO YB	5839.0758	−1729.9783	−2413.4444	1.8352032	10.102526	−3.8400436	11.84	10.50	8.334	15.902	7.243	9.211
DACO XA	5840.1876	−1729.5077	−2413.9399	1.8338174	10.101666	−3.8404395	0.2019	0.3338	0.4881	0.8323	0.1897	0.3086
DACO XB	5840.7132	−1728.6373	−2415.5449	1.8314503	10.101078	−3.8411077	0.2504	0.4202	0.7125	1.102	0.2747	0.3900
DACO YC	5839.8568	−1730.1002	−2413.4197	1.8351946	10.102020	−3.8396398	0.3023	0.5075	0.8375	1.327	0.3294	0.4608
DACO XC	5839.3517	−1730.9422	−2412.0304	1.8374025	10.102555	−3.8389599	0.2832	0.4783	0.7603	1.238	0.3098	0.4602
DACO XD	5839.8461	−1730.1183	−2413.3816	1.8352447	10.102032	−3.8396284	0.2233	0.3712	0.5241	0.9227	0.2117	0.3278
DACO YE	5839.8441	−1730.1211	−2413.3797	1.8352527	10.102035	−3.8396220	0.2276	0.3790	0.5503	0.9466	0.2173	0.3197
NOMA XA	5839.8287	−1730.1451	−2413.3135	1.8353257	10.102051	−3.8396200	0.2163	0.3588	0.5238	0.9011	0.2085	0.3050
NOMA YA	5839.8346	−1730.1342	−2413.3302	1.8352996	10.102046	−3.8396274	0.2187	0.3626	0.5315	0.9089	0.2079	0.2956
NOMA YB	5839.9020	−1730.0234	−2413.4860	1.8350247	10.101986	−3.8397032	0.1393	0.2338	0.3581	0.5915	0.1428	0.2238
NOMA XB	5839.9173	−1729.9993	−2413.5088	1.8349660	10.101973	−3.8397281	0.1155	0.1961	0.3113	0.5000	0.1263	0.2140
LAPM YA	5839.9416	−1729.9584	−2413.5816	1.8348623	10.101950	−3.8397466	0.07225	0.1276	0.2206	0.3320	0.0936	0.1786
LAPM XA	5839.9354	−1729.9697	−2413.5520	1.8348917	10.101957	−3.8397498	0.0770	0.1356	0.2370	0.3527	0.0987	0.1882
LAPM YB	5839.9470	−1729.9497	−2413.5977	1.8348388	10.101945	−3.8397519	0.0708	0.1252	0.2161	0.3256	0.0921	0.1772
LAPM XB	5839.9479	−1729.9490	−2413.5916	1.8348365	10.101943	−3.8397610	0.0716	0.1269	0.2226	0.3304	0.0941	0.1847
LAPM YC[a]	5839.9485	−1729.9473	−2413.6036	1.8348321	10.101943	−3.8397522	0.0701	0.1242	0.2141	0.3229	0.0917	0.1789
PRCL YC[b]	5839.9676	−1729.9084	−2413.6501	1.8347366	10.10912	−3.8398219	0.1161	0.2079	0.3829	0.5715	0.1697	0.2839

[a]Orbit used for midcourse maneuver computations.

[b]Current best estimate, premaneuver as of May 1, 1967.

Table 9. Summary of premaneuver DSS tracking data used in orbit computations for Surveyor *III*

Orbit identification	DSS	Data type[a]	Data span, GMT h:min:s Beginning (Apr. 17, 1967)	Ending	Number of points	Standard deviation[a]	Root mean square[a]	Mean residual,[a] (O − C)	Sample rate, s
PROR YA	42	CC3	08:01:57	08:17:49	93	0.0189	0.0189	0.000478	10
		HA	07:57:42	08:17:52	104	0.0210	0.0210	−0.000318	10
		Dec	07:57:42	08:17:52	104	0.0438	0.0438	−0.00103	10
PROR XA	42	CC3	08:04:37	08:22:07	99	0.0271	0.0902	−0.0861	10
		HA	07:57:42	08:22:12	107	0.0106	0.0106	−0.000196	10
		Dec	07:57:42	08:22:12	106	0.00500	0.00501	−0.000335	10
ICEV YA	42	CC3	08:01:57	09:20:32	319	0.0382	0.0389	0.00735	10 and 60
		HA	07:58:02	09:21:02	331	0.00672	0.00825	−0.00479	10 and 60
		Dec	07:58:02	09:21:02	331	0.0200	0.0216	−0.00818	10 and 60
ICEV XA	42	CC3	08:04:37	09:55:32	318	0.0375	0.0382	0.00720	10 and 60
		HA	07:58:02	09:56:02	329	0.00791	0.00969	−0.00558	10 and 60
		Dec	07:58:02	09:56:02	329	0.0187	0.0203	−0.00787	10 and 60
PREL XA	42	CC3	08:04:37	10:24:32	342	0.0190	0.0190	0.000420	10 and 60
PREL YA	42	CC3	08:01:57	10:24:32	364	0.0453	0.0462	0.00869	10 and 60
		HA	07:58:02	10:25:02	383	0.0087	0.0107	−0.00629	10 and 60
		Dec	07:58:02	10:25:02	383	0.0211	0.0243	−0.0121	10 and 60
UPDATE XB	42	CC3	08:04:37	11:45:32	401	0.0176	0.0176	0.00018	10 and 60
	51	CC3	12:23:32	13:41:32	67	0.00907	0.00907	−0.000364	60
UPDATE YA	42	CC3	08:01:57	11:45:32	427	0.0169	0.0169	−0.000056	10 and 60
	51	CC3	12:23:32	13:47:32	63	0.00809	0.00810	−0.000349	60
	61	CC3	14:32:32	14:41:32	10	0.0456	0.0456	−0.00132	10
UPDATE YB	42	CC3	08:01:57	08:56:32	287	0.0201	0.0201	0.0000817	10
		CC3	08:57:32	11:45:32	139	0.00429	0.00429	−0.000302	60
	51	CC3	12:23:32	14:27:32	94	0.00879	0.00881	−0.000473	60
	61	CC3	14:32:32	15:44:32	39	0.0151	0.0151	−0.000313	60
DACO YA	42	CC3	08:01:57	08:56:32	287	0.0201	0.0201	0.000116	10
	42	CC3	11:45:32	11:45:32	139	0.00422	0.00423	−0.00033	60
	61	CC3	12:23:32	14:32:32	1	0.0000	0.000977	−0.000977	60
	61	CC3	14:33:32	16:49:32	55	0.0154	0.0154	0.0000888	60
DACO YB	51	CC3	08:01:57	14:27:32	93	0.00844	0.00847	−0.00080	60
		CC3	17:04:32	18:16:32	45	0.00984	0.00989	−0.00106	60
	61	CC3	14:32:32	14:32:32	1	0.0000	0.000977	−0.000977	60
		CC3	14:33:32	16:49:32	55	0.0153	0.0154	−0.00103	60
DACO XA	61	CC3	14:32:32	14:32:32	1	0.0000	0.000488	0.000488	60
		HA	14:22:02	14:32:02	5	0.00402	0.0076	0.0064	60
		Dec	14:22:02	14:32:02	5	0.00402	0.0120	−0.011	60
		CC3	14:33:32	16:52:32	83	0.0470	0.0478	0.00923	60
		HA	14:33:02	16:53:02	112	0.0122	0.0123	0.00121	60
		Dec	14:33:02	16:53:02	112	0.0160	0.0276	0.0225	60
		HA	17:07:02	17:33:02	13	0.00577	0.0065	−0.00299	60
		Dec	17:07:02	17:33:02	13	0.00773	0.011	0.00781	60
DACO XA	51	CC3	12:23:32	14:27:32	49	0.0121	0.0131	0.00504	60
		HA	12:16:02	14:28:02	115	0.00533	0.0572	0.0570	60
		Dec	12:16:02	14:28:02	115	0.00505	0.0353	−0.0349	60
		CC3	17:04:32	17:58:32	36	0.0101	0.0118	−0.00613	60
		HA	14:34:32	18:02:02	166	0.0071	0.055	0.0545	60
		Dec	14:34:32	18:02:02	166	0.0102	0.0299	−0.0281	60
	42	CC3	08:04:37	08:52:47	276	0.038	0.038	0.00198	10
		HA	07:58:02	08:55:02	283	0.00586	0.00722	−0.00422	10
		Dec	07:58:02	08:55:02	283	0.00666	0.0472	−0.0467	10
		HA	08:57:02	08:57:02	1	0.000	0.00219	0.00219	60
		Dec	08:57:02	08:57:02	1	0.000	0.0516	−0.0516	60
		CC3	08:57:32	08:57:32	1	0.000	0.040	0.04	60
		CC3	08:58:32	11:45:32	124	0.0367	0.0385	−0.0117	60

[a]Hour angle (HA) and declination (dec) are expressed in degrees; and two-way doppler (CC3), in Hz.

Table 9 (contd)

Orbit identification	DSS	Data type[a]	Data span, GMT h:min:s Beginning (Apr. 17, 1967)	Ending	Number of points	Standard deviation[a]	Root mean square[a]	Mean residual,[a] (O − C)	Sample rate, s
DACO XA (contd)	42 (contd)	HA	08:58:02	11:51:02	137	0.00669	0.0158	−0.0143	60
		Dec	08:58:02	11:51:02	137	0.00445	0.0478	−0.0476	60
		HA	12:28:02	14:19:02	98	0.0102	0.0353	−0.0338	60
		Dec	12:28:02	14:19:02	97	0.0103	0.0373	−0.0359	60
DACO XB	61	HA	12:16:02	14:32:02	5	0.00403	0.00907	0.00812	60
		Dec	12:16:02	14:32:02	5	0.00404	0.0154	−0.0149	60
		HA	14:33:02	16:53:02	112	0.0122	0.0125	0.00284	60
		Dec	14:33:02	16:53:02	112	0.0159	0.0244	0.0185	60
		HA	17:07:02	18:44:02	16	0.00653	0.00720	−0.00304	60
		Dec	17:07:02	18:44:02	16	0.0165	0.0169	−0.00388	60
	51	CC3	12:23:32	14:27:32	99	0.00986	0.0109	0.00454	60
		CC3	17:21:32	17:21:32	1	0.000	0.0337	0.0337	60
		CC3	17:22:32	18:42:32	62	0.0118	0.0306	0.282	60
	42	CC3	08:04:37	08:52:47	276	0.0334	0.0346	0.00903	10
		HA	07:58:02	08:55:02	283	0.00594	0.00595	−0.00023	10
		Dec	07:58:02	08:55:02	283	0.00953	0.0406	−0.395	10
		HA	08:57:02	08:57:02	1	0.000	0.00548	0.00548	60
		Dec	08:57:02	08:57:02	1	0.000	0.0487	−0.0487	60
		CC3	08:57:32	08:57:32	1	0.000	0.0352	0.0352	60
		CC3	08:58:32	11:45:32	124	0.0401	0.0495	−0.0289	60
		HA	08:58:02	15:51:02	137	0.0069	0.0137	−0.0119	60
		Dec	08:58:02	11:51:02	137	0.00503	0.0484	−0.0481	60
		HA	12:28:02	14:19:02	98	0.0102	0.0337	−0.0321	60
		Dec	12:28:02	14:19:02	97	0.0101	0.0403	−0.039	60
DACO YC	42	CC3	08:01:57	08:56:32	288	0.0204	0.0204	0.000268	10
		CC3	08:57:32	11:45:32	139	0.00432	0.00432	0.000102	60
	51	CC3	12:23:32	17:21:32	94	0.00836	0.00836	0.0000779	60
		CC3	17:22:32	18:41:32	61	0.00923	0.00923	0.00064	60
DACO XC	61	HA	14:22:02	14:32:02	5	0.00403	0.00465	0.00233	60
		Dec	14:22:02	14:32:02	5	0.00400	0.0114	−0.0107	60
		HA	14:33:02	16:53:02	112	0.0122	0.0125	−0.00283	60
		Dec	14:33:02	16:53:02	112	0.0162	0.0287	0.0237	60
		HA	17:07:02	19:21:12	176	0.00547	0.0166	−0.0156	60
		Dec	17:07:02	19:21:12	176	0.0122	0.0323	−0.0299	60
	51	CC3	12:23:32	14:27:32	99	0.00843	0.0137	0.0108	60
		HA	07:58:02	14:28:02	115	0.00532	0.0529	0.0526	60
		Dec	07:58:02	14:28:02	115	0.00493	0.0354	−0.0350	60
		HA	14:34:02	17:21:02	128	0.00678	0.0525	0.0520	60
		Dec	14:34:02	17:21:02	128	0.0102	0.0313	−0.0296	60
		CC3	17:21:32	17:21:32	1	0.000	0.0259	−0.0259	60
		CC3	17:22:32	19:20:32	103	0.0172	0.0306	−0.0254	60
		HA	17:22:02	19:21:02	117	0.00509	0.0447	0.0444	60
		Dec	17:22:02	19:21:02	117	0.00476	0.0135	−0.0126	60
	42	CC3	08:04:37	08:52:47	276	0.0227	0.0238	−0.00689	10
		↓	08:57:32	08:57:32	1	0.0000	0.00195	−0.00195	60
		↓	08:58:32	11:45:32	124	0.0141	0.0220	0.0169	60
DACO XD	61	↓	14:32:32	14:32:32	1	0.000	0.0176	−0.0176	60
		↓	14:33:32	16:52:32	83	0.0464	0.0497	−0.0178	60
	51	↓	12:23:32	14:27:32	99	0.00847	0.0183	−0.0162	60
		↓	17:21:32	17:21:32	1	0.000	0.0244	−0.0244	60
		↓	17:22:32	19:44:32	121	0.0160	0.0273	−0.0221	60
	42	↓	08:04:37	08:52:47	276	0.0211	0.0223	−0.00742	10
		↓	08:57:32	08:57:32	1	0.000	0.00488	−0.00488	60
		CC3	08:58:32	11:45:32	124	0.00460	0.0130	−0.0122	60

Table 9 (contd)

Orbit identification	DSS	Data type[a]	Data span, GMT h:min:s Beginning (Apr. 17, 1967)	Ending	Number of points	Standard deviation[a]	Root mean square[a]	Mean residual,[a] (O − C)	Sample rate, s
DACO YE	61	CC3	14:32:32	14:32:32	1	0.000	0.00146	−0.00146	60
			14:33:32	16:49:32	55	0.0153	0.0153	−0.0000089	60
	51		12:23:32	17:21:32	94	0.00840	0.00846	−0.00103	60
			17:22:32	19:44:32	122	0.0161	0.0162	−0.00164	60
	42		08:01:57	08:56:32	287	0.0201	0.0201	−0.000362	10
			08:57:32	11:45:32	139	0.00423	0.00423	−0.0000703	60
NOMA XA	61		14:32:32	14:32:32	1	0.000	0.00684	−0.00684	60
			14:33:32	20:31:27	54	0.0155	0.0160	−0.00380	60
			20:31:37	22:02:32	84	0.0137	0.0160	0.00824	60
	51		12:23:32	17:21:32	100	0.00841	0.00841	0.0000293	60
			17:22:32	20:29:32	145	0:0106	0.0115	−0.00435	60
	42		08:04:37	08:57:32	274	0.0205	0.0205	0.000127	10
			08:58:32	11:45:32	124	0.00440	0.00445	0.000665	60
NOMA YA	61		14:32:32	14:32:32	1	0.000	0.00684	−0.00684	60
			14:33:23	20:31:27	55	0.0155	0.0161	−0.00435	60
			20:31:37	22:07:32	86	0.0146	0.0162	0.00696	60
	51		12:23:32	17:21:32	92	0.00772	0.00772	−0.000138	60
			17:22:32	20:29:32	133	0.00793	0.00903	−0.00431	60
	42		08:01:57	08:56:32	275	0.0186	0.0186	0.000087	10
			08:57:32	11:45:32	139	0.00439	0.00439	0.000239	60
NOMA YB	61		14:32:32	14:32:32	1	0.000	0.00586	−0.00586	60
			14:33:32	20:31:32	55	0.0155	0.0156	−0.00171	60
			20:31:57	22:07:32	84	0.0161	0.0185	0.00917	60
	51		12:23:32	17:21:32	90	0.00777	0.00851	−0.00347	60
			17:22:32	20:28:32	134	0.00807	0.00845	−0.00249	60
	42		08:01:57	08:56:32	272	0.0187	0.0187	0.000582	10
			08:57:32	11:45:32	139	0.00564	0.00565	0.000341	60
	11		22:18:32	23:00:32	10	0.00426	0.0170	0.0165	60
NOMA XB	61		14:32:32	20:31:32	52	0.0121	0.0122	−0.00199	60
			20:31:57	22:07:32	82	0.0119	0.0151	0.00923	60
	51		12:23:32	17:21:32	93	0.00756	0.00888	−0.00466	60
			17:22:32	20:28:32	132	0.00846	0.00888	−0.00270	60
	42		08:04:37	08:57:32	260	0.0189	0.0189	0.000193	10
			08:58:32	11:45:32	124	0.00636	0.00638	−0.000441	60
	11		22:18:32	23:16:32	21	0.00426	0.0101	0.00918	60
LAPM YA	61		14:32:32	20:31:32	56	0.0154	0.0156	−0.00245	60
			20:31:57	22:07:32	84	0.0160	0.0176	0.00733	60
	51		12:23:32	17:21:32	84	0.00718	0.0100	−0.00699	60
			17:22:32	20:28:32	132	0.00841	0.00911	−0.00350	60
	42		08:01:57	08:56:32	275	0.0193	0.0193	0.000151	10
			08:57:32	11:45:32	139	0.00697	0.00719	−0.00175	60
	11		22:18:32	00:28:32	119	0.00562	0.00594	0.00193	60
LAPM XA	61		14:32:32	20:31:32	52	0.0120	0.0122	−0.00221	60
			20:31:57	22:07:32	82	0.0120	0.0146	0.00841	60
	51		12:23:32	17:21:32	89	0.00733	0.00935	−0.00581	60
			17:22:32	20:28:32	130	0.00847	0.00911	−0.00336	60
	42		08:04:37	08:57:32	258	0.0188	0.0188	−0.0000927	10
			08:58:32	11:45:32	124	0.00697	0.00710	−0.00131	60
	11	CC3	22:18:32	00:20:32	92	0.00461	0.00522	0.00245	60

Table 9 (contd)

Orbit identification	DSS	Data type[a]	Data span, GMT h:min:s — Beginning (Apr. 17, 1967)	Ending	Number of points	Standard deviation[a]	Root mean square[a]	Mean residual,[a] (O − C)	Sample rate, s
LAPM YB	61	CC3	14:32:32	20:31:32	56	0.0154	0.0154	−0.000872	60
			20:31:57	22:07:32	84	0.0160	0.0182	0.00862	60
	51		12:23:32	17:21:32	84	0.00724	0.00971	−0.00648	60
			17:22:32	20:28:32	134	0.00846	0.00896	−0.00296	60
	42		08:01:57	08:56:32	275	0.0193	0.0193	0.000914	10
			08:57:32	11:45:32	139	0.00706	0.00719	−0.00138	60
	11		22:18:32	00:57:32	145	0.00666	0.00767	0.00380	60
LAPM XB	61		14:32:32	20:31:32	52	0.0120	0.0210	−0.0000563	60
			20:31:57	22:07:32	82	0.0120	0.0156	0.0101	60
	51		12:23:32	17:21:32	89	0.00723	0.00952	−0.00619	60
			17:22:32	20:28:32	131	0.00841	0.00886	−0.00278	60
	42		08:04:37	08:57:32	277	0.0216	0.0216	0.00162	10
			08:58:32	11:45:32	124	0.00716	0.00730	−0.00144	60
	11		22:18:32	01:19:32	156	0.00731	0.00877	0.00484	60
LAPM YC	61		14:32:32	20:31:32	56	0.0154	0.0157	−0.00308	60
			20:31:57	22:07:32	83	0.0149	0.0162	0.00635	60
	51		12:23:32	17:21:32	77	0.00641	0.0102	−0.00796	60
			17:22:32	20:28:32	131	0.00830	0.00983	−0.00526	60
	42		08:01:57	08:56:32	274	0.0190	0.0190	0.000672	10
			08:57:32	11:45:32	139	0.00735	0.00801	−0.00318	60
	11		22:18:32	01:22:32	165	0.00719	0.00728	0.00117	60
PRCL YC	11		22:18:32	04:37:32	344	0.00969	0.0109	0.00490	60
			04:39:32	04:46:32	43	0.0214	0.0245	0.0119	60
	42		08:01:57	08:52:47	288	0.0221	0.0222	0.00254	10
			08:55:32	11:45:32	141	0.00950	0.0110	−0.00549	60
	51		12:23:32	18:48:32	155	0.00844	0.0115	−0.00779	60
			18:49:37	18:52:37	19	0.0358	0.0385	−0.0141	60
		CC3	18:54:32	20:24:32	68	0.00825	0.0179	−0.0159	60

C. Postmaneuver Orbit Estimates

The first postmidcourse orbit computation was completed approximately 9 h 7 min after the midcourse maneuver. For this computation, approximately 3 h 24 min of DSS 11 and 5 h of DSS 42 two-way doppler data were available. The starter values for the first postmidcourse orbit were the conditions obtained from mapping the PRCL YC conditions to an epoch at the end of midcourse burn and adding the midcourse velocity increment. *A priori* information from the premaneuver tracking data was not used. When the first postmidcourse orbit was mapped to the moon, it indicated that unbraked impact point to be approximately 1.5 km north and 8.4 km west of the aiming point. Subsequent inflight postmidcourse orbit computations refined the estimated unbraked impact point to 1.8 km south and 4.2 km west of the aiming point.

During the postmidcourse phase a problem occurred with the DSS 51 data. A pass of DSS 51 two-way doppler data appeared to be biased from the DSS 11 and DSS 61 two-way doppler data and it was therefore ignored in the subsequent orbit computations. The cause of this bias has not been determined. It has been verified that the correct transmitter frequency was used for this pass of DSS 51 data.

A decision must be made by 6 h before the retrofiring whether to track the spacecraft with DSS 51 or DSS 61, along with DSS 11, during the terminal phase. DSS 51 had the two-way doppler bias problem and DSS 61 had the counter problem during the premidcourse phase. It was decided to track with DSS 61 because the counter problem appeared to have been solved. The final spacecraft terminal attitude maneuver computations were based on the fifth postmidcourse orbit solution (5 POM YD) completed approximately 4½ h before nominal retro-ignition.

Numerical results of the inflight postmidcourse orbit computations are presented in Tables 10 and 11. Figure 13 is a plot showing the postmidcourse unbraked impact points obtained from these solutions. The current best

Table 10. Postmaneuver computations for *Surveyor III*

Orbit identification	Time computed		Target statistics										Selenocentric conditions at unbraked impact			Type solution	Data used	
	Start h:min	Stop h:min	B, km	B · TT, km	B · RT, km	T_L, h	SMAA, km (1σ)	SMIA, km (1σ)	θ_T, deg	$\sigma_{T, impact}$, s (1σ)	ϕ_{90}, deg	SVFIXR, m/s (1σ)	Latitude, deg (south)	Longitude, deg	GMT h:min:s Apr. 20, 1967		DSS	Data
1 POM YA	12:03	12:16	1529.0	1460.23	−453.47	43.133	1357.3	130.9	99.1	1847.2	66.96	1.389	−1.724	336.50	00:03:14.342	6×6	11, 42	CC3
1 POM YD	13:54	14:07	1517.58	1464.665	−397.23	43.11	205.1	24.86	63.07	105.1	2.786	0.6372	−2.826	336.65	00:01:59.756	6×6	11, 42	
2 POM YA	17:23	17:43	1513.25	1462.96	−386.90	43.11	23.19	6.5	55.15	7.99	0.5792	0.6095	−3.036	336.62	00:01:51.561	6×6	11, 42, 51, 61	
2 POM YD	19:09	20:15	1515.16	1465.13	−386.12	43.11	11.655	3.09	44.92	5.305	0.3554	0.6087	−3.047	336.68	00:01:49.445	6×6	11, 42, 51, 61	
3 POM YA	00:08	00:26	1515.72	1465.55	−386.74	43.110	11.312	3.04	44.25	5.197	0.3471	0.6086	−3.033	336.68	00:01:49.178	6×6	11, 42, 51, 61	
3 POM YE	02:12	02:54	1521.75	1470.72	−390.77	43.109	4.6859	1.899	59.22	1.785	0.1197	0.6082	−2.939	336.800	00:01:45.782	6×6	11, 42, 61	
4 POM XF	11:34	12:13	1521.59	1470.62	−390.53	43.109	2.838	1.432	79.28	0.950	0.055	0.6089	−2.937	336.82	00:01:46.415	6×6	11, 42, 51, 61	
4 POM YF	12:12	12:35	1521.36	1470.48	−390.18	43.109	2.734	1.411	80.78	0.9316	5.25	0.6089	−2.945	336.81	00:01:46.483	6×6	11, 42, 61	
5 POM YA	18:31	18:58	1520.81	1469.97	−389.97	43.109	2.652	0.9324	86.40	0.7071	0.0389	0.6089	−2.951	336.80	00:01:46.779	6×6	11, 42, 61	
5 POM YD[a]	20:42	21:11	1520.35	1469.35	−390.50	43.109	2.601	0.5601	82.90	0.5393	0.0356	0.6089	−2.941	336.79	00:01:47.191	6×6	11, 42, 61	
5 POM XD	20:42	20:52	1520.04	1468.96	−390.70	57.61	2.731	0.7601	82.56	0.5786	0.0374	0.6089	−2.938	336.78	00:01:47.496	6×6	61	
FINAL YA	22:03	22:20	1519.16	1468.34	−389.64	57.61	2.583	0.7492	89.92	0.5684	0.0349	0.6089	−2.961	336.77	00:01:47.418	6×6	61	
FINAL XA	22:05	22:20	1519.63	1468.82	−389.67	57.61	2.625	0.7518	82.93	0.5688	0.0354	0.6089	−2.959	336.78	00:01:47.632	6×6	61	
FINAL YB	22:39	22:51	1519.05	1468.42	−388.91	57.61	2.577	0.7467	83.60	0.5631	0.0347	0.6089	−2.976	336.77	00:01:47.578	6×6	61	
FINAL XB	22:37	22:46	1521.74	1469.36	−395.84	57.61	2.372	0.7461	82.05	0.5551	0.0320	0.6089	−2.835	336.78	00:01:48.427	6×6	11, 61	
FINAL YC	22:55	23:06	1521.39	1469.01	−395.76	57.61	2.338	0.7425	82.05	0.5513	0.0316	0.6089	−2.837	336.78	00:01:48.380	6×6	11, 61	
FINAL XC	22:50	23:10	1522.36	1469.22	−398.72	57.61	2.533	0.5983	86.84	0.5068	0.0354	0.6089	−2.776	336.78	00:01:47.928	6×6	11	
FINAL YD	23:11	23:24	1520.35	1468.33	−394.32	57.61	2.292	0.7307	82.76	0.5299	0.0312	0.6089	−2.868	336.76	00:01:47.971	6×6	11, 61	
FINAL XD	23:13	23:22	1523.51	1469.52	−401.98	57.61	2.161	0.5958	87.58	0.4819	0.0306	0.6089	−2.709	336.78	00:01:48.322	6×6	11	
FINAL YE	23:37	23:55	1520.05	1468.10	−393.96	57.61	2.203	0.7071	84.98	0.5024	0.0303	0.6089	−2.876	336.76	00:01:47.646	6×6	11, 61	
POST 1[b]	NA[c]	NA[c]	1519.63	1468.90	−389.37	43.11	3.343	0.7476	81.76	0.6324	0.0448	0.6089	−2.966	336.78	00:01:47.317	12×12	42, 51, 61, 11	CC3

[a]Orbit used for terminal maneuver computations.
[b]Current best estimate, postmaneuver as of May 1, 1967.
[c]Not applicable.

Table 11. Postmaneuver position and velocity for *Surveyor III* at injection epoch

Orbit identification	Geocentric space-fixed position, km			Geocentric space-fixed velocity, km/s			Uncertainties (1σ)					
							Position, km			Velocity, m/s		
	X	Y	Z	DX	DY	DZ	σ_X	σ_Y	σ_Z	σ_{DX}	σ_{DY}	σ_{DZ}
1 POM YA	−152090.04	111756.66	43614.824	−1.3825557	0.60936115	0.51981518	494.44	412.25	2828.60	8.009	11.372	13.000
1 POM YD	−152110.38	111773.96	43733.391	−1.3822504	0.60980822	0.51924782	38.89	53.79	209.0	0.2042	0.4958	1.813
2 POM YA	−152112.92	111776.95	43746.498	−1.3822246	0.60985777	0.51915663	2.087	4.886	5.684	0.0854	0.0662	0.1449
2 POM YD	−152113.00	111777.16	43749.388	−1.382209	0.60987654	0.51915170	1.779	2.467	3.519	0.556	0.0452	0.0731
3 POM XA	−152113.08	111777.01	43749.589	−1.3822064	0.60987806	0.51915632	1.749	2.396	3.432	0.0545	0.0447	0.0708
3 POM YE	−152114.04	111775.96	43751.033	−1.3821719	0.60990536	0.51919761	1.1368	1.3843	2.163	0.01959	0.01867	0.03246
4 POM XF	−152114.03	111776.04	43750.883	−1.3821726	0.60990521	0.51919647	0.9529	1.041	1.945	0.00977	0.0128	0.0209
4 POM YF	−152114.15	111776.07	43750.370	−1.3821729	0.60990553	0.51919630	0.9627	1.016	2.033	0.0093	0.0126	0.0230
5 POM YA	−152114.10	111776.22	43749.992	−1.3821761	0.60990234	0.51919457	0.9454	0.9705	1.865	0.0067	0.0106	0.0199
5 POM YD	−152113.98	111776.36	43749.554	−1.3821805	0.60989582	0.51919667	0.9367	0.9591	1.797	0.0046	0.0079	0.0197
5 POM XD	−289766.26	163392.01	100073.78	−0.78552219	0.29053491	0.37827816	0.7441	1.240	1.741	0.0121	0.0193	0.0266
FINAL YA	−289766.28	163392.31	100072.90	−0.78552884	0.29052667	0.37826901	0.7366	1.191	1.619	0.0113	0.0186	0.0254
FINAL XA	−289766.20	163392.41	100073.02	−0.78552864	0.29052742	0.37826794	0.7364	1.210	1.643	0.0112	0.0186	0.0256
FINAL YB	−289765.99	163392.66	100072.42	−0.78553638	0.29051731	0.37825889	0.7256	1.187	1.613	0.0109	0.0182	0.0251
FINAL XB	−289765.88	163389.96	100076.71	−0.78555579	0.29047802	0.37829382	0.7061	1.119	1.496	0.0104	0.0170	0.0248
FINAL YC	−289764.64	163389.93	100076.53	−0.78556329	0.29046747	0.37828987	0.6984	1.105	1.477	0.0101	0.0167	0.0245
FINAL XC	−289765.54	163388.23	100079.05	−0.78552301	0.29051344	0.37830580	0.5611	1.246	1.623	0.0074	0.0077	0.0206
FINAL YD	−289765.32	163390.86	100075.47	−0.78556304	0.29046588	0.37829373	0.6446	1.084	1.449	0.0097	0.0161	0.0244
FINAL XD	−289765.15	163386.64	100081.11	−0.78552465	0.29050294	0.37831737	0.5397	1.066	1.393	0.0074	0.0065	0.0200
FINAL YE	−289765.99	163389.75	100075.38	−0.78554669	0.29049334	0.37829746	0.5691	1.047	1.404	0.0095	0.0154	0.0244
POST 1	−152114.15	111776.63	43748.41	−1.3821823	0.60989540	0.51919357	1.2134	1.0707	3.5490	0.0056	0.0154	0.0285

NOTE
1 POM YA through 5 POM YD are at midcourse epoch.
5 POM XD through FINAL YE are at unbraked impact minus 5 h 40 min.

estimate of landed spacecraft location is 2.4 km south and 3.6 km west of the aiming point. The amounts of tracking data used in the various postmidcourse orbit computations, together with the associated noise statistics, are given in Table 12.

D. AMR Backup Computations

After the 5 POM YD computation, primary OD emphasis was placed on obtaining the best estimate of unbraked impact time to be used for sending a ground command to back up the onboard AMR. All subsequent computations used *a priori* information from all postmaneuver tracking data up to the time of the last data point in 5 POM YD. This information was in the form of a covariance matrix mapped to an epoch a few minutes past the time of the last data point in 5 POM YD. The covariance matrix was degraded and expanded as discussed in Section IV. In addition to being able to account for the SPODP model errors by using this method, a considerable saving in program running time is achieved by working from the updated epoch. This is very important since the basic philosophy is that the near-moon data will yield the best estimate of unbraked impact time. This requires that as much near-moon data as possible be included in the orbit solution while still being able to provide the results at retro minus 40 min ($R - 40$ min), the lead time required to implement the backup command.

For the AMR backup computations, a lunar elevation of 1736.1 km at the predicted unbraked impact point was used. This lunar elevation was obtained from NASA Langley Research Center (LRC) and it agreed closely with the elevation obtained from the appropriate ACIC lunar chart less 2.4 km. The 2.4 km is the amount by which the elevation obtained from the appropriate ACIC lunar chart exceeds the elevation obtained from the *Ranger VI, VII* and *VIII* tracking data. An *a priori* 1-σ uncertainty of ± 1 km (roughly equivalent to ± 0.4 s) was assigned to the elevation.

During the AMR backup computations, an inconsistency appeared between the DSS 61 and DSS 11 data. At that time it was believed that the inconsistency was caused by small biases in the DSS 61 data since DSS 61 had a counter problem earlier. (However, it was discovered later, during postflight analysis, that an incorrect frequency input was made for DSS 11). Therefore, the FINAL XC and XD solutions were run with only the DSS 11 data. The FINAL YE orbit solution using DSS 61

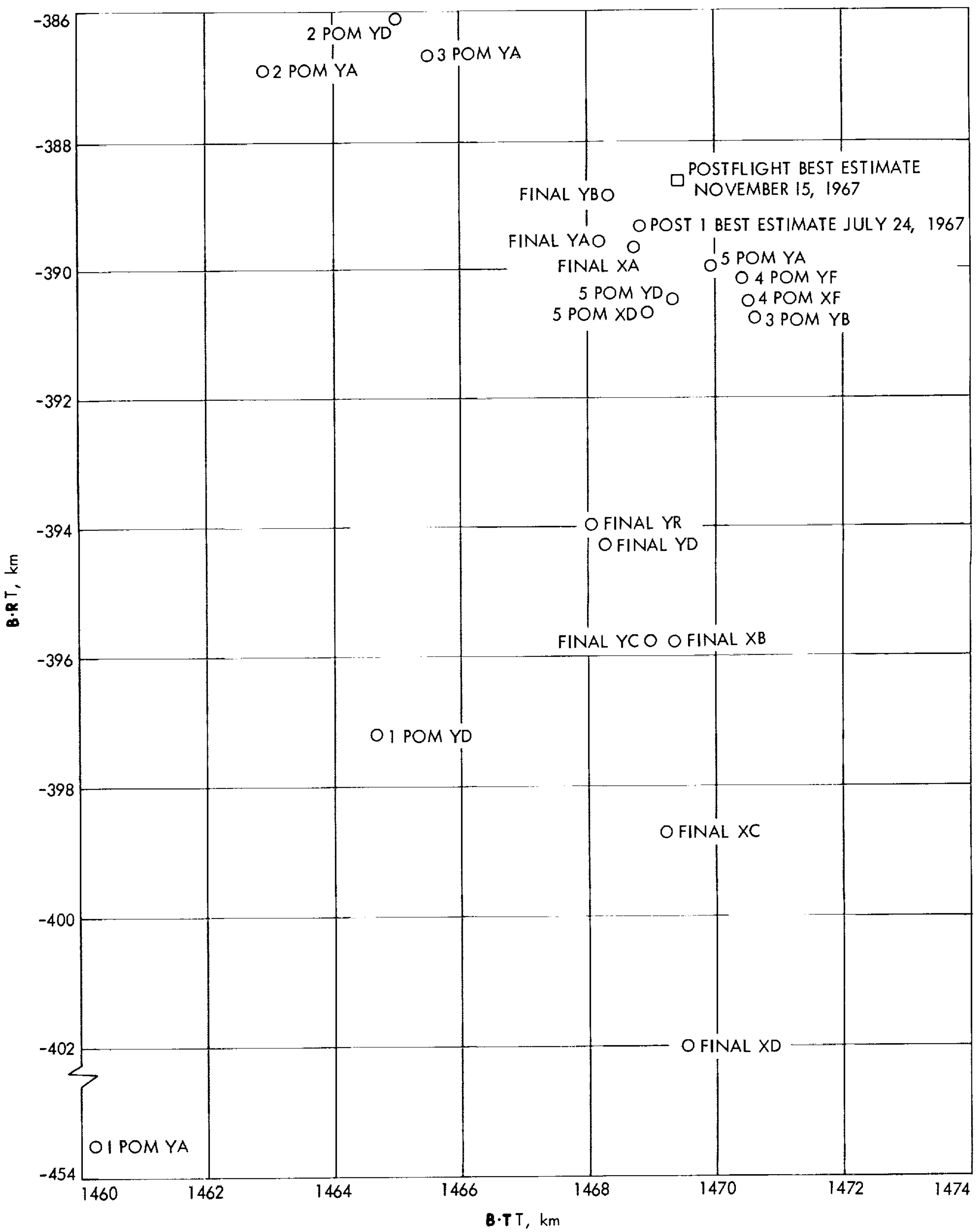

Fig. 13. Estimated postmidcourse unbraked impact point for Surveyor III

Table 12. Summary of postmaneuver DSS tracking data used in orbit computations for *Surveyor III*

Orbit identification	DSS	Data type	Data span, GMT				Number of points	Standard deviation, Hz	Root mean square, Hz	Mean residual (O − C), Hz	Sample rate, s
			Beginning		Ending						
			1967	h:min:s	1967	h:min:s					
1 POM YA	42	CC3	4/18	08:43:32	4/18	09:59:32	76	0.00534	0.00534	0.000077	60
	11			05:09:12		05:12:12	19	0.0346	0.0362	−0.0105	10
				05:14:32		08:33:32	182	0.00428	0.00429	0.000278	60
1 POM YD	11			05:09:12		05:12:12	19	0.0346	0.0372	−0.0137	10
				05:14:32		08:33:32	180	0.0043	0.00431	0.000301	60
	42			08:43:32		13:44:32	288	0.00585	0.00585	0.0000543	60
2 POM YA	11			05 01:92		05:12:12	19	0.0345	0.0371	−0.0138	10
				05:14:32		08:33:32	18	0.00429	0.0043	0.000168	60
	42			08:43:32		14:39:32	338	0.00638	0.0638	−0.0000455	60
	51			16:42:32		17:07:32	26	0.00846	0.00853	−0.00106	60
	61			14:43:32		16:33:32	94	0.00528	0.00529	0.000183	60
2 POM YD	11			05:09:12		05:12:12	10	0.0148	0.0172	−0.00869	10
				05:14:32		08:33:32	180	0.00505	0.00505	−0.0000814	60
				22:23:32		23:21:32	56	0.00422	0.00842	0.00728	60
	42			08:43:32		14:39:32	338	0.00611	0.00627	0.00138	60
	51			16:42:32		21:11:32	75	0.00771	0.0139	−0.0115	60
				21:12:32		22:19:32	62	0.00844	0.00952	−0.00429	60
	61			14:43:32		16:33:32	94	0.00550	0.00735	−0.00488	60
				18:13:32		21:03:32	153	0.00618	0.00760	0.00442	60
3 POM YA	11			05:09:12		05:12:12	10	0.0146	0.0163	−0.00725	10
				05:14:32		08:33:32	180	0.00475	0.00476	0.000281	60
				22:23:32		23:50:32	85	0.00480	0.00817	0.00667	60
	42			08:43:32		14:39:32	338	0.00616	0.00629	0.00125	60
	51			16:42:32		21:11:32	75	0.00781	0.0147	−0.0124	60
	51			21:12:32		22:19:32	62	0.00851	0.00939	−0.00397	60
	61			14:43:32		16:33:32	94	0.00539	0.00824	−0.00623	60
				18:13:32		21:03:32	153	0.00629	0.00749	0.00408	60
3 POM YE	11			05:09:12		05:12:12	11	0.0135	0.0144	−0.00510	10
			4/18	05:14:32	4/18	08:38:32	169	0.00566	0.00600	0.00201	60
			4/18	22:23:32	4/19	00:07:32	102	0.00530	0.00532	0.000511	60
			4/18	02:22:32	4/19	06:34:32	246	0.00522	0.00524	−0.000429	60
	42		4/18	08:43:32	4/18	14:33:32	290	0.00607	0.00625	−0.00149	60
			4/19	06:43:32	4/19	07:33:32	37	0.00593	0.0119	−0.0103	60
	61		4/18	16:42:32	4/18	16:33:32	93	0.00581	0.00637	−0.00260	60
			4/18	18:13:32	4/19	00:28:32	151	0.00629	0.00683	−0.00267	60
			4/19	00:29:32	4/19	02:11:32	94	0.00836	0.00906	0.00349	60
4 POM XF	11		4/18	05:09:12	4/18	05:12:12	12	0.0161	0.0163	−0.00222	10
			4/18	05:14:32	4/18	08:33:32	169	0.00553	0.00596	0.00223	60
			4/18	22:23:32	4/19	00:07:32	86	0.00508	0.00516	0.000887	60
			4/19	02:22:32	4/19	06:34:32	246	0.00512	0.00515	−0.000558	60
	42		4/18	08:43:32	4/18	14:33:32	275	0.00465	0.00471	−0.000785	60
			4/19	06:43:32	4/19	14:19:32	318	0.00586	0.00661	0.00305	60
	51		4/18	21:11:32	4/18	21:11:32	1	0.000	0.00684	−0.00684	60
			4/18	21:12:32	4/18	22:13:32	59	0.00711	0.0106	−0.00788	60
	61		4/18	14:43:32	4/18	16:33:32	71	0.00460	0.00554	−0.00310	60
	61		4/18	18:13:32	4/19	00:28:32	151	0.00624	0.00681	−0.00272	60
			4/19	00:29:32	4/19	02:11:32	71	0.00900	0.00989	0.00410	60
			4/19	14:23:32	4/19	16:18:32	50	0.00903	0.0104	−0.00517	60
4 POM YF	11		4/18	05:01:92	4/18	05:12:12	19	0.0346	0.0348	−0.00320	10
			4/18	05:14:32	4/18	08:33:32	180	0.00623	0.00624	0.000412	60
			4/18	22:23:32	4/19	00:13:32	92	0.00519	0.00528	0.000983	60
			4/19	02:22:32	4/19	06:34:32	242	0.00500	0.00573	−0.00281	60
	42		4/18	08:43:32	4/18	14:33:32	287	0.00442	0.00444	−0.000419	60
		CC3	4/19	06:43:32	4/19	14:19:32	329	0.00512	0.00549	0.00196	60

Table 12 (contd)

Orbit identification	DSS	Data type	Data span, GMT Beginning 1967	Beginning h:min:s	Ending 1967	Ending h:min:s	Number of points	Standard deviation, Hz	Root mean square, Hz	Mean residual (O − C), Hz	Sample rate, s
4 POM YF (contd)	61 (contd)	CC3	4/18	21:11:32	4/18	16:33:32	72	0.00453	0.00488	0.00182	60
			4/18	18:13:32	4/19	00:28:32	155	0.00586	0.00586	0.000197	60
			4/19	00:29:32	4/19	02:13:32	67	0.00829	0.00833	−0.000813	60
			4/19	14:23:32	4/19	16:28:32	61	0.00981	0.00995	−0.00165	60
5 POM YA	11		4/18	05:09:12	4/18	05:12:12	19	0.0346	0.0346	−0.00204	10
			4/18	05:14:32	4/18	08:33:32	180	0.00617	0.00649	0.00200	60
			4/18	22:23:32	4/19	00:13:32	92	0.00508	0.00508	0.00000398	60
			4/19	02:22:32	4/19	09:38:32	272	0.00512	0.00605	−0.00322	60
	42		4/18	08:43:32	4/18	14:33:32	287	0.00438	0.00461	−0.00144	60
			4/19	06:43:32	4/19	14:19:32	329	0.00525	0.00649	0.00381	60
	61		4/18	21:11:32	4/18	16:33:32	72	0.00455	0.00490	0.00181	60
			4/18	18:13:32	4/19	00:28:32	155	0.00582	0.00584	−0.000438	60
			4/19	00:29:32	4/19	02:13:32	67	0.00830	0.00957	−0.00477	60
			4/19	14:23:32	4/19	17:54:32	140	0.00990	0.00993	−0.000746	60
5 POM YD	11		4/18	05:09:12	4/18	05:12:12	19	0.0345	0.0346	0.00227	10
			4/18	05:14:32	4/18	08:33:32	180	0.00618	0.00882	0.00629	60
	11		4/18	22:23:32	4/19	00:13:32	92	0.00468	0.00729	−0.00559	60
			4/19	02:22:32	4/19	09:38:32	272	0.00565	0.00700	−0.00412	60
	42		4/18	08:43:32	4/18	14:33:32	287	0.00442	0.00544	−0.00317	60
			4/19	06:43:32	4/19	14:19:32	329	0.00647	0.00791	0.00454	60
	61		4/18	21:11:32	4/18	16:33:32	72	0.00456	0.00462	−0.000744	60
			4/18	18:13:32	4/19	00:28:32	155	0.00583	0.00604	−0.00156	60
			4/19	00:29:32	4/19	02:13:32	67	0.00838	0.0131	−0.0101	60
			4/19	14:23:32	4/19	20:34:32	236	0.0104	0.0109	0.00308	60
5 POM XD	61		4/19	18:49:32	4/19	20:32:32	87	0.00625	0.00625	0.0000884	60
FINAL YA	61		4/19	18:21:32	4/19	21:52:32	162	0.00766	0.00766	0.000190	60
FINAL XA	61			18:21:32		21:57:32	151	0.00779	0.00779	0.000125	60
FINAL YB	61			18:21:32		22:09:32	173	0.00779	0.00779	0.0000734	60
FINAL XB	11			22:18:32		22:25:32	8	0.00312	0.00990	0.00940	60
	61			18:49:32		22:11:32	157	0.00949	0.00949	−0.000304	60
FINAL YC	11			22:18:32		22:26:32	9	0.00384	0.00952	0.00871	60
	61			18:21:32		22:12:32	176	0.00896	0.00896	−0.000153	60
FINAL XC	11			22:18:32		22:40:32	23	0.0127	0.0128	0.00202	60
FINAL YD	11			22:18:32		22:45:32	28	0.0111	0.0111	0.00142	60
	61			18:21:32		22:12:32	176	0.00949	0.00949	−0.000221	60
FINAL YD	11			22:18:32		22:50:32	33	0.00797	0.00811	0.00154	60
FINAL YE	11			22:18:32		22:56:32	39	0.00349	0.00413	0.00221	60
	61		4/19	18:21:32	4/19	22:12:32	176	0.0111	0.0111	−0.000298	60
POST 1	11		4/18	05:09:12	4/18	05:12:12	19	0.0344	0.0355	0.0085	10
			4/18	05:14:32	4/18	08:38:32	169	0.0072	0.0117	0.0092	60
			4/18	22:23:32	4/18	00:07:32	86	0.0049	0.0049	0.0003	60
			4/19	02:22:32	4/19	08:43:32	247	0.0050	0.0075	−0.0056	60
	42		4/18	08:43:32	4/18	14:33:32	275	0.0051	0.0062	−0.0035	60
			4/19	06:43:32	4/19	14:19:32	318	0.0052	0.0061	0.0032	60
	51		4/19	21:11:32	4/18	21:11:32	1	0.0000	0.0010	0.0010	60
			4/18	21:12:32	4/19	18:44:32	100	0.0069	0.0069	0.0004	60
	61		4/18	14:43:32	4/18	16:33:32	71	0.0046	0.0116	−0.0106	60
			4/18	18:13:32	4/19	00:28:32	151	0.0068	0.0095	−0.0067	60
			4/19	00:29:32	4/19	02:11:32	71	0.0090	0.0090	−0.0008	60
		CC3	4/19	14:23:32	4/19	22:11:32	288	0.0141	0.0151	0.0055	60

and DSS 11 data indicated an unbraked impact time of 00:01:47.646 GMT and the FINAL XD orbit solution using only DSS 11 data showed an unbraked impact time of 00:01:48.322. The FINAL XD solution contained DSS 11 data taken up to 1 h 12 min before encounter; the YE solution contained DSS 11 and DSS 61 data taken up 1 h 6 min before encounter. The unbraked impact time that was used for the AMR backup computations was 00:01:48.000, which was obtained by averaging the FINAL XD and YE solutions. With this unbraked impact time, the estimated nominal AMR mark time was computed as 00:01:11.52 GMT, April 20, 1967. This time was used as the basic reference point from which the desired time of backup command transmission from the ground station was calculated. The backup command was transmitted from DSS 11 at such a time that it was predicted to arrive at the spacecraft 1.73 s after the nominal AMR mark time. The time at which the AMR provided a mark pulse onboard the spacecraft was 00:01:11.61 ±50 ms. This observed time was 0.09 s later than the nominal AMR mark time used for the backup command computations. The AMR backup command arrived at the spacecraft at 00:01:13.13 ±0.1 s about 1.52 s after the AMR MARK. The inflight results of AMR backup computations are given in Table 13 and the comparison between inflight and postflight AMR backup computations can be seen in Table 14. Even though an incorrect frequency was used for the last pass of DSS 11 data, the difference between the estimated unbraked impact time provided for the AMR backup and the current best estimate is well within the 0.5-s desired 1-σ orbit determination accuracy.

Table 13. Inflight results of orbit determination AMR backup computations, *Surveyor III*

Orbit solution data span		Predicted selenocentric conditions at unbraked impact		
From	To	Latitude, deg (minus, south)	Longitude, deg	GMT, h:min:s (Apr. 20, 1967)
Midcourse[a]	*E* − 5 h 40 min[b]	−2.951	336.803	00:01:46.779[a]
E − 5 h 40 min	*E* − 2 h 09 min	−2.961	336.767	00:01:47.418
E − 5 h 40 min	*E* − 1 h 52 min	−2.976	336.769	00:01:47.578
E − 5 h 40 min	*E* − 1 h 35 min	−2.837	336.777	00:01:48.380
E − 5 h 40 min	*E* − 1 h 16 min	−2.868	336.763	00:01:47.971
E − 5 h 40 min	*E* − 1 h 05 min	−2.876	336.758	00:01:47.646
E − 5 h 40 min	*E* − 1 h 48 min	−2.852	336.768	00:01:47.912
Best estimate of unbraked impact time				00:01:48.159

[a]*Midcourse* refers to initial postmidcourse epoch. Solution used for initial estimate of AMR mark time.

[b]*E* refers to lunar encounter.

Table 14. Comparisons of inflight and postflight AMR backup computations, *Surveyor III*

Orbit solution data span		Unbraked impact, GMT		Difference between solutions, s
From	To	Inflight computations, h:min:s	Postflight computations,[a] h:min:s	
Midcourse[b]	*E* − 5 h 40 min	00:01:46.779	00:01:46.779	0
E − 5 h 40 min	*E* − 2 h 9 min	00:01:47.418	00:01:47.777	0.359
E − 5 h 40 min	*E* − 1 h 52 min	00:01:47.578	00:01:47.895	0.317
E − 5 h 40 min	*E* − 1 h 35 min	00:01:48.380	00:01:48.094	0.286
E − 5 h 40 min	*E* − 1 h 16 min	00:01:47.971	00:01:48.069	0.098
E − 5 h 40 min	*E* − 1 h 05 min	00:01:47.646	00:01:48.006	0.360
E − 5 h 40 min	*E* − 48 min	00:01:47.912	00:01:48.014	0.102

[a]With corrected DSS 11 frequency and lunar radius.

[b]Postmidcourse epoch at end of reorientation after motor burn.

VI. *Surveyor III* Postflight Orbit Determination Analysis

A. Introduction

This section presents the best estimate of the *Surveyor III* flight path, and other significant results obtained from the DSS tracking data. The analysis verified that both the premaneuver and postmaneuver inflight orbit solutions were within the orbit determination accuracy requirements of the *Surveyor* Project. The inflight philosophy of estimating only a minimum parameter set (i.e., the 6 components of the spacecraft position and velocity vectors) for the orbital computations was again proved valid.

For the postflight orbital computations and analysis, only two-way doppler data were used. Column I of Table 6 summarizes the data used for the premaneuver orbit computation in the postflight analysis. A comparison between columns D (amount of data used inflight) and I of Table 6 shows that fewer two-way doppler data points were used for the postflight computations. This was the result of removing some noisy DSS 61 data caused by the counter problem and rejecting some suspected bad data points. Column I of Table 6 summarizes the data used for postmaneuver orbit computations in postflight analysis. Once again the amount of data used for postflight computations was smaller than the amount of data used for inflight computation, the difference being the rejection of data obtained at an elevation angle below 17 deg.

B. Premaneuver Orbit Estimate

All the known or suspected bad data points were removed in the orbit data generator program (ODG) before the analysis of the premaneuver orbit data was begun. The DSS 61 data, which were disregarded on the preclean orbit computation immediately after midcourse because of its counter problem, was reexamined. The reexamination indicated that approximately 1½ h of usable data were obtained after the counter was fixed. Therefore this span of data was added in the postflight analysis. An orbit solution, based on estimating only the standard 6 parameters (position and velocity) using DSS 11, 42, 51, and 61 data was obtained and mapped forward to the target. The plot of observed minus computed (O − C) residuals showed that the data were not fitting as well as they should. A number of computer runs were made for data consistency checks. These runs indicated that the data were fairly consistent, with possibly very small biases in the DSS 51 and DSS 11 data. An attempt was made to remove the effect of these small biases and obtain a better data fit by expanding the set of estimated parameters from 6 to 18 to include the three station location parameters (radius, latitude, longitude) for DSS 11, 42, 51, and 61. An 18 × 18 orbit solution was then obtained and mapped forward to target. The O − C residual plots from this solution showed excellent data fit. The maximum difference between the estimated station-location and the nominal station-location parameters was in the longitude of DSS 11. This difference was 0.00019 deg or approximately 19 m. This longitude change could represent a station timing error of approximately 45.6 ms, or it could be caused by an error in station longitude, or a combination of both. It does not seem likely that the entire 19-m difference was due to an error in station longitude, since the uncertainty in the station locations was determined from the *Ranger* mission to be less than 15 m. The causes of this small bias are still being investigated. Even though the 6 × 6 orbit solution used the biased data in its orbit computations, the solution is well within the accuracy requirement for the orbit determination. The difference in the predicted unbraked impact point between the 6 × 6 and 18 × 18 orbit solutions is 0.01 deg in latitude and 0.03 deg in longitude.

Table 15. Summary of postflight orbit parameters, *Surveyor III*

Parameter	Premidcourse	Postmidcourse
Epoch, GMT	07:38:39.838 (Apr 17, 1967)	05:00:05.000 (Apr 18, 1967)
Geocentric position and velocity at epoch		
X, km	5839.9228 ±0.3794 (1σ)	−152113.39 ±2.92
Y, km	−1730.0102 ±0.5975	111775.36 ±2.55
Z, km	−2413.5785 ±1.1268	43749.888 ±7.638
DX, km/s	1.8349446 ±0.0017087	−1.3821714 ±0.0000480
DY, km/s	10.101593 ±0.000521	0.60990978 ±0.00005690
DZ, km/s	−3.8397087 ±0.0008211	0.51919389 ±0.00004215
Target statistics		
B, km	822.7767	1520.0479
B · **TT**, km	816.9932	1469.5219
B · **RT**, km	−97.3867	−388.65516
SMAA, km	10.0	7.0
SMIA, km	2.0	5.0
θ_T, deg	77.33	85.20
$\sigma_{T,\ impact}$ s	2.74	0.500
ϕ_{99}, deg	0.504073	0.106929
SVFIXR, m/s	0.608185	0.611175
Latitude, deg	−10.085561	−2.9760013
Longitude, deg	323.04465	336.79968
Unbraked impact, GMT	23:58:16.297 (April 19, 1967)	00:01:48.158 (April 20, 1967)

Note
Current best estimate, as of November 15, 1967.

The 18 × 18 solution is considered the best estimate of the spacecraft premaneuver orbit. The uncorrected unbraked impact point predicted by this solution (latitude = 10.09°S, longitude = 36.96°W) was 6.76 deg south and 13.79 deg west of the prelaunch targeted site (latitude = 3.33°S, longitude = 23.17°W). This is roughly equivalent to 202.8 km and 413.7 km, respectively. Other numerical values from this solution are presented in Table 15 and the number of data points, together with data noise statistics, are given in Table 16. A graphical comparison between the predicted unbraked impact (in the **B**-plane system) of this solution and the inflight solution may be seen in Fig. 11.

C. Postmaneuver Orbit Estimate

Before the analysis of the postmaneuver tracking data was started, all known or suspected bad data points were removed. An objective of the postflight analysis was to obtain an orbit solution by processing all postmaneuver tracking data in one block. This differed from the inflight computations which required that the data be processed in two blocks in order to meet the AMR backup requirements.

A 6 × 6 orbit solution based on all postmaneuver data and a lunar radius of 1736.1 km was obtained and mapped forward to the target. The value of 1736.1 was based on *Lunar Orbiter* photographs of the landing area. Examination of the residual plots indicated a very poor fit. The unbraked impact location predicted from this solution was in good agreement with the inflight results, but the impact time was approximately 0.460 s earlier than the observed time. A number of 6 × 6 orbit computations were made with various combinations of data from three stations. A comparison of the resulting orbit solutions indicated that all data were consistent. Consequently, the value of the lunar radius was suspected to be in error. The lunar radius was then changed to 1735.7 km, a value obtained by subtracting 2.4 km from the radius shown on the ACIC charts (2.4 km is the amount by which the ACIC elevations exceed the elevations obtained from *Rangers VI, VII* and *VIII* tracking data). The impact time obtained using this radius in a 6 × 6 solution was only 0.330 s earlier than the observed time. An attempt was then made to improve the fit by expanding the set of estimated parameters to 18 to include the station location parameters of the four stations. Examination of the residual plots from this 18 × 18 solution indicated a poor, but improved, fit; but

Table 16. Summary of data used in postflight orbit solutions, *Surveyor III*

DSS	Time data, GMT: Beginning, 1967	Beginning, h:min:s	Ending, 1967	Ending, h:min:s	Number of points	Standard deviation, Hz	Root mean square, Hz	Mean residual (O − C), Hz
Premidcourse								
11	4/17	22:18:32	4/18	04:37:32	341	0.00422	0.00437	−0.00114
11	4/18	04:39:32	4/18	04:46:32	37	0.0162	0.0162	0.000501
42	4/17	08:01:57	4/17	08:52:42	277	0.0196	0.0196	0.000328
42	4/17	08:55:32	4/17	11:45:32	141	0.00436	0.00456	−0.00134
51	4/17	12:23:32	4/17	18:48:32	154	0.00828	0.00836	−0.00116
51	4/17	18:49:37	4/17	18:52:37	17	0.0258	0.0261	−0.00419
51	4/17	18:54:32	4/17	20:24:32	68	0.00777	0.00842	−0.00324
61	4/17	20:37:07	4/17	22:07:32	67	0.0138	0.0138	−0.000743
Postmidcourse								
11	4/18	05:09:17	4/18	05:12:12	17	0.0242	0.0266	−0.0110
11	4/18	05:14:32	4/18	08:38:32	169	0.00462	0.00463	0.000347
11	4/18	22:41:32	4/19	00:07:32	84	0.00395	0.00399	−0.000564
11	4/19	02:22:32	4/19	23:12:32	315	0.00519	0.00520	−0.000267
42	4/18	08:43:32	4/18	13:40:32	275	0.00456	0.00457	−0.000316
42	4/19	06:43:32	4/19	13:46:32	315	0.00467	0.000953	
51	4/18	21:12:32	4/19	18:44:32	100	0.00718	0.00719	−0.000398
61	4/18	15:07:32	4/18	16:33:32	71	0.00456	0.00518	0.00244
61	4/18	18:13:32	4/19	00:28:32	146	0.00493	0.00493	0.000187
61	4/19	00:29:32	4/19	01:39:32	61	0.00505	0.00506	−0.000372
61	4/19	15:10:32	4/19	22:11:32	273	0.00726	0.00726	0.0000510

Note
Only two-way doppler data were used.

the predicted target parameters did not agree with any previous results.

A number of orbital computations were made using the Mod II ODP in an attempt to improve the data fit by solving for nongravitational trajectory perturbations and thereby provide a refined estimate of the postmaneuver orbit. The formulation referred to in this paragraph is discussed in Section II.A. The coefficients of the time polynomial (α_1, α_2) were not estimated for any case, and for most cases the solar radiation coefficients (G_R, G_T, G_N) were not estimated. In such computations, Eq. (1) was reduced to simply

$$\Delta\ddot{\mathbf{r}} = f_1\mathbf{U} + f_2\mathbf{T} + f_3\mathbf{N} \quad (2)$$

A 17×17 orbit solution, using all postmaneuver data, was obtained and mapped to target. This solution was based on an estimation of the standard 6 parameters; the station location parameters radius and longitude for the four stations (8 total); and the three accelerations (f_1, f_2 and f_3) for the entire trajectory. Examination of the doppler residual plots (Figs. 14, 15) indicated that the fit had been significantly improved. Also, the predicted unbraked impact point agreed very well with the inflight results, and the predicted impact time agreed with the observed time to within 0.07 s. This 17×17 orbit solution using all postmaneuver data is considered the current best estimate of the *Surveyor III* postmaneuver orbit.

The following are the nongravitational acceleration perturbations estimated in the 17×17 solution:

$$f_1 = 0.14 \times 10^{-9}\,\text{km/s}^2$$

$$f_2 = 0.70 \times 10^{-10}\,\text{km/s}^2$$

$$f_3 = -0.95 \times 10^{-10}\,\text{km/s}^2$$

$$[\Delta\ddot{\mathbf{r}}] \cong 0.183 \times 10^{-9}\,\text{km/s}^2$$

These results indicate that some perturbations did exist in the postmaneuver trajectory and that their effect can be accounted for by solving for nongravitational acceleration perturbations. The causes of these perturbations in the acceleration have not yet been determined and are still under investigation. However, the solar radiation pressure, uncanceled velocity increment from normal operations of the attitude control system, possible attitude jet misalignment, and possible gas or propellant leaks would be some of the causes for the perturbations. Even though these trajectory perturbations were not accounted for during inflight computations, the orbit determination requirements were met. Numerical values from the best estimate 17×17 postmaneuver orbit solutions are presented in Table 15. The amount of data used in this solution, together with the associated noise statistics, is shown in Table 16.

D. Evaluation of Midcourse Maneuver from DSIF Tracking Data

The *Surveyor III* midcourse maneuver can be evaluated by examining the velocity change at midcourse epoch, and by comparing the maneuver aim point with the target parameters from the best-estimate solution of the postmidcourse orbit.

The *observed* velocity change due to midcourse thrust is determined by differencing the velocity components of best-estimate orbit solutions derived from postmaneuver data only and premaneuver data only. These solutions are independent; i.e., *a priori* information from premaneuver data is not used during the processing of postmaneuver data. The estimated maneuver execution errors, at midcourse epoch, are determined by differencing the observed velocity changes and the commanded maneuver velocity increments. The remaining source of major contribution to the total maneuver error is made by the orbit determination process and includes ODP computational and model errors, and errors in tracking data. These errors may be obtained by differencing the velocity components, at midcourse epoch, of the best-estimate solution of the premaneuver orbit and the inflight orbit used for the maneuver computations. Numerical results of this part of the evaluation are presented in Table 17, in which it can be seen that the execution errors in *DX*, *DY* and *DZ* were only -0.0375 m/s, $+0.0103$ m/s, and -0.0074 m/s respectively. The orbit determination errors are also very small. Total maneuver errors for *Surveyor III* are well within specifications.

A more meaningful evaluation can be made by examining certain critical target parameters. Since the primary objective of the midcourse maneuver is to achieve lunar encounter at the selected landing site, the maneuver unbraked aim point is used as the basic reference for this evaluation. The unbraked aim point for *Surveyor III* was 2.88° S lat and 336.93° E lon. Trajectory corrections were based on the predicted unbraked impact point from the best estimate inflight orbit solution (LAPM YC) to achieve landing at the desired site. To evaluate the total maneuver error at the target, the maneuver aim point is compared with the predicted unbraked impact point from the current best estimate postmaneuver orbit solution.

Table 17. Midcourse maneuver evaluated at midcourse epoch, *Surveyor III*

Current best estimate of premaneuver velocity, m/s	Inflight[a] estimate of premaneuver velocity, m/s	Current best estimate of postmaneuver velocity at midcourse epoch,[b] m/s	Observed velocity change due to maneuver (best post—best pre), m/s	Commanded[a] maneuver velocity change, m/s	Total maneuver errors: Execution errors (observed change —commanded change), m/s	Total maneuver errors: Orbit determination errors (best pre-inflight), m/s
$DX = -1385.9217$	−1385.9256	−1382.1752	$\Delta DX = 3.7465$	3.7840	−0.0375	+0.0039
$DY = 610.82415$	610.81945	609.90406	$\Delta DY = -0.9201$	−0.9304	+0.0103	0.0047
$DZ = 517.65969$	517.66004	519.19749	$\Delta DZ = 1.5378$	1.5452	−0.0074	−0.0004

Note

All velocity components are given in geocentric space-fixed Cartesian coordinates.

[a]Based on inflight premaneuver orbit solution (LAPM YC) used for midcourse maneuver computations.

[b]Midcourse epoch ≃ end of reorientation after motor burn, April 18, 1967, 05:00:05.000 GMT.

Orbit determination errors can be obtained by differencing the unbraked target parameters of the current best estimate premaneuver orbit solution and the inflight orbit solution used for maneuver computations. Execution errors, consisting of both attitude maneuver errors and engine system errors, are then determined by differencing the total and the orbit determination errors. Numerical results of these computations are presented in Table 18, in which it can be seen that landing was achieved within 0.10 deg south and 0.13 deg west of the desired aiming point. These differences in latitude and longitude are roughly equivalent to 3.0 km and 3.9 km, respectively, on the lunar surface. The orbit determination **B**-space position errors ($\Delta \mathbf{B} \cdot \mathbf{T}T = 1.39$ km, $\Delta \mathbf{B} \cdot \mathbf{R}T = 0.458$ km) are well within the 9×2 km, one standard deviation, expected accuracy.[7] The accuracy of the *Surveyor III* midcourse maneuver was well within *Surveyor* Project specifications. It should be noted that these results cannot be used to precisely evaluate the *Centaur* injection accuracy since the inflight aim point was not exactly the same as the prelaunch aim point.

Table 18. Lunar unbraked impact points, *Surveyor III*

Source	Latitude, deg (south)	Longitude, deg (east)
Best estimate of premidcourse	−10.09	323.04
Inflight premidcourse orbit (LAPM YC)	−10.08	323.01
Best estimate of postmidcourse	−2.98	336.80
Maneuver unbraked aim point	−2.88	336.93

Estimated midcourse errors mapped to unbraked impact point

Source	Δ Latitude: deg (minus, south)	Δ Latitude: ≈km	Δ Longitude: deg (minus, west)	Δ Longitude: ≈km
OD errors[a]	−0.01	−0.3	0.03	0.9
Maneuver errors[b]	−0.09	−2.7	−0.16	−4.8
Overall errors[c]	−0.10	−3.0	−0.13	−3.9

[a]Orbit determination errors: Current best premaneuver estimate *minus* orbit used for maneuver computations (LAPM YC).

[b]Maneuver errors: Overall errors *minus* OD errors.

[c]Overall errors: Current best postmaneuver estimate *minus* aiming point.

E. Estimated Tracking Station Locations and Physical Constants

1. Introduction. Computations were made to determine the best estimate of GM_{earth}, GM_{moon} and station location parameters for *Surveyor III* mission. The parameters estimated in these computations were the spacecraft position and velocity at an epoch; GM_{earth}; GM_{moon}; spacecraft acceleration perturbations f_1, f_2 and f_3; the solar radiation constant G; and two components (geocentric radius and longitude) of station locations for each of DSSs 11, 42, 51 and 61. These solutions were computed using only the two-way doppler data from stations 11, 42, 51 and 61 for both the premidcourse and postmidcourse phases. In an effort to obtain the best estimate of the parameters to be solved for, the premidcourse data block was combined with the postmidcourse data block. The procedure of combining the two data blocks is to fit only the premidcourse data, accumulate the normal equations at the injection epoch, and map the converged estimate to the midcourse epoch with a linear mapping of the inverted normal equation matrix (i.e., covariance matrix). The estimate is then incremented with the best estimate of the maneuver, and the mapped covariance matrix is corrupted in the velocity increment and used as *a priori* for the postmidcourse data fit. The ephemeris used in the reduction was the JPL DE-19 with the updated mass ratios and Eckert's corrections.

[7]See Ref. 9 for expected accuracy of orbit determination.

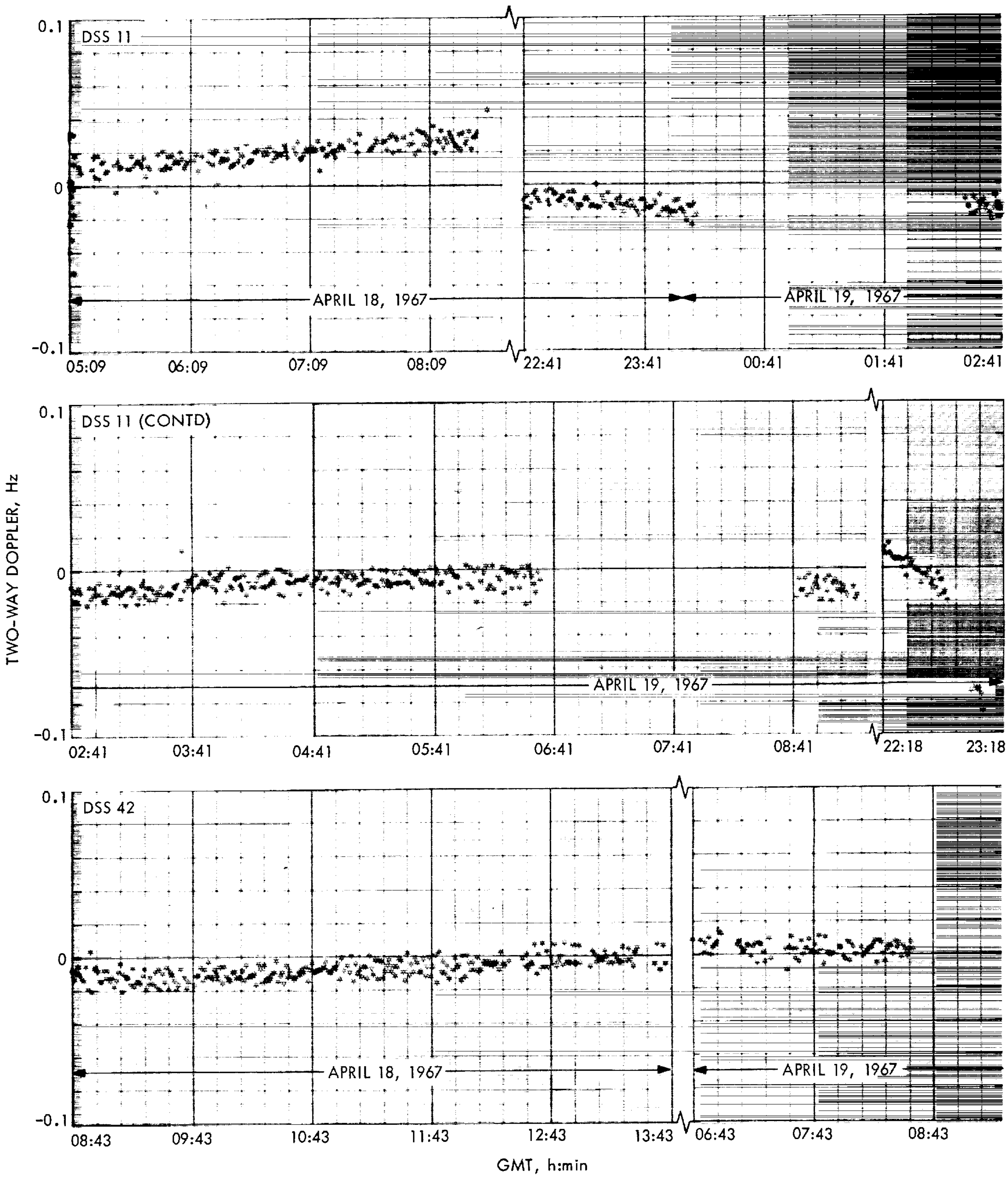

Fig. 14. *Surveyor III* **postmaneuver two-way doppler residuals, trajectory not corrected for perturbations**

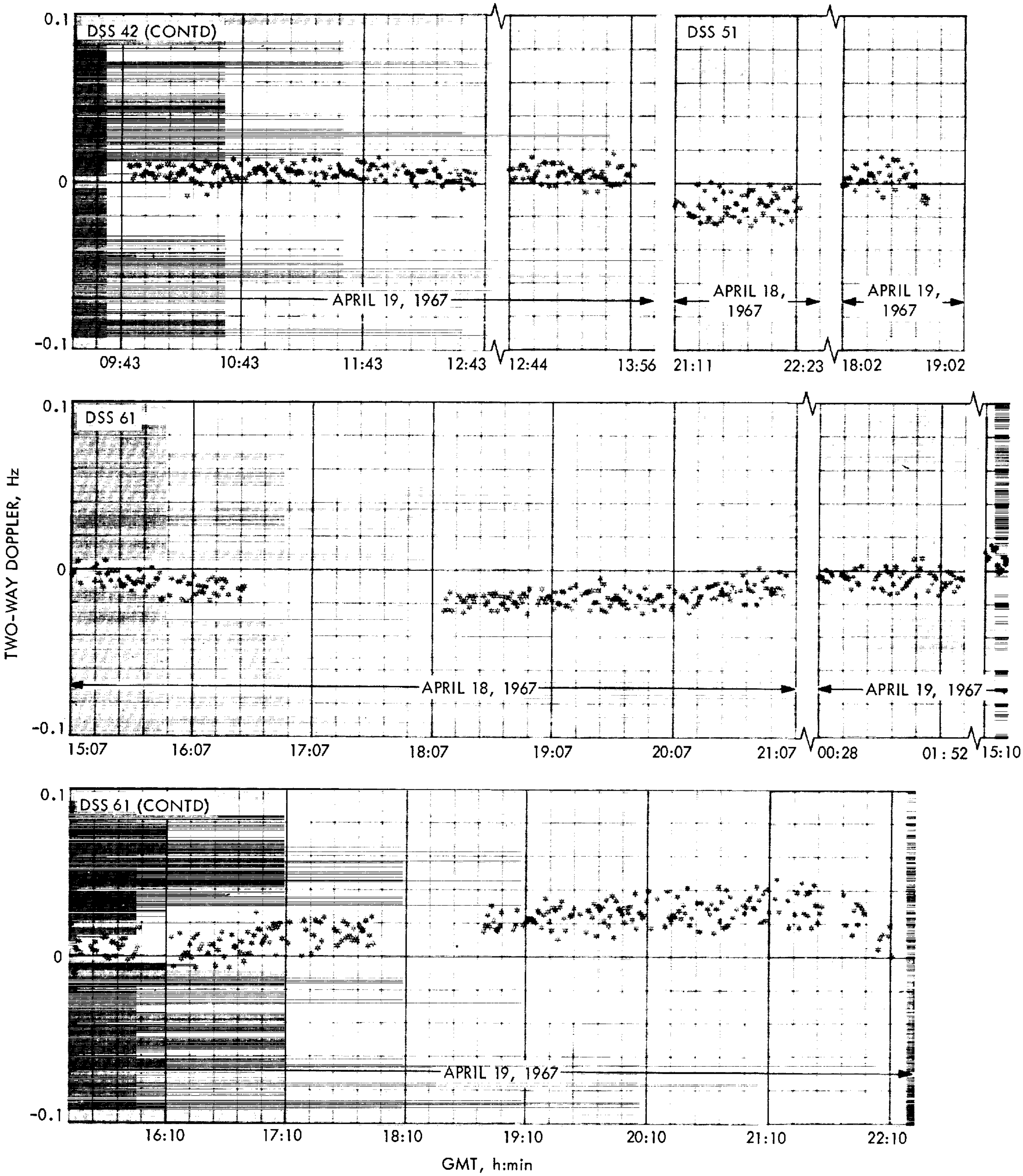

DSS 42 (CONTD)
DSS 51
APRIL 19, 1967
APRIL 18, 1967
APRIL 19, 1967
09:43
10:43
11:43
12:43
12:44
13:56
21:11
22:23
18:02
19:02
DSS 61
APRIL 18, 1967
APRIL 19, 1967
15:07
16:07
17:07
18:07
19:07
20:07
21:07
00:28
01 : 52
15:10
DSS 61 (CONTD)
APRIL 19, 1967
16:10
17:10
18:10
19:10
20:10
21:10
22:10
TWO-WAY DOPPLER, Hz
0.1
0
-0.1
GMT, h:min

Fig. 14 (contd)

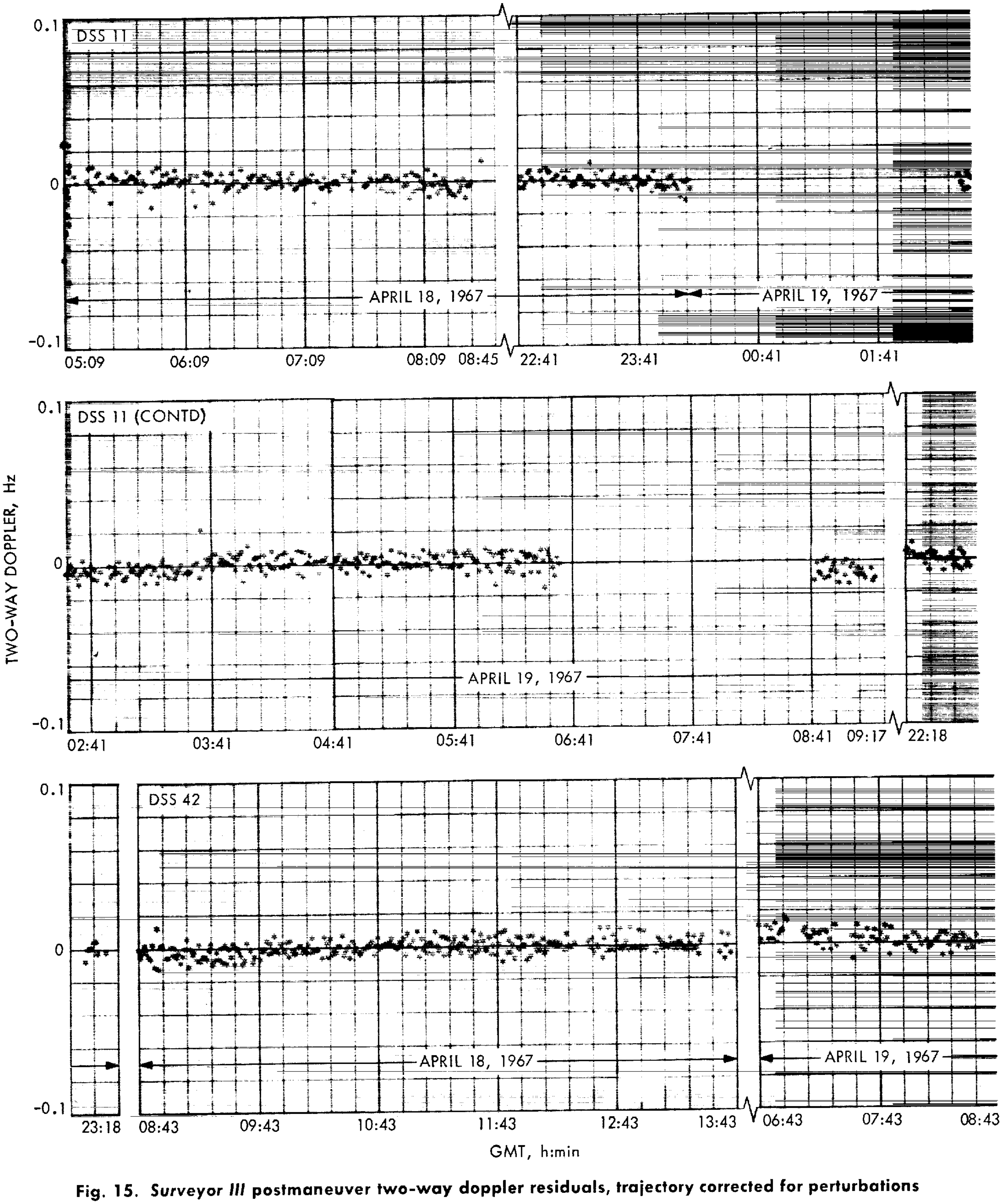

Fig. 15. ***Surveyor III* postmaneuver two-way doppler residuals, trajectory corrected for perturbations**

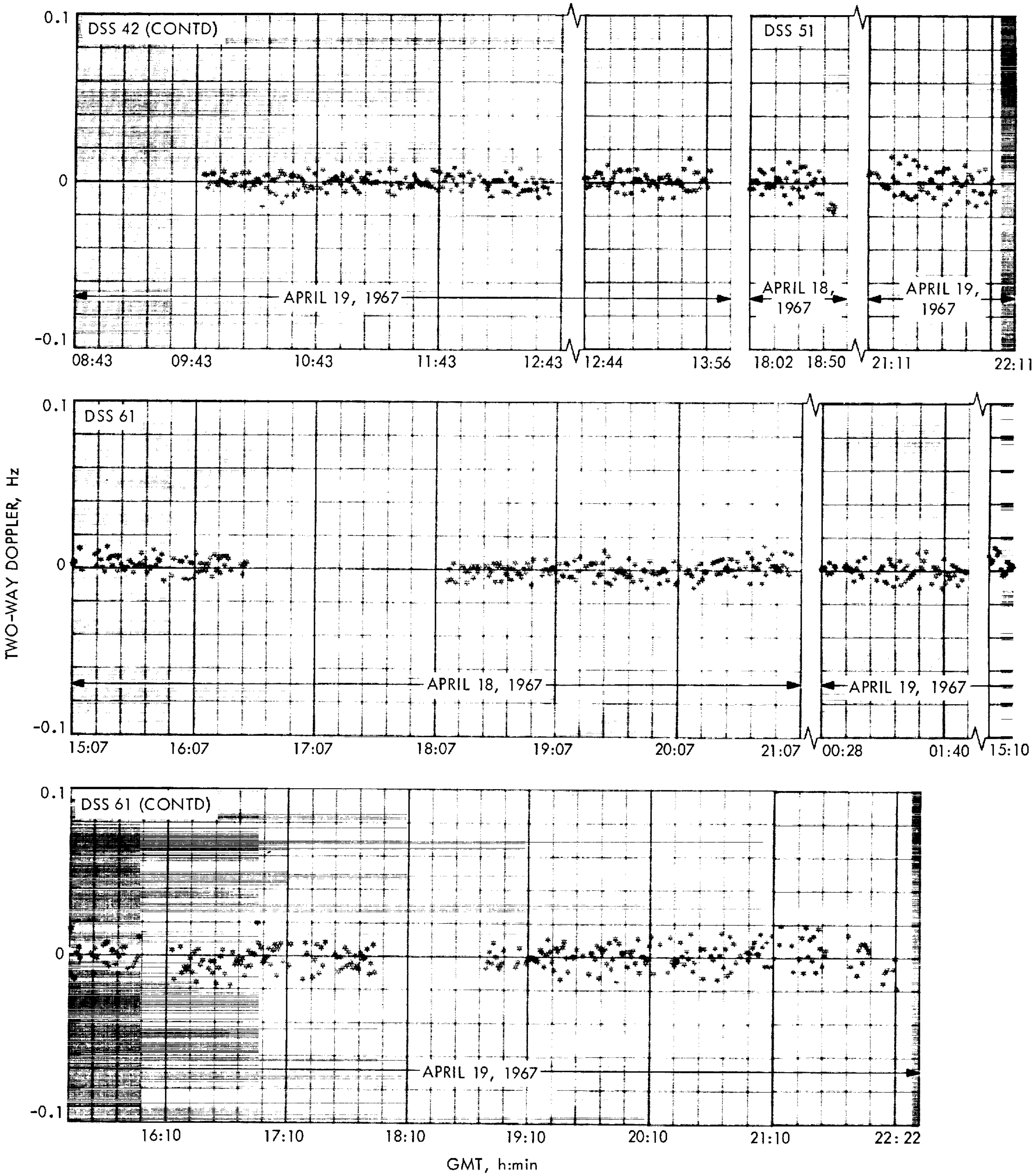

DSS 42 (CONTD)
DSS 51
APRIL 19, 1967
APRIL 18, 1967
APRIL 19, 1967
0.1
0
-0.1
08:43
09:43
10:43
11:43
12:43
12:44
13:56
18:02
18:50
21:11
22:11
DSS 61
APRIL 18, 1967
APRIL 19, 1967
15:07
16:07
17:07
18:07
19:07
20:07
21:07
00:28
01:40
15:10
DSS 61 (CONTD)
APRIL 19, 1967
16:10
17:10
18:10
19:10
20:10
21:10
22:22
TWO-WAY DOPPLER, Hz
GMT, h:min

Fig. 15 (contd)

2. Results. The results of these computations are presented in Table 19 in an unnatural station coordinate system (geocentric radius, latitude, and longitude) and in a natural coordinate system (r_s, λ, Z) where r_s is the distance off the spin axis (in the station meridian), λ is the longitude, and Z is a line along the earth spin axis (Fig. 16).

The numerical results indicate that the values obtained for r_s and longitude for DSS 11, and r_s for DSS 42, are a few meters higher than any of the previous solutions listed (except by Goddard). The value of r_s for DSS 61 is only slightly lower (<1 m) than previous solutions. This may be due to the abundance of low elevation data incorporated in the solution and the improved values[8] of DSS indices of refraction used in the solution. The new indices improved the data fit for all stations which took low elevation data. Previous to the availability of new indices, a value of 340 was used for all Deep Space Stations.

Surveyor I and *III* solutions for longitude of DSS 42 are both higher than previous solutions. However, these values are consistent with all the other *Surveyor* solutions which have been computed in postflight analysis of the tracking data. Therefore, the estimate for DSS 42 longitude is considered a good one. All other station locations estimated for *Surveyor III* are within the range of the previous solutions listed. The statistics obtained with the station locations are higher than those of most other missions because larger effective data weights were used for

[8]Indices of refraction obtained from A. S. Liu, JPL: DSS 11 = 240, DSS 42 = 310, DSS 51 = 240, DSS 61 = 300.

Table 19. Station locations and statistics, *Surveyor III* (referenced to 1903.0 pole)

DSS	Data source	Distance off spin axis r_s, km	r_s Standard deviation (1σ), m	Geocentric longitude, deg	Longitude standard deviation (1σ), m	Geocentric radius, deg	Geocentric latitude[a], deg
11	*Mariner II*	5206.3357	3.9	243.15058	8.8	6372.0044	35.208035
	Mariner IV, cruise	404	10.0	067	20.0	.0188	08144
	Mariner IV, postencounter	378	37.0	072	40.0	.0161	08151
	Pioneer VI, Dec. 1965–June 1966	359	9.6	092	10.3	.0286	08030
	Goddard Land Survey, Aug. 1966	718	29.0	094	35.0	.0640	08230
	Surveyor I, post-touchdown	276	2.9	085	23.8	.6446	16317
	Surveyor I, inflight	417	49.3	125	46.0	.0240	08192
	Surveyor III, inflight	431	22.1	086	45.0	.0258	08192
42	*Mariner IV*, cruise	5205.3478	10.0	148.98136	20.0	6371.6882	−35.219410
	Mariner IV, postencounter	.3480	28.0	134	29.0	.6824	19333
	Pioneer VI, Dec. 1965–June 1966	.3384	5.0	151	8.1	.6932	19620
	Goddard Land Survey, Aug. 1966	.2740	52.0	000	61.0	.7030	20750
	Surveyor I, post-touchdown	.3474	3.5	130	22.1	.6651	19123
	Surveyor I, inflight, postmidcourse only	74	29.2	161	41.0	.6845	19372
	Surveyor III, inflight	74	25.3	156	42.0	.6847	19372
51	Combined *Rangers*, LE-3[b]	5742.9315	8.5	27.68572	22.2	6375.5072	−25.739169
	Ranger VI, LE-3	203	19.7	572	69.3	.4972	9215
	Ranger VII, LE-3	211	25.5	583	61.3	.4950	9157
	Ranger VIII, LE-3	372	22.3	548	85.0	.5130	9159
	Ranger IX, LE-3	626	56.6	580	49.5	322	8993
	Mariner IV, cruise	363	10.0	540	20.0	120	9148
	Mariner IV, postencounter	365	40.0	557	38.0	143	9198
	Pioneer VI, Dec. 1965–June 1966	332	11.6	569	12.0	094	9176
	Goddard Land Survey, Aug. 1966	706	39.0	586	43.0	410	8990
	Surveyor I, inflight	382	33.9	572	41.2	146	9169
	Surveyor III, inflight	347	32.7	570	45.0	108	9169
61	*Lunar Orbiter II*, doppler	4862.6067	9.6	355.75115	44.4	6369.9932	40.238566
	Lunar Orbiter II, doppler and ranging	6118	3.4	138	4.0	69.9999	566
	Mariner IV, postencounter	6063	14.0	099	24.0	70.0009	655
	Pioneer VI, Dec. 1965–June 6, 1966	59	8.8	103	10.4	60	715
	Surveyor III, inflight	65	21.2	124	45.0	54	701

[a]Latitude was not estimated for *Surveyor* inflight solutions.
[b]Lunar ephemeris 3 (DE-15); all *Surveyor* inflight solutions used LE-4 (DE-19).

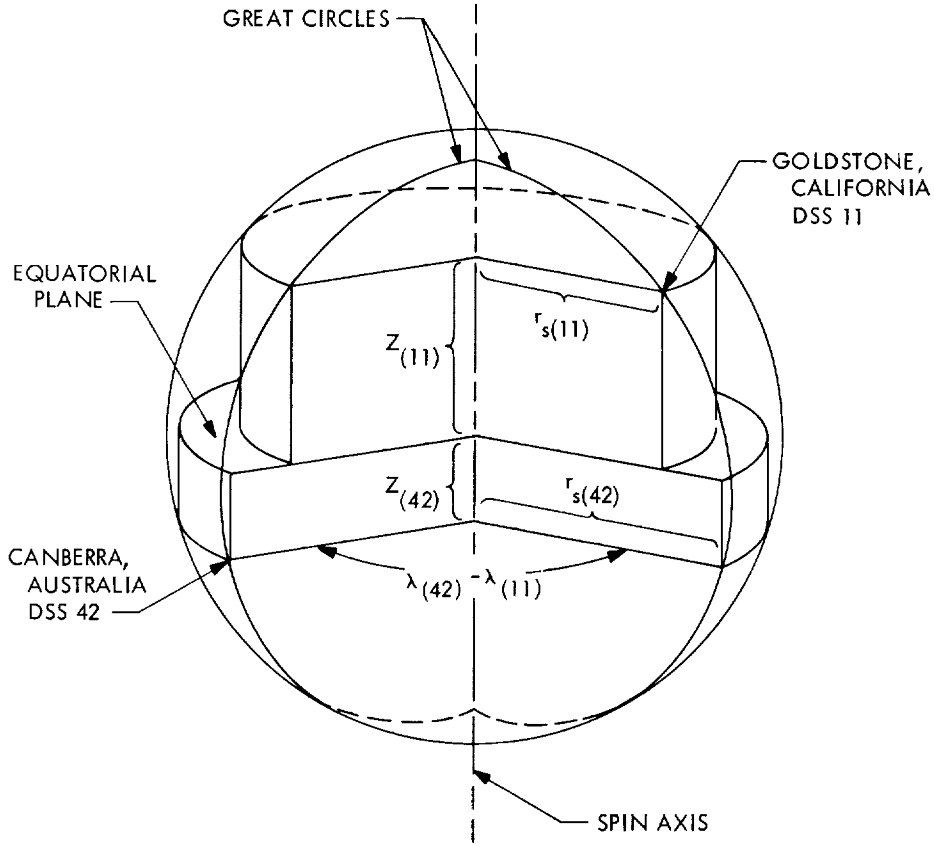

Fig. 16. Station coordinate system

Surveyor missions and the amount of data available is generally smaller.

The GM_{earth} and GM_{moon} estimates for *Surveyor III* are given in Table 20 along with previous solutions. The value for GM_{earth} is slightly lower than most of the *Ranger* solutions, but is well within 1 σ of the combined *Ranger* estimates. The value obtained for GM_{moon} is within the range of the *Ranger* estimates and slightly higher than the combined *Ranger* values. The correlation matrix on postmaneuver data with premaneuver data as *a priori* is given in Table 21.

3. Conclusion. The GM_{earth} and GM_{moon} estimates are within the same range as previous individual *Ranger* and *Lunar Orbiter* estimates. Other than DSS 11 r_s and longitude, and DSS 42 longitude, the station location parameters are in good agreement with the *Ranger*, *Mariner*, *Lunar Orbiter*, and *Pioneer* missions. However, additional solutions are being made for other *Surveyor* missions which indicate the value for DSS 42 longitude is consistent. The results of successive *Surveyor* estimates will be presented in their associated flight path reports. For *Surveyor IV* estimates, see Section X. E.

Table 20. Physical constants and statistics, *Surveyor III*

Data source	GM_{earth}, km^3/s^2	Standard deviation (1σ), km^3/s^2	GM_{moon}, km^3/s^2	Standard deviation (1σ), km^3/s^2
Lunar Orbiter II (doppler)	398600.88	2.14	4902.6605	0.29
Lunar Orbiter II (doppler and range)	398600.37	0.68	4902.7562	0.13
Combined *Rangers*	398601.22	0.37	4902.6309	0.074
Ranger VI	398600.69	1.13	4902.6576	0.185
Ranger VII	398601.34	1.55	4902.5371	0.167
Ranger VIII	398601.14	0.72	4902.6304	0.119
Ranger IX	398601.42	0.60	4902.7073	0.299
Surveyor I	398600.62	0.63	4902.6529	0.236
Surveyor III	398600.78	0.72	4902.7102	0.230

Table 21. Correlation matrix of estimated parameters, *Surveyor III* (solution on postmaneuver data with premaneuver data as a *priori* at maneuver epoch)

Standard deviation		X	Y	Z	DX	DY	DZ	GM_{earth}	G	GM_{moon}	f_1	f_2	f_3	R_{11}	Lon_{11}	R_{42}	Lon_{42}	R_{51}	Lon_{51}	R_{61}	Lon_{61}
X	1.178	1.000	0.680	0.226	−0.277	0.055	−0.444	−0.360	0.001	−0.117	−0.057	−0.080	0.057	−0.058	−0.579	0.032	−0.530	0.159	−0.592	0.068	−0.607
Y	1.700		1.000	−0.555	−0.289	0.290	−0.532	0.113	−0.001	0.144	−0.110	−0.206	0.260	−0.547	−0.737	−0.436	−0.848	−0.267	−0.827	−0.420	−0.713
Z	3.072			1.000	0.139	−0.257	0.241	−0.530	0.002	−0.353	0.154	0.254	−0.334	0.685	0.255	0.606	0.478	0.544	0.370	0.633	0.193
DX	0.021				1.000	0.702	0.743	0.025	0.001	−0.512	0.964	0.854	−0.528	0.253	−0.163	0.085	−0.047	0.081	−0.030	0.116	−0.204
DY	0.023					1.000	0.079	0.164	−0.000	−0.403	0.726	0.484	−0.165	−0.332	−0.626	−0.351	−0.553	−0.204	−0.516	−0.288	−0.581
DZ	0.041						1.000	−0.016	0.001	−0.261	0.694	0.753	−0.549	0.580	0.265	0.363	0.301	0.210	0.325	0.360	0.162
GM_{earth}	0.725							1.000	0.008	0.175	−0.016	−0.091	0.133	−0.393	−0.001	−0.359	−0.192	−0.193	−0.134	−0.293	0.007
G	0.1								1.000	−0.003	−0.004	0.001	−0.002	0.002	−0.001	0.002	0.000	0.001	0.003	0.002	0.000
GM_{moon}	0.230									1.000	−0.502	−0.268	0.046	−0.243	0.118	−0.267	0.037	−0.172	0.007	−0.271	0.058
f_1	0.37×10^{-9}										1.000	0.852	−0.408	0.244	−0.321	0.100	−0.218	0.113	−0.199	0.167	−0.379
f_2	0.46×10^{-9}											1.000	−0.861	0.382	−0.245	0.099	−0.075	0.141	−0.114	0.102	−0.337
f_3	0.29×10^{-9}												1.000	−0.399	0.120	−0.064	−0.090	−0.149	0.004	−0.009	0.210
R_{11}	0.027													1.000	0.314	0.581	0.460	0.502	0.355	0.547	0.224
Lon_{11}	0.00045														1.000	0.385	0.891	0.213	0.893	0.282	0.923
R_{42}	0.031															1.000	0.383	0.436	0.410	0.558	0.319
Lon_{42}	0.00042																1.000	0.299	0.888	0.324	0.860
R_{51}	0.036																	1.000	0.115	0.372	0.125
Lon_{51}	0.00045																		1.000	0.331	0.872
R_{61}	0.028																			1.000	0.244
Lon_{61}	0.00045																				1.000

Units of measure

X, Y, Z: km
DX, DY, DZ: m/s
GM_{earth}, GM_{moon}: km^3/s^2
f_1, f_2, f_3: km/s^2
G (solar radiation coefficient), unitless
Lon, deg
R, km

VII. Observations and Conclusions From *Surveyor III* Mission

A. Tracking Data Evaluation

The only significant loss of prime two-way doppler data during the *Surveyor III* mission occurred during the first pass over DSS 61. At 14:32:02 GMT, on April 17, DSS 61 began taking two-way doppler data, and approximately 15 min later the results of the data monitor program indicated excessive noise in the DSS 61 data. The problem was traced to a dropped 8-bit in the least significant digit of the doppler counter. A transfer to DSS 51 could not be scheduled until 17:00:00 because of Canopus acquisition. At 17:33:02, DSS 61 stopped three-way tracking to repair the counter, and resumed three-way tracking at 18:36:31. Investigation disclosed that now bits were being dropped from the fifth significant digit in the doppler counter, and DSS 61 stopped tracking from 19:24:32 to 19:51:22 to again repair the doppler counter. After 19:51:22, no further such problems were encountered.

In general, doppler data yields far greater accuracy in the determination of a spacecraft orbit than does angle data and is therefore used almost exclusively in the orbit determination process during most of the mission. The one exception is the launch phase, when little doppler data is available and a quick determination of the orbit necessitates the use of both doppler and angle data. During the *Surveyor III* mission, angle data from DSS 42, DSS 61, and DSS 51 were used in the orbit determination program during the premidcourse phase. To improve the quality of the angle data to be used in the orbit determination program, it is first corrected for antenna optical pointing error as discussed in Section II.B.

Experience gained in past missions has shown that the correction coefficients of the optical printing error do not remove all systematic pointing errors. This was verified again during the *Surveyor III* mission when examination of residual plots revealed a definite bias in angle data with respect to the doppler data.[9] During the third orbit computation period (PREL), a comparison was made between orbit solutions with angle data and those without. The result was a difference of 132 km in **B** space when the resulting orbit solutions were mapped to target encounter.

Results of the midcourse maneuver burn can be seen in the DSS 11 two-way doppler data shown in Fig. 17. Results of the retromotor burn as seen in the one-way doppler data from DSS 11 are presented in Fig. 18.

[9]See Figs. 1 to 4.

B. Comparison of Inflight and Postflight Results

The results of the inflight orbit determination can be evaluated by comparing them with the results obtained from the postflight computations. The degree to which these results agree is primarily influenced by the success attained in detecting and eliminating bad or questionable tracking data from the inflight computations, and accounting for all trajectory perturbations. Of these, the largest variations are usually caused by bad or questionable data resulting from equipment malfunction, incorrect time information, or incorrect frequency information. Other than gross blunder points, these data are not easily detected unless two-way doppler data are available from more than one station. That is, the least-squares method used to fit data in the ODP gives no information on constant data biases when data are available from only one station. Therefore, a comparison can be made only when data from more than one station are available. Furthermore, data must be available from three or more stations in order for bad blocks of data to be isolated.

The best comparison between the results of inflight and postflight orbit determinations can be made by examining the critical target parameters; namely, the unbraked impact time and the impact location. Table 22, which summarizes these results, shows that the inflight premaneuver impact point was in error by 0.01 deg in latitude and 0.03 deg in longitude. This is well within the uncertainty associated with the inflight estimate. The inflight postmaneuver impact point associated with orbit solution (5 POM YD) used for the terminal attitude maneuver computations was in error by 0.035 deg in latitude and 0.01 deg in longitude. These errors are also within the stated uncertainties associated with the inflight estimates. The inflight predicted unbraked impact time used to provide the AMR backup differed from the observed time by 0.159 s which was within the 1 σ uncertainty of 0.500 s. Part of this error was due to an incorrect input of DSS 11 station frequency. Had the correct frequency been used, this error would have been reduced to 0.145 s.

The best estimate of the landing point determined by transit tracking data (i.e., current best postmaneuver orbit), and the landing points determined by independent observations are presented in Table 22. One of the independent observations was obtained by processing tracking data from the landed spacecraft. The other one was obtained by optical methods; i.e., correlating television photos of surrounding lunar horizon features taken by *Surveyor III* with the photos of the same lunar region taken by *Lunar Orbiter*. In the table it can be seen that the estimated location based on the preliminary analysis of the landed

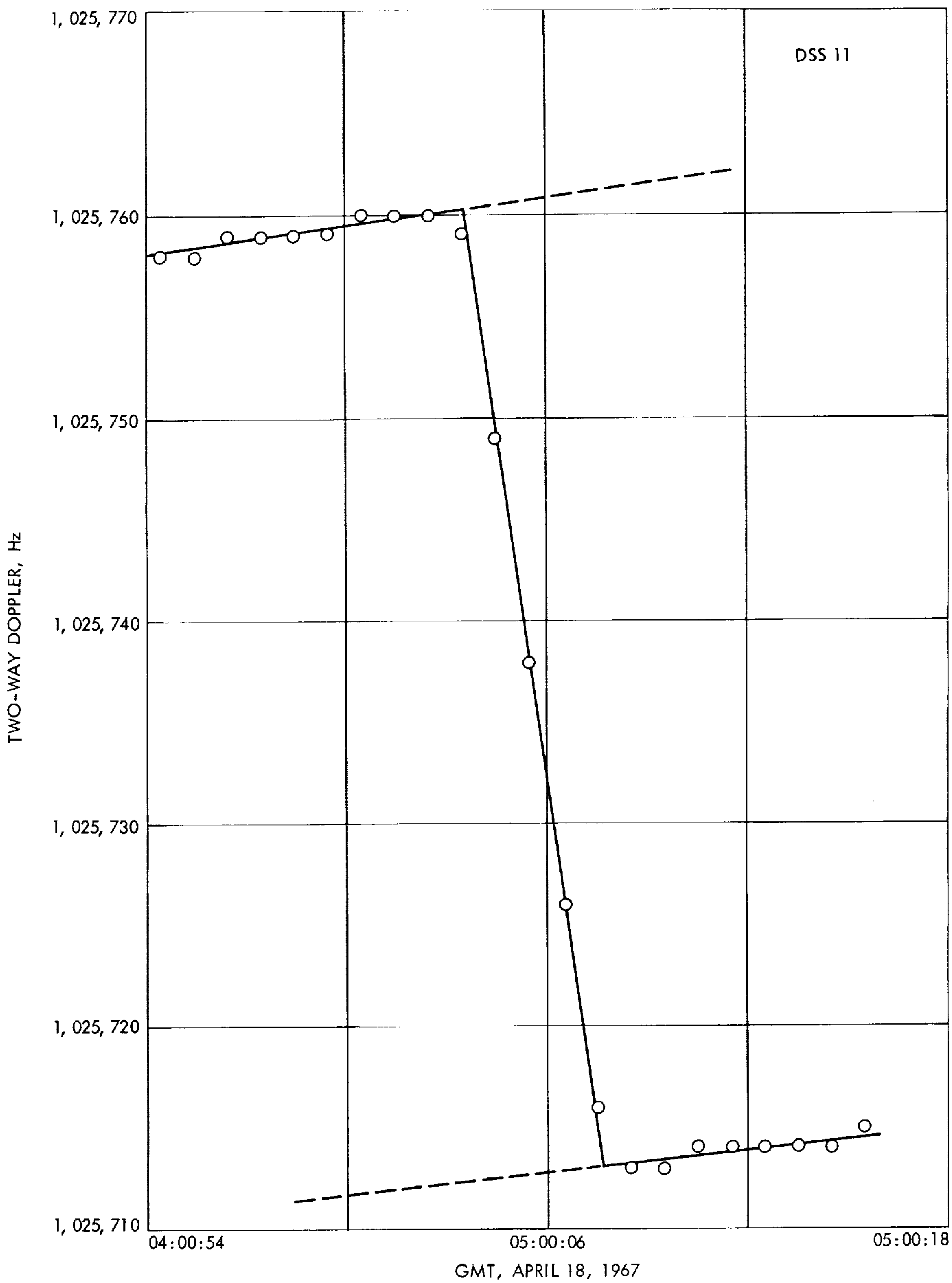

Fig. 17. DSS 11 midcourse maneuver doppler data for Surveyor *III*

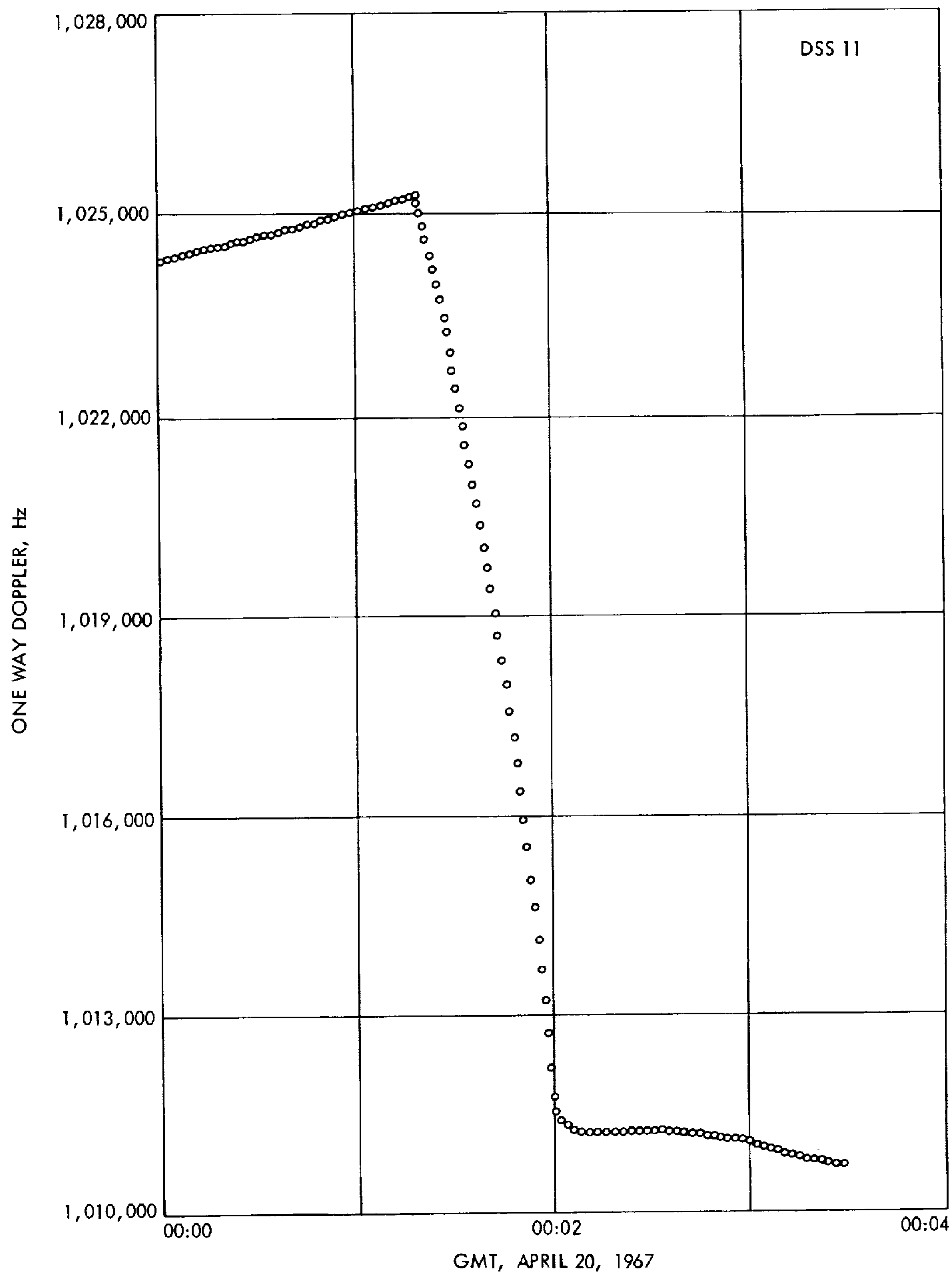

Fig. 18. DSS 11 main retromotor burn phase doppler for Surveyor III

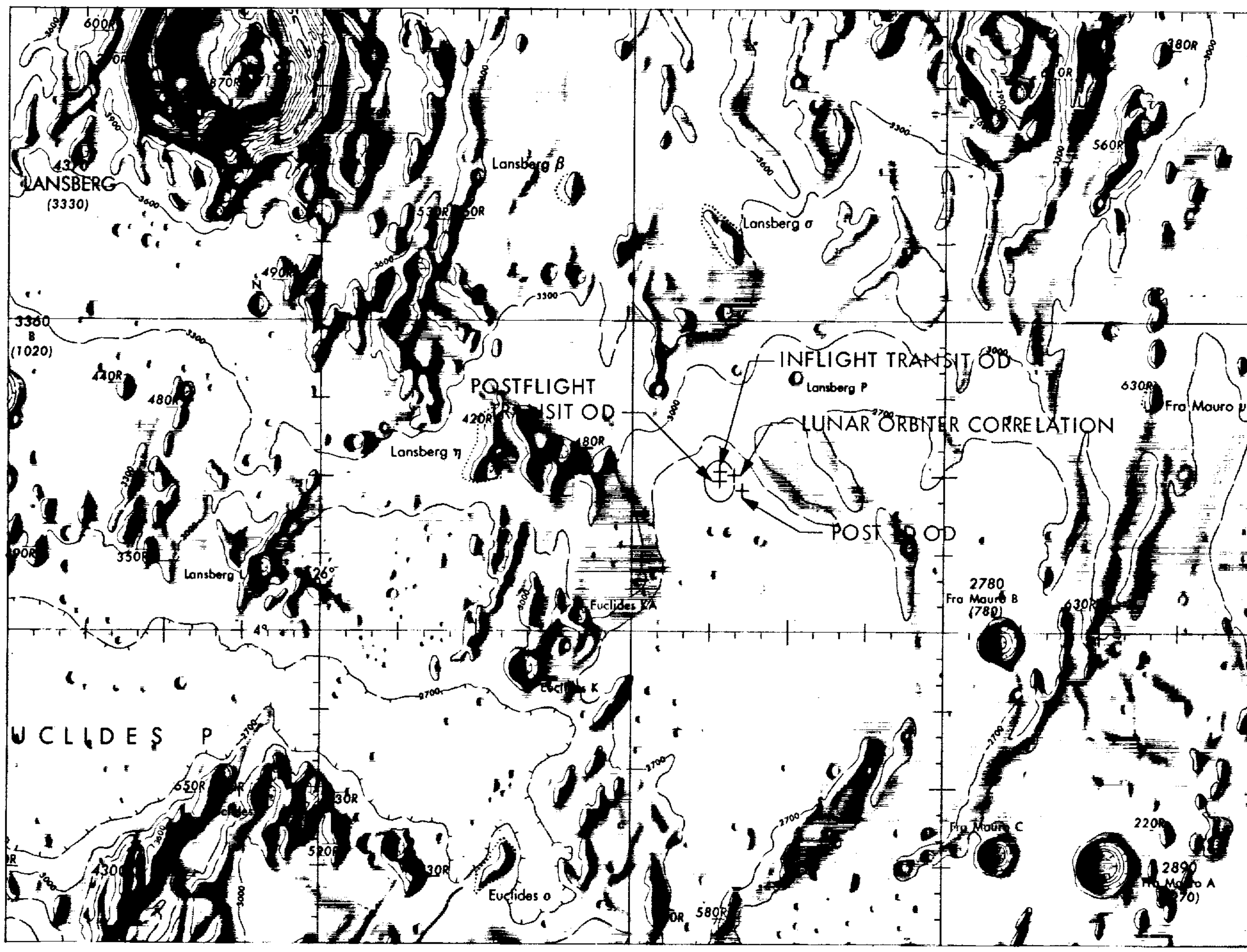

Fig. 19. *Surveyor III* estimated landed location on lunar surface

Table 22. Summary of target impact parameters, *Surveyor III*

Source	Estimated unbraked impact location		Uncertainty about estimated impact point (1 σ dispersion ellipse)			Estimated unbraked impact time, GMT h:min:s	Uncertainty in estimated unbraked impact time (1σ), s
	Latitude, deg (south)	Longitude, deg	SMAA, km	SMIA, km	θ_T, deg		
Premaneuver (uncorrected)							
Inflight OD	−10.08	323.01	10.0	2.0	71.395	23:58:16.856	2.74
Postflight OD	−10.09	323.04	10.0	2.0	77.330	23:58:16.297	2.74
Postmaneuver (transit)							
Inflight OD	−2.94	336.79	7.0	5.0	82.90	00:01:48.000	0.500
Postflight OD	−2.98	336.80	7.0	5.0	85.207	00:01:48.159	0.500
Observed unbraked impact	—	—	—	—	—	00:01:48.09	0.050
Post-landing							
Postflight OD (adjusted)	−3.01	336.59					
Lunar Orbiter correlation	−2.94	336.66					
Post touchdown OD	−3.06	336.71					

spacecraft tracking data falls outside of the 1-σ dispersion ellipse associated with the transit location (Fig. 19). However, it is well within the 3-σ dispersion ellipse. The estimate based on the *Lunar Orbiter* photos is within the 1-σ uncertainty of the transit estimate. The unbraked impact time *observed* and the impact time predicted by the current best postmaneuver orbit solution (based on a lunar elevation of 1735.7 km) differ by only 0.069 s.

Based on the results of the comparison between inflight and postflight results, the following conclusions may be made: (1) the premaneuver OD requirements were met; (2) the postmaneuver OD requirements were met even with an incorrect frequency input for a pass of DSS 11 data.

VIII. Analysis of Air Force Eastern Test Range Tracking Data—*Surveyor III*

A. Introduction

During *Surveyor* missions, the Air Force Eastern Test Range (AFETR) is responsible for providing injection conditions and classical orbital elements for the parking orbit, the spacecraft transfer orbit, and the *Centaur* postretro orbit. The AFETR is also responsible for providing initial acquisition information to the SFOF for possible use by the deep space tracking stations. These data are computed with *Centaur* C-band tracking data obtained from the downrange AFETR tracking stations. Results of these calculations are transmitted to the SFOF for possible retransmission to the tracking stations. The injection conditions are sometimes used as starter values for the initial JPL orbit calculations. However, since *Surveyor III* experienced a near-nominal launch, the nominal injection conditions available before launch were used as starter values for the initial JPL orbits.

In addition to the above requirements, the AFETR transmits the C-band pulse radar data obtained during the parking orbit, the transfer orbit, and the *Centaur* postretro orbit to the SFOF. The transfer orbit data are used during flight operations to provide a check and a backup to the AFETR computations. The *Centaur* postretro data are important for verifying the *Centaur* retromaneuver and the *Centaur* postretro orbit. The retromaneuver is performed to ensure that the *Centaur* does not impact the lunar surface and to provide a separation between the *Centaur* and the spacecraft so that the Canopus seeker does not lock on the *Centaur* rather than Canopus.

Centaur C-band preretro data were obtained from Bermuda, Pretoria, Ascension, Antigua and Grand Turk. However, all the data from Bermuda and Grand Turk were from the burn period between launch and CACO[10] and were not used in any JPL orbit computations. Postretro data were obtained from Carnarvon only. Elevation angles for the *usable* data were as follows:

(1) Carnarvon $14 \leq el \leq 81$ deg

(2) Pretoria $17 \leq el \leq 23$ deg

(3) Ascension $5 \leq el \leq 12$ deg

(4) Antigua $0 \leq el \leq 11$ deg

[10]CACO means *Centaur* achieves circular orbit at the end of the first 100-lb thrust propellant settling phase.

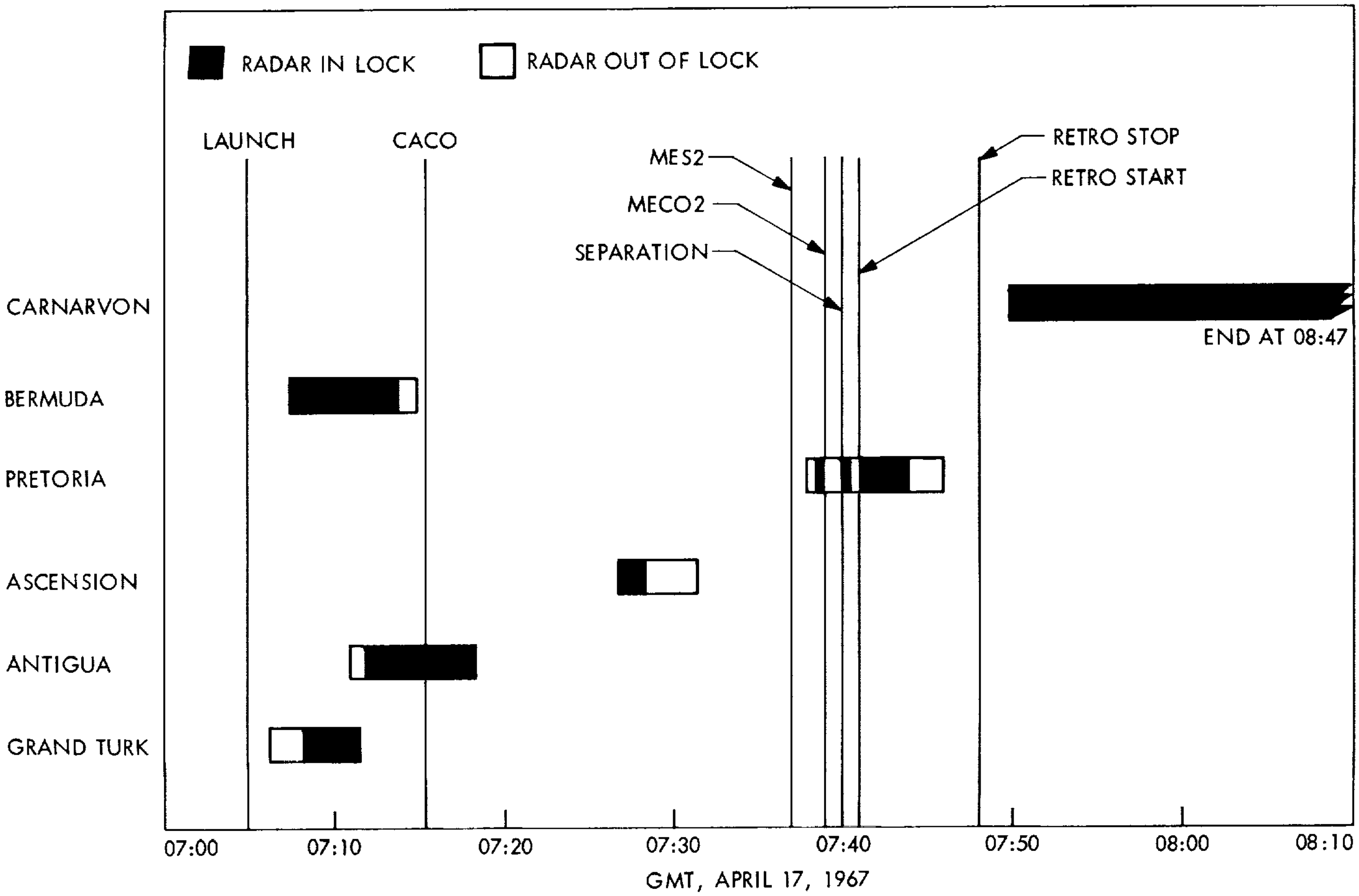

Fig. 20. AFETR tracking coverage for *Surveyor III*

The AFETR data coverage and associated spacecraft events are shown in Fig. 20.

B. Analysis of the Parking Orbit Data

The parking orbit computed at JPL used 23 points of angle and range data from Antigua and 14 points of range and 11 points of angle data from Ascension. These data were all between CACO and *Centaur* second main engine start (MES2). The converged earth-fixed spherical injection conditions are given in Table 23 for orbit determinations computed by both JPL and AFETR. Although the epochs used are slightly different, they are near enough to see good agreement between the JPL and AFETR computations. The tracking data residuals are shown in Fig. 21. The type and amounts of data are shown in Table 24 along with their associated noise statistics.

C. Analysis of the Transfer Orbit Data

The *Centaur* transfer orbit was computed using angle and range data from Pretoria obtained during the period

Table 23. Parking orbit injection conditions, *Surveyor III*

Description	JPL orbit	AFETR orbit
Epoch, GMT	07:15:50.118 (Apr. 17, 1967)	07:16:05.7 (Apr. 17, 1967)
Radius, km	6537.04	6537.0
Latitude, deg	21.598	21.171
Longitude, deg	303.078	304.168
Velocity, km/s	7.403	7.401
Flight path angle, deg	0.0036	0
Azimuth, deg	112.543	112.985
Semimajor axis, km	6546.0	6544.0
Eccentricity, deg	0.0013675	0.0010187
C_3 (vis viva integral), km²/s²	−60.89	−60.91
True anomaly, deg	2.506	0.102
Inclination, deg	29.96930	29.96304
Longitude of ascending node, deg	120.129	120.1372
Argument of perigee, deg	130.02739	133.58394

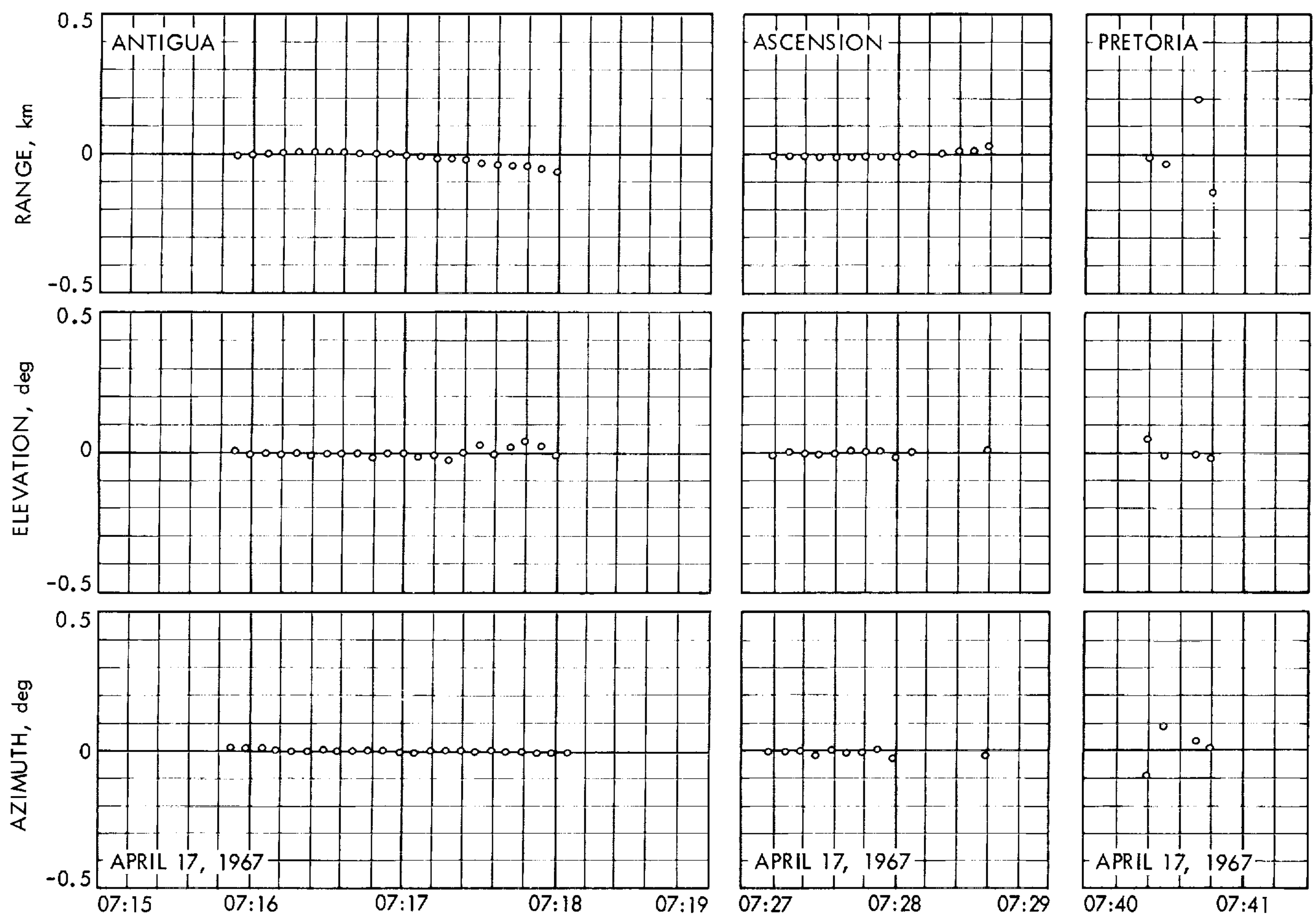
ANTIGUA
ASCENSION
PRETORIA
RANGE, km
ELEVATION, deg
AZIMUTH, deg
0.5
0
-0.5
APRIL 17, 1967
07:15
07:16
07:17
07:18
07:19
07:27
07:28
07:29
07:40
07:41

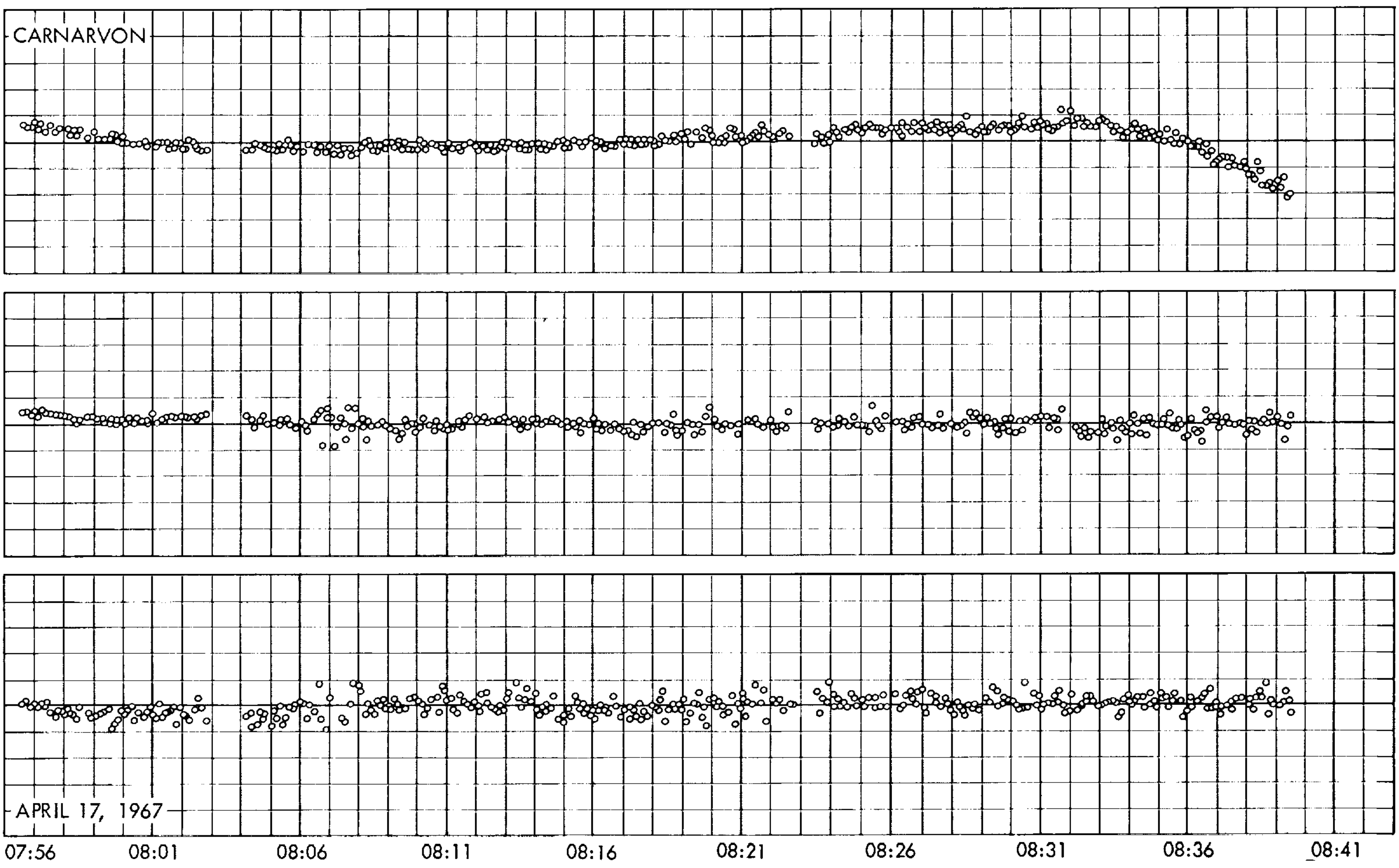

Fig. 21. AFETR tracking data residuals for *Surveyor III*

Table 24. Summary of AFETR tracking data used in orbit computations for *Surveyor III/Centaur*

Orbit identification	AFETR station	Data type[a]	Beginning data time (month/date-GMT) 1967	h:min:s	End data time (month/date-GMT) 1967	h:min:s	Number of points	Standard deviation[a]	Root mean square[a]	Mean error residual[a] (O − C)
AFETR parking orbit	74	Az	4/17	07:15:54	4/17	07:18:18	23	0.00404	0.00448	0.00193
		El		07:15:54		07:18:06	22	0.0161	0.0165	0.00357
		R		07:15:54		07:18:18	22	0.0222	0.0260	−0.0135
	75	Az		07:27:12		07:28:36	11	0.0245	0.0306	−0.0183
		El		07:27:12		07:28:36	11	0.00773	0.00868	−0.00395
		R		07:27:12		07:28:36	14	0.00945	0.00955	−0.00135
AFETR transfer orbit	76	Az		07:40:24		07:40:48	4	0.0663	0.0663	−0.000775
		El		07:40:24		07:40:48	4	0.0238	0.0239	−0.00122
		R		07:40:24		07:40:48	4	0.120	0.120	0.000137
AFETR postretro orbit	83	Az		07:56:42		08:39:36	385	0.0132	0.0134	−0.00184
		El		07:56:42		08:39:36	372	0.00789	0.00791	0.000634
		R	4/17	07:56:42	4/17	08:39:36	390	0.0185	0.0185	0.000259

[a]Azimuth (az) and elevation (el) are expressed in degrees; Range (R), in kilometers.

Stations
Station 74, Antigua
Station 75, Ascension
Station 76, Pretoria
Station 83, Carnarvon

between separation and the beginning of the *Centaur* retromaneuver. Because of problems in locking onto the *Centaur*, no usable data were available between main engine cutoff and separation. The AFETR converged conditions (geocentric Cartesian position and velocity) are given in the top of Table 25. Since the AFETR and JPL transfer orbits were computed with different epochs, the JPL converged conditions were mapped to the AFETR epoch for comparison. The most significant differences revealed by this comparison were those in the X and Z velocity components of 18.8 and 48.7 m/s, respectively. However, differences this large are considered normal for these transfer orbit calculations. The differences may be attributed to the different data spans used in the orbits. The AFETR real-time orbits were computed before the mark times were known and, consequently, include some data taken during the *Centaur* retromaneuver. The JPL transfer orbit used only four points of data obtained between separation and start of *Centaur* retro.

Pretoria had problems locking-on with its radar. Out of 20 potential data points received from Pretoria between *Centaur* second main engine cutoff (MECO 2) and the beginning of retromaneuver, only 5 had a data condition code indicating an *in-lock* condition. Out of these 5 points only 4 were considered usable for the JPL orbit. The AFETR transfer orbit was computed with 17 points of data which, as already noted, include some burn data taken during *Centaur* retro.

Table 25. Converged conditions at injection epoch in space-fixed cartesian coordinates, *Surveyor III*

Parameter	AFETR transfer orbit by JPL	AFETR transfer orbit	Difference between orbits by JPL and AFETR
Epoch, GMT 07:42:17.9 (Apr. 17, 1967)			
X, km	6047.2997	6046.7853	−0.5144
Y, km	492.59301	506.50451	3.91150
Z, km	−3162.9813	−3161.8319	1.1491
DX, km/s	0.10297172	0.08416453	−0.01880719
DY, km/s	10.289004	10.290564	0.001560
DZ, km/s	−3.0536272	−3.0049606	0.0486666
Epoch, GMT 07:38:39.838 (Apr. 17, 1967)			
		Best DSS orbit	
X, km	5836.2944	5839.9109	3.6165
Y, km	−1742.4379	−1730.0228	12.4151
Z, km	−2405.2075	−2413.5618	−8.3543
DX, km/s	1.8607523	1.8349779	−0.0259744
DY, km/s	10.096772	10.101964	0.005192
DZ, km/s	−3.8775678	−3.8396961	0.0388717

The orbital elements obtained from the best premaneuver orbit computed from DSIF data only are reasonably consistent with the JPL transfer orbit computed from Pretoria data. When comparing these two orbits, it should be kept in mind that the DSIF is tracking the spacecraft and the AFETR is tracking the *Centaur*. Since the Pretoria

Table 26. Transfer orbit parameter solutions, *Surveyor III*

Parameter	Best DSIF orbit	AFETR transfer orbit by JPL	AFETR transfer orbit	Difference between transfer orbits by JPL and DSIF orbit	Difference between transfer orbits by JPL and AFETR
Epoch, GMT	07:38:39.838 (Apr. 17, 1967)	07:38:39.838 (Apr. 17, 1967)	07:42:17.9 (Apr. 17, 1967)		(Since JPL and AFETR used different Epochs, the differences between injection conditions would be meaningless)
Radius, km	6551.5651	6548.5450	6842.0	−3.0201	
Latitude, deg	−21.616922	−21.548509	−27.522	0.068413	
Longitude, deg	24.083007	23.961265	44.461	−0.121742	
Velocity, km/s	10.549416	10.562811	10.298	0.013395	
Flight path angle, deg	2.0786519	2.1485487	12.475	0.0698968	
Azimuth, deg	112.17171	112.34263	102.808	0.17092	
Semimajor axis, km	261992.97	307887.81	252520.7	45894.84	−5536.1
Eccentricity	0.97502421	0.97875873	0.9740863	0.00373452	−0.0046724
Inclination, deg	29.980849	30.046146	29.93845	0.065297	−0.09770
Longitude of node, deg	120.11426	120.32213	119.9996	0.20787	−0.3225
Argument of perigee, deg	223.44343	223.00454	223.53038	0.43889	−0.52584
C_3, km^2/s^2	−1.5214196	−1.2946315	−1.57	0.2267781	−0.26
Encounter					
B, km	821.98308	9749.1163	2714.3445	8927.1332	−7034.7718
B · RT, km	−97.110296	7098.2878	−1008.8109	7195.3981	−8107.0987
B · TT, km	816.22667	−6682.7819	2519.9140	−7499.0086	9202.6959
Latitude, deg	−10.092257	−38.751088	12.781923	−28.658831	51.533011
Longitude, deg	323.02872	186.612	2.8061422	−136.416	−183.806

data were taken after separation, it is logical that the orbit based on those data would differ some from the orbit based on DSIF data only. The values for the orbital elements obtained from the AFETR transfer orbits and the DSIF orbit are given in Table 26 which also lists the differences between the orbits being compared. The amount and types of tracking data used, and their associated data noise statistics, are given in Table 24. The tracking data residuals (O − C) for the transfer orbit are shown in Fig. 21.

D. Analysis of the Postretro Orbit Data

Approximately one hour of postretro data from Carnarvon is available for analysis. These data are relatively noise-free, thus lending to a highly reliable postretro orbit computation. The AFETR postretro orbit computation was based on a data span of 12 min 50 s, from 07:50:06 to 08:02:56 GMT, which included 129 points of Carnarvon data. The JPL postretro orbit was based on approximately 390 points of range and angular data taken during the time span 07:56:42 to 08:39:36. Since the data were of high quality and the JPL solution contained three times as many points as the AFETR solution, confidence in the JPL solution is higher. Comparison of the two solutions reveals no outstanding differences. The AFETR solution gave a **B**-plane miss of 38,568 km, while the JPL solution gave a miss of 39,235 km, a difference of 667 km. However, this is considered reasonable for the postretro solutions. The orbit parameters for the JPL and AFETR postretro orbit solutions are given in Table 27. The tracking data residuals for the JPL solution are given in Fig. 21.

E. Conclusions

Although limited in quantity and quality, the Pretoria transfer orbit data were useful during flight operations for verifying the initial DSIF orbit estimate.

The inclusion of burn data in the transfer orbit computed by the AFETR was not a discrepancy on the part of the AFETR. They were responsible for computing a *quick-look* orbit to provide initial acquisition information to the DSIF. They fulfilled this obligation.

Table 27. Postretro parameter solutions, *Surveyor III*

Parameter	JPL orbit with Carnarvon data	AFETR orbit	Difference between orbits by JPL and AFETR
Epoch, GMT	07:56:32.9 (Apr. 17, 1967)	07:56:32.9 (Apr. 17, 1967)	—
Radius, km	10428.581	10435.	6.
Latitude, deg	−25.781722	−25.772	−0.010
Longitude, deg	99.213737	99.267	0.053
Velocity,[a] km/s	8.1047094	8.102	−0.003
Flight path angle,[a] deg	40.017568	40.039	0.021
Azimuth,[a] deg	72.440034	72.420	−0.020
Semimajor axis, km	182487.62	183166.7	679.1
Eccentricity	0.96414709	0.9642721	0.0001250
Inclination, deg	29.970017	29.96997	−0.00005
Longitude of node, deg	120.00405	120.0248	0.0207
Argument of perigee, deg	223.40281	223.40566	0.00285
C_3, km^2/s^2	−2.1842647	−2.17	−0.01
B, km	39235.485	38568.279	−667.206
B • **T**T, km	36347.191	35678.663	−668.528
B • **R**T, km	−14775.132	−14647.360	127.772

[a]Earth-fixed.

IX. *Surveyor IV* Inflight Orbit Determination Analysis

A. View Periods and Tracking Patterns

Figure 22 summarizes the tracking station view periods and their data coverage for the period from launch to loss of signal. Figures 23 through 27 are tracking station stereographic projections for the tracking stations which show the trace of the spacecraft trajectory for the view periods in Fig. 22.

B. Premaneuver Orbit Estimates

Table 28 summarizes the tracking data used for both the inflight and postflight orbital calculations and analyses. This table provides a general picture of the performance of the data recording and handling system. The first estimate of the spacecraft orbit (PROR Y) calculated from DSS data only was completed at launch plus 2 h 00 min (L + 02 h 00 min), based on approximately one hour of DSS 72 two-way doppler and angle (az–el) data and 20 min of DSS 51 two-way doppler and angle (HA–dec) data. When mapped to the moon, this orbit solution indicated that the correction required to achieve encounter at the prelaunch aiming point was well within the nominal midcourse correction capability. These results were verified by the second (ICEV) orbit computation completed at L + 2 h 54 min and the third (PREL) at L + 5 h 07 min.

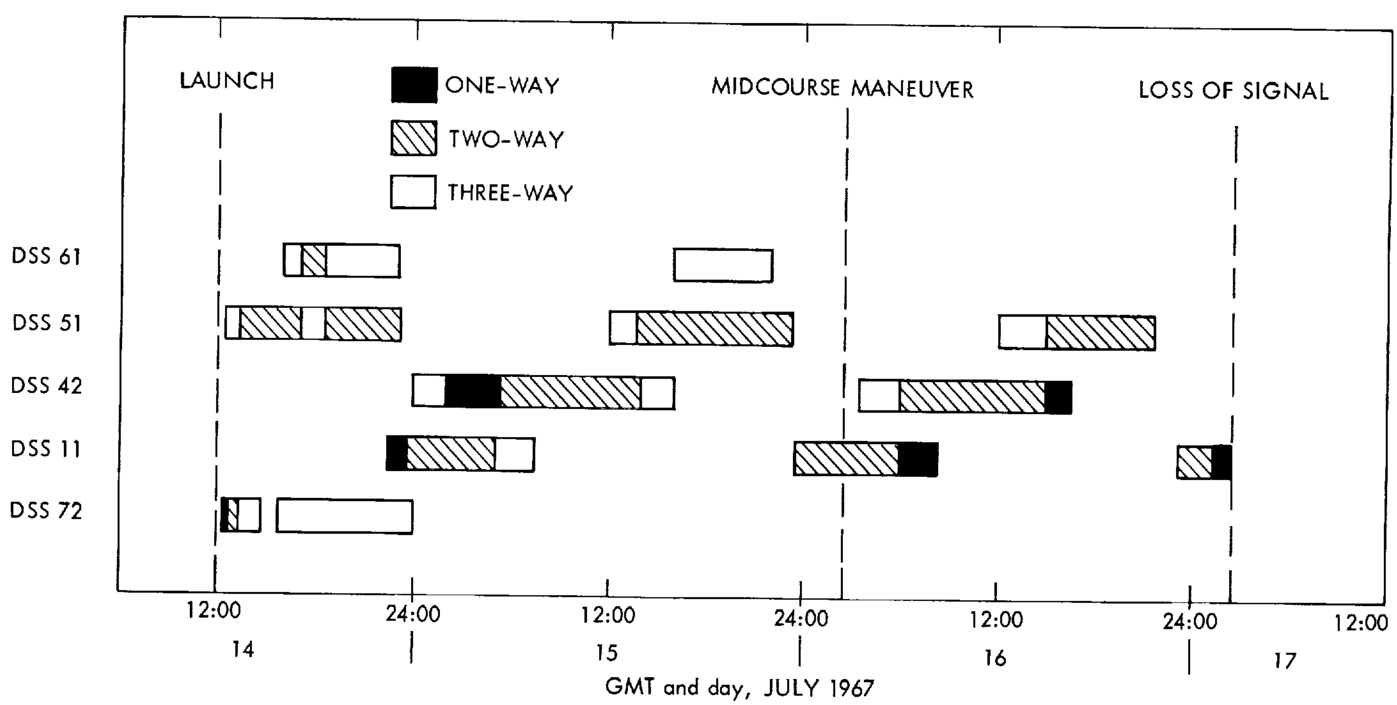

Fig. 22. Tracking station view periods and doppler data coverage for *Surveyor IV*

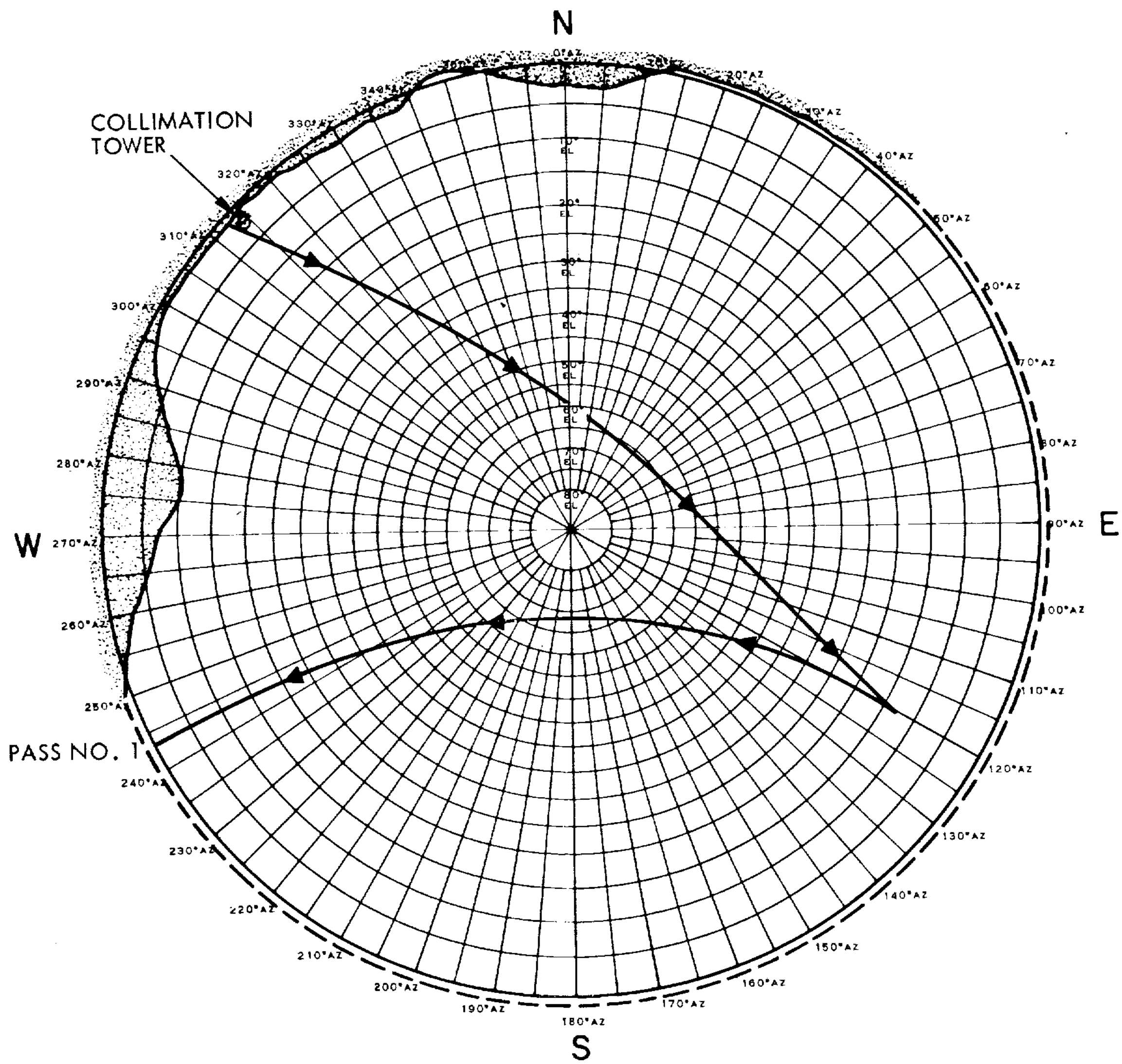

Fig. 23. DSS 72 stereographic projection for Surveyor *IV*

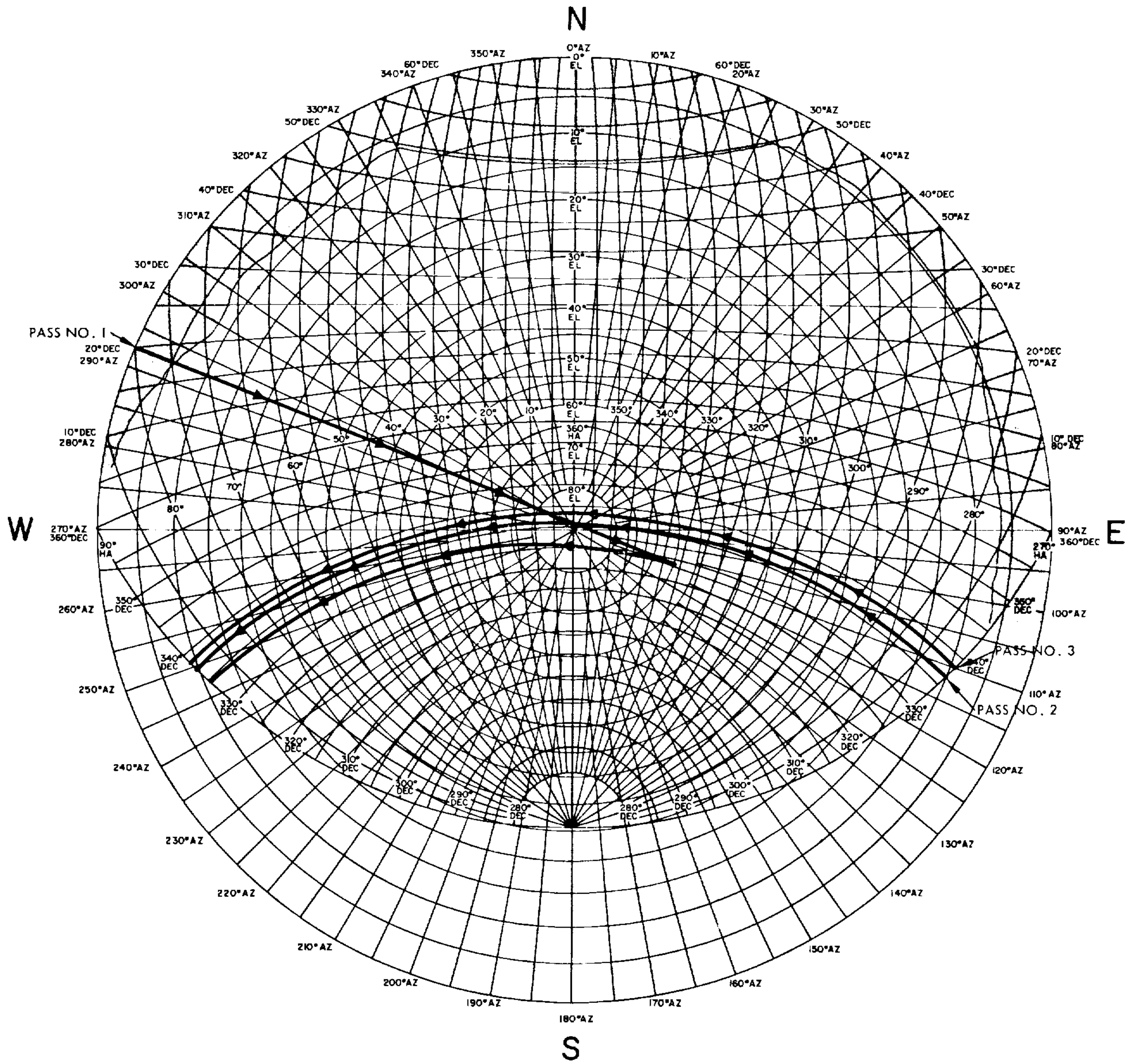

Fig. 24. DSS 51 stereographic projection for Surveyor IV

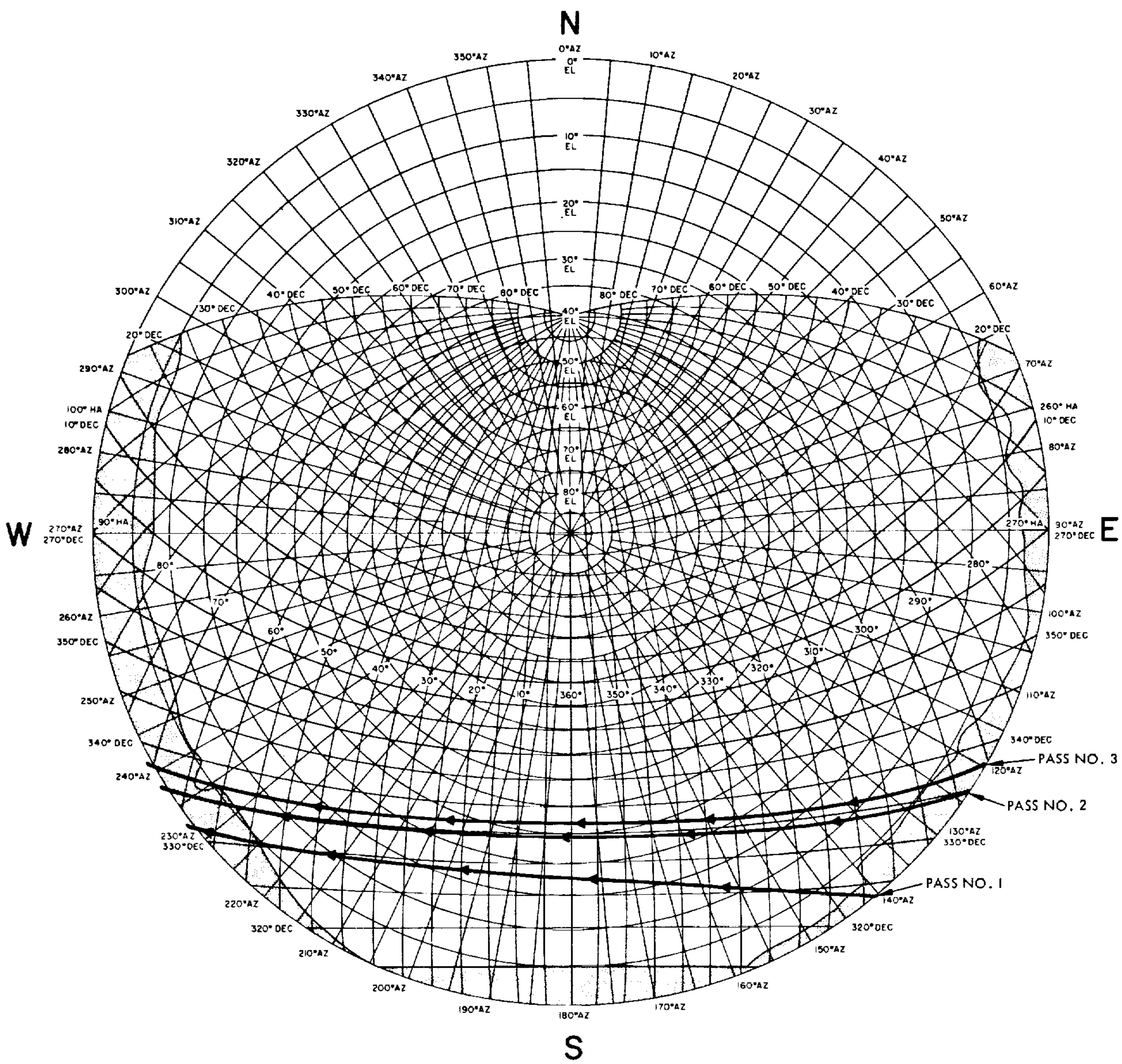

Fig. 25. DSS 61 stereographic projection for Surveyor IV

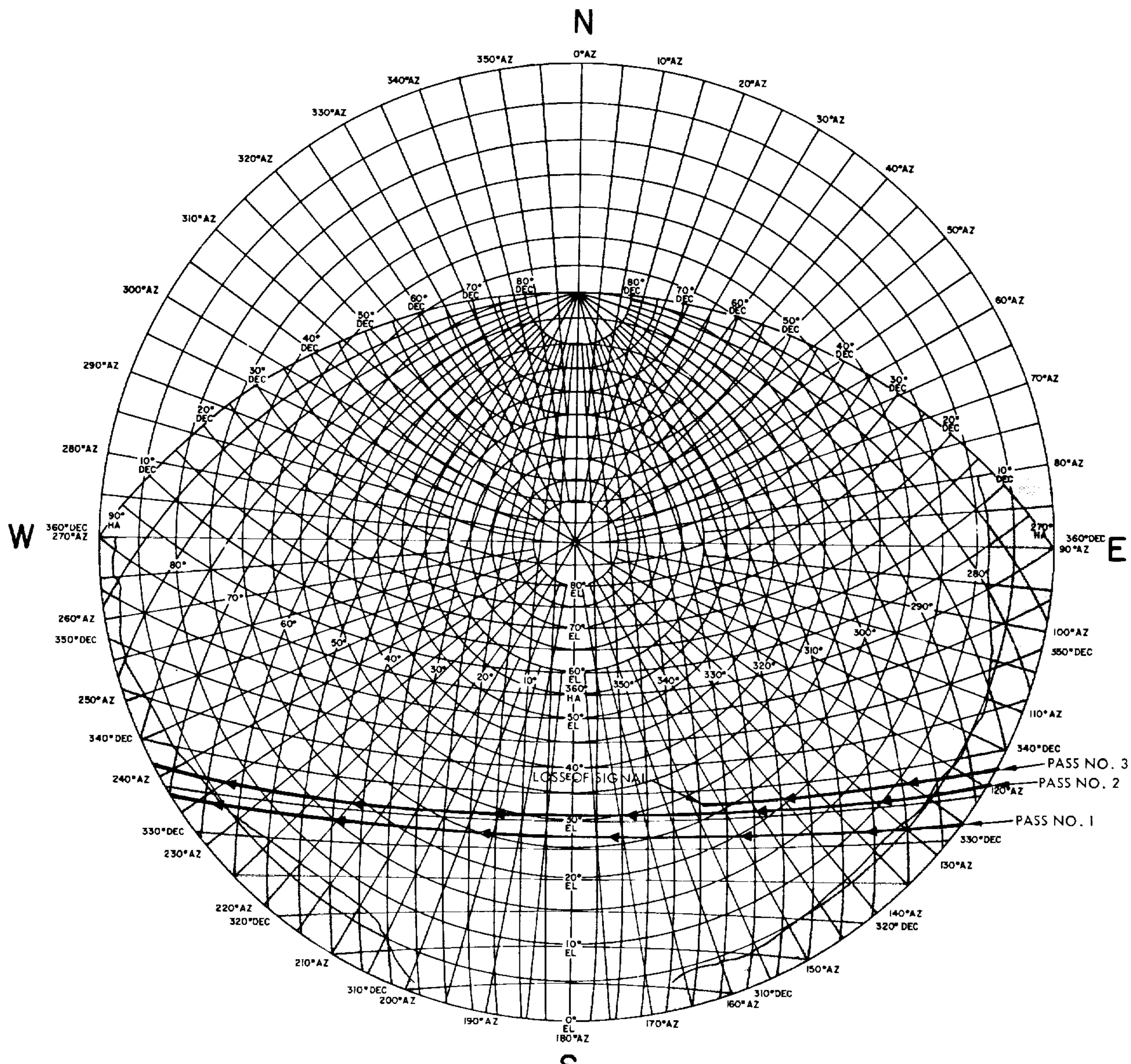

Fig. 26. DSS 11 stereographic projection for *Surveyor IV*

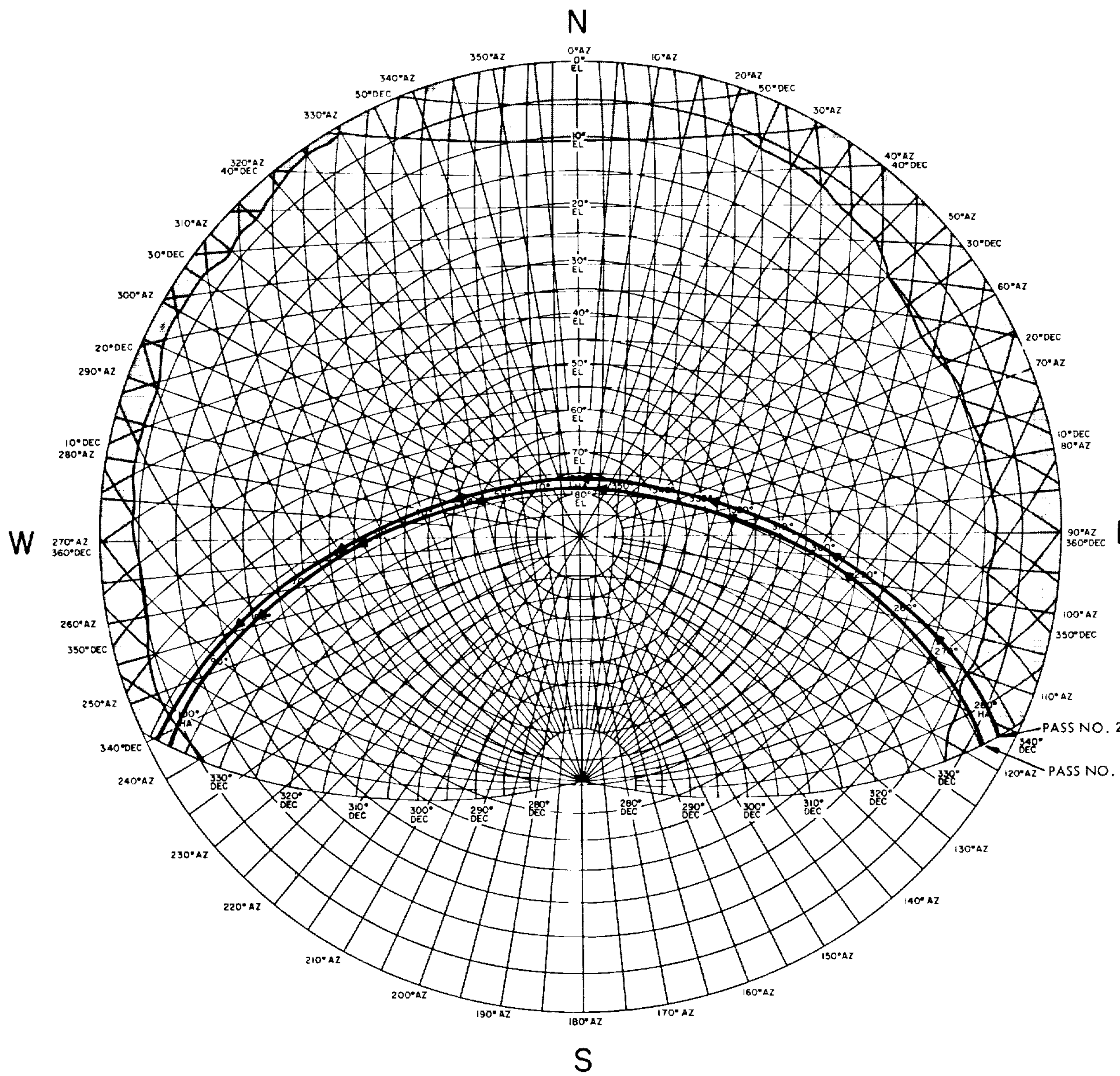

Fig. 27. DSS 42 stereographic projection for Surveyor IV

Table 28. Summary of premaneuver and postmaneuver data used in orbit determination for *Surveyor IV*

DSS	Data type	Points received	Number of points used in real time, % of received		Bad format, % of received		Bad data condition, % of received		Blunder points, % of received		Rejection limits on blunder points	Points used in postflight analysis
			Points	%	Points	%	Points	%	Points	%		
(A)	(B)	(C)	(D)		(E)		(F)		(G)		(H)	(I)
Premaneuver data												
11	CC3	719	575	80.0	5	0.7	3	0.4	8	1.1	0.114	556
	HA	791	0	0.0	8	1.0	7	0.9	—	—	—	0
	Dec	791	0	0.0	8	1.0	7	0.9	—	—	—	0
42	CC3	545	519	95.2	4	0.7	5	0.9	1	0.2	0.021	519
	HA	790	0	0.0	8	1.0	11	1.4	—	—	—	0
	Dec	790	0	0.0	8	1.0	11	1.4	—	—	—	0
51	CC3	1066	914	85.7	52	4.9	20	1.9	6	0.6	0.029	869
	HA	1516	171	11.3	61	4.0	1	0.1	12	0.8	0.098	0
	Dec	1516	171	11.3	61	4.0	1	0.1	9	0.6	0.088	0
61	CC3	90	39	43.3	4	4.4	7	7.8	20	22.2	0.100	0
	HA	919	0	0.0	27	2.9	62	6.7	—	—	—	0
	Dec	919	0	0.0	27	2.9	62	6.7	—	—	—	0
72	CC3	209	118	56.5	10	4.8	41	19.6	33	15.8	0.079	95
	Az	816	182	22.3	29	3.6	19	2.3	13	1.6	0.600	0
	El	816	182	22.3	29	3.6	19	2.3	11	1.3	0.240	0
Postmaneuver data												
11	CC3	362	289	79.8	39	10.8	1	0.3	1	0.3	0.030	286
42	CC3	541	505	93.3	0	0.0	9	1.7	2	0.4	0.021	505
51	CC3	498	463	93.0	1	0.2	29	5.8	0	0.0	0.022	462

As additional data were received and used in the orbit computations, it became clear that the angle data were biased with respect to the two-way doppler data. This was partly due to the bias caused by mechanical deflection as the antenna moves from horizon to horizon. Consequently, the angle data were weighted out of the orbit solutions computed during the third orbit (PREL) period. Eliminating the angle data resulted in a change of approximately 40 km in **B**-space when the solution was mapped to target.

During the data consistency (DACO) orbit computation period, the first data from DSS 61 were received. As these data were added to the data already received from DSS 72 and DSS 51, it became evident that the data were not consistent. DACO orbits, which provided a comparison of the data from DSS 51, 72 and 61, influenced the decision not to use DSS 61 in any later orbit computations because of an apparent bias and excessive noise. Also, during the DACO period, the first DSS 11 data were processed and found to be consistent with DSS 51 and 72. Eleven orbits were computed during the DACO period, giving a good comparison of the relative consistency of the two-way doppler data. As mentioned earlier, the angle data were dropped from the solutions during the PREL orbit period.

By the end of the DACO orbit period ($L + 9$ h 49 min) it had been decided to delay the midcourse maneuver to approximately $L + 39$ h during the second view period at Goldstone. Orbit computations indicated a very small miss; consequently, executing the maneuver during the first Goldstone view period was dismissed in favor of the increased accuracy which could be achieved by the later one.

During the period from $L + 9$ h 49 min to $L + 16$ h 40 min, 9 additional orbits were run to update the two-way doppler solution and continue data consistency checks as new data came in. No problems were encountered during this time.

At the beginning of the last premidcourse (LAPM) orbit computation period, the following amount of usable two-way doppler data was available: 5 h 18 min from DSS 11, 8 h 46 min from DSS 42, 13 h 38 min from DSS 51, and 36 min from DSS 72.

The LAPM orbit solutions indicated that the data from DSS 42 were consistent with the data from DSS 11, 51 and 72. After updating the ODP data file the final premidcourse orbit was run (LAPM YC) using all the data (except DSS 61) to $MC - 3$ h 40 min. When mapped to target, this solution predicted an unbraked impact point at 2.00° S lat and 354.1° E lon approximately 178 km southwest of the initial aiming point.

The numerical results of the premaneuver orbit computations are presented in Tables 29 and 30. Amounts and types of tracking data used in the various orbit computations, together with the associated noise statistics, are given in Table 31. Figure 28 is representative of premidcourse residual plots for two-way doppler data used in *Surveyor IV* orbit solutions. Representative premidcourse unbraked impact points are shown in Fig. 29.

C. Postmaneuver Orbit Estimates

The first postmidcourse orbit computation (1 POM) was completed approximately 10 h 30 min after maneuver execution. For the final (1 POM XF) orbit computation during this period, approximately 3 h 20 min of DSS 11 and 5 h 35 min of DSS 42 two-way doppler data were used. The initial values for the first postmidcourse orbit estimation were the conditions obtained by mapping the PRCL YB conditions to the epoch at the end of the midcourse burn and adding the midcourse velocity increment. *A priori* information from the premaneuver tracking data was not used. When the 1 POM XF orbit was mapped to the moon, it indicated the unbraked impact point as approximately 3.06 km south and 10.5 km west of the aim point. Subsequent inflight postmidcourse orbit computations refined the estimated unbraked impact point to 0.3 km north and 8.1 km west of the aim point.

A decision had to be made no later than 6 h before the *Surveyor* retrofiring sequence to determine whether to track the spacecraft with DSS 51 or DSS 61 just before switching to DSS 11 during the terminal phase. Since DSS 61 data had exhibited an unexplained bias and excessive data noise from the recurring counter problem, it was decided to track with DSS 51. The final terminal maneuver computations were based on the 3 POM YD orbit solution.

Numerical results of the inflight postmidcourse orbit solutions are presented in Tables 32 and 33. Figure 30 is a plot showing the postmidcourse unbraked impact points obtained from these solutions. The amounts of tracking data used in the various postmidcourse orbit computations, together with the associated data statistics, are given in Table 34. Representative two-way doppler residuals are presented in Fig. 31.

D. AMR Backup Computations

After retrofire minus 2 h ($R - 2$ h), primary emphasis was placed on obtaining the best estimate of unbraked impact time to be used for sending the ground command to back up the *Surveyor* AMR. The AMR backup computations were characterized by a consistent estimated unbraked impact time (EUBIT) between 02:02:29.593 and 02:02:30.397 GMT. The last orbit (3 POM YD) computation made before changing to FINAL ($R - 5$ h 40 min) epoch gave a EUBIT of 02:02:29.645, which is unusually close to the time indicated by the FINAL orbits. Some change in estimated unbraked time is expected as more near-encounter data are used in the orbit solution. This was seen as the FINAL YF orbit solution yielded a EUBIT of 02:02:30.397. This solution was used as the basis for computing the AMR backup time, using data up to $R - 1$ h 40 min consisting of 53 min of two-way doppler from DSS 11 and 3 h from DSS 51. Another solution (POST 1) was computed later which included all data from the end of midcourse burn to $R - 40$ min. This solution gave a EUBIT of 02:02:30.228 GMT, thus increasing confidence in the solution chosen for the AMR backup.

Since all the postmidcourse data fitted well and appeared consistent with the near-encounter data, it was felt that the FINAL YF solution was good within the 1-σ stated uncertainty of 0.5 s. The estimated AMR mark time based on this solution was July 17, 1967, 02:01:53.99 GMT. It was used as the basic reference point from which the desired time of backup command transmission from the ground was calculated. The uncertainty (orbit determination and manual implementation) associated with executing the AMR backup command was determined as 0.72 s (1 σ). With the use of this value and the amount of predicted vernier engine propellant available, a backup delay of 1.17 s was specified. Known fixed delays such as the propagation delay, operator delay, command generator and command decoder delays totaled 2.27 s. The final GMT for transmission of the AMR backup command was rounded up to the next second, yielding 02:01:53.0. This backup mark command should have arrived at the spacecraft approximately 1.27 s after the predicted mark. Telemetry records show that the backup command arrived at the spacecraft 1.25 s after the actual AMR mark time. Table 35 summarizes the results of the inflight orbit determinations performed to back up the AMR.

Table 29. Premaneuver computations for *Surveyor IV*

Orbit identification	Time computed		Target statistics										Selenocentric conditions at unbraked impact			Type solution	Data used	
	Start h:min	Stop h:min	B, km	B • TT, km	B • RT, km	T_L, h	SMAA, km (1σ)	SMIA, km (1σ)	θ_T, deg	$\sigma_{T,\,impact}$, s (1σ)	ϕ_{99}, deg	SVFIXR, km/s (1σ)	Latitude, deg (south)	Longitude, deg	GMT, h:min:s July 17, 1967		DSS	Data
ETR	12:27	12:42	3882.77	2498.0	2972.5	61.43	8224.0	1485.4	28.58	0.488E11	706.7	0.0282	−29.15	102.5	01:50:12.319	6x6		
PROR YA	13:25	13:53	1881.97	1878.4	115.33	62.19	93.42	35.80	97.31	60.93	3.14	0.000627	−8.75	357.2	02:12:59.134	6x6	72, 51	CC3, Angles
PROR XA	13:45	14:21	1823.17	1819.9	−108.73	62.18	92.87	17.43	96.81	40.20	2.187	0.000617	−4.47	355.4	02:12:09.999	6x6		CC3, Angles
ICEV YA	14:25	14:49	1824.92	1823.7	66.86	62.20	89.48	6.80	99.19	36.45	1.835	0.000615	−7.93	355.8	02:13:42.463	6x6		CC3, Angles
ICEV XA	14:28	14:47	1806.21	1805.3	−57.29	62.19	75.90	7.71	98.99	29.22	1.573	0.000613	−5.52	355.1	02:12:48.886	6x6		CC3, Angles
PREL XB	15:39	15:53	1785.30	1767.4	−251.9	62.17	55.82	5.78	104.1	17.24	1.044	0.000612	−1.74	354.0	02:11:39.209	6x6	72, 51	CC3
PREL YB	16:43	17:00	1785.69	1768.7	−246.0	62.17	26.46	5.29	109.3	7.59	0.452	0.000611	−1.86	354.1	02:11:41.012	6x6	72, 51	CC3
DACO XB	18:28	18:43	1787.95	1772.6	−234.1	62.17	16.60	4.98	114.3	4.68	0.265	0.000610	−2.09	354.2	02:11:44.535	6x6	72, 51	CC3
DACO YB	18:46	19:02	1783.01	1767.8	−232.4	62.17	91.21	37.8	174.3	26.63	0.686	0.000629	−2.13	354.1	02:11:45.090	6x6	51, 61	CC3
DACO YC	20:43	21:07	1786.40	1770.2	−240.1	62.17	5.01	3.93	55.76	1.501	0.103	0.000610	−1.97	354.1	02:11:43.937	6x6	72, 51, 61	CC3
DACO XF	20:56	21:10	1786.24	1769.9	−240.6	62.17	4.9523	2.62	64.84	1.630	0.111	0.000610	−1.96	354.2	02:11:42.518	6x6	72, 51	CC3
DACO XH	21:25	21:42	1785.14	1769.237	−237.8	62.17	3.3263	2.23	46.3	1.4957	1.0636	0.000610	−2.02	354.1	02:11:42.003	6x6	11, 72, 51	CC3
NOMA YA	00:59	01:21	1785.07	1769.207	−237.5	62.17	3.012	1.93	34.69	1.4161	0.1026	0.000610	−2.03	354.09	02:11:41.925	6x6	11, 72, 51	CC3
NOMA YD	11:40	11:59	1784.26	1768.4	−237.2	62.17	2.469	1.798	49.86	0.9485	0.0733	0.000610	−2.03	354.1	02:11:42.388	6x6	72, 42, 51	CC3
NOMA YE	11:59	12:25	1781.68	1765.9	−236.7	62.17	6.133	2.946	147.67	1.373	0.1416	0.000610	−2.05	354.0	02:11:43.204	6x6	72, 11, 42	CC3
NOMA YF	12:27	13:25	1784.06	1768.3	−236.7	62.17	2.137	1.567	33.33	0.8641	0.0660	0.000610	−2.04	354.1	02:11:42.470	6x6	72, 11, 42, 51	CC3
LAPM XA	21:23	21:44	1782.68	1766.9	−236.8	42.26	1.848	1.41	34.91	0.762	0.0564	0.000610	−2.05	354.0	02:11:42.614	6x6	42, 51	CC3
LAPM YB	22:27	23:04	1784.19	1768.2	−238.7	62.17	7.21	3.18	82.59	2.027	0.1603	0.000610	−2.01	354.1	02:11:42.121	18x18	72, 11, 42, 51	CC3
LAPM XC	22:09	22:29	1781.78	1765.8	−237.7	42.26	4.00	3.12	89.49	1.412	0.1085	0.000610	−2.03	354.0	02:11:42.752	6x6	42, 51	CC3
LAPM XE	22:50	23:19	1781.70	1765.7	−238.0	42.26	1.82	1.27	32.52	0.7519	0.0555	0.000610	−2.02	354.0	02:11:42.819	6x6	42, 51	CC3
LAPM YC[a]	23:12	23:43	1784.01	1768.0	−238.7	62.17	2.07	1.22	35.00	0.8223	0.0626	0.000610	−2.00	354.1	02:11:42.145	6x6	72, 11, 42, 51	CC3
PRCL YB[b]	04:33	05:58	1778.7	1763.0	−236.2	62.18	48.14	9.12	83.05	16.80	1.163	0.000712	−2.07	354.0	02:11:45.992	6x6	72, 11, 42, 51	CC3

[a]Orbit used for midcourse computations.

[b]Current best estimate, premaneuver as of July 24, 1967.

SMAA = Semimajor axis of dispersion ellipse.

SMIA = Semiminor axis of dispersion ellipse.

θ_T = Orientation angle of dispersion ellipse measured counterclockwise from B • TT axis.

$\sigma_{T,\,impact}$ = Uncertainty in predicted unbraked impact time.

ϕ_{99} = 99% velocity vector pointing error.

SVFIXR = Uncertainty in magnitude of velocity vector at unbraked impact.

Table 30. Premaneuver position and velocity at injection epoch,[a] *Surveyor IV*

Orbit identification	Geocentric space-fixed position, km			Geocentric space-fixed velocity, km/s			Uncertainties (1σ)					
							Position, km			Velocity, m/s		
	X	Y	Z	DX	DY	DZ	σ_X	σ_Y	σ_Z	σ_{DX}	σ_{DY}	σ_{DZ}
ETR	3098.4646	5358.3490	2140.6742	−8.0054246	6.1087959	−4.3545489	0.5546	0.6189	0.3257	27.05	31.15	14.49
PROR YA	3086.5737	5361.6350	2138.8208	−8.0390635	6.0652971	−4.3562983	1.189	1.179	1.601	0.6071	0.1893	0.9458
PROR XA	3086.9832	5364.9950	2135.5580	−8.0388224	6.0603508	−4.3596912	0.7629	1.090	1.503	0.4550	1.573	0.8266
ICEV YA	3085.4966	5362.9185	2138.8048	−8.0397978	6.0628234	−4.3572016	0.5236	1.119	1.424	0.3092	1.581	0.9961
ICEV XA	3086.1033	5364.6475	2136.6177	−8.0393009	6.0605345	−4.3592688	0.4806	0.9204	1.185	0.3115	1.323	0.7652
PREL XB	3087.0362	5367.1017	2133.5783	−8.0396596	6.0569386	−4.3606015	0.2847	0.7651	0.8512	0.4023	1.130	0.9905
PREL YB	3087.0036	5367.0326	2133.6613	−8.0396324	6.0570451	−4.3605965	0.2365	0.4447	0.4271	0.4173	0.6391	1.024
DACO XB	3086.9892	5366.8527	2133.8468	−8.0396035	6.0573190	−4.3604621	0.2323	0.3415	0.2973	0.4139	0.4704	1.006
DACO YB	3086.7373	5366.8889	2133.8368	−8.0400841	6.0571453	−4.3600178	4.324	3.969	2.641	3.407	5.011	12.55
DACO YC	3087.0555	5366.8391	2133.8549	−8.0399126	6.0572518	−4.3599387	0.2140	0.1609	0.1229	0.3439	0.1824	0.8014
DACO XF	3086.9770	5366.9696	2133.7339	−8.0395975	6.0571463	−4.3606039	0.1902	0.1367	0.1259	0.3925	0.1186	0.8343
DACO XH	3086.8602	5367.0487	2133.6730	−8.0393869	6.0570837	−4.3611032	0.106694	0.08313	0.09723	0.28117	0.07207	0.51466
NOMA YA	3086.8471	5367.0578	2133.6650	−8.0393592	6.0570775	−4.3611659	0.0840	0.07003	0.08895	0.2495	0.06294	0.42122
NOMA YD	3086.8385	5367.0451	2133.6892	−8.0394281	6.0570733	−4.3610587	0.0750	0.0475	0.0568	0.1588	0.0540	0.2238
NOMA YE	3086.8241	5367.0160	2133.7534	−8.0396188	6.0570534	−4.3607564	0.0936	0.0809	0.0976	0.3537	0.1489	0.5234
NOMA YF	3086.8311	5367.0373	2133.6971	−8.0394506	6.0570777	−4.3610265	0.0714	0.0414	0.0515	0.1487	0.0491	0.2092
LAPM XA[a]	−119963.34	−120517.78	−77576.644	−0.83177353	−1.3500233	−0.56701688	0.6386	0.6618	0.6670	0.0085	0.0053	0.0095
LAPM YB	3086.8492	5367.0903	2133.6695	−8.0393941	6.0570272	−4.3611099	0.1421	0.0970	0.0909	0.1806	0.1205	0.2637
LAPM XC[a]	−119963.21	−120517.92	−77576.751	−0.83176856	−1.3500302	−0.56701319	0.9044	0.9487	1.017	0.0211	0.0197	0.0250
LAPM XE[a]	−119963.16	−120517.87	−77576.768	−0.83176783	−1.3500318	−0.56701197	0.6272	0.6266	0.6434	0.0084	0.0049	0.0091
LAPM YC[b]	3086.8478	5367.0926	2133.6705	−8.0393992	6.0570216	−4.3611047	0.0706	0.0401	0.0498	0.1513	0.0408	0.2068
PRCL YB[c]	3086.8904	5367.0377	2133.6794	−8.0394324	6.0570880	−4.3609970	0.1348	0.1832	0.2694	0.5559	0.1343	0.9716

[a] Injection epoch is July 14, 1967, 12:05:6.480 GMT, for all solutions except for the LAPM XA, LAPM XC, and LAPM XE solutions, for which it is July 15, 8:00:5.000 GMT.

[b] Orbit used for midcourse maneuver computations.

[c] Current best estimate premaneuver as of July 24, 1967.

Table 31. Summary of premaneuver DSS tracking data used in orbit computations for *Surveyor IV*

Orbit identification	DSS	Data type[a]	Data span, GMT: Beginning 1967	Beginning h:min:s	Ending 1967	Ending h:min:s	Number of points	Standard deviation[a]	Root mean square[a]	Mean residual[a] (O − C)	Sample rate, s
ETR	91	Az	7/14	12:05:12	7/14	12:06:18	10	0.0126	0.0217	0.0177	6
		El		12:05:12		12:06:06	9	0.0139	0.0298	−0.0263	6
		R		12:05:12		12:06:18	9	0.00343	0.00906	0.00839	6
	77	Az		12:05:15		12:05:33	4	0.0198	0.0928	−0.0906	6
		El		12:05:15		12:05:33	4	0.123	0.446	0.428	6
		R		12:05:15		12:05:33	4	0.0487	0.111	−0.0999	6
PROR YA	72	CC3		12:26:08		13:04:32	118	0.136	0.144	−0.0478	10
		Az		12:16:23		13:17:02	149	0.0223	0.0292	−0.0189	10
		El		12:16:23		13:17:02	154	0.0323	0.0367	0.0174	10
	51	HA		12:42:11		13:04:02	35	0.0175	0.0202	−0.0100	60
		Dec		12:42:11		13:04:02	35	0.00456	0.0141	−0.0133	60
		CC3		13:14:32		13:16:32	3	0.0392	0.179	−0.174	60
		HA		13:14:02		13:17:02	4	0.00102	0.00905	−0.00900	60
		Dec		13:14:02		13:17:02	4	0.00240	0.00255	−0.000865	60
PROR XA	72	CC3		12:26:08		13:04:32	113	0.0926	0.0944	−0.0183	10
		Az		12:26:53		13:37:02	135	0.0186	0.0386	−0.0338	10
		El		12:26:53		13:37:02	134	0.0239	0.0454	0.0387	10
	51	HA		12:42:11		13:04:02	152	0.0114	0.0181	0.0140	60
		Dec		12:42:11		13:04:02	152	0.0136	0.0217	−0.0169	60
		CC3		13:14:32		13:35:32	18	0.0744	0.0744	0.00255	60
		HA		13:14:02		13:36:02	19	0.00283	0.0182	0.0180	60
		Dec		13:17:02		13:36:02	19	0.00147	0.00330	−0.00295	60
ICEV YA	72	CC3		12:26:08		13:04:32	115	0.0797	0.0801	−0.00810	10
		Az		12:26:53		14:16:02	182	0.0177	0.0332	−0.0280	10
		El		12:26:53		14:16:02	182	0.0227	0.0482	0.0425	10
	51	CC3		13:14:32		14:14:32	61	0.0259	0.0262	−0.00382	60
		HA		12:42:11		14:15:02	97	0.0111	0.0128	0.00641	60
		Dec		12:42:11		14:15:02	97	0.00912	0.0103	0.00479	60
ICEV XA	72	CC3		12:26:08		13:04:32	110	0.0353	0.0355	−0.00400	10
		Az		12:26:53		14:16:02	165	0.0169	0.0372	−0.0332	10
		El		12:26:53		14:16:02	164	0.0238	0.0513	0.0455	10
	51	HA		12:18:51		12:26:21	28	0.00559	0.0355	0.0351	60
		Dec		12:18:51		12:26:21	27	0.00689	0.0351	−0.0344	60
		CC3		13:18:32		14:15:32	53	0.0293	0.0294	0.00254	60
		HA		12:26:31		14:16:02	180	0.0102	0.0195	0.0166	60
		Dec		12:26:31		14:16:02	180	0.0157	0.0189	−0.0106	60
PREL XB	72	CC3		12:26:48		13:04:32	101	0.0212	0.0212	−0.000387	10
	51			13:18:32		15:24:32	115	0.00725	0.00729	−0.000713	60
PREL YB	72			12:26:48		13:04:32	96	0.0208	0.0208	0.0000509	10
	51			13:18:32		16:13:32	164	0.00775	0.00776	−0.000408	60
DACO XB	51			13:18:32		16:59:32	199	0.0514	0.0514	−0.0000810	60
	72			12:26:48		13:04:32	96	0.0207	0.0207	−0.000346	60
DACO YB	51			12:26:48		16:58:32	205	0.00788	0.00788	−0.000119	60
	61	CC3	7/14	17:03:32	7/14	17:46:32	33	0.0190	0.0190	−0.000163	60

[a]Hour angle (HA), declination (dec), azimuth (az), and elevation (el) are expressed in degrees; two-way doppler (CC3), in Hz; and range (R), in kilometers.

Table 31 (contd)

Orbit identification	DSS	Data type[a]	Data span, GMT Beginning 1967		Data span, GMT Ending 1967		Number of points	Standard deviation[a]	Root mean square[a]	Mean residual[a] (O − C)	Sample rate, s
			1967	h:min:s	1967	h:min:s					
DACO YC	72	CC3	7/14	12:26:48	7/14	13:04:32	96	0.0268	0.0273	0.00545	10
	51			13:18:32		16:58:32	205	0.0104	0.0134	−0.00837	60
	51			18:33:32		20:27:32	61	0.0102	0.0103	−0.00183	60
	61			17:03:32		18:23:32	39	0.0135	0.0342	0.0314	60
DACO XF	72			12:26:48		13:04:32	96	0.0208	0.0208	0.00107	10
	51			13:18 32		16:58:32	205	0.00928	0.00931	0.000724	60
	51			18:33:32		22:24:32	145	0.00837	0.00843	−0.00099	60
DACO XH	11			23:38:32		23:57:32	20	0.00824	0.0209	0.0193	60
	51			13:18:32		16:38:32	205	0.0106	0.0108	−0.00201	60
	51		7/14	18:33:32	7/14	23:04:32	172	0.00767	0.00771	−0.000713	60
NOMA YA	11		7/14	23:38:32	7/15	00:42:32	65	0.00958	0.0118	0.00684	60
	72		7/14	12:26:48	7/14	13:04:32	96	0.0358	0.0368	0.00838	60
	51		7/14	13:18:32	7/14	16:58:32	205	0.0108	0.0111	−0.00231	60
	51		7/14	18:33:32	7/14	23:04:32	215	0.00809	0.00809	−0.000357	60
NOMA YD	72		7/14	12:28:08	7/14	13:04:32	95	0.0308	0.0324	0.0100	10
	42		7/14	23:38:32	7/15	11:30:32	373	0.00840	0.00842	−0.000586	60
	51		7/14	13:18:32	7/14	16:58:32	205	0.0114	0.0118	−0.00301	60
	51		7/14	18:33:32	7/14	23:04:32	215	0.00860	0.00867	0.00109	60
NOMA YE	72		7/14	12:28:08	7/14	13:04:32	95	0.0262	0.0268	0.00599	10
	11		7/14	23:38:32	7/15	04 56:32	317	0.00782	0.0101	0.00644	60
	42		7/15	05:13:32	7/15	11:30:32	373	0.00707	0.0114	0.00899	60
NOMA YF	72		7/14	12:28 08	7/14	13:04:32	95	0.0316	0.0340	0.0125	10
	11		7/14	23:38:32	7/15	04:56:32	317	0.00822	0.00895	0.00354	60
	42		7/15	05:13:32	7/15	13:15 32	478	0.00786	0.00795	−0.00121	60
	51		7/14	13:18:32	7/14	16:58:32	205	0.0115	0.0126	−0.00504	60
	51		7/14	18:33:32	7/14	23:04:32	215	0.00839	0.00854	0.00158	60
LAPM XA	42		7/15	08:00:32	7/15	13:59:32	355	0.00700	0.00712	−0.00131	60
	51		7/15	14:15:32	7/15	19:59:32	324	0.00762	0.00787	−0.00197	60
LAPM YB	72		7/14	12:28:08	7/14	13:04:32	95	0.0292	0.0299	0.00652	10
	11		7/14	23:38 32	7/15	04:56:32	299	0.00815	0.00817	−0.000523	60
	42		7/15	05:13:32	7/15	13:59 32	519	0.00689	0.00700	−0.00126	60
	51		7/14	14:00:32	7/14	16:58:32	162	0.0102	0.0103	−0.00134	60
	51		7/14	18:33:32	7/14	23:04:32	220	0.00910	0.00948	−0.00265	60
	51		7/15	14:15:32	7/15	21:58:32	425	0.00881	0.00885	−0.000793	60
LAPM XC	42		7/15	08:00:32	7/15	13:59:32	355	0.00719	0.00719	−0.000287	60
	51		7/15	14:15:32	7/15	21:53:32	429	0.0133	0.0133	0.000228	60
LAPM XE	42		7/15	08:00:32	7/15	13:59:32	355	0.00711	0.00711	−0.00217	60
	51		7/15	14:15:32	7/15	22:29:32	441	0.00730	0.00730	0.000117	60
LAPM YC	72		7/14	12:28:08	7/14	13:04:32	95	0.0288	0.0296	0.00707	10
	11		7/14	23:38:32	7/15	04:56:32	299	0.00805	0.00810	0.000873	60
	42		7/15	05:13:32	7/15	13:59:32	519	0.00694	0.00694	−0.000270	60
	51		7/14	14 00:32	7/14	16:58:32	162	0.0105	0.0105	0.000193	60
	51		7/14	18:33:32	7/14	23 04:32	220	0.00967	0.00997	−0.002243	60
	51		7/15	14:15:32	7/15	22:50:32	454	0.00917	0.00931	0.00158	60
PRCL YB	72		7/14	12:28:08	7/14	13:04:32	95	0.0269	0.0275	−0.00600	10
	11		7/14	23:38 32	7/15	04:56:32	299	0.00861	0.00874	0.00147	60
	11		7/15	23:41:32	7/16	02:29 59	258	0.0382	0.0386	0.00519	60
	42		7/15	05:13:32	7/15	13:59:32	519	0.00685	0.00687	0.000425	60
	51		7/14	14:00:32	7/14	16:58:32	162	0.00991	0.00995	−0.000922	60
	51		7/14	18:33:32	7/14	23:04:32	220	0.00797	0.00801	−0.000801	60
	51	CC3	7/15	14:15:32	7/15	23 32:32	489	0.00748	0.00750	0.000477	60

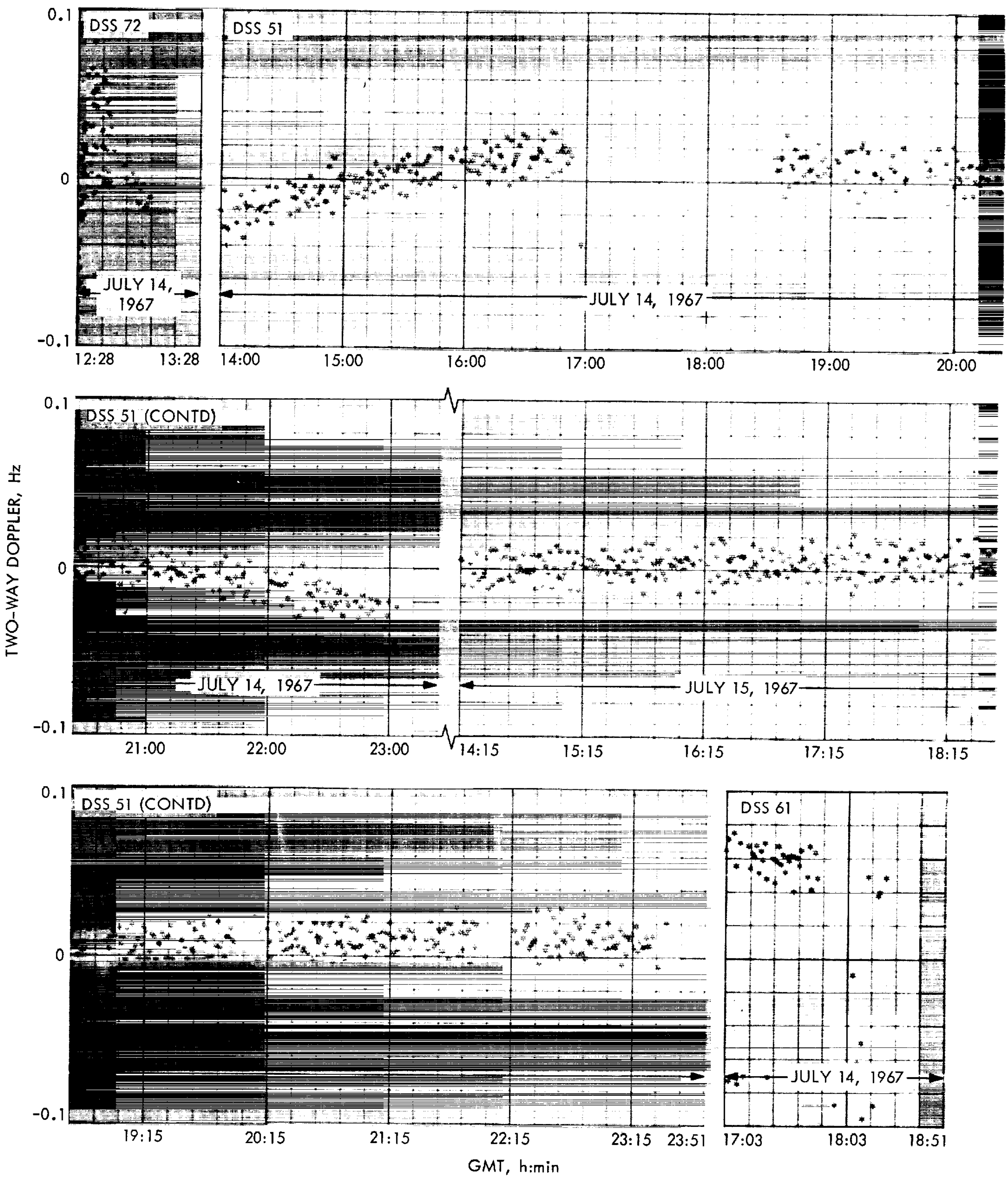

Fig. 28. Premaneuver two-way doppler residuals for *Surveyor IV*, trajectory not corrected for perturbations

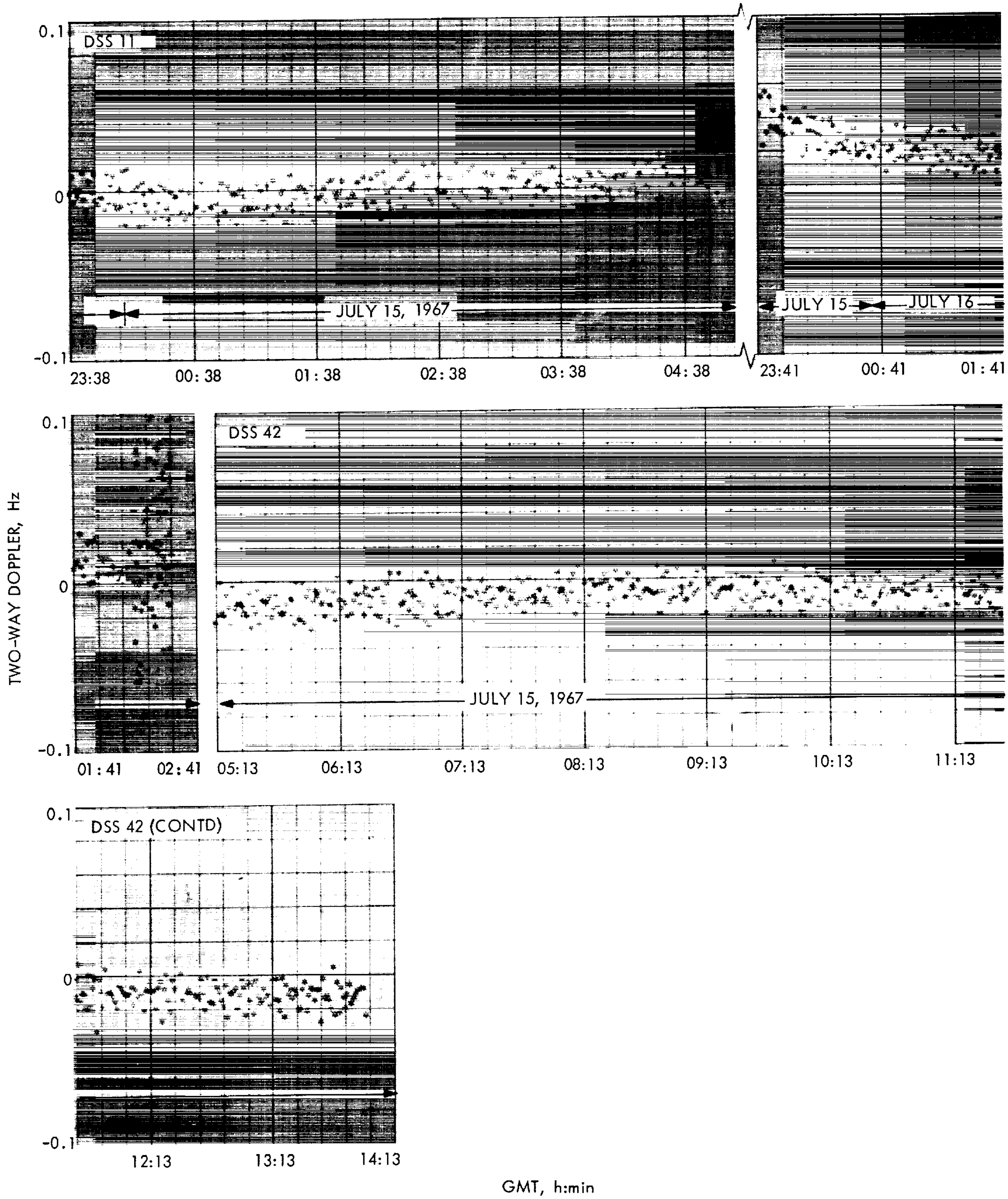

0.1
0
-0.1
DSS 11
JULY 15, 1967
JULY 15
JULY 16
23:38
00:38
01:38
02:38
03:38
04:38
23:41
00:41
01:41
TWO-WAY DOPPLER, Hz
DSS 42
01:41
02:41
05:13
06:13
07:13
08:13
09:13
10:13
11:13
DSS 42 (CONTD)
12:13
13:13
14:13
GMT, h:min

Fig. 28 (contd)

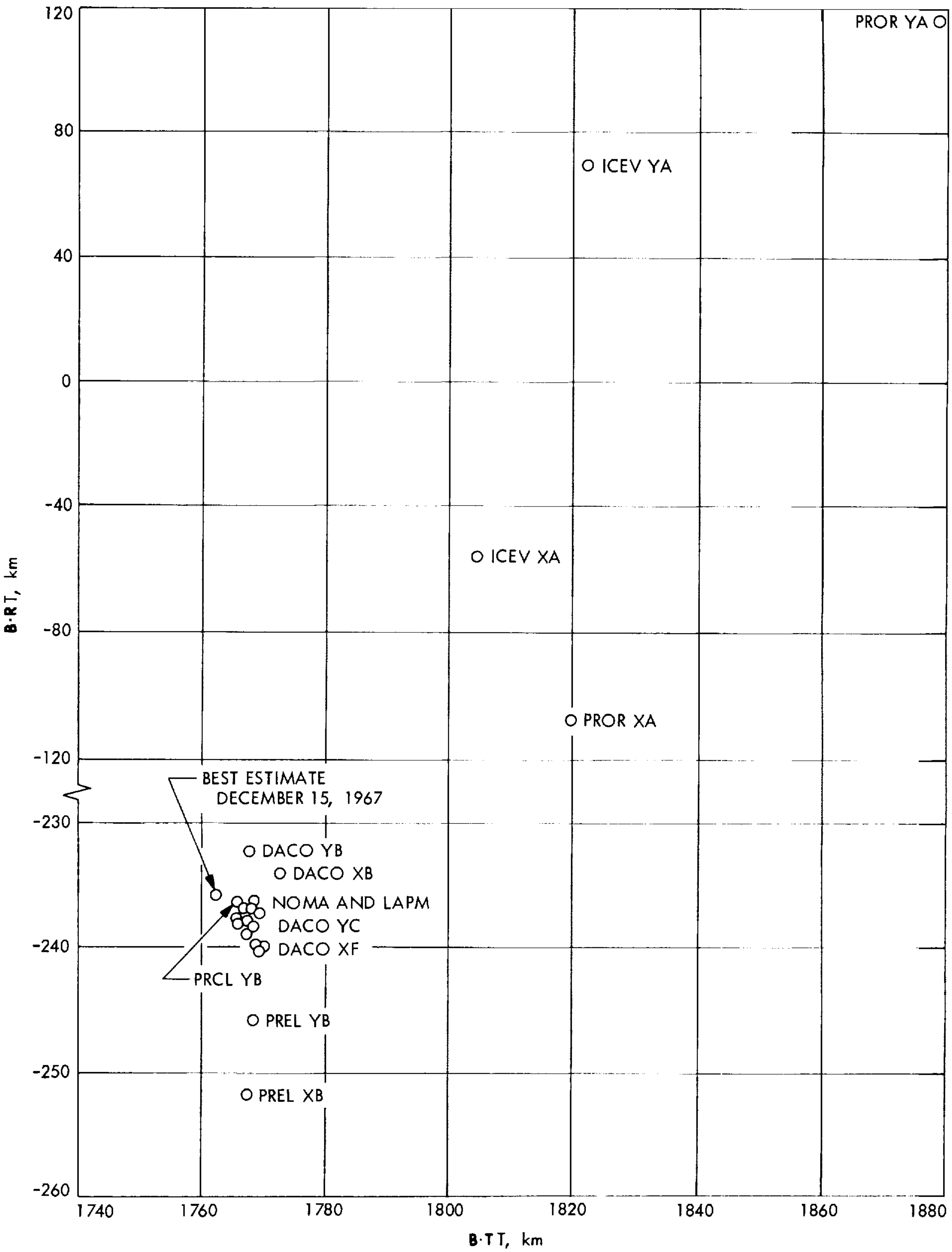

Fig. 29. Estimated premidcourse unbraked impact point for *Surveyor IV*

Table 32. Postmaneuver computations for *Surveyor IV*

Orbit identification	Time computed		Target statistics										Selenocentric conditions at unbraked impact			Type solution	Data used	
	Start h:min	Stop h:min	B, km	B • TT, km	B • RT, km	T_L, h	SMAA, km (1σ)	SMIA, km (1σ)	θ_T' deg	$\sigma_{T,\,impact}$, s (1σ)	ϕ_{99}, deg	SVFIXR, km/s (1σ)	Latitude, deg	Longitude, deg	GMT, h:min:s July 17, 1967		DSS	Data
1 POM YC	09:20	09:34	1966.58	1945.6	−286.5	23.58	1009.8	102.5	92.24	206.6	16.32	0.0016	−0.661[a]	358.49	02:02:17.992	6x6	11, 42	CC3
1 POM XE	10:37	10:37	1977.88	1947.8	−343.5	23.59	477.3	56.69	99.56	104.3	8.317	0.00114	0.466	358.52	02:02:29.648	6x6	11, 42	
1 POM YE	10:53	11:09	1975.46	1943.5	−354.1	23.59	340.2	50.08	102.5	75.31	6.10	0.000991	0.665	358.41	02:02:31.887	6x6	11, 42	
1 POM XF	11:50	12:05	1978.44	1949.3	−338.2	23.59	126.2	42.03	113.8	27.82	2.497	0.000738	0.365	358.56	02:02:28.432	6x6	11, 42	
2 POM XA	12:30	12:48	1977.51	1948.9	−335.0	23.59	73.66	0.50	121.7	16.80	1.537	0.000678	0.301	358.54	02:02:27.620	6x6	11, 42	
2 POM YA	13:27	13:39	1978.40	1950.2	−332.6	23.59	39.71	22.37	48.59	9.59	0.546	0.000624	0.256	358.58	02:02:26.964	6x6	11, 42	
2 POM XC	13:48	14:04	1978.64	1950.3	−333.6	23.59	40.19	30.00	44.94	10.13	0.687	0.000631	0.275	358.58	02:02:27.249	6x6	11, 42	
2 POM YC	15:49	16:03	1984.08	1954.8	−339.5	23.59	13.60	9.84	111.4	3.842	0.299	0.000613	0.401	358.69	02:02:28.946	6x6	11, 42, 51	CC3
3 POM YA	20:53	21:07	1983.20	1953.9	−339.5	23.59	12.26	3.41	89.29	3.361	0.202	0.000611	0.400	358.66	02:02:29.020	6x6	11, 42, 51	
3 POM YC	22:36	22:49	1982.57	1953.3	−339.4	23.59	12.21	2.78	89.92	3.353	0.202	0.000611	0.396	358.65	02:02:28.990	6x6	11, 42, 51	
3 POM XB	21:56	22:07	1982.57	1953.3	−339.3	23.59	12.20	2.79	90.02	3.348	0.202	0.000611	0.393	358.65	02:02:28.938	6x6	11, 42, 51	
3 POM YD[b]	22:54	23:06	1982.15	1952.4	−341.9	23.59	11.30	2.26	87.22	3.139	0.181	0.000610	0.443	358.62	02:02:29.645	6x6	11, 42, 51	
FINAL XA	23:45	23:54	1982.10	1952.1	−343.8	57.40	10.04	1.99	85.94	2.839	0.158	0.000610	0.480	358.62	02:02:30.158	6x6	51	
FINAL XD	00:36	00:48	1981.73	1951.8	−342.8	57.40	2.95	1.27	53.68	1.246	0.034	0.000609	0.461	358.62	02:02:29.93	6x6	11, 51	
FINAL YA	00:21	00:30	1981.89	1952.0	−343.0	57.40	2.80	1.22	50.91	1.189	0.030	0.000609	0.464	358.62	02:02:30.024	6x6	11, 51	
FINAL XE	00:52	01:00	1981.93	1952.0	−343.0	57.40	2.72	1.20	49.66	1.153	0.029	0.000609	0.465	358.62	02:02:30.046	6x6	11, 51	
FINAL YB	00:34	00:42	1981.85	1952.0	−342.9	57.40	2.54	1.19	48.18	1.076	0.027	0.000609	0.463	358.62	02:02:29.996	6x6	11, 51	
FINAL YC	00:45	00:55	1981.89	1952.0	−343.0	57.40	2.09	1.18	51.16	0.8852	0.024	0.000609	0.464	358.62	02:02:30.018	6x6	11, 51	
FINAL XH	NA[c]	NA[c]	1980.93	1951.1	−342.3	57.40	1.51	0.896	83.34	0.5805	0.021	0.000609	0.450	358.60	02:02:29.593	6x6	11, 51	
FINAL YE	00:58	01:06	1981.16	1951.3	−342.5	57.40	1.48	0.816	87.76	0.5499	0.022	0.000609	0.453	358.60	02:02:29.690	6x6	11, 51	
FINAL YF	01:10	01:19	1982.91	1952.9	−343.5	57.40	1.43	0.509	96.17	0.4748	0.021	0.000609	0.477	358.64	02:02:30.397	6x6	11, 51	
POST 1[d]	03:52	04:17	1982.41	1952.3	−344.0	23.59	2.31	1.32	64.42	0.808	0.029	0.000609	0.484	358.63	02:02:30.228	6x6	11, 42, 51	CC3

[a] Minus denotes south.

[b] Orbit used for terminal maneuver computations.

[c] Not available.

[d] Current best estimate, postmaneuver as of July 24, 1967.

Table 33. Postmaneuver position and velocity for *Surveyor IV* at injection epoch

Orbit identification	Geocentric space-fixed position, km			Geocentric space-fixed velocity, km/s			Uncertainties (1σ)					
							Position, km			Velocity, m/s		
	X	Y	Z	DX	DY	DZ	σ_X	σ_Y	σ_Z	σ_{DX}	σ_{DY}	σ_{DZ}
1 POM YC	−163930.13	−197947.25	−107718.92	−0.54590966	−1.0145030	−0.36380790	35.85	202.4	407.5	4.266	6.149	5.288
1 POM XE	−163929.24	−197934.88	−107696.62	−0.54572961	−1.0148241	−0.36348289	32.09	82.54	200.8	2.703	3.225	2.104
1 POM YE	−163930.66	−197933.92	−107691.66	−0.54564363	−1.0149091	−0.36345131	30.03	55.81	144.8	2.140	2.386	1.393
1 POM XF	−163928.77	−197935.66	−107699.00	−0.54576651	−1.0147841	−0.36350271	23.35	21.36	54.83	1.098	0.9932	0.4513
2 POM XA	−163928.91	−197936.62	−107700.22	−0.54577585	−1.0147660	−0.36352205	19.74	17.48	31.89	0.7681	0.6154	0.3397
2 POM YA	−163928.39	−197936.99	−107701.45	−0.54580227	−1.0147424	−0.36352693	12.80	16.74	11.72	0.3306	0.2224	0.3207
2 POM XC	−163928.39	−197936.64	−107701.07	−0.54579803	−1.0147488	−0.36352155	14.35	16.92	13.97	0.4104	0.2790	0.3261
2 POM YC	−163926.73	−197933.64	−107699.55	−0.54582115	−1.0147636	−0.36346257	6.129	6.917	6.606	0.1797	0.1432	0.0846
3 POM YA	−163927.08	−197933.78	−107699.35	−0.54580950	−1.0147697	−0.36346802	4.635	6.771	5.708	0.1104	0.1116	0.0690
3 POM YC	−163927.42	−197933.90	−107699.25	−0.54580488	−1.0147729	−0.36347323	4.521	6.739	5.696	0.1079	0.1111	0.6658
3 POM XB	−163927.35	−197933.99	−107699.34	−0.54580350	−1.0147715	−0.36347320	4.529	6.735	5.696	0.1082	0.1112	0.6644
3 POM YD	−163928.87	−197932.63	−107697.82	−0.54576737	−1.0148022	−0.36346779	3.781	6.324	5.117	0.0906	0.0987	0.0650
FINAL XA	−195243.91	−256945.42	−127512.74	−0.47410485	−0.84318697	−0.26018892	2.210	1.708	7.431	0.0860	0.0827	0.0504
FINAL XD	−195244.08	−256945.46	−127513.43	−0.47410837	−0.84318072	−0.26019648	0.5056	1.661	2.067	0.0207	0.0216	0.0315
FINAL YA	−195244.05	−256945.35	−127513.28	−0.47410674	−0.84318242	−0.26019540	0.4842	1.635	1.905	0.0161	0.0185	0.0314
FINAL XE	−195244.05	−256945.32	−127513.24	−0.47410620	−0.84318296	−0.26019512	0.4726	1.612	1.818	0.0137	0.0170	0.0313
FINAL YB	−195244.06	−256945.38	−127513.33	−0.47410725	−0.84318189	−0.26019573	0.4494	1.546	1.664	0.0106	0.0146	0.0310
FINAL YC	−195244.06	−256945.35	−127513.30	−0.47410684	−0.84318232	−0.26019547	0.3945	1.310	1.391	0.0092	0.0120	0.0290
FINAL XH	−195244.22	−256945.99	−127513.86	−0.47410549	−0.84317895	−0.26020567	0.3073	0.8561	1.068	0.0090	0.0104	0.0247
FINAL YE	−195244.18	−256945.84	−127513.73	−0.47410614	−0.84317958	−0.26020306	0.2981	0.8090	1.041	0.0089	0.0104	0.0242
FINAL YF	−195243.87	−256944.72	−127512.88	−0.47411540	−0.84318265	−0.26018002	0.2732	0.6806	0.9840	0.0082	0.0103	0.0226
FINAL YG	−195243.95	−256944.97	−127513.04	−0.47411162	−0.84318265	−0.26018649	0.2753	0.6904	0.9873	0.0083	0.0103	0.0228
POST 1	−163929.68	−197931.45	−107696.87	−0.54574736	−1.0148227	−0.36345852	1.395	1.564	1.750	0.0174	0.0123	0.0317

NOTE

All *POM* and *POST 1* orbits are at midcourse epoch.

All *FINAL* orbits are at unbraked impact minus 5 h 40 min.

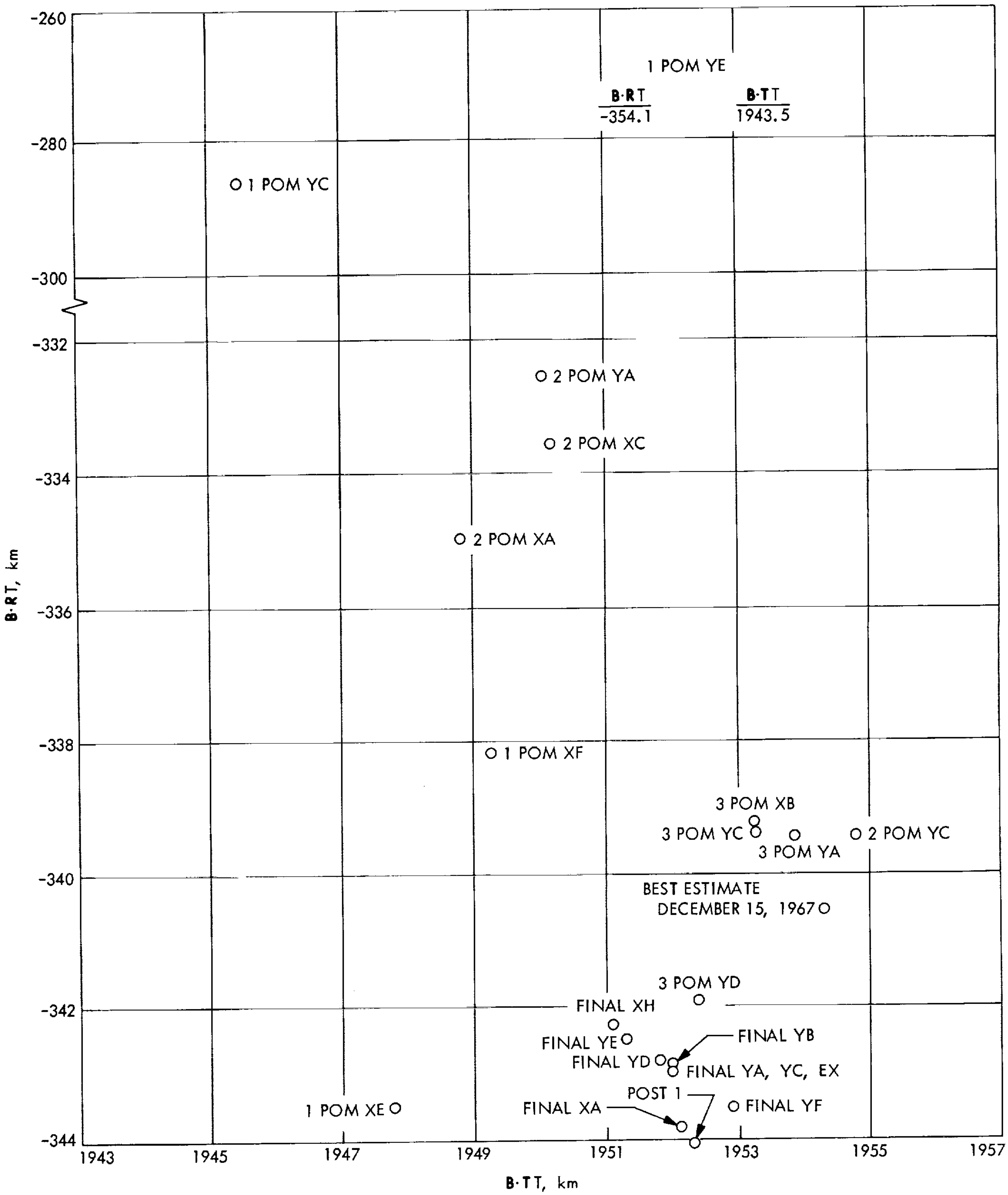

Fig. 30. Estimated postmidcourse unbraked impact point for Surveyor IV

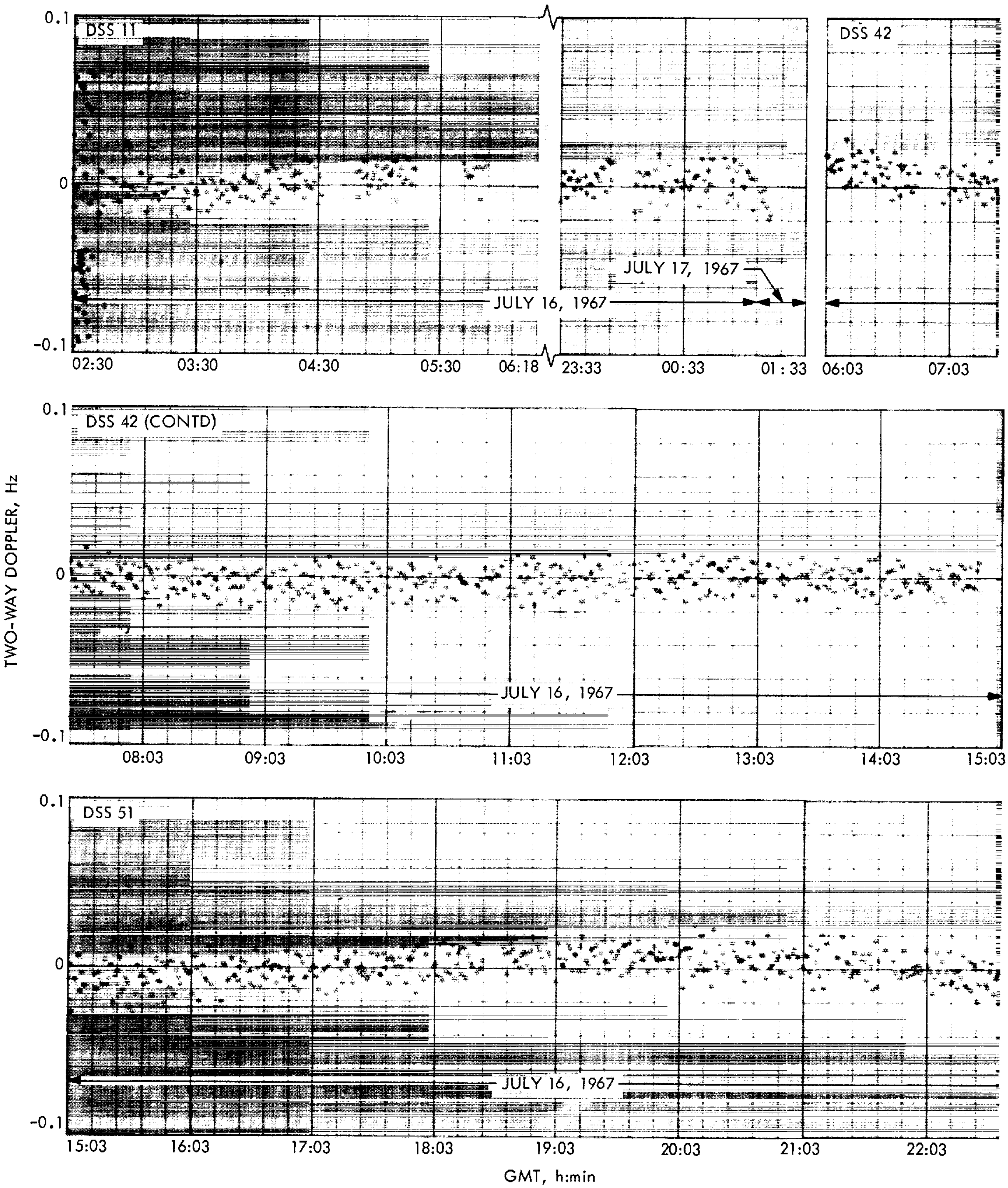

Fig. 31. Postmaneuver two-way doppler residuals for *Surveyor IV*, trajectory not corrected for perturbations

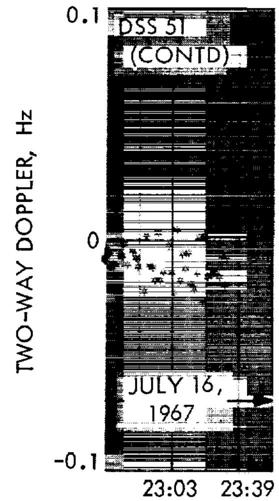

Fig. 31 (contd)

Table 34. Summary of postmaneuver DSS tracking data used in orbit computations for *Surveyor IV*

Orbit identification	DSS	Data type	Data span, GMT				Number of points	Standard deviation, Hz	Root mean square, Hz	Mean residual (O − C)	Sample rate, s
			Beginning		Ending						
			1967	h:min:s	1967	h:min:s					
1 POM YC	11	CC3	7/16	02:30:19	7/16	02:40:19	50	0.0498	0.0508	−0.0101	10
	11			02:43:32		05:53:32	149	0.00662	0.00666	0.000670	60
	42			06:03:32		09:01:32	166	0.00711	0.00711	−0.0000287	60
1 POM XE	11			02:30:19		02:40:19	50	0.0498	0.0511	−0.0116	10
	11			02:43:32		05:53:32	148	0.00670	0.00672	0.000576	60
	42			06:03:32		10:13:32	235	0.00715	0.00715	0.0000291	60
1 POM YE	11			02:30:19		02:40:19	49	0.0516	0.0539	−0.0156	10
	11			02:43:32		05:53:32	149	0.00690	0.00699	0.00109	60
	42			06:03:32		10:34:32	256	0.00718	0.00718	0.0000057	60
1 POM XF	11			02:30:19		02:40:19	50	0.0498	0.0512	−0.0117	10
	11			02:43:32		05:53:32	148	0.00669	0.00671	0.000610	60
	42			06:03:32		11:39:32	315	0.00723	0.00723	−0.0000093	60
2 POM XA	11			02:30:19		02:40:19	48	0.0507	0.0530	−0.0155	10
	11			02:43:32		05:53:32	148	0.00682	0.00689	0.00101	60
	42			06:03:32		12:18:32	353	0.00728	0.00728	0.0000145	60
2 POM YA	11			02:30:19		02:40:19	49	0.0517	0.0543	−0.0168	10
	11			02:43:32		05:53:32	149	0.00689	0.00698	0.00116	60
	42			06:03:32		14:09:32	462	0.00725	0.00725	0.00000766	60
2 POM XC	11			02:30:19		02:40:19	48	0.0508	0.0532	−0.0159	10
	11			02:43:32		05:53:32	148	0.00684	0.00690	0.000958	60
	42			06:03:32		13:39:32	428	0.00721	0.00721	−0.0000074	60
2 POM YC	11			02:30:24		02:40:19	48	0.0509	0.0550	−0.0208	10
	11			02:43:32		05:53:32	149	0.00668	0.00674	0.000927	60
	42			06:03:32		14:53:32	505	0.00722	0.00722	0.000220	60
	51			15:03:32		16:42:32	90	0.00754	0.00757	−0.000677	60
3 POM YA	11			02:30:24		02:40:19	48	0.0508	0.0549	−0.0208	10
	11			02:43:32		05:53:32	149	0.00669	0.00673	0.000749	60
	42			06:03:32		14:53:32	505	0.00722	0.00723	0.000369	60
	51			15:03:32		20:20:32	291	0.00731	0.00732	−0.000343	60
3 POM YC	11			02:30:24		02:40:19	48	0.0509	0.0550	−0.0208	10
	11			02:43:32		05:53:32	149	0.00666	0.00668	0.000495	60
	42			06:03:32		14:53:32	505	0.00722	0.00723	0.000421	60
	51	CC3	7/16	15:03:32	7/16	21:39:32	352	0.00815	0.00816	−0.000248	60

Table 34 (contd)

Orbit identification	DSS	Data type	Data span, GMT				Number of points	Standard deviation, Hz	Root mean square, Hz	Mean residual (O − C), Hz	Sample rate, s
			Beginning		Ending						
			1967	h:min:s	1967	h:min:s					
3 POM XB	11	CC3	7/16	02:30:24	7/16	02:40:19	52	0.0590	0.0638	−0.0242	10
	11			02:43:32		05:53:32	148	0.00663	0.00671	0.000985	60
	42			06:03:32		14:53:32	501	0.00726	0.00727	0.000526	60
	51			15:03:32		21:39:32	356	0.00775	0.00777	−0.000453	60
3 POM YD	11			02:30:24		02:40:19	48	0.0508	0.0552	−0.0216	10
	11			02:43:32		05:53:32	149	0.00708	0.00711	0.000601	60
	42			06:03:32		14:53:32	505	0.00751	0.00751	0.0000147	60
	51			15:03:32		22:38:32	418	0.00942	0.00942	0.000239	60
FINAL XA	51			20:21:32		22:06:32	80	0.00696	0.00696	0.0000641	60
FINAL XD	11			23:33:32		23:54:32	22	0.00557	0.00558	0.000139	60
	51			20:21:32	7/16	23:23:32	174	0.00738	0.00738	−0.0000182	60
FINAL YA	11			23:33:32	7/17	00:10:32	29	0.00724	0.00724	0.0000210	60
	51			20:21:32	7/16	23:23:32	171	0.00742	0.00742	0.000124	60
FINAL XE	11			23:33:32	7/17	00:13:32	32	0.00770	0.00770	0.00000381	60
	51			20:21:32	7/16	23:23:32	174	0.00736	0.00736	−0.0000982	60
FINAL YB	11			23:33:32	7/17	00:22:32	41	0.00841	0.00841	0.000134	60
	51			20:21:32	7/16	23:23:32	171	0.00743	0.00743	−0.0000200	60
FINAL YC	11			23:33:32	7/17	00:37:32	56	0.00771	0.00771	0.000142	60
	51			20:21:32	7/16	23:23:32	171	0.00741	0.00741	−0.0000514	60
FINAL XH	11			23:33:32	7/17	00:58:32	72	0.00814	0.00814	0.0000559	60
	51			20:21:32	7/16	23:23:32	174	0.00735	0.00735	−0.0000379	60
FINAL YE	11			23:33:32	7/17	01:01:32	75	0.00840	0.00840	0.0000309	60
	51			20:21:32	7/16	23:23:32	171	0.00740	0.00740	0.00000428	60
FINAL YF	11			23:33:32	7/17	01:15:32	87	0.00989	0.00990	0.000281	60
	51			20:21:32	7/16	23:23:32	171	0.00744	0.00744	−0.000136	60
POST 1	11			02:30:24	7/16	02:40:19	52	0.0590	0.0647	−0.0267	10
	11			02:43:32	7/16	05:53:32	149	0.00787	0.00793	0.000957	60
	11			23:33:32	7/17	01:16:32	88	0.0105	0.0106	0.000610	60
	42			06:03:32	7/16	14:53:32	505	0.00796	0.00796	−0.000198	60
	51	CC3	7/16	15:03:32	7/16	23:23:32	462	0.00964	0.00965	0.000420	60

Table 35. Inflight results of orbit determination AMR backup computations for *Surveyor IV*

Orbit solution data span		Predicted selenocentric conditions at unbraked impact		
From	To	Latitude, deg (minus, south)	Longitude, deg	GMT, h:min:s (July 17, 1967)
Midcourse[a]	*E* − 5 h 40 min[b]	−0.400	358.666	02:02:29.020
E − 5 h 40 min	*E* − 1 h 50 min	−0.464	358.619	02:02:30.024
E − 5 h 40 min	*E* − 1 h 38 min	−0.463	358.618	02:02:29.996
E − 5 h 40 min	*E* − 1 h 23 min	−0.464	358.619	02:02:30.018
E − 5 h 40 min	*E* − 1 h 14 min	−0.464	358.619	02:02:30.014
E − 5 h 40 min	*E* − 59 min	−0.453	358.603	02:02:29.690
E − 5 h 40 min	*E* − 45 min	−0.477	358.641	02:02:30.397
Best estimate of unbraked impact time				02:02:31.171

[a] *Midcourse* refers to initial postmidcourse epoch. Solution used for initial estimate of AMR mark time.

[b] *E* refers to lunar encounter.

X. *Surveyor IV* Postflight Orbit Determination Analysis

A. Introduction

This section presents the best estimate of the *Surveyor IV* flight path and other significant results obtained from analysis of the DSIF tracking data. The analysis verified that both the premaneuver and postmaneuver inflight orbit solutions were within the *Surveyor* Project orbit determination accuracy requirements. The inflight philosophy of estimating only a minimum parameter set (i.e., the 6 components of the spacecraft position and velocity vectors) for the orbital computations was again proved valid.

For the postflight orbital computations and analysis, only two-way doppler data were used. Column I of Table 28 summarizes the data used for the premaneuver orbit computation in the postflight analysis. A comparison between columns D (amount of data used inflight) and I of Table 28 shows that, in general, fewer two-way doppler data points were used for the postflight computations. This was the result of removing some noisy DSS 61 data caused by the counter problem and rejecting some suspected bad data points. Column I of Table 28 summarizes the data used for postmaneuver orbit computations in postflight analysis. Once again the amount of data used for postflight computations was smaller than the amount of data used for inflight computation. The major difference is the rejection of data obtained at elevation angles below 17 deg.

B. Premaneuver Orbit Estimate

All the known bad data points were removed in the orbit data generator program (ODG) before the start of the postflight analysis. However, further analysis revealed that additional data, not previously suspected, were bad. This included the 60-s sample rate data from DSS 72 shortly after acquisition and some 10-s sample rate data from DSS 11 just before midcourse maneuver. When included in the fit with data from DSS 11, 42, and 51, the 60-s data from DSS 72 were not consistent. They showed a bias of approximately 0.04 Hz. An attempt to compensate for this bias by estimating the station location parameters (radius, latitude, longitude) failed to improve the fit significantly, so these data were eliminated from the final best-estimate orbit solution. The 10-s data from DSS 11 taken just before the midcourse motor burn were eliminated because of perturbations caused by spacecraft orientation (yaw and roll) maneuvers. Data below 17 deg elevation were also eliminated.

Because of the large amount of premidcourse data (38 h) available from *Surveyor IV*, it was difficult to fit the premidcourse data as well as on previous missions. An orbit solution based on estimating only the standard 6 parameters (position and velocity) with DSS 11, 42, 51, and 72 data was obtained and mapped forward to the target. The residual plots indicated a rather poor fit, but the parameters resulting when the solution was mapped to target were consistent with inflight results. Several runs made to check the consistency of data between stations showed that the data were fairly consistent. In an attempt to remove the remaining perturbations in the data, an orbit solution was computed estimating the station location parameters (radius, latitude, longitude). Although this improved the fit, it was still not as good as desired. At this point it became apparent that long spans of data (greater than 20 h) are difficult to fit with the customary "6×6" or "6×6 plus station locations" type orbit solution. It was decided to expand the list of estimated parameters to include estimates of acceleration due to nongravitational forces[11] such as solar radiation pressure, uncancelled attitude jet forces, etc. The resulting 17×17 solution significantly improved the data fit and gave results reasonably consistent with the inflight solution. The 17 parameters estimated included position and velocity (6), geocentric radius, and longitude of DSS 11, 42, 51 and 72 (8), and the accelerations due to nongravitational forces (3). All estimated station-location parameters were within 3 m of nominal values. The accelerations estimated[11] are as follows:

$$f_1 = 0.42 \times 10^{-9}\ \mathrm{km/s^2}$$

$$f_2 = 0.31 \times 10^{-9}\ \mathrm{km/s^2}$$

$$f_3 = -0.42 \times 10^{-9}\ \mathrm{km/s^2}$$

$$[\Delta\ddot{\mathbf{r}}] = 0.52 \times 10^{-9}\ \mathrm{km/s^2}$$

The 17×17 solution is considered the best estimate of the spacecraft premaneuver orbit. The uncorrected unbraked impact point predicted by this solution (latitude = 2.067°S, longitude = 353.943°E) is approximately 2.7 deg south and 5.5 deg west of the prelaunch unbraked aiming point. This is approximately equal to 81 km and 165 km, respectively. Other numerical values from this solution are presented in Table 36 and the number of data points, together with data noise statistics, are given in Table 37. A graphic comparison between the predicted unbraked impact points (in the **B**-plane) of this solution and the inflight solutions may be seen in Fig. 29. The residual plots are presented in Fig. 32.

[11]See Section II.A for explanation of the model used to estimate these accelerations.

Table 36. Summary of postflight orbit parameters, *Surveyor IV*

Parameter	Premidcourse	Postmidcourse
Epoch, GMT	12:05:06.480 (7/14/67)	02:30:10.461 (7/16/67)
Geocentric position and velocity at epoch		
X, km	3086.8998 ±0.1573 (1 σ)	−163926.88 ±4.92
Y, km	5367.0501 ±0.1543	−197932.47 ±5.08
Z, km	2133.6768 ±0.2245	−107696.98 ±9.20
DX, km/s	−8.0394010 ±0.0005463	−0.54579016 ±0.00008009
DY, km/s	6.0570800 ±0.0000717	−1.0147810 ±0.0000767
DZ, km/s	−4.3610388 ±0.0008395	−0.36347278 ±0.00009955
Target statistics		
B, km	1778.1800	1983.7764
B • **TT**, km	1762.4350	1954.3440
B • **RT**, km	−236.1143	−340.46074
SMAA, km	10.0	7.0
SMIA, km	2.0	5.0
θ_T, deg	34.71	77.47
$\sigma_{T,\,impact}$ s	2.66	0.500
$\phi_{\psi\psi}$, deg	0.222126	0.154230
SVFIXR, m/s	0.610626	0.610880
Latitude, deg	−2.0674965	358.69741
Longitude, deg	353.94333	0.42522965
Unbraked impact, GMT	02:11:44.824 (July 17, 1967)	02:02:31.171 (July 17, 1967)

Note
Current best estimate as of December 15, 1967.

Table 37. Summary of data used in postflight orbit solutions, *Surveyor IV*

DSS	Time data, GMT[a]				Number of points	Standard deviation, Hz	Root mean square, Hz	Mean residual (O − C), Hz
	Beginning		Ending					
	1967	h:min:s	1967	h:min:s				
				Premidcourse				
72	7/14	12:28:08	7/14	12:44:48	75	0.0253	0.0257	0.00445[b]
11	7/14	23:38:32	7/15	04:56:32	245	0.00730	0.00740	0.00118
11	7/15	23:41:32	7/16	02:09:32	89	0.00771	0.00837	−0.00325
42	7/15	05:13:32	7/15	13:59:32	519	0.00773	0.00809	−0.00241
51	7/14	14:00:32	7/14	16:58:32	162	0.0104	0.0106	−0.00209
51	7/14	18:33:32	7/14	23:04:32	196	0.00784	0.00791	0.00105
51	7/15	14:15:32	7/15	23:32:32	476	0.00757	0.00786	0.00211
				Postmidcourse				
11	7/16	02:30:39	7/16	02:40:19	47	0.0520	0.0539	−0.0140[b]
11	7/16	02:43:32	7/16	05:53:32	149	0.00670	0.00676	0.00945
11	7/16	23:33:32	7/17	01:16:32	88	0.00801	0.00801	0.000233
42	7/16	06:03:32	7/16	14:53:32	505	0.00722	0.00723	0.000145
51	7/16	15:03:32	7/16	23:23:32	462	0.00727	0.00727	0.00000106

[a]Only two-way doppler data were used in postflight analyses.
[b]These data have a 10-s sample rate; all other data have 60 s.

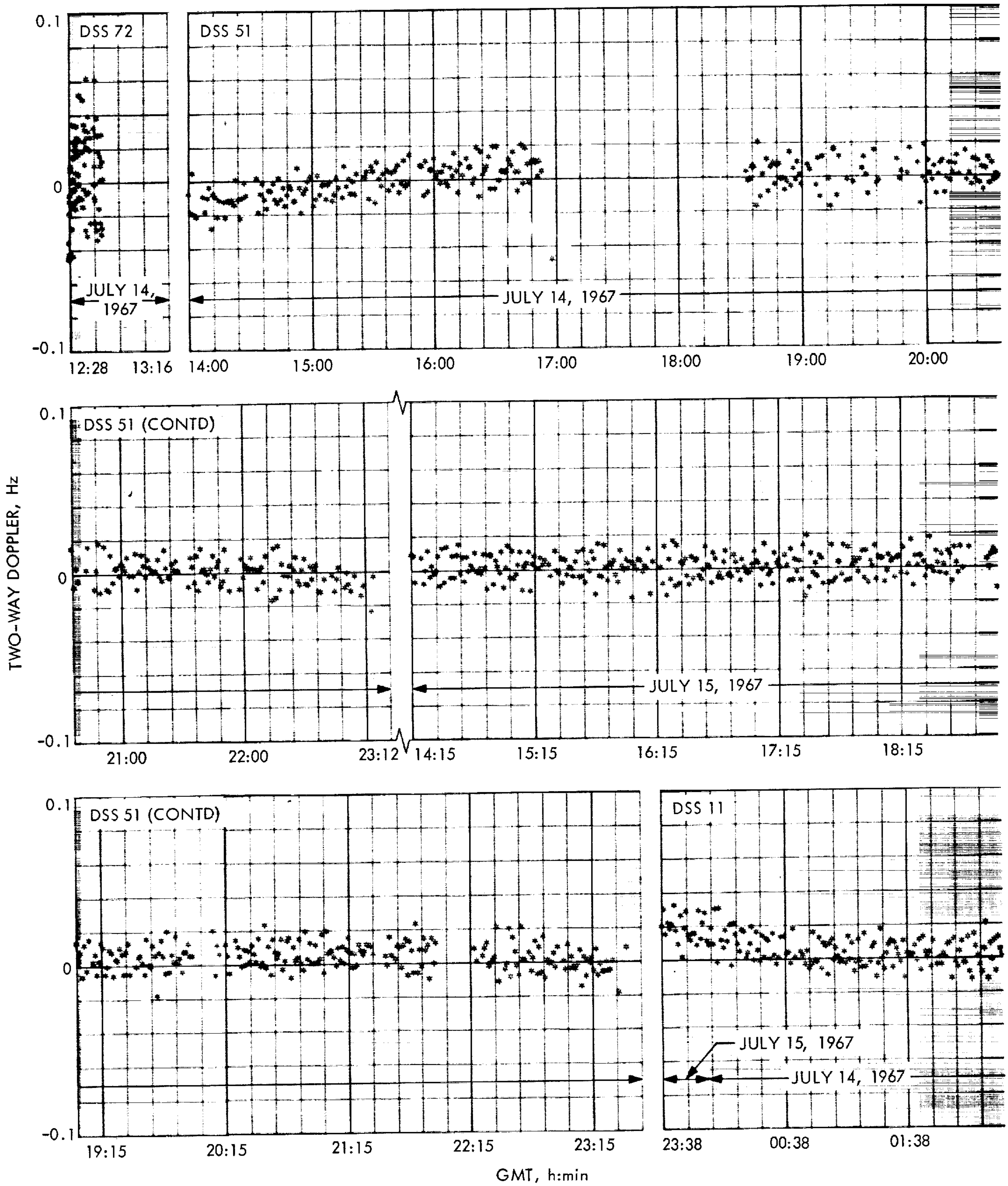

Fig. 32. Premaneuver two-way doppler residuals for *Surveyor IV*, trajectory corrected for perturbations

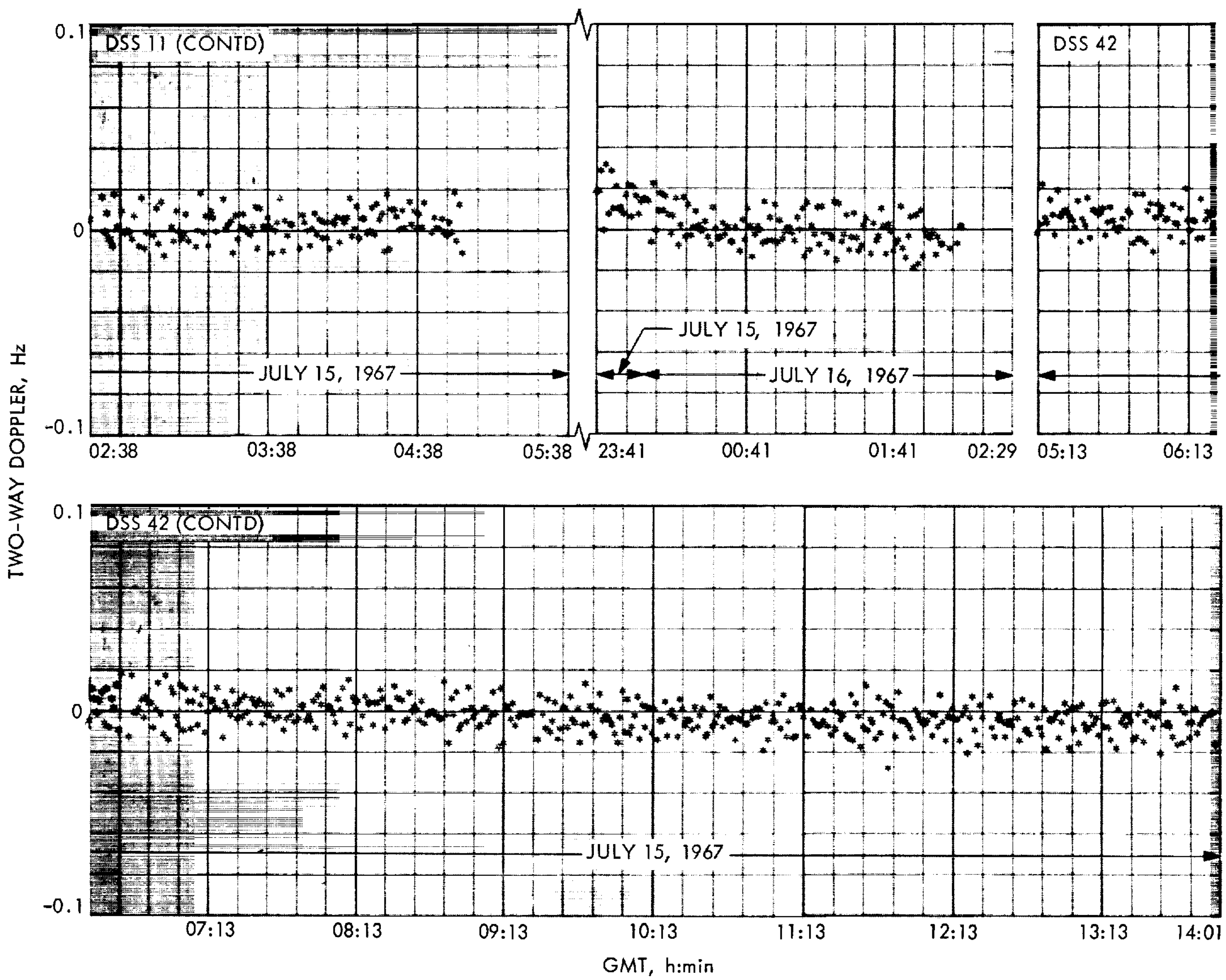

Fig. 32 (contd)

C. Postmaneuver Orbit Estimate

Before the analysis of the postmaneuver tracking data was started, all known or suspected bad data points were removed. The objective of the analysis in this section was to obtain an orbit solution based on processing all postmaneuver tracking data in one block. This differed from the inflight computations which required that the data be processed in two blocks in order to meet the AMR backup requirements. A 6 × 6 orbit solution based on all postmaneuver data was obtained and mapped forward to target. Examination of residual plots indicated a very poor fit. The predicted unbraked impact location from this solution was in very good agreement with the inflight results, but the impact time was approximately 1.079 s earlier than the observed time, indicating that the lunar radius of 1736.8 km at the impact location, which was based on *Lunar Orbiter* data, might be in error. It was therefore decided to try a radius of 1735.7 km, which was obtained by subtracting 2.4 km from the elevation shown on the ACIC charts. The 2.4 km is the amount by which the ACIC elevations exceed those obtained from *Rangers VI*, *VII*, and *VIII* tracking data. Furthermore, it was discovered that an incorrect DSS 11 station frequency had been used in the above solution and inflight. Correcting this frequency input and using the 1735.7 km lunar radius yielded an improved 6 × 6 solution with an impact time only 0.595 s earlier than the observed time.

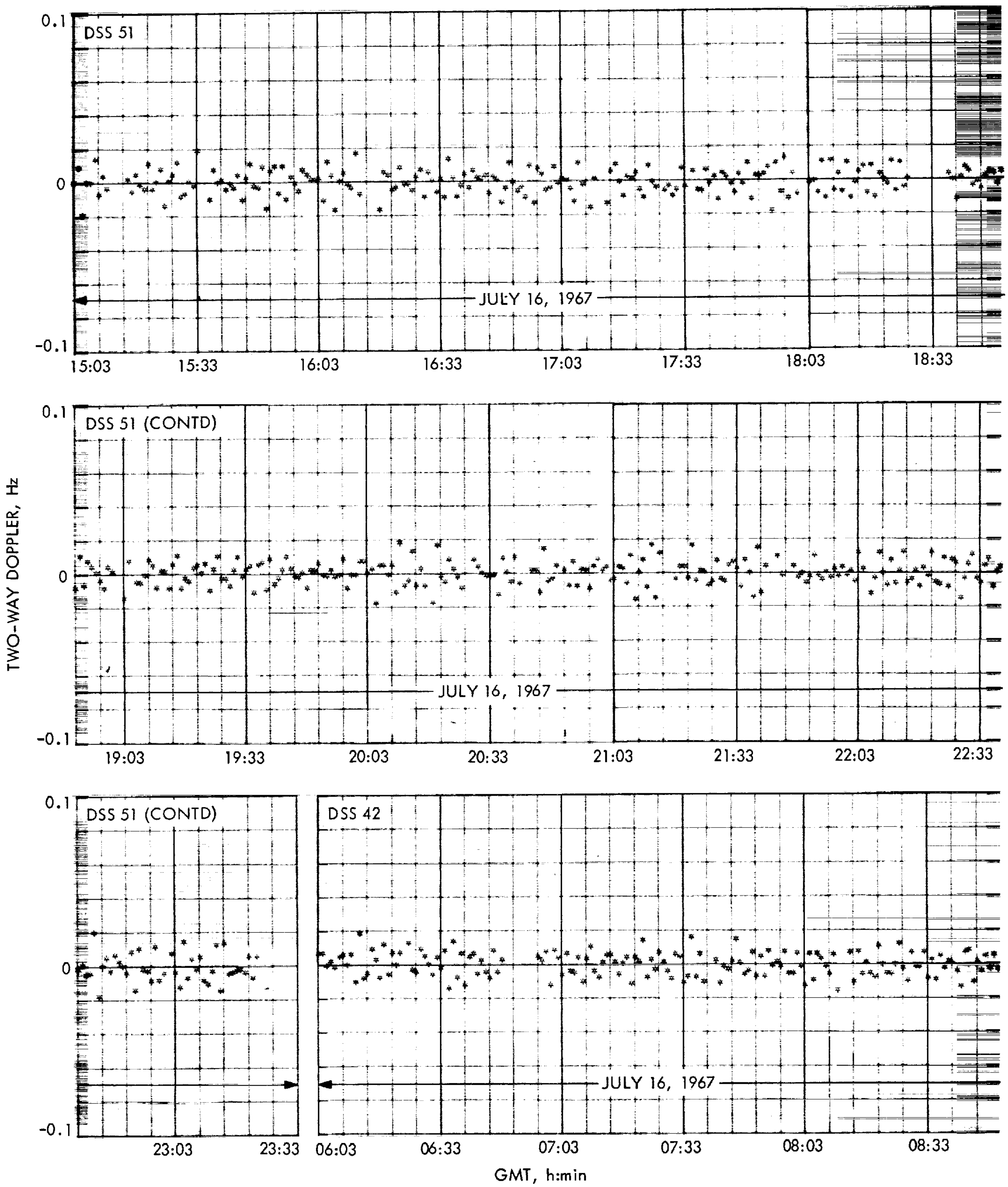

Fig. 33. Postmaneuver two-way doppler residuals for *Surveyor IV*, trajectory corrected for perturbations

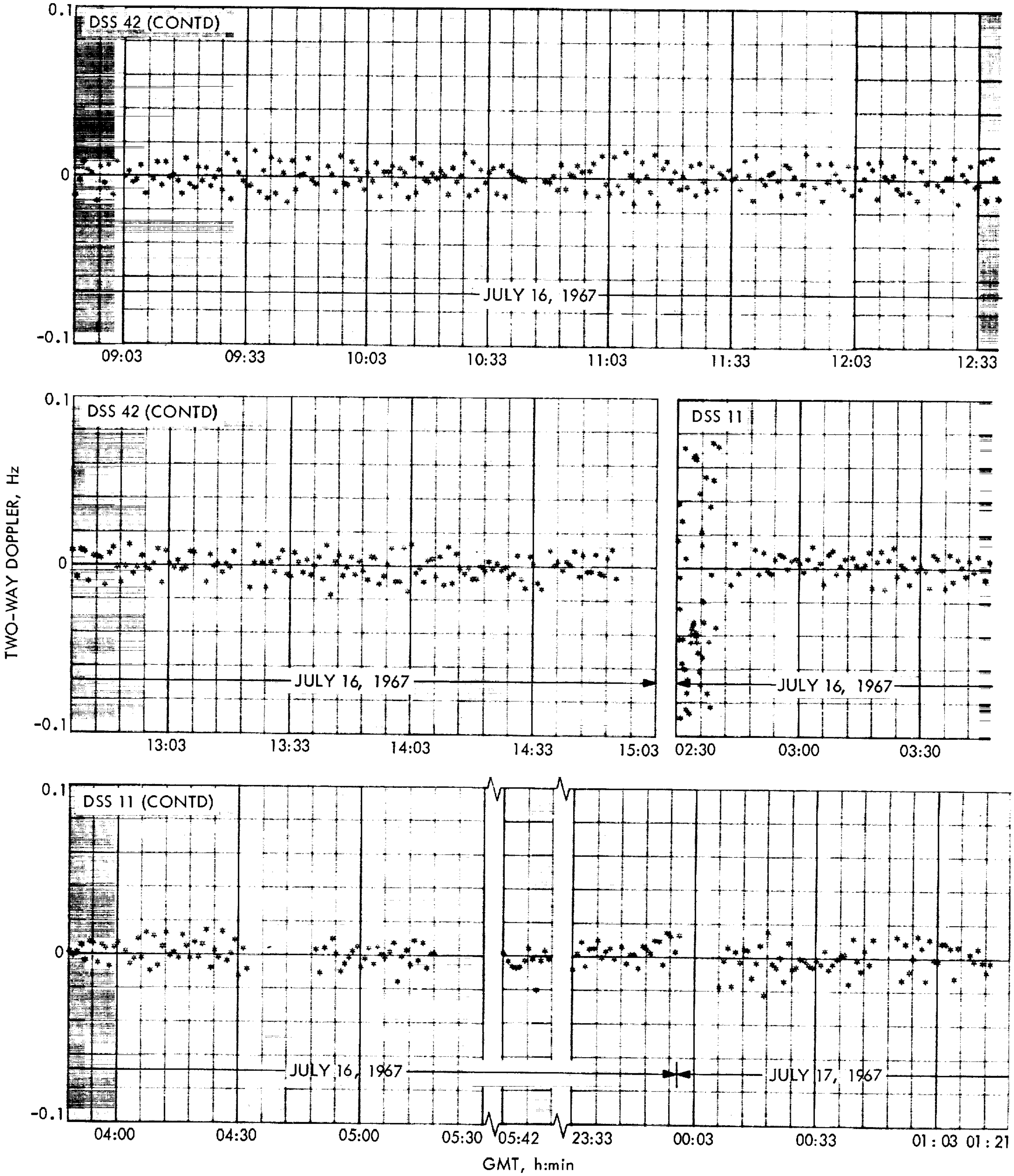
0.1
0
-0.1
DSS 42 (CONTD)
JULY 16, 1967
09:03
09:33
10:03
10:33
11:03
11:33
12:03
12:33
TWO-WAY DOPPLER, Hz
DSS 42 (CONTD)
JULY 16, 1967
13:03
13:33
14:03
14:33
15:03
DSS 11
JULY 16, 1967
02:30
03:00
03:30
DSS 11 (CONTD)
JULY 16, 1967
JULY 17, 1967
04:00
04:30
05:00
05:30
05:42
23:33
00:03
00:33
01 : 03
01 : 21
GMT, h:min

Fig. 33 (contd)

A number of 6 × 6 orbit computations were made with various combinations of data from three stations. A comparison of the results showed that all data were consistent. An attempt was made to improve the fit by expanding the set of estimated parameters from 6 to 18 to include the station location parameters of the four stations. Examination of the residual plots from this 18 × 18 solution still indicates a poor fit, although the predicted target parameters did agree with previous results. A total of 25 orbit solutions was computed by estimating various combinations of physical constants and trajectory perturbations.

A number of orbital computations were made using the MOD II ODP in an attempt to improve the data fit by solving for nongravitational trajectory perturbations and thereby provide a refined estimate of the postmaneuver orbit. The formulation referred to in this paragraph is discussed in Section II.A. The coefficients of the time polynomial (α_1, α_2) were estimated for two cases, but the data fit was not improved. For most cases the solar radiation coefficients (G_R, G_T, G_N) were not estimated. In such computations, where the α's and G's were not estimated, Eq. (1) was reduced to simply

$$\Delta\ddot{\mathbf{r}} = f_1\mathbf{U} + f_2\mathbf{T} + f_3\mathbf{N} \qquad (2)$$

An 18 × 18 orbit solution, using all postmaneuver data, was obtained and mapped to target. This geocentric solution was based on estimating the standard 6 parameters, the station location parameters (radius, latitude, longitude) for the three stations, and the three accelerations (f_1, f_2 and f_3) for the entire trajectory. Examination of the doppler residual plots (Fig. 33) indicated that the fit had been significantly improved. Also, the predicted unbraked impact point agreed very well with the inflight results, and the predicted impact time agreed with the observed time to within 0.136 s. Table 38 presents a comparison of the inflight and postflight determination of unbraked impact time. The 18 × 18 orbit solution using all postmaneuver data is considered to be the current best estimate of the *Surveyor IV* postmaneuver orbit.

The following are the nongravitational acceleration perturbations estimated in the 18 × 18 solution:

$$f_1 = 0.94 \times 10^{-10}\ \mathrm{km/s^2}$$

$$f_2 = 0.11 \times 10^{-9}\ \mathrm{km/s^2}$$

$$f_3 = 0.23 \times 10^{-9}\ \mathrm{km/s^2}$$

$$[\Delta\ddot{\mathbf{r}}] \cong 0.272 \times 10^{-9}\ \mathrm{km/s^2}$$

Table 38. Comparisons of inflight and postflight AMR backup computations for *Surveyor IV*

Orbit solution data span		Unbraked impact, GMT		Difference between solutions, s
From	To	Inflight computations h:min:s	Postflight computations[a] h:min:s	
Midcourse[b]	E − 5 h 40 min	02:02:29.020	02:02:29.495	0.475
E − 5 h 40 min	E − 1 h 50 min	02:02:30.024	02:02:30.500	0.476
E − 5 h 40 min	E − 1 h 38 min	02:02:29.996	02:02:30.462	0.466
E − 5 h 40 min	E − 1 h 23 min	02:02:30.018	02:02:30.484	0.466
E − 5 h 40 min	E − 1 h 14 min	02:02:30.014	02:02:30.470	0.456
E − 5 h 40 min	E − 59 min	02:02:29.690[c]	02:02:30.698	1.008
E − 5 h 40 min	E − 45 min	02:02:30.397	02:02:30.967	0.570

[a]With corrected DSS 11 frequency and lunar radius.
[b]Postmidcourse epoch at end of motor burn.
[c]Bad run because of computer problems encountered.

These results indicate that some perturbations did exist in the postmaneuver trajectory and that their effect can be accounted for by solving nongravitational acceleration perturbations. The causes of these perturbations in the acceleration are still being investigated. However, the solar radiation pressure, uncancelled velocity increment from normal operations of the attitude control system, possible attitude jet misalignment, and possible gas and propellant leaks could be some of the causes for the perturbations. Even though these trajectory perturbations were not accounted for during inflight computations, the orbit determination requirements were met. Numerical values from the best estimate 18 × 18 postmaneuver orbit solutions are presented in Table 36. The amount of data used in this solution, together with the associated noise statistics, is shown in Table 37. From this current best estimate, and the assumption of a nominal landing sequence, the *Surveyor IV* spacecraft is estimated to be at 358.450°E lon and 0.373°N lat. This is 0.044 deg (≈1.3 km) south and 0.217 deg (≈6.5 km) west of the final soft landing aim point.

D. Evaluation of Midcourse Maneuver from DSIF Tracking Data

The *Surveyor IV* midcourse maneuver can be evaluated by examining the velocity change at the midcourse epoch and by comparing the maneuver aim point with the target parameters from the best-estimate postmidcourse orbit solution.

Table 39. Midcourse maneuver evaluated at midcourse epoch, *Surveyor IV*

Current best estimate of premaneuver velocity, m/s	Inflight[a] estimate of premaneuver velocity, m/s	Current best estimate of postmaneuver velocity at midcourse epoch,[b] m/s	Observed velocity change due to maneuver (best post—best pre), m/s	Commanded[a] maneuver velocity change, m/s	Total maneuver errors: Execution errors (observed change —commanded change), m/s	Total maneuver errors: OD errors (best pre-inflight), m/s
$DX = -535.8995$	−535.9417	−545.7902	$\Delta DX = -9.8907$	−9.9447	0.0540	0.0422
$DY = -1014.3888$	−1014.3666	−1014.7810	$\Delta DY = -0.3922$	−0.3421	−0.0501	−0.0222
$DZ = -366.0315$	−366.0038	−363.4728	$\Delta DZ = 2.5587$	2.5494	0.0093	−0.0277

Note

All velocity components are given in geocentric space-fixed Cartesian coordinates.

[a]Based on inflight premaneuver orbit solution (LAPM YC) used for midcourse maneuver computations.

[b]Midcourse epoch ≃ end of reorientation after motor burn, July 16, 1967, 02:30:10.461 GMT.

The *observed* change in velocity owing to midcourse thrust is determined by differencing the velocity components of best-estimate orbit solutions taken from postmaneuver data only and premaneuver data only. These solutions are independent; i.e., *a priori* information from premaneuver data is not used during the processing of postmaneuver data. The estimated maneuver execution errors, at midcourse epoch, are determined by differencing the observed velocity changes and the commanded maneuver velocity increments. The remaining major contribution to the total maneuver error is made by the orbit determination process. This error source includes ODP computational and model errors, and errors in tracking data. These errors may be obtained by differencing the velocity components, at midcourse epoch, of the best-estimate premaneuver orbit and the inflight orbit solution used for the maneuver computations. Numerical results of this part of the evaluation are presented in Table 39 in which it can be seen that the execution errors in DX, DY and DZ were only $+0.0540$ m/s, -0.0501 m/s, and $+0.0093$ m/s, respectively. The OD errors are also very small. The total maneuver errors for *Surveyor IV* were well within specifications.

A more meaningful evaluation can be made by examining certain critical target parameters. Since the primary objective of the midcourse maneuver is to achieve lunar encounter at the selected landing site, the maneuver unbraked aim point is used as the basic reference for this evaluation. The unbraked aim point for *Surveyor IV* was 0.469°N lat and 358.914°E lon. To achieve landing at the desired site, trajectory corrections were based on the predicted unbraked impact point from the best estimate inflight orbit solution (LAPM YC). To evaluate the total maneuver error at the target, the maneuver aim point is compared with the predicted unbraked impact point from the current best-estimate postmaneuver orbit solution. Orbit determination errors can be obtained by differencing the unbraked target parameters of the current best-estimate premaneuver orbit solution and the inflight orbit solution used for maneuver computations. Execution errors, consisting of both attitude maneuver errors and engine system errors, are then determined by differencing the total and the orbit determination errors. Numerical results of these computations, presented in Table 40, show that encounter was achieved within 0.044 deg south and 0.217 deg west of the desired aiming point. These differences in latitude and longitude are roughly equivalent to 1.32 km and 6.51 km, respectively, on the lunar surface. The OD **B**-space position errors ($\Delta \mathbf{B} \cdot \mathbf{T}T = -5.0$ km, $\Delta \mathbf{B} \cdot \mathbf{R}T = 2.5$ km) are well within the expected

Table 40. Lunar unbraked impact points, *Surveyor IV*

Source	Latitude, deg (minus, south)	Longitude, deg (east)
Best estimate of premidcourse	−2.067	353.943
Inflight premidcourse orbit (LAPM YC)	−2.005	354.070
Best estimate of post-midcourse	0.425	358.697
Maneuver unbraked aim point	0.469	358.914

Estimated midcourse errors mapped to unbraked impact point

Source	Δ Latitude: deg (minus, south)	Δ Latitude: ≈km	Δ Longitude: deg (minus, west)	Δ Longitude: ≈km
OD errors[a]	−0.062	−1.86	−0.127	−3.81
Maneuver error[b]	0.018	0.54	−0.090	−2.70
Overall errors[c]	−0.044	−1.32	−0.217	−6.51

[a]Orbit determination errors: Current best premaneuver estimate *minus* orbit used for maneuver computations (LAPM YC).

[b]Maneuver errors: Overall errors *minus* OD errors.

[c]Overall errors: Current best postmaneuver estimate *minus* aiming point.

Table 41. Station locations and statistics, *Surveyor IV* (referenced to 1903.0 pole)

DSS	Data source	Distance off spin axis r_s, km	r_s Standard deviation (1σ), m	Geocentric longitude, deg	Longitude standard deviation (1σ), m	Geocentric radius, deg	Geocentric latitude,[a] deg
11	*Mariner II*	5206.3357	3.9	243.15058	8.8	6372.0044	35.208035
	Mariner IV, cruise	404	10.0	067	20.0	.0188	08144
	Mariner IV, postencounter	378	37.0	072	40.0	.0161	08151
	Pioneer VI, Dec. 1965–June 1966	359	9.6	092	10.3	.0286	08030
	Goddard Land Survey, Aug. 1966	718	29.0	094	35.0	.0640	08230
	Surveyor I, post-touchdown	276	2.9	085	23.8	.6446	16317
	Surveyor I, inflight	417	49.3	125	46.0	.0240	08192
	Surveyor III, inflight	431	22.1	086	45.0	.0258	08192
	Surveyor IV, inflight	326	41.1	097	49.0	.0129	08192
42	*Mariner IV*, cruise	5205.3478	10.0	148.98136	20.0	6371.6882	−35.219410
	Mariner IV, postencounter	.3480	28.0	134	29.0	.6824	19333
	Pioneer VI, Dec. 1965–June 1966	.3384	5.0	151	8.1	.6932	19620
	Goddard Land Survey, Aug. 1966	.2740	52.0	000	61.0	.7030	20750
	Surveyor I, post-touchdown	.3474	3.5	130	22.1	.6651	19123
	Surveyor I, inflight, postmidcourse only	74	29.2	161	41.0	.6845	19372
	Surveyor III, inflight	74	25.3	156	42.0	.6847	19372
	Surveyor IV, inflight	87	34.8	161	49.0	.6861	19372
51	Combined *Rangers*, LE-3[b]	5742.9315	8.5	27.68572	22.2	6375.5072	−25.739169
	Ranger VI, LE-3	203	19.7	572	69.3	.4972	9215
	Ranger VII, LE-3	211	25.5	583	61.3	.4950	9157
	Ranger VIII, LE-3	372	22.3	548	85.0	.5130	9159
	Ranger IX, LE-3	626	56.6	580	49.5	322	8993
	Mariner IV, cruise	363	10.0	540	20.0	120	9148
	Mariner IV, postencounter	365	40.0	557	38.0	143	9198
	Pioneer VI, Dec. 1965–June 1966	332	11.6	569	12.0	094	9176
	Goddard Land Survey, Aug. 1966	706	39.0	586	43.0	410	8990
	Surveyor I, inflight	382	33.9	572	41.2	146	9169
	Surveyor III, inflight	347	32.7	570	45.0	108	9169
	Surveyor IV, inflight	337	39.3	575	46.8	096	9169

[a]Latitude was not estimated for *Surveyor* inflight solutions.

[b]Lunar ephemeris 3 (DE-15); all *Surveyor* inflight solutions used LE-4 (DE-19).

accuracy.[12] In general, the accuracy of the *Surveyor IV* midcourse maneuver is well within the *Surveyor* Project specifications. These results cannot be used to precisely evaluate the *Centaur* injection accuracy since the inflight aim point was not exactly the same as the prelaunch aim point.

E. Estimated Tracking Station Locations and Physical Constants

*1. **Introduction.*** Computations were made to determine the best estimate of GM_{earth}, GM_{moon} and station location parameters for *Surveyor IV* mission. The parameters estimated in these computations were the spacecraft position and velocity at an epoch; GM_{earth}; GM_{moon}; spacecraft acceleration perturbations f_1, f_2 and f_3; the solar radiation constant G; and two components (geocentric radius and longitude) of station locations for each of DSS 11, 42, 51 and 61. These solutions were computed using only the two-way doppler data from stations 11, 42, 51 and 61 for both the premidcourse and postmidcourse phases. In an effort to obtain the best estimate of the parameters to be solved for, the premidcourse data block was combined with the postmidcourse data block. The procedure of combining the two data blocks is to fit only the premidcourse data, accumulate the normal equations at the injection epoch, and map the converged estimate to the midcourse epoch with a linear mapping of the inverted normal equation matrix (i.e., covariance matrix). The estimate is then incremented with the best estimate of the maneuver, and the mapped covariance matrix is corrupted in the velocity increment and used as *a priori* for the postmidcourse data fit. The ephemeris used in the reduction was the JPL DE-19 with the updated mass ratios and Eckert's corrections.

*2. **Results.*** The results of these computations are presented in Table 41 in an unnatural station coordinate system (geocentric radius, latitude and longitude) and in a natural coordinate system (r_s, λ, Z) where r_s is the distance off the spin axis (in the station meridian), λ is the longitude, and Z is a line along the earth spin axis (see Fig. 16).

The numerical results indicate that the value obtained for r_s for DSS 11 is a few meters smaller than most of the previous solutions listed. All other station location parameters estimated are consistent with previous solutions. As with *Surveyors I* and *III*, the improved values[13] of DSS indices of refraction were used in the solution. The new indices improved the data fit for all stations which took low elevation data. Previous to the availability of new indices, a value of 340 was used for all Deep Space Stations.

The *Surveyor I* solution for longitude of DSS 42 is higher than previous solutions. However, the *Surveyor IV* solution is consistent with this and all the other *Surveyor* solutions which have been computed in postflight analysis of the tracking data. Therefore, the estimate for DSS 42 longitude is considered a good one. All other station locations estimated for *Surveyor IV* are within the range of the previous solutions listed. The statistics obtained with the station locations are higher than those of most other missions because larger effective data weights were used for *Surveyor* missions and the amount of data available is generally smaller.

Table 42. Physical constants and statistics, *Surveyor IV*

Data source	GM_{earth}, km^3/s^2	Standard deviation (1σ), km^3/s^2	GM_{moon}, km^3/s^2	Standard deviation (1σ), km^3/s^2
Lunar Orbiter II (doppler)	398600.88	2.14	4902.6605	0.29
Lunar Orbiter II (doppler and range)	398600.37	0.68	4902.7562	0.13
Combined *Rangers*	398601.22	0.37	4902.6309	0.074
Ranger VI	398600.69	1.13	4902.6576	0.185
Ranger VII	398601.34	1.55	4902.5371	0.167
Ranger VIII	398601.14	0.72	4902.6304	0.119
Ranger IX	398601.42	0.60	4902.7073	0.299
Surveyor I	398600.62	0.63	4902.6529	0.236
Surveyor III	398600.78	0.72	4902.7102	0.230
Surveyor IV	398601.19	0.99	4902.6297	0.247

The GM_{earth} and GM_{moon} estimates for *Surveyor IV* are given in Table 42 along with previous solutions. The value for GM_{earth} is consistent with the combined *Ranger* solutions. It is also within the range of individual *Ranger* solutions. The value obtained for GM_{moon} is consistent when compared with the other solutions, being slightly lower than previous *Surveyors*. It is within the value plus $1\ \sigma$ of the combined solutions for *Ranger*. The correlation matrix on postmaneuver data with premaneuver data as *a priori* is given in Table 43.

*3. **Conclusion.*** The GM_{earth} and GM_{moon} estimates were well within the standard deviation ($1\ \sigma$) of the combined *Ranger* estimates, but differ slightly from estimates of *Surveyors I* and *III*. The station location parameters are

[12]See Ref. 8 for expected accuracy of orbit determination.

[13]Indices of refraction obtained from A. S. Liu, JPL: DSS 11 = 240, DSS 42 = 310, DSS 51 = 240.

Table 43. Correlation matrix of estimated parameters, *Surveyor IV* (solution on postmaneuver data with premaneuver data as *a priori* at maneuver epoch)

Standard deviation		X	Y	Z	DX	DY	DZ	GM_{earth}	G	GM_{moon}	f_1	f_2	f_3	R_{11}	Lon_{11}	R_{42}	Lon_{42}	R_{51}	Lon_{51}
X	2.32	1.000	−0.375	−0.287	−0.770	0.651	0.299	−0.107	0.000	0.052	0.592	0.308	0.286	0.141	0.293	0.151	0.349	0.152	0.512
Y	2.60		1.000	−0.707	0.093	−0.080	−0.108	0.021	0.000	0.011	−0.149	−0.023	−0.121	0.579	0.661	0.717	−0.679	0.741	−0.672
Z	4.52			1.000	0.532	−0.520	−0.031	−0.012	0.000	−0.081	−0.410	−0.191	−0.229	−0.814	0.492	−0.914	0.383	−0.860	0.373
DX	0.088				1.000	−0.796	−0.442	0.035	0.000	0.234	−0.947	−0.558	−0.405	−0.420	−0.037	−0.413	−0.148	−0.318	−0.250
DY	0.062					1.000	−0.188	−0.060	0.000	−0.159	0.749	0.017	0.727	−0.422	−0.154	0.417	0.152	0.298	0.038
DZ	0.079						1.000	0.033	0.000	−0.158	0.435	0.871	−0.403	0.013	0.370	−0.013	0.102	0.006	0.418
GM_{earth}	0.99							1.000	0.000	0.003	0.001	0.027	−0.033	0.051	0.036	0.021	0.003	−0.010	−0.023
G	0.10								1.000	0.000	−0.001	0.000	0.000	0.000	0.000	0.000	0.000	0.000	0.000
GM_{moon}	0.247									1.000	−0.334	−0.099	−0.221	0.104	0.048	0.110	0.073	0.071	0.050
f_1	0.17×10^{-8}										1.000	0.507	0.517	0.344	0.076	0.302	0.224	0.143	0.255
f_2	0.14×10^{-8}											1.000	−0.473	0.219	0.111	0.183	−0.110	0.224	0.167
f_3	0.19×10^{-8}												1.000	0.127	−0.027	0.131	0.343	−0.082	0.106
R_{11}	0.050													1.000	−0.419	0.732	−0.359	0.672	−0.440
Lon_{11}	0.00049														1.000	−0.531	0.854	−0.521	0.897
R_{42}	0.043															1.000	−0.457	0.875	−0.418
Lon_{42}	0.00049																1.000	−0.531	0.859
R_{51}	0.044																	1.000	−0.444
Lon_{51}	0.00047																		1.000

Units of measure

X, Y, Z: km

DX, DY, DZ: m/s

GM_{earth}, GM_{moon}: km^3/s^2

f_1, f_2, f_3: km/s^2

G (solar radiation coefficient), unitless

Lon, deg

R, km

in good agreement with the *Ranger*, *Mariner*, *Lunar Orbiter*, and *Pioneer* missions. The results of successive *Surveyor* estimates will be presented in their associated flight path reports. For *Surveyor III* estimates, see Section VI.E.

XI. Observations and Conclusions from Surveyor IV

A. Tracking Data Evaluation

The most serious loss of two-way doppler data during the *Surveyor IV* mission occurred during the first pass at DSS 61. DSS 61 began taking two-way doppler data at 17:03:02 GMT on July 14, and approximately 20 min later the results of the data monitor program indicated excessive noise in the DSS 61 doppler data. The problem was traced to a dropped 8-bit in the least significant digit of the doppler counter. A transfer to DSS 51 could not be effected until 18:30:00 on July 14, at which time DSS 51 reacquired good two-way doppler data. This problem at DSS 61, which resulted in the loss of approximately 1½ h of two-way doppler, almost parallels the problem which occurred during the first pass of DSS 61 on the *Surveyor III* mission. Minor losses of data occurred during the initial acquisition at DSS 72, when a loss of the uplink was responsible for a 10-min loss of prime early data, and during the second pass at DSS 11, when an intermittent loss of the most significant digit of the doppler counter accounted for a 30-min loss of data. The effect from these data losses on the mission was negligible.

1. Premidcourse phase angular tracking. Because doppler data yield far greater accuracy in the determination of a spacecraft orbit than angle data do, they are used almost exclusively in the orbit determination process. The one exception is during the launch phase, when little doppler data are available and a quick determination of the orbit necessitates the use of both doppler and angle data. During the *Surveyor IV* mission, angle data from DSS 72 and DSS 51 were used in the orbit determination program during the premidcourse phase of the mission. To improve the quality of the angle data to be used in the orbit determination program, they are first corrected for antenna optical pointing error as discussed in Section II.B.

Since DSS 72 was the initial acquisition station, the angle data taken by it was the most important angle data for use in the early orbits. These data, when fitted through the final postflight orbit, show a bias of +0.046 deg in azimuth and +0.097 deg in elevation, and a standard deviation of 0.210 deg. Considering these biases and the high noise level, the DSS 72 angle data are poor. The quality of these angle data match that of the very poor angle data taken by DSS 72 during its first pass of *Surveyor III*, in contrast to the better angle data taken by DSS 72 on the *Atlas–Centaur 9* and *Surveyor II* missions. First-pass angle data from DSS 51, when fitted through the final postflight orbit, shows biases of +0.028 deg in hour angle and −0.018 deg in declination. These values correlate well with past experience on *Surveyor* missions. For instance, the DSS 51 hour angle and declination biases averaged over *Atlas–Centaur 9*, *Surveyor II*, and *Surveyor III* were +0.028 deg and −0.020 deg, respectively.

2. Doppler tracking. The first prime station to see the spacecraft after injection, DSS 72, began taking good two-way, 10-s-count doppler data at 12:16:23 GMT on July 14, 1967. However, two-way lock was lost at 12:17:03 and was not recovered until 12:25:54. At this time DSS 72 resumed taking good 10-s-count two-way doppler data. The sample rate was changed to 60 s at 12:45:02 and two-way tracking was transferred to DSS 51 at 13:11:02. These early data from DSS 72 were quite acceptable, showing a standard deviation of 0.026 Hz. Results of the midcourse maneuver burn can be seen in the DSS 11 two-way doppler data shown in Fig. 34.

All post-midcourse orbit computations used only two-way doppler from the prime stations DSS 11, DSS 42, and DSS 51. Very good two-way doppler data were obtained throughout the postmidcourse phase without exception. The doppler data from all stations indicated a standard deviation of 0.007 Hz during this period, and any biases in the data were minuscule. Results of the retroengine burn as seen in the one-way doppler data over DSS 11 are presented in Fig. 35.

B. Comparison of Inflight and Postflight Results

The orbit determination inflight results can be evaluated by comparing them with the results obtained from the postflight computations. The degree to which these results agree is primarily influenced by the success attained in detecting and eliminating bad or questionable tracking data from the inflight computations, and accounting for all trajectory perturbations. Of these, the largest variations are usually caused by bad or questionable data resulting from equipment malfunctions, incorrect time information, or incorrect frequency information. Other than obvious blunder points, these data are not easily detected. Having data from more than two stations is necessary to isolate bad data.

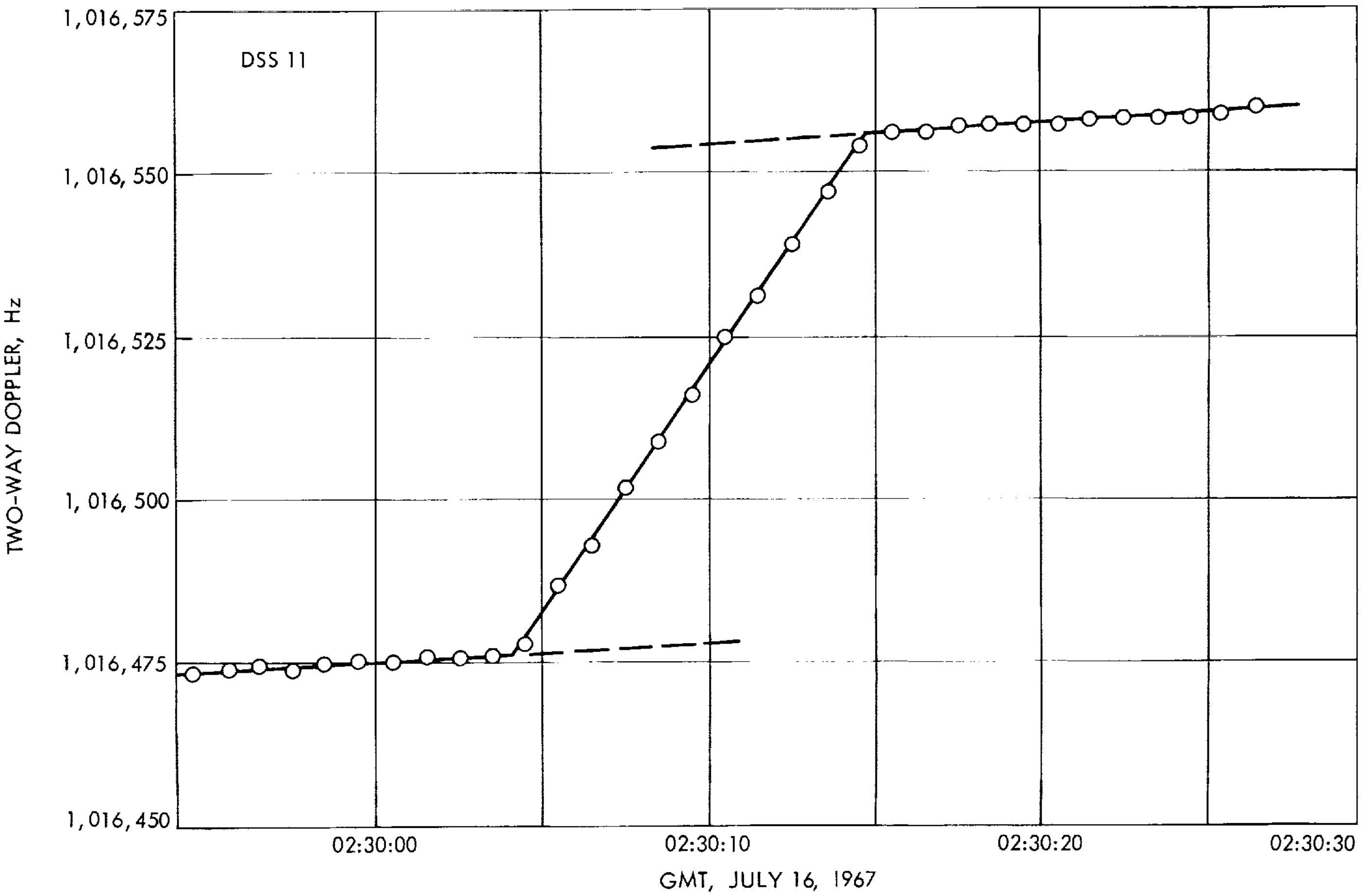

Fig. 34. Midcourse maneuver doppler for Surveyor IV

The most meaningful comparison between inflight and postflight orbit determination results can be made by examining the critical target parameters—the unbraked impact time and impact location. These results, summarized in Table 44, show that the inflight premaneuver impact point was in error by 0.07 deg in latitude and 0.13 deg in longitude. This is well within the uncertainty associated with the inflight estimate. The inflight postmaneuver impact point associated with the orbit solution (3 POM YD) used for the terminal attitude maneuver

Table 44. Summary of target impact parameters, Surveyor IV

Source	Estimated unbraked impact location		Uncertainty about estimated impact point (1 σ dispersion ellipse)			Estimated unbraked impact time, GMT h:min:s	Uncertainty in estimated unbraked impact time (1 σ), s
	Latitude, deg (minus, south)	Longitude, deg	SMAA, km	SMIA, km	θ_T, deg		
Premaneuver (uncorrected)							
Inflight OD	−2.00	354.07	10.0	2.0	35.00	02:11:42.145	2.66
Postflight OD	−2.07	353.94	10.0	2.0	34.71	02:11:44.824	2.66
Postmaneuver (transit)							
Inflight OD	0.44	358.63	7.0	5.0	87.22	02:02:29.645	0.500
Postflight OD	0.43	358.70	7.0	5.0	77.47	02:02:31.171	0.500
Observed unbraked impact	—	—	—	—	—	02:02:31.267	0.050

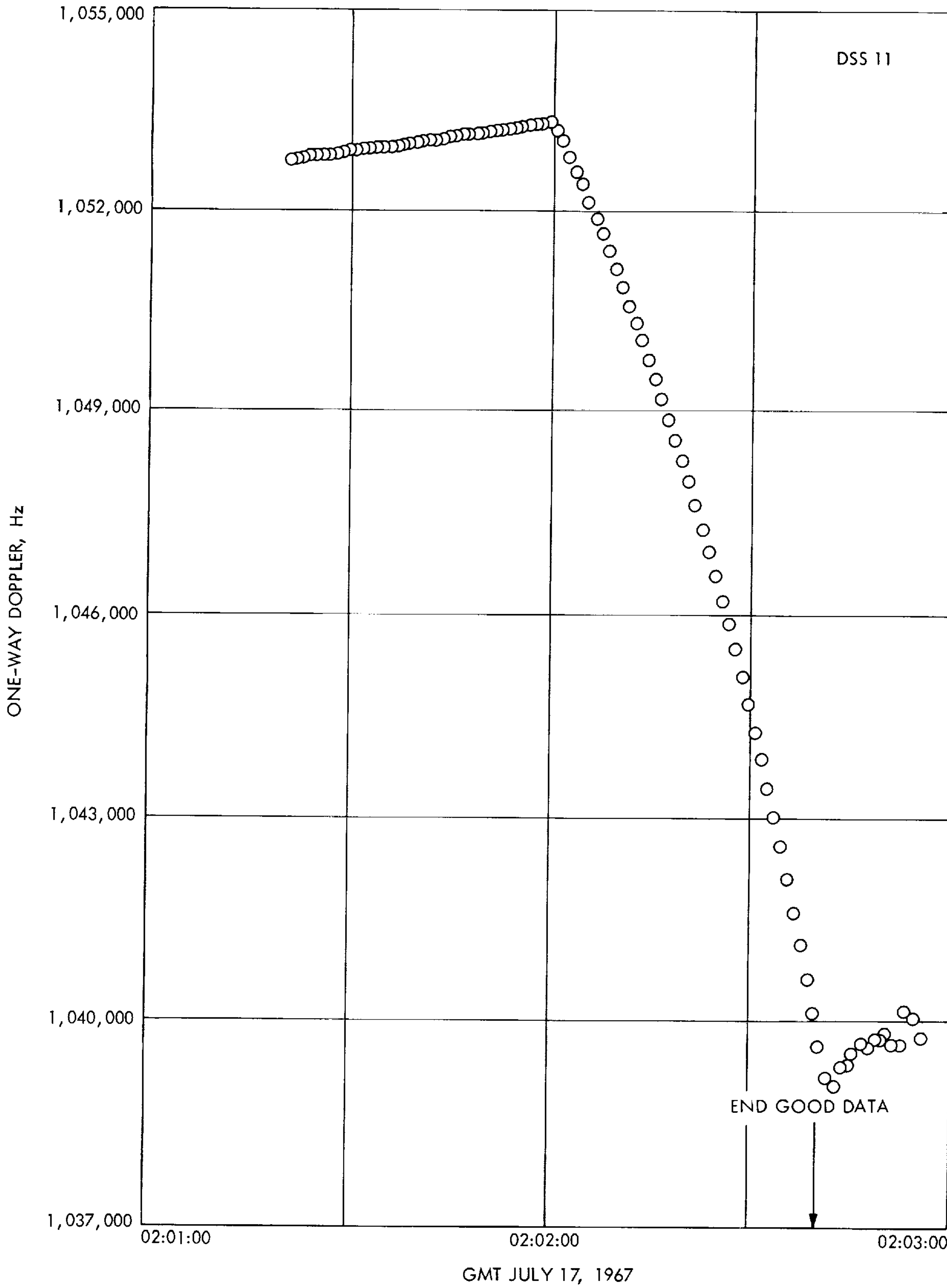

Fig. 35. Main retromotor burn phase doppler for Surveyor IV

computations was in error by 0.018 deg in latitude and 0.068 deg in longitude. These errors are also within the stated uncertainties associated with the inflight estimates. The inflight predicted unbraked impact time used to provide the AMR backup was in error by 0.774 s which was within 2-σ uncertainty of 1.000 s. Part of this error was caused by an incorrect input of DSS 11 station frequency and part was caused by an incorrect input of lunar elevation as discussed in Section X. C. Had the correct frequency and lunar elevation been used, this error would have been reduced to 0.340 s.

Since no posttouchdown data are available from *Surveyor IV*, no independent estimates of impact location can be based on posttouchdown tracking data or photo correlation with *Lunar Orbiter*. The *observed* unbraked impact time and impact time predicted by the current best postmaneuver orbit solution (based on a lunar elevation of 1735.7 km) differ by only 0.136 s.

The following conclusions may be made from the results of the comparison between inflight and postflight results: (1) the premaneuver guaranteed OD accuracies were met; (2) the postmaneuver guaranteed OD accuracies were met even though an incorrect frequency was used for the last few points of DSS 11 data.

XII. Analysis of Air Force Eastern Test Range Tracking Data—*Surveyor IV*

A. Introduction

The AFETR supports the *Surveyor* missions by computing injection conditions and classical orbital elements for the parking orbit, the spacecraft transfer orbit, and the *Centaur* postretro orbit. However, since *Surveyor IV* was a direct ascent mission, parking orbit computations were not applicable. The injection conditions computed by the AFETR are relayed to the SFOF in Pasadena where they may be used as the initial values for early JPL orbit computations. The AFETR also transmits initial acquisition information to the SFOF, which may be relayed to the Deep Space Stations. The input for the AFETR calculations is the *Centaur* C-band tracking data obtained from various AFETR and MSFN tracking stations,[14] the locations of which are given in Table 45.

In addition to fulfilling these requirements, the AFETR transmits the C-band tracking data taken during the transfer orbit and the *Centaur* postretro orbit to the SFOF.

[14]Trinidad uses skin tracking of the *Centaur* vehicle; it does not have C-band tracking capability.

Table 45. AFETR station locations used for Surveyor IV

Station	Radar type	Geocentric radius, km	Geocentric latitude, deg (minus, south)	Longitude, deg
Pretoria	MPS-25	6375.7617	−25.7960	28.35670
Ascension	TPQ-18	6377.9609	−7.9223	345.59729
Trinidad[a]	FPS-43	6377.7316	10.6717	298.39093
Antigua	FPQ-6	6376.3798	17.0349	298.20663
Grand Turk	TPQ-18	6375.3547	21.3313	288.86751

[a]Trinidad uses skin tracking of the *Centaur* vehicle; it does not have C-band tracking capability.

The transfer orbit data are used to compute an early JPL transfer orbit based solely on the C-band data that are used as a backup should unusual circumstances cause a failure of the AFETR orbit computation system. Under normal conditions, the early JPL orbit is used as a quick check on the AFETR transfer orbit. The *Centaur* postretro orbit is made available to verify that the *Centaur* retromaneuver was performed properly, ensuring that the *Centaur* will not impact the moon and that the spacecraft will be separated from the *Centaur* sufficiently so that the Canopus sensor on board the spacecraft will not lock up on the *Centaur*. The AFETR tracking coverage for *Surveyor IV* is shown in Fig. 36.

B. Analysis of the Transfer Orbit Data

The inflight transfer orbit computed at JPL from the C-band tracking data used only data taken during the time span from *Centaur* main engine cutoff to separation of the spacecraft from the *Centaur*. All data before main engine cutoff are unusable since the vehicle is experiencing a high-thrust acceleration that would perturb any transfer orbit solution. Any C-band data taken after separation of the spacecraft from the *Centaur* are questionable for use in a spacecraft transfer orbit solution because the C-band radars are actually tracking the *Centaur* and not the spacecraft. After separation, the *Centaur* executes a turnaround maneuver and lateral thrust maneuver preparatory to the *Centaur* retromaneuver.

Centaur transfer orbit data were obtained from the Trinidad and Antigua tracking stations. About 18 s of low-elevation data at a rate of 1 point/6 s was obtained from Trinidad skin-tracking during the unpowered part of the flight. About 48 s of free-flight data was obtained from Antigua C-band tracking at the same sample rate but at somewhat higher elevation angles. Figure 37 shows the elevation angles at Antigua and Trinidad during the time free-flight data were being taken.

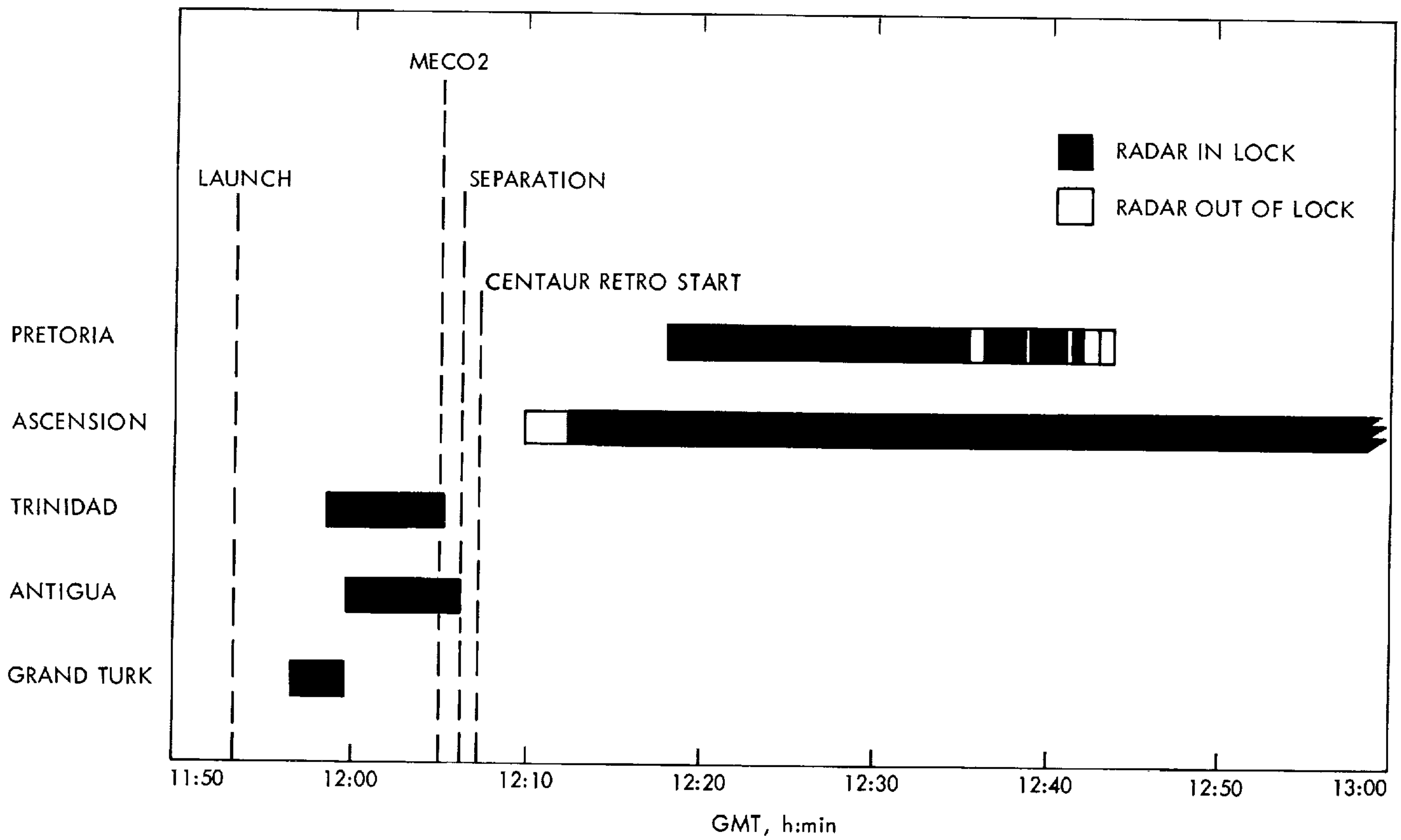

Fig. 36. AFETR tracking coverage for *Surveyor IV*

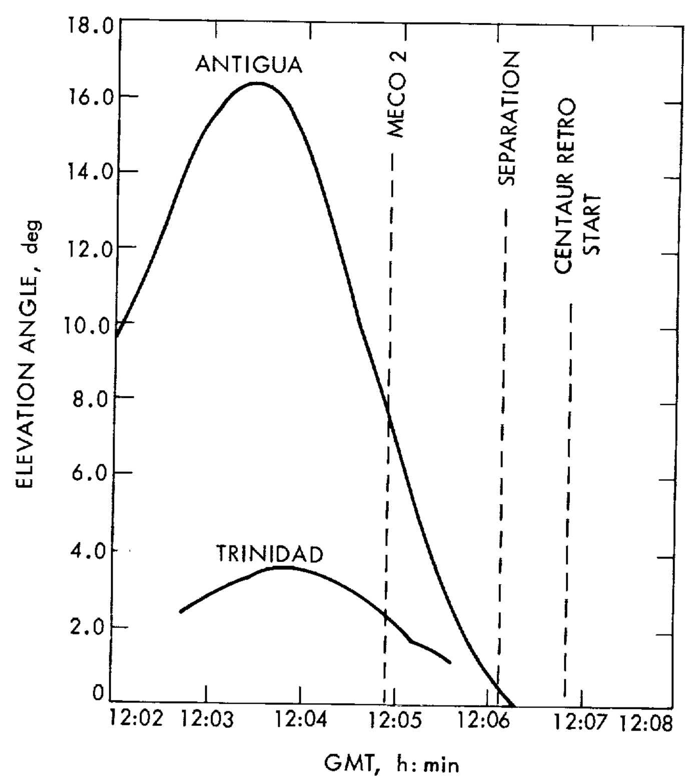

Fig. 37. AFETR station elevation angles for *Surveyor IV*

A comparison of the AFETR and JPL injection conditions is given in Table 46. The inflight best-estimate of the transfer orbit, also shown, is based on premidcourse DSIF data. Table 47 shows the data spans used for the JPL inflight transfer orbit on AFETR data and the associated statistics for the tracking data residuals. Figure 38 shows a time history of the residuals.

Table 46. Transfer orbit solutions, *Surveyor IV*

Parameter	Best inflight orbit computed by AFETR	Inflight orbit computed from AFETR data by JPL	Best DSIF orbit computed from premidcourse data
Epoch, GMT 12:05:06.480 (July 14, 1967)			
Geocentric position and velocity at epoch			
X, km	3084.3324	3098.4646	3086.8904
Y, km	5367.6490	5358.3490	5367.0377
Z, km	2133.4062	2140.6742	2133.6794
DX, km/s	−8.0374844	−8.0054246	−8.0394324
DY, km/s	6.0574391	6.1087959	6.0570880
DZ, km/s	−4.3658312	−4.3545489	−4.3609970
Unbraked impact quantities			
B, km	1781.04	3882.77	1778.7325
B • **T**T, km	1778.32	2497.99	1762.9854
B • **R**T, km	−98.51	2972.54	−236.16865
Latitude, deg	−4.78	−29.15	−2.0651264
Longitude, deg	354.48	102.452	353.95643
SMAA, km	Value not available	8224.	48.14
Unbraked impact, GMT	02:11:06.400 (July 17, 1967)	01:50:12.319 (July 17, 1967)	02:11:45.992 (July 17, 1967)

Table 47. Statistics of real-time transfer orbit tracking data residuals, *Surveyor IV*

Station and data type	Data span, GMT		Number of points	Standard deviation	Mean residual (O − C)
	Beginning h:min:s	Ending h:min:s			
Trinidad					
Range, km	12:05:15	12:05:33	4	0.049	−0.100
Azimuth, deg	12:05:15	12:05:33	4	0.020	−0.091
Elevation, deg	12:05:15	12:05:33	4	0.123	0.428
Antigua					
Range, km	12:05:12	12:06:00	9	0.003	0.008
Azimuth, deg	12:05:12	12:06:06	10	0.013	0.018
Elevation, deg	12:05:12	12:06:00	9	0.014	−0.026

The AFETR solution agrees very closely to the best inflight DSIF orbit computed from premidcourse data. The AFETR solution represents a remarkable solution when one considers that it was based on a short span of data. The JPL transfer orbit computed from the AFETR data does not compare quite as well with the DSIF orbit. However, the unbraked impact point of the best DSIF solution falls well within the impact dispersion ellipse of the JPL transfer orbit computed from the AFETR data. For this reason the three transfer orbit solutions are considered consistent. The AFETR solution is a fairly accurate one and the JPL solution is consistent with it and serves as a good check on the AFETR solution.

The fact that there is a difference between the AFETR solution and the JPL solution should not be alarming because some difference has always existed between the two solutions for all *Surveyor* missions. Five possible causes for the difference in the solutions are advanced:

(1) *Modifications made to the raw data used by the AFETR to compute the transfer orbit.* Before launch, the AFETR obtains the latest weather information from the various tracking stations to determine the index of refraction for each station. The AFETR is thus able to apply refraction corrections based on the current local atmospheric conditions. The SPODP program used by JPL applies a refraction correction to the computed observations but does not consider local conditions. The difference in refraction corrections used by the AFETR and JPL could account for a few meters in the range observable and a few hundredths of a degree in angle data. This difference in the data observables would also mean some difference in the converged transfer orbit solutions.

(2) *Difference in the tracking station locations used by the AFETR and JPL.* Since there is an uncertainty associated with the location of any tracking station, there is always a difference of opinion about which station location is best. As a part of the postflight analysis for *Surveyor IV*, a short study was made to determine the sensitivity of the AFETR transfer orbit solution to station-location variation. The conclusion drawn from this study was that minor station-location variations could not account for

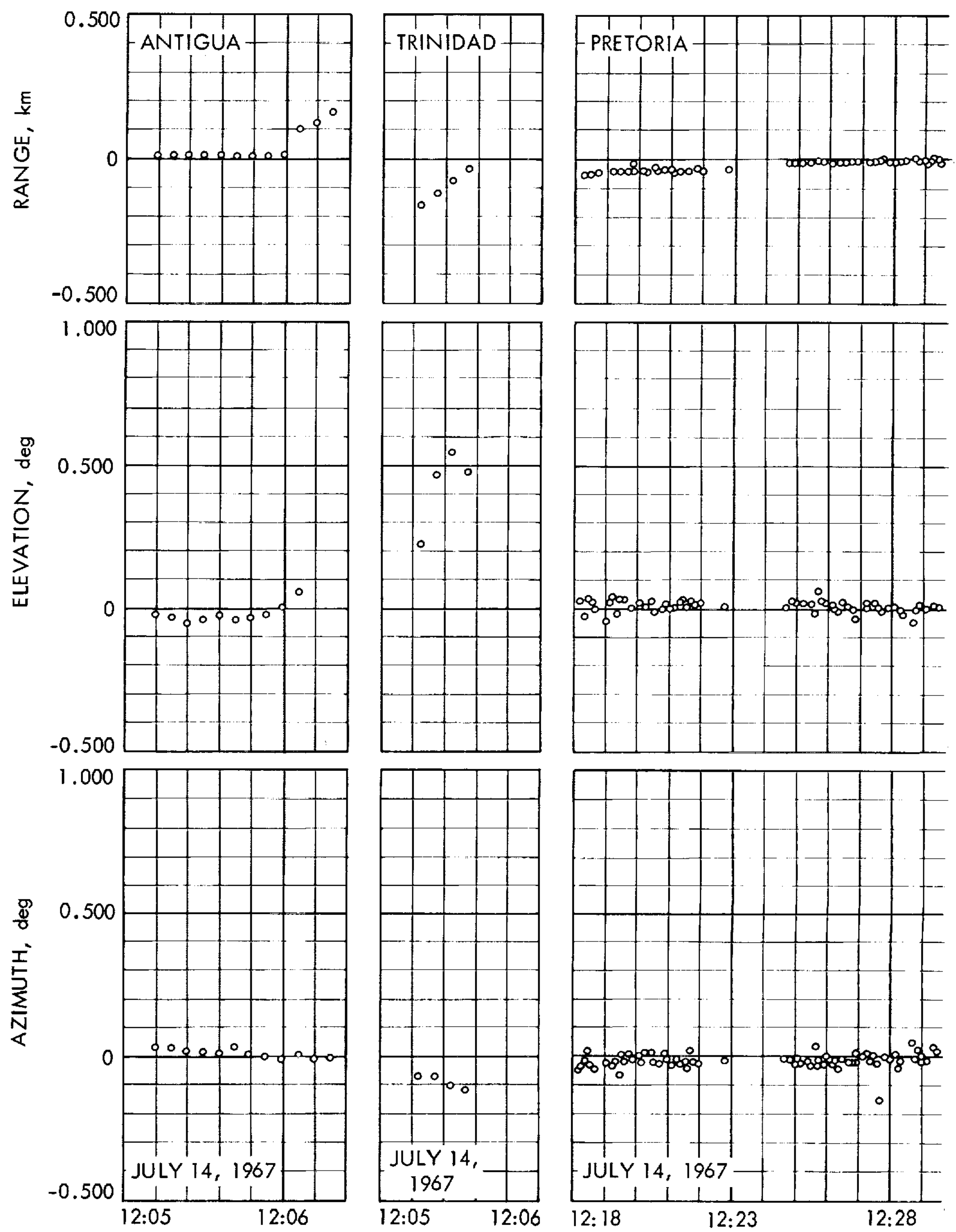

0.500
ANTIGUA
TRINIDAD
PRETORIA
RANGE, km
0
-0.500
1.000
ELEVATION, deg
0.500
0
-0.500
1.000
AZIMUTH, deg
0.500
0
-0.500
JULY 14, 1967
JULY 14, 1967
JULY 14, 1967
12:05
12:06
12:05
12:06
12:18
12:23
12:28

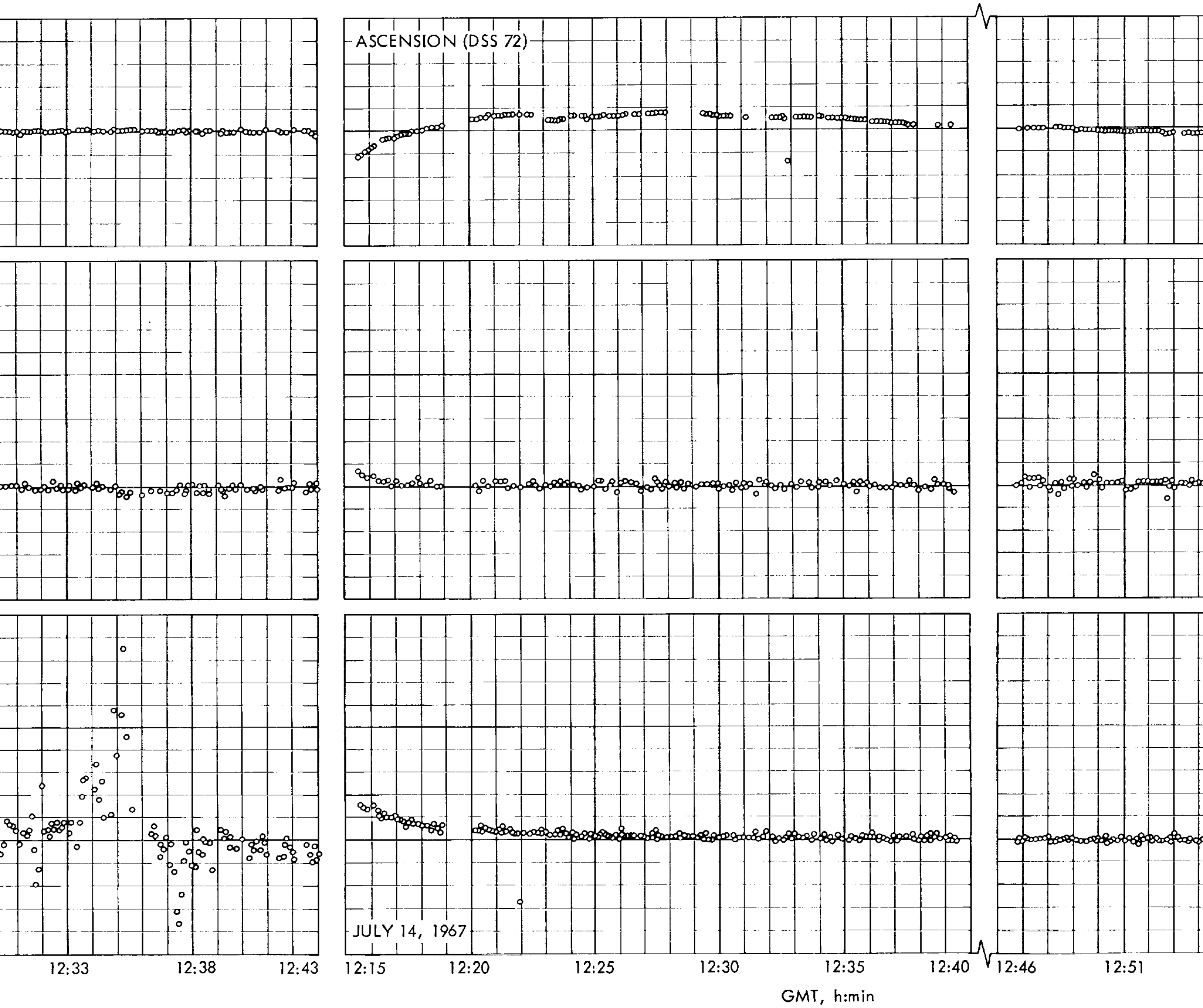
ASCENSION (DSS 72)
JULY 14, 1967
12:33
12:38
12:43
12:15
12:20
12:25
12:30
12:35
12:40
12:46
12:51
GMT, h:min

Fig. 38. AFETR tracking data residuals for *Surveyor IV*

the relatively large difference in the geocentric inertial position and velocity of the JPL and AFETR transfer orbit solutions.

(3) *Different epochs associated with the JPL and AFETR transfer orbit solutions.* The epoch used for the AFETR orbit solution was 12:04:55.600 GMT. To compare this solution with the JPL solution, the AFETR converged conditions had to be mapped to the JPL epoch of 12:05:06.480. Some accuracy could be lost by the mapping but this should have only a minor effect.

(4) *Different data spans used by AFETR and JPL to compute a transfer orbit.* During the postflight analysis, it was not possible to determine which data were used in the various AFETR solutions. Consequently, additional postflight analysis was performed using various data spans in the transfer orbit solution in an attempt to match the best AFETR solution. Three additional postflight transfer orbits were computed and the solutions are given in Table 48. Table 49 shows the data spans used for these postflight transfer orbit solutions and the associated statistics for the tracking data residuals.

The first solution is based on only the C-band tracking data received from Antigua. The time span used is from main engine cutoff to just before separation of the spacecraft from *Centaur.* No Trinidad data were used in the solution since the small amount of Trinidad data available did not appear

Table 48. Postflight transfer orbit solutions, *Surveyor IV*

Parameter	Solution using Antigua data only	Solution using burn data from Antigua and Trinidad	Solution using DSS 72 angle data with Antigua and Trinidad
Epoch, GMT 12:05:06.480 (July 14, 1967)			
Geocentric position and velocity at epoch			
X, km	3098.3648	3098.4306	3099.0084
Y, km	5358.5347	5358.7887	5358.9018
Z, km	2140.0163	2140.1980	2140.9097
DX, km/s	−8.0202025	−8.0963849	−8.0406861
DY, km/s	6.0849217	5.9829855	6.0729472
DZ, km/s	−4.3556044	−4.4015518	−4.3768332
Unbraked impact quantities			
B, km	2868.93	14037.1	12067.6
B · TT, km	2827.33	−13234.5	−8031.20
B · RT, km	486.81	4678.2	9007.00
Latitude, deg	−12.23	−17.44	−44.10
Longitude, deg	24.58	217.31	205.88
Unbraked impact, GMT	02:15:11.353 (July 17, 1967)	23:48:18.721 (July 16, 1967)	23:14:59.077 (July 16, 1967)

Table 49. Statistics of postflight transfer orbit tracking data residuals, *Surveyor IV*

Station and data type	Data span, GMT		Number of points	Standard deviation	Mean residual (O − C)
	Beginning h:min:s	Ending h:min:s			
Antigua data only					
Antigua					
Range, km	12:05:06	12:05:54	9	0.002	0.000664
Azimuth, deg	12:05:06	12:05:54	9	0.0075	0.000002
Elevation, deg	12:05:06	12:05:54	9	0.0148	0.00668
Burn data from Antigua and Trinidad					
Antigua					
Range, km	12:04:48	12:05:54	12	0.217	0.0704
Azimuth, deg	12:04:48	12:06:00	13	0.0290	0.00540
Elevation, deg	12:04:48	12:05:54	12	0.126	0.0763
Trinidad					
Range, km	12:04:51	12:05:27	7	0.245	0.0212
Azimuth, deg	12:04:51	12:05:33	8	0.0353	−0.0967
Elevation, deg	12:04:51	12:05:27	7	0.254	0.188
DSS 72 angle data with Antigua and Trinidad					
Antigua					
Range, km	12:05:06	12:05:54	9	0.0545	−0.0219
Azimuth, deg	12:05:06	12:05:54	9	0.0153	0.0167
Elevation, deg	12:05:06	12:05:54	9	0.0325	−0.00706
Trinidad					
Range, km	12:05:09	12:05:33	5	0.0952	−0.0601
Azimuth, deg	12:05:09	12:05:33	5	0.0261	−0.0880
Elevation, deg	12:05:09	12:05:33	5	0.190	0.317
DSS 72					
Azimuth, deg	12:16:23	12:28:53	47	3.70	−0.0250
Elevation, deg	12:16:23	12:28:53	47	0.224	0.0116

to be good. This solution is very close to the inflight transfer orbit solution computed by JPL.

A second transfer orbit solution used Antigua and Trinidad tracking data from before main engine cutoff to separation of the spacecraft from *Centaur*. The time span was chosen to add two points of burn data (data received before main engine cutoff) to the data span for each station. Since the AFETR real-time orbits were computed before the actual mark times were known, it was thought that an error in main engine cutoff mark time had perhaps brought some burn data into their solutions. However, a comparison of this postflight solution with the AFETR real-time solution shows that this was probably not true.

Both Antigua and Trinidad lost track of the spacecraft–*Centaur* before their separation (Fig. 36). This rules out any possibility that data taken during *Centaur* retrothrust could have been used in the AFETR real-time transfer orbit solution. So an error in the *Centaur* retro mark time would not affect the AFETR transfer orbit solution.

The third postflight transfer orbit solution contained data from DSS 72 in addition to the Trinidad and Antigua data. In the past the AFETR transfer orbit solutions have been based only on tracking data from the AFETR and MSFN tracking stations. But the AFETR personnel indicated they had used early data from DSS 72 in one of their transfer orbit solutions. A transfer orbit solution using the first 10 min of two-way doppler data and angle data from DSS 72 showed that the poor quality of the doppler data made a converged solution impossible. When only the angle data from DSS 72 and the data from Trinidad and Antigua were used, a converged solution was possible. From this solution (Table 48) it is clear that the early DSS 72 data was inconsistent with the data from Trinidad and Antigua.

(5) *Different orbit determination programs used by the AFETR and JPL.* The fact that the inflight AFETR transfer orbit solution is very close to the best DSIF solution while the inflight JPL solution did not give as close a comparison should not be alarming. The AFETR orbit determination program is designed specifically to deal with short spans of data and can make special corrections for the AFETR data (e.g., refraction corrections). The JPL orbit determination program is designed to yield very accurate solutions from long spans of data. With such a small amount of data, it is difficult to find the accurate solution for the orbital parameters. Thus the JPL inflight solution was considered a good one for the amount of data available.

C. Analysis of the Postretro Orbit Data

Centaur C-band tracking data from Pretoria and Ascension were available for postretro orbit computations. Approximately 30 min of data from Pretoria and 90 min of data from Ascension were used in the JPL postflight postretro orbit solution. The AFETR personnel were unable to provide information on the data used in their

Table 50. Summary of *Centaur* postretro orbit injection conditions, *Surveyor IV*

Parameter	Inflight orbit computed by AFETR	Postflight orbit computed by JPL
Epoch, GMT 12:15:30.000 (July 14, 1967)		
Geocentric position and velocity at epoch		
X, km	−2289.6226	−2277.9752
Y, km	7557.4279	7555.1903
Z, km	−895.16378	−885.98453
DX, km/s	−8.5209694	−8.5240357
DY, km/s	1.1773870	1.1875719
DZ, km/s	−4.9415631	−4.9420839
Unbraked impact quantities		
B, km	26479.433	26472.925
B • TT, km	22427.062	22490.459
B • RT, km	−14077.900	−13964.061

Table 51. Statistics of JPL postflight *Centaur* postretro orbit tracking data residuals, *Surveyor IV*

Station and data type	Data span, GMT		Number of points	Standard deviation	Mean residual (O − C)
	Beginning h:min:s	Ending h:min:s			
Pretoria					
Range, km	12:15:36	13:37:06	476	0.0850	−0.00423
Azimuth, deg	12:15:36	13:37:06	673	0.0225	0.00182
Elevation, deg	12:15:36	13:37:06	673	0.0169	0.00721
Ascension					
Range, km	12:18:12	12:43:06	179	0.0169	−0.00860
Azimuth, deg	12:18:12	12:43:06	182	0.158	0.0224
Elevation, deg	12:18:12	12:43:06	180	0.0164	0.000961

solution. The AFETR and JPL postretro solutions are given in Table 50. The data used for the JPL solution and the statistics of the postretro orbit tracking data residuals are given in Table 51.

D. Conclusions

The AFETR data and the early DSS 72 data were not consistent. In fact, the early DSS 72 data were of such poor quality that they were not useful in any transfer orbit solutions. The elevation angles at Trinidad were so low that these data were also of poor quality. The best postflight transfer orbit solution computed from early data was from the C-band data received from Antigua after main engine cutoff and before separation. This orbit solution agrees closely with the inflight transfer orbit computed on AFETR data. The elevation angles at Antigua were all below 10 deg and these data were not considered good enough to accurately define the transfer orbit.

The data used for the JPL postretro orbit solution were obtained at elevation angles above 10 deg. The relatively large amount of postretro data that were available yielded a reliable postretro orbit solution. The JPL and AFETR solutions agree closely, particularly in the **B**-plane quantities.

Appendix A
Definition of Doppler Data Types

Three types of doppler data were obtained by the DSN tracking stations – one-way, two-way, and three-way doppler. The following sketches and definitions distinguish the methods.

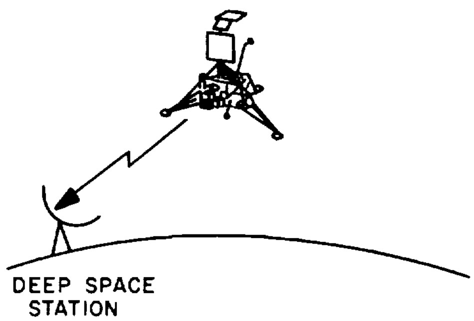

ONE-WAY DOPPLER

The spacecraft transmits to the ground station. The ground station operates in receive mode, only.

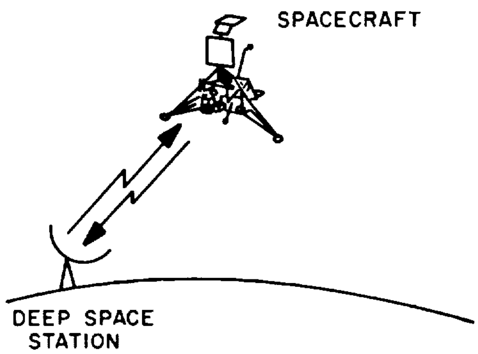

TWO-WAY DOPPLER

The ground station transmits to the spacecraft; the spacecraft retransmits signal to the same ground station. The ground station operates in both transmit and receive modes.

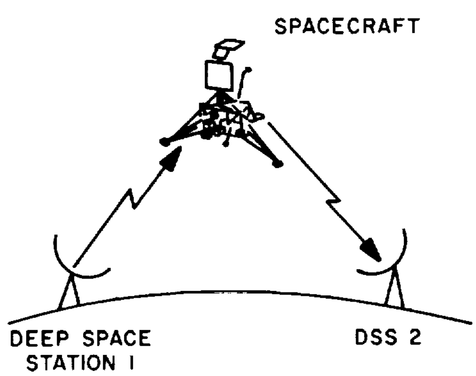

THREE-WAY DOPPLER
(NONCOHERENT)

The first ground station transmits a signal to the spacecraft; the spacecraft retransmits the signal to the second ground station. Station 1 does *not* transmit a reference frequency to station 2.

Appendix B

Definition of the Miss Parameter B

The miss parameter **B** is used at JPL to measure miss distances for lunar and interplanetary trajectories; it is described by W. Kizner in Ref. 10. The parameter has the desirable feature of being very nearly a linear function of changes in injection conditions.

The osculating conic at closest approach to the target body is used in defining **B**, which is the vector from the target's center of mass, perpendicular to the incoming asymptote. Let $\mathbf{S}_I$ be a unit vector in the direction of the incoming asymptote. The orientation of **B** in the plane normal to $\mathbf{S}_I$ is described in terms of two unit vectors, **R** and **T**, normal to $\mathbf{S}_I$. Unit vector **T** is taken parallel to a fixed *reference plane*, and **R** completes a right-handed orthogonal system. Figure B-1 illustrates the system.

For *Surveyor*, two reference planes have been used: the plane of the earth's equator **T***Q* or the plane of the moon's equator **T***T*.

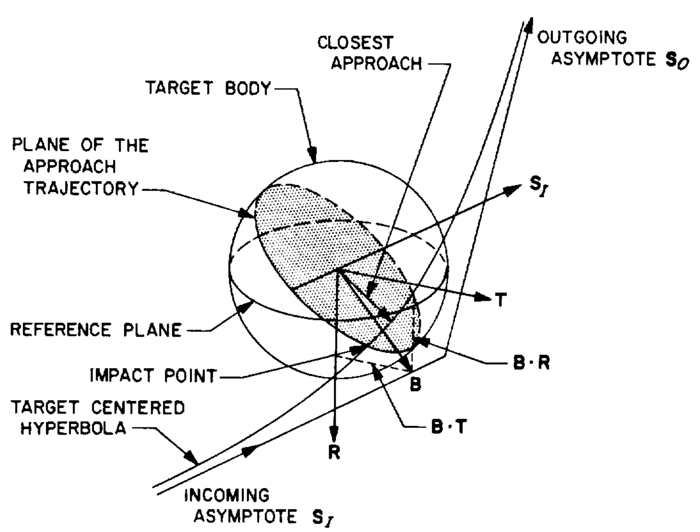

Fig. B-1. Definition of B·T, B·R system

Glossary

Abbreviations

ACIC	Air Force Aeronautical Chart and Information Center
AMR	altitude marking radar
az	azimuth
CACO	*Centaur* achieves circular orbit
dec	declination angle
el	elevation
E	lunar encounter (when shown with *time*)
EUBIT	estimated unbraked impact time
HA	hour angle
L	launch (when shown with *time*)
lat	latitude
lon	longitude
LaRC	Langley Research Center
O − C	observed value *minus* computed value (residual)
OD	orbit determination
ODG	orbit data generator program
MECO	*Centaur* main engine cutoff
MC	midcourse
R	radius; retromaneuver (when shown with *time*)
SPODP	single precision orbit determination program
TDP	tracking data processor program
AFETR	Air Force Eastern Test Range

Parameters

C_3	*vis viva* integral (twice the energy per unit mass)

Parameters (contd)

DX, DY, DZ	geocentric space-fixed velocity
SMAA	semimajor axis of one-sigma dispersion ellipse
SMIA	semiminor axis of one-sigma dispersion ellipse
SVFIXR	one-sigma uncertainty in magnitude of velocity vector at unbraked impact (Sigma Velocity at **FIX**ed **R**adius)
T_L	time of launch
X, Y, Z	geocentric space-fixed position
$\sigma_{T,\,impact}$	one-sigma uncertainty in predicted unbraked impact time
$\sigma_x, \sigma_y, \sigma_z$	one-sigma uncertainties in position
$\sigma_{DX}, \sigma_{DY}, \sigma_{DZ}$	one-sigma uncertainties in velocity.
$\theta_{\mathbf{T}}$	orientation angle of dispersion ellipse measured counterclockwise from $\mathbf{B}\cdot\mathbf{T}T$ axis
ϕ_{99}	99% velocity vector pointing error

Orbit identifications

DACO	data consistency orbit
ETR	orbit computed at AFETR real-time computer complex
FINAL	AMR backup computation orbit
ICEV	initial condition evaluation orbit
LAPM	last premidcourse orbit
NOMA	nominal maneuver orbit
POM	postmidcourse orbit
PRCL	premidcourse data cleanup orbit
PREL	preliminary evaluation orbit
PROR	predict orbit
PTD	post touchdown orbit

References

1. *Surveyor III Mission Report, Part I. Mission Description and Performance,* Technical Report 32-1177. Jet Propulsion Laboratory, Pasadena, Calif., Sept. 1, 1967.

2. *Surveyor IV Mission Report. Mission Description and Performance,* Technical Report 32-1210. Jet Propulsion Laboratory, Pasadena, Calif., Jan. 1, 1968.

3. Warner, M. R., and Nead, M. W., *SPODP-Single Precision Orbit Determination Program,* Technical Memorandum 33-204. Jet Propulsion Laboratory, Pasadena, Calif., Feb. 15, 1965.

4. White, R. J., et al., *SPACE-Single Precision Cowell Trajectory Program,* Technical Memorandum 33-198. Jet Propulsion Laboratory, Pasadena, Calif., Jan. 15, 1965.

5. Holzman, R. E., *User's Guide to the Tracking Data Processor and Orbit Data Generator Programs,* Reorder No. 62-205, Jet Propulsion Laboratory, Pasadena, Calif., May 27, 1965.

6. Vegos, C. J., and Trask, D. W., "Ranger Combined Analysis, Part II: Determination of the Masses of the Earth and Moon from Radio Tracking Data," in *The Deep Space Network,* Space Programs Summary 37-44, Vol. III, Jet Propulsion Laboratory, Pasadena, Calif., Mar. 31, 1967.

7. Clarke, V. C., Jr., *Constants and Related Data for Use in Trajectory Calculations,* Technical Report 32-604. Jet Propulsion Laboratory, Pasadena, Calif., Mar. 6, 1964.

8. Wollenhaupt, W. R., *Surveyor HAC-JPL Orbit Determination Interface Agreement,* Project Document No. 62, Jet Propulsion Laboratory, Pasadena, Calif., Mar. 30, 1966.

9. Labrum, R. G., *HAC-JPL Orbit Determination Interface Agreement for Surveyor Parking Orbit Trajectories,* Project Document No. 602-26, Jet Propulsion Laboratory, Pasadena, Calif., June 6, 1967.

10. Kizner, W. A., *A Method of Describing Miss Distances for Lunar and Interplanetary Trajectories,* External Publication No. 674, Jet Propulsion Laboratory, Pasadena, Calif., Aug. 1, 1959.